# Electrochemical studies of the ligand 1-hydroxyl-3-aminopropilydenediphosphonic acid (APD) towards bone cancer therapy

by

**Philemon Podile Magampa**

Submitted in partial fulfillment of the requirements for the degree **Master of Science**

in the Faculty of Natural & Agricultural Sciences

University of Pretoria

Pretoria

October, 2006

## Declaration

I hereby declare that this dissertation is my own original work. It is submitted for the partial fulfillment of the degree of Master of Science in the faculty of Natural and Agricultural science at the University of Pretoria. The work in this dissertation has never been submitted before for any degree or examination in any university.

……...

**P.P. Magampa**

……day of ……the year……

## Abstract

The stability constants for the ligand 1-hydroxyl-3-aminopropilydene diphosphonic acid (APD) or Pamidronate with metal ions $Cd^{II}$, $Pb^{II}$ and $Zn^{II}$ were established in this work by sampled direct current polarography ($DC_{TAST}$). Due to precipitation of the metal-ligand complexes in the pH range about 4.0 to 5.0 at typical glass electrode potentiometric conditions, these systems could not be studied by glass electrode potentiometry (GEP). The concept of Virtual Potentiometry (VP) was used in the modelling of the metal-ligand system and refinement of stability constants to evaluate further the metal-ligand models derived from $DC_{TAST}$. Virtual potentiometry uses virtual potentials to refine polarographic data by employing dedicated potentiometric software, ESTA. The structure of the metal complexes determined in this work is also proposed and compared to the reported crystal structures of the metal complexes of the ligand APD.

The Linear Free Energy Relationship, LFER (log $K_{ML'}$ vs. log $K_{M(OH)}$) for the ligand APD is derived here for the first time using the log $K_{ML'}$ values from literature as well as the values for $Cd^{II}$, $Pb^{II}$ and $Zn^{II}$ determined in this work. The log $K_{ML'}$ values of $^{153}Sm^{III}$–APD and $^{166}Ho^{III}$–APD, which cannot be determined by these two techniques (GEP and $DC_{TAST}$), were predicted in this work using the LFER methodology.

## Acknowledgements

I would like to take this opportunity to express my sincere thanks to the following people:

- My project supervisor Prof. I. Cukrowski for his guidance, understanding, patience, 30 years plus experience and intellectual input in this work. Your commitment in this project is much appreciated.

- The NRF for financial assistance, the entire Electrochemistry Research Group especially Tumaini, Daniel and Castelo for their inputs and opinions in this work. Winny for her continued encouragement since our honours level at Wits University.

- I would like to acknowledge my family (especially my late father Mr. Manoke Magampa) for their continued support over the years, their patience, belief and trust in me. My friends Legase, Charles, Selele and Ouma for their moral support during hard and challenging times in my studies.

- Above all, God almighty for giving me strength to hold on and persevere challenges in my life.

# Table of contents

## List of figures

**Figure 4.42** The species distribution diagram for the $Zn^{II}$–APD system studied by $DC_{TAST}$ at $[L_T]:[M_T] = 28$, initial $[M_T] = 8.961\times10^{-5}$ M, at ionic strength $\mu$ = 0.15 M NaCl and 25 °C. The model consists of species $M(H_3L)$, $M(H_2L)$ and $M_2L$ with refined stability constants as log $\beta$ values 30.16±0.02, 25.64±0.06 and 20.54±0.05, respectively.

**Figure 4.43** The species distribution diagram for the $Zn^{II}$–APD system studied by $DC_{TAST}$ at $[L_T]:[M_T] = 28$, initial $[M_T] = 8.961\times10^{-5}$ M, at ionic strength $\mu$ = 0.15 M NaCl and 25 °C. The model consists of species $M(H_3L)$, $M_2(HL)$ and MHL with refined stability constants as log $\beta$ values 30.19±0.01, 25.38±0.07 and 20.75±0.03, respectively.

**Figure 4.44** The plot for virtual half-wave potential, $E_{1/2}^{r}$(virt) vs. log [M] for $Zn^{II}$–APD system studied by $DC_{TAST}$ at $[L_T]:[M_T]$ ratio 28, $[M_T] = 8.961\times10^{-5}$ M, at ionic strength $\mu$ = 0.15 M (NaCl) and 25 °C. This plot is for model: $M(H_3L)$, $M(H_2L)$ and MHL with refined stability constants as log $\beta$ values 30.15±0.02, 25.64±0.05 and 20.72±0.03, respectively.

**Figure 4.45** The linear free energy relationship (LFER) between the log $K_{M(OH)}$ and log $K_{MHL}$ for indicated metal ions (all divalent) and the ligand APD.

**Figure 4.46** The linear free energy relationship (LFER) between the log $K_{M(OH)}$ and log $K_{MHL}$ for indicated metal ions (all divalent) and the ligand APD. The log $K_{MHL}$ value for $Mg^{II}$ determined in this work was used.

**Figure 4.47** The linear free energy relationship (LFER) between the log $K_{M(OH)}$ and log $K_{MHL}$ for indicated metal ions (all divalent) and the ligand APD. The log $K_{MHL}$ value for $Mg^{II}$ was not used at all.

**Figure 4.48** The linear free energy relationship (LFER) between the log $K_{M(OH)}$ and log $K_{ML'}$ for indicated metal ions (all divalent) and the ligand APD. The log $K_{ML'}$ value for $Mg^{II}$ was not used at all.

## List of tables

## List of symbols and abbreviations

| | |
|---|---|
| APD | 1-hydroxyl-3-aminopropilydene diphosphonic acid |
| EDTMP | Ethylenediammine-tetramethylenephosphonic acid |
| MDP | Methylene diphosphonic acid |
| HEDP | 1-hydroxyethylenediphosphonic acid |
| FHMA | 1,1-dihydroperflouroheptyl methacrylate |
| IDA | Iminodiacetic acid |
| MIDA | N-methyliminodiacetic acid |
| t | Temperature/ °C |
| μ | Ionic strength/ $mol.L^{-1}$ |
| DPP | Differential Pulse Polarography |
| GEP | Glass Electrode Potentiometry |
| $DC_{TAST}$ or DCP | Direct Current Polarography |
| ESTA | Equilibrium Simulation and Titration Analysis |
| *p*, *q* and *r* | Stoichiometric coefficients for given reactants M, L and H, respectively |
| $\beta_{pqr}$ | Thermodynamic overall formation constant for the complex, $M_pL_qH_r$ |

| | |
|---|---|
| $K_1 ... K_n$ | Stepwise stabiliy or formation constants |
| $K_1^H \ldots K_n^H$ | Stepwise protonation constants |
| $E$ | Potential |
| $E°$ | Standard redox potential |
| R | Gas constant (= 8.31 J.mol$^{-1}$.K$^{-1}$) |
| T | Absolute temperature/ K |
| F | Faraday constant (= 96,500 C/mol) |
| $T_i^r$ | Real or experimental concentration of component *i* |
| $T_i^c$ | Calculated total concentration of component *i* |
| °C | Degrees Celcius |
| $X_i$ | Free concentration of the *i*th component |
| $r_{jn}$ | Stoichiometric coefficient of component *i* in complex *j* |
| $C_i^V$ | Initial concentration of *i*th component in the vessel |
| $C_{im}^B$ | Concentration of ith component in the *m*th burette |
| $V°$ | Initial vessel volume |
| $NB$ | Number of burettes |
| $\gamma_n$ | Activity coefficients of species *n* |

| | |
|---|---|
| $\gamma_j$ | Activity coefficients of species *j* |
| $E_k$ | Electrode potential at *k*th step |
| $E_k^\circ$ | Electrode response intercept |
| $E_k^{IS}$ | Electrode selectivity |
| $E_k^{LJ}$ | Liquid junction potential |
| $S_k$ | Electrode response slope |
| $K_{ki}$ | Selectivity coefficient of the *i*th component |
| $\alpha$ | Electron transfer coefficient |
| $z_i$ | Charge on the *i*th component |
| $\lambda_i^s, \lambda_i^b$ | Ionic conductance of the *i*th components in test and bridge solution, respectively |
| $\{S_i^s\}, \{S_i^b\}$ | Activity of *i*th components in the test and bridge solution, respectively |
| $E_k^{LJ0}$ | Liquid junction between the bridge solution and a solution containing the bridge ions at the reference ionic strength |
| $\overline{Z}_H$ | Average number of protons bound to the ligand |
| $\overline{Z}_M$ | Average number of ligands bound to the metal ion |
| $K_w$ | Dissociation constant for water |
| $H_T$ or [H] | Total proton concentration |

| | |
|---|---|
| $L_T$ or $[L_T]$ | Total ligand concentration |
| DME | Dropping mercury electrode |
| $I_d$ | Limiting diffusion current |
| $n$ | Number of electrons |
| $D$ | Diffusion coefficient |
| $m$ | Mass flow rate of mercury |
| $t_d$ | Drop time |
| $C$ | Concentration of electroactive species in the bulk solution |
| $E_{1/2}$ | Half-wave potential |
| $E_{1/2}^{r}$ | Reversible half-wave potential |
| $E_{1/2}^{irr}$ | Irreversible half-wave potential |
| $E_{1/2}(M)$ or $E(M_{Free})$ | Half-wave potential for the free metal ion |
| $E_{1/2}(C)$ | Half-wave potential for the complexed metal ion |
| $\beta_0$ | Stability constant of zero complex |
| *I(C)* or *I(comp)* | Current for complexed metal ion |
| *I(M)* | Current for free or uncomplexed metal ion |
| [L] or L | Free ligand concentration |

| | |
|---|---|
| [M] | Free metal ion concentration |
| $\Delta E$ | Shift in $E_{1/2}$ due to complexation of free metal ion |
| $E_{1/2}$(virt) or $E$(virt) | Virtual half-wave potential |
| BC | Background current |
| $C_O(0)$ | Surface concentration of oxidised species |
| $C_R(0)$ | Surface concentration of reduced species |
| $I$ | Current |
| $D_O$ | Diffusion coefficient of oxidised form |
| $D_R$ | Diffusion coefficient of reduced form |
| $I_p(M_{comp})(i)$ | Height of the DPP peak recorded at *i*th pH value |
| $I_p(M_{Free})(i)$ | Calculated DPP peak height of the free metal ion, one would observe at *i*th pH value if complexes are not formed |
| $[M_T](i)$ | Total metal ion concentration at *i*th pH value |
| $[M_{Free}](i)$ | Free metal ion concentration at *i*th pH value |
| ECFC | Experimental Complex Formation Curve |
| CCFC | Calculated Complex Formation Curve |
| pH | Negative logarithm of proton concentration |

| | |
|---|---|
| $\delta$, Delta | Parameter which relates to electrochemical reversibility of the metal-ligand system, it is close to 1 for fully reversible system |
| VP | Virtual potentiometry |
| VP-DC | Combined virtual potentiometry and direct current polarography |
| $X$ | Applied potential |

# CHAPTER 1

# INTRODUCTION

# 1. General introduction

Normal bone remodelling refers to a dynamic process in which a delicate and coordinated balance between bone-resorbing cells (called osteoclasts) and bone-forming cells (called osteoblasts) is maintained. This balance results in the replacement of old bone with new, stronger bone. The process of bone remodelling depends on the adequate amounts of vitamin D, calcium and phosphate [1].

Cancer is one of the most death causing disease, bone cancer is the focus of our study. The bone is one of the most preferential metastatic target sites for several cancers, including breast, prostate, and lung cancer because it possess unique biological features that enable circulating cancer cells to home, survive and proliferate. More often than not bone cancer occurs as a result of cancer cells spreading from the primary tumour site (usually breast, prostate and lung) to the bone where they metastasize and develop into secondary tumours which lead to bone dissolution.

The process of bone metastasis, commonly known as bone cancer, consists of three steps:

- Proliferation and invasion of cancer cells at the primary site.
- Migration of cancer cells to the bone surface.
- Attachment to bone surfaces, osteoclastic bone destruction and colonization of cancer cells in bone [2].

Osteolysis is the process in which a bone tissue is remodelled through 'normal' physiological process or is degenerated through disease. Osteolytic bone metastases that cause pain, pathological fracture and hypocalcaemia are frequently seen in patients with a variety of malignant tumours. Progressive skeletal destruction may lead to increasing immobility, deteoriation in the quality of life and premature death [3].

Methods of treating cancer patients include radiation therapy, chemotherapy and hormone therapy. The cancer treatment is performed in order to suppress pain caused by cancer or to cure cancer completely. Radioisotopes are systematically administered on patients for the palliation of pain, which originates from bone cancer. These radioisotopes are administered in the form of radiopharmaceuticals, i.e. radioisotopes complexed to the bone-seeking ligands such as bisphosphonates. Radiopharmaceuticals, such as $^{153}$Sm-EDTMP, have

produced satisfactory results in the pain palliation therapy [4, 5]. Intravenous radioisotopes such as $^{89}$Sr and $^{153}$Sm have been used to treat bone cancer in radiation therapy [6]. However the mechanism by which the cancer pain is lessened is not yet known. One theory on how radiopharmaceuticals work in the pain palliation treatment is that the complexed bisphosphonate ligand delivers the radioisotope to the areas of increased osteoblastic activity. Radiation due to the isotope will then cause death to the percentage of cancer cells within the β-range (3 mm for $^{153}$Sm and 8 mm for $^{166}$Ho) [7].

### 1.1 Bisphosphonate ligands

Bisphosphonates are class of compounds containing two phosphonate groups linked by a carbon atom (i.e. they contain P-C-P structure). It is through this structure by which the bisphosphonates bind strongly to calcified bone matrix (hydroxyapatite) and inhibit bone resorption. The bisphosphonates' ability to bind the bone and their anti-resorptive ability depends on the side chains attached to the carbon atom. Bisphosphonates containing a primary nitrogen atom (e.g. APD) are more potent than non-nitrogen bisphosphonates (e.g. MDP), whilst modifying the primary amine (e.g. APD) to form tertiary amine (e.g. ibandronate) increases potency even further. Bisphosphonates have anti-tumour effects, which include inhibition of cell growth, prohibition of adhesion and spreading of cells. Bisphosphonates increase osteoclast apoptosis (a biological process which result in the reduction in tumour cell-induced bone resorption and destruction) and inhibit tumour cell invasion. They also inhibit osteoclast activity [8, 9].

Bisphosphonates are resistant to chemical and enzymatic hydrolysis [10, 11]. Bisphosphonates are bone seeking ligands and are key drugs in control of hypocalcaemia caused by malignant tumours such as multiple myeloma, Paget's disease and bone metastases from diverse solid tumours. They are also used in the absence of hypocalcaemia [12].

A variety of bisphosphonates has been used in the treatment of bone metastases in humans and animals. In human clinical trials, significant number of patients with bone metastases responded to the treatment well when evaluated for pain relief and mobility. Experiments on animals have also shown reduction in bone metastases as well as a decrease in the

invasion and resorption of bone by contiguous tumours following bisphosphonates treatment [10].

It appears therefore that bisphosphonates are choice drugs in slowing down and prohibiting bone resorption and destruction. Bisphosphonates also increase bones mass in cortical and trabecular bone but are poorly absorbed in the gastrointestinal tract. Bisphosphonates have high bone uptake and when injected they target the bone [12]. The bisphosphonate of interest in this study is 1-hydroxyl-3-amino-propilydene diphosphonic acid (APD).

### 1.1.1 1–hydroxyl–3–aminopropilydene diphosphonic acid, APD.

This ligand is being produced commercially by Ciba company in Switzerland since 1994 under trade name Pamidronate. This ligand binds to the bone surface thereby inhibiting resorption, the functioning of the osteoclast, and interferes with osteoclast precursors [13]. APD also increases the mobility of $Ca^{II}$ and $Mg^{II}$ ions in blood plasma such that these metal ions deposition on the bone tissue is easier, thus assisting in regenerating the bone. It stops the "eating away" of bone by the cancer cells and repairs the damaged bone. APD has palliative effects on its own and can also be used as therapeutic radiopharmaceutical when complexed to radioactive nuclides such as $^{153}Sm$ and $^{166}Ho$ to deliver these trivalent lanthanides to the bone in order to kill the cancer cells [14].

## 1.2 The use of radiopharmaceuticals

A radiopharmaceutical is a radioactive pharmaceutical or compound that is used as a tracer for diagnosis in radiotherapy. This compound elicits no physiological response from the patient when it is administered for the purpose of diagnosis. Radiopharmaceuticals are classified into two categories in accordance with their properties. i.e. ideal-diagnostic radiopharmaceuticals and ideal-therapeutic radiopharmaceuticals [15].

### 1.2.1 Ideal diagnostic radiopharmaceuticals

Ideal diagnostic radiopharmaceuticals possess a radioactive isotope with characteristics of a gamma ray emitter. The ideal imaging energy range for this particular radioisotope is 100 to 250 keV and must decay by electron capture or isomeric transition. Examples of these radioisotopes are $^{201}$Tl and $^{133}$Xe which emit photons of energies 70-80 keV. The most important property of radioisotope is its half-life. The effective half-life of a radiopharmaceutical should ideally be 1.5 times the duration of the diagnostic procedure. This is essential for minimisation of the radiation dose to the patient [15].

The most widely used nuclide in diagnostic nuclear medicine is the metastable isotope of Technetium ($^{99m}$Tc). Its main advantage is in that it is a pure gamma emitter and has a half-life of only 6 hours. This time is long enough to perform a diagnostic study, such as bone scintigraphy, but short enough to keep patient dose to a minimum. $^{99m}$Tc can be labelled with a variety of compounds called chelators or ligands, which stabilise the nuclide and direct it to the part of the body that needs to be imaged. For example, methyl diphosphonate (MDP) is taken up by osteoblasts and therefore $^{99m}$Tc-MDP is used for bone scintigraphy. $^{99m}$Tc is an ideal diagnostic imaging radioisotope because it has the ability to bind easily to a variety of compounds at the physiological conditions [16].

The most important aspect of ideal diagnostic radiopharmaceutical is the target organ. The ideal diagnostic radiopharmaceutical should have minimum target ratio of 5:1 for target organ to non-target organ [15].

### 1.2.2 Ideal therapeutic radiopharmaceuticals

Therapeutic radiopharmaceuticals are radioactive pharmaceutical compounds that are designed to destroy the target cells. These compounds are beta particle emitters and are controllable in terms of distribution in tissue and are easily detectable when spilled. One example of radioactive therapeutic isotope is $^{131}$I, which emits beta particles that can damage estimated 90 % of tissue. Ideal radionuclide therapy requires high-energy particles because they destroy cells and beta emitter with maximum energy greater than 1 meV is preferred. Ideal radiopharmaceuticals must have effective half-life measured in hours or

days. An example of this kind of radiopharmaceutical is $^{166}$Ho-FHMA (FHMA stands for 1,1-dihydroperflouroheptyl methacrylate) with the effective half-life of 1.2 days. The ratio of uptake of therapeutic radiopharmaceutical in terms of target to non target organ should not be too low because this may result in insufficient treatment of the primary disease and delivery of potentially lethal radiation dose to bone marrow.

Radiopharmaceuticals are relatively safe, sterile and apyrogenic. They must be effective at physiological pH of approximately 7.5 and the administration dose to the patient should be within ±10 % of the prescribed dose.

Every radiopharmaceutical is designed based on the physiological functions of the target organ and the mechanism in which it is localised at the target organ depends on the processes occurring at the target organ [15].

### 1.3 Linear Free Energy Relationships.

Many relationships between free energies or rates of complex formation and various properties of metal ions, ligands, or complexes can be discovered using the concept of linear free energy relationship (i.e. LFER). These relationships do not require strict thermodynamics in their derivation and hence they are called extra-thermodynamic relationships. These relationships provide understanding into the factors governing complex formation and also allow prediction of unknown formation or rate constants.
The first LFER in coordination chemistry was observed between the protonation constant of a ligand and log $K_{ML}$ with a variety of metal ions [17]. An example of this correlation is seen in Figure 1.1. The linearity of this relationship shows that any factors increasing or decreasing the p$K_a$ of the ligand by increasing or decreasing basicity (or electron density) of the oxygen atom on the $RO^-$ ligand also affect the log $K_{ML}$ value in a parallel fashion [18].

The LFER of log $K_{ML}$ for metal ions or ligands can be derived against the non-themodynamic properties as well. For example, in Figure 1.2, a correlation of log $K_{ML}(F^-)$ for various metal ions vs. $Z^2/r$ (where Z = cationic charge and r = ionic radius) for the

metal ions is shown. This correlation shows that the M-F bonds are largely electrostatic by nature [19].

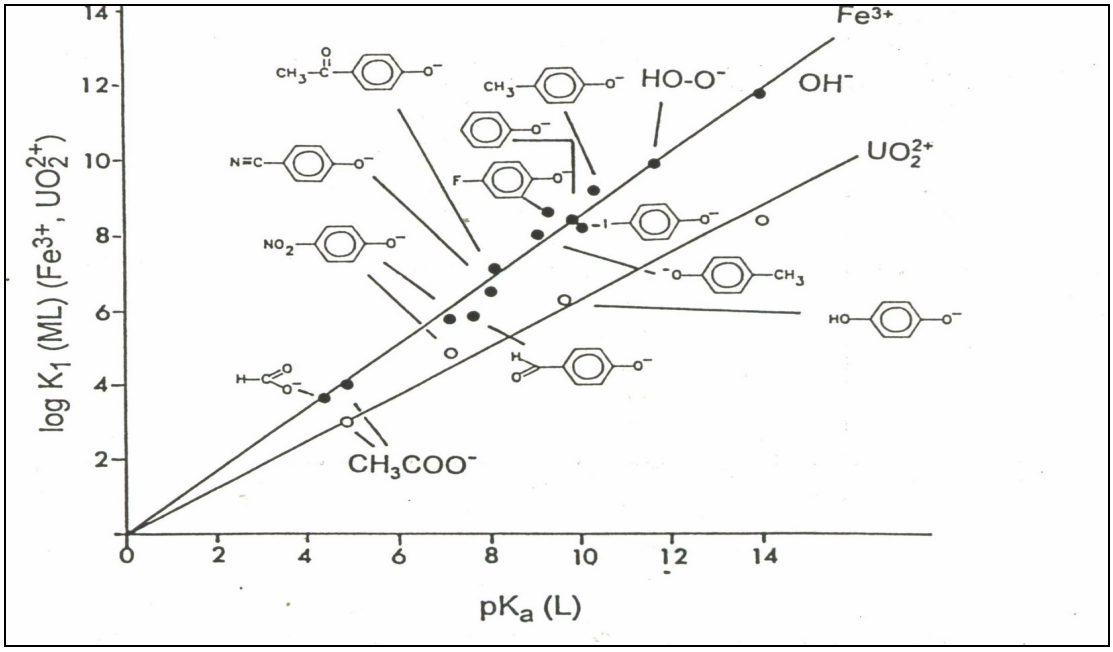


**Figure 1.1**: The linear free energy relationship for log $K_{ML}$ for $Fe^{3+}$ and $UO_2^{2+}$ vs. $pK_a$ for unidentate ligands containing negatively charged oxygen donor atoms. (ionic strength, μ = 0 M and temperature, t = 25 °C). Graph taken from reference [18].

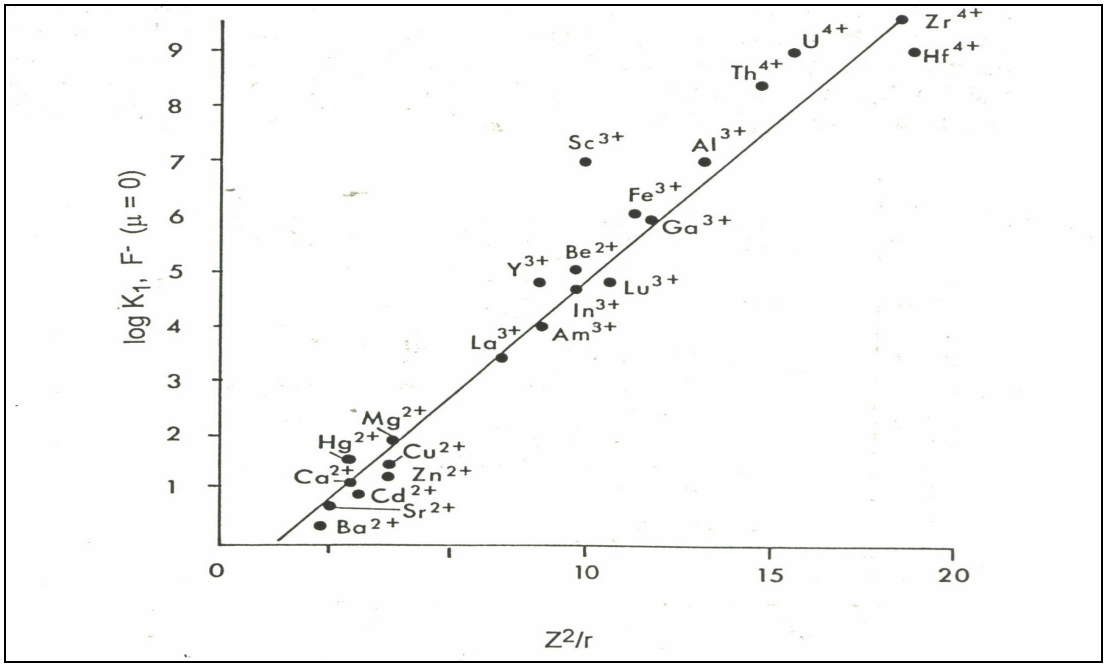


**Figure 1.2**: The LFER between log $K_{ML}(F^-)$ complexes of metal ions vs. $Z^2/r$, where Z is the cationic charge on the metal ion and r the ionic radius. (μ = 0 M and t = 25 °C) plot taken from reference [18].

The LFER approach was also employed previously for the estimation of first formation constants of trivalent lanthanides $^{153}Sm^{III}$ and $^{166}Ho^{III}$ complexed with the ligand 1-hydroxyethylenediphosphonic acid, HEDP [20, 21] using the first formation constants of the ligand HEDP with several metal ions $Ca^{II}$, $Mg^{II}$, $Ni^{II}$, $Zn^{II}$, and $Sn^{II}$ as shown in Figure 1.3.

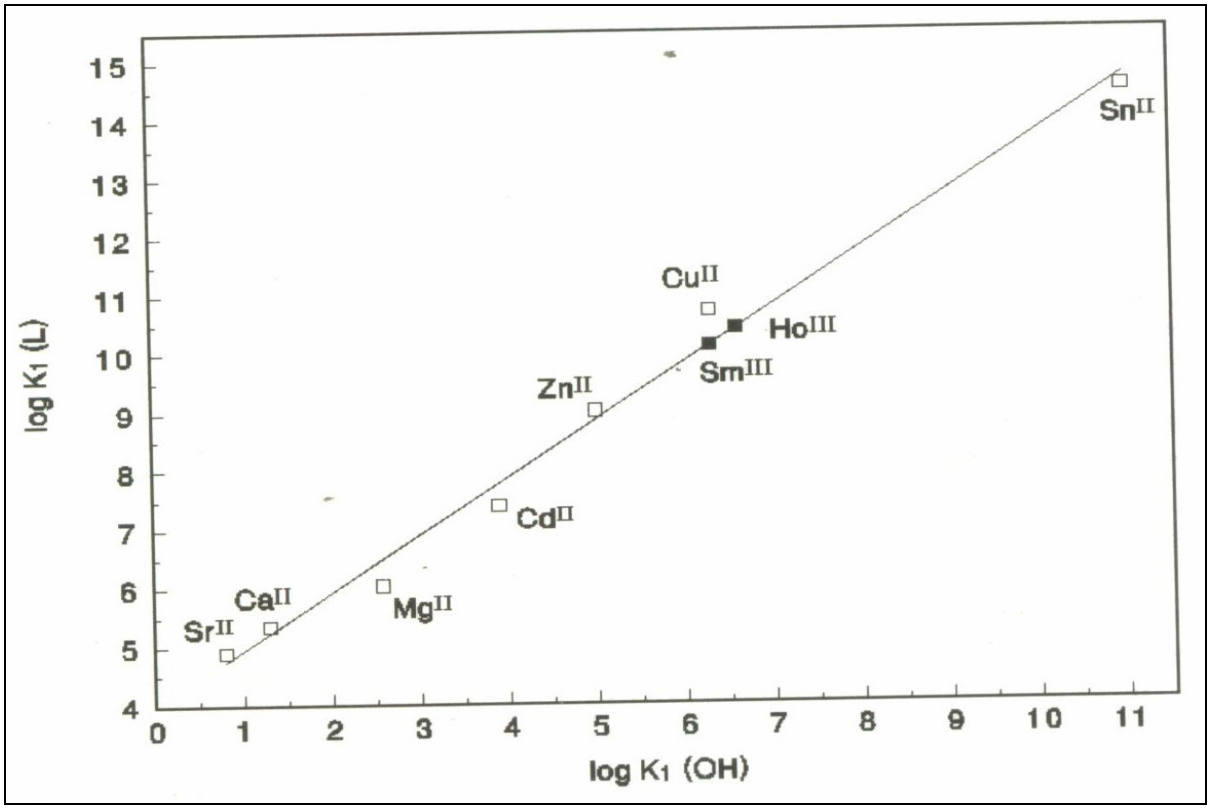


**Figure 1.3**: The LFER showing the relationship between the first formation constant, log $K_{ML}$(HEDP) and the log $K_{ML}$(OH) for different metal ions for the bisphosphonate ligand, HEDP. Graph taken from reference [20].

The LFER methodology was used recently [22, 23] to predict the first formation constants (log $K_{ML}$) for the ligand, methylene diphosphonic acid, MDP with $^{153}Sm^{III}$ and $^{166}Ho^{III}$ using the log $K_{ML}$ values form literature and the log $K_{ML}$ for $Cd^{II}$, $Zn^{II}$ and $Pb^{II}$ attained by Cukrowski et al [23]. The plot is shown in Figure 1.4.

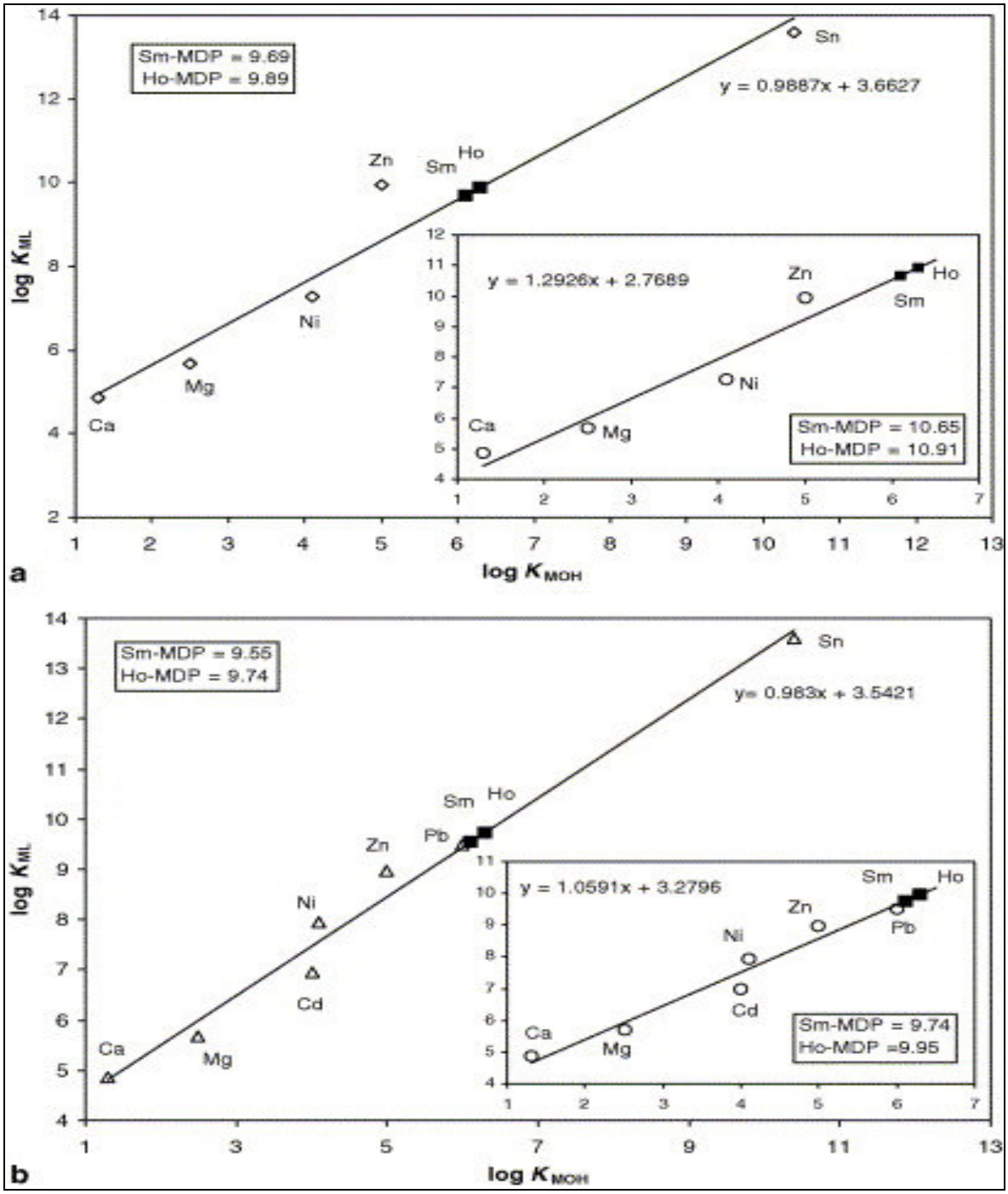


**Figure 1.4**: The Linear Free Energy Relationship (LFER) between log $K_{M(OH)}$ and log $K_{ML}$ for indicated metal ions (all divalent) and the ligand MDP. The inserts do not include stability constants for $Sn^{II}$. (a)-LFER generated for literature data [25, 26, 27] and (b)-LFER generated for data reported in [23].

### 1.4 Previous studies on bisphosphonate ligands.

A number of studies have been conducted in the use of trivalent lanthanides complexed to mainly bisphosphonates. The use of $^{153}Sm$ complexed to the ligand ethylene-diaminetetramethylenephosphonate (EDTMP) in pain palliation therapy for metastatic bone cancer is well established and has been studied in clinical trials in several countries including South Africa. However, it has been found (using baboon model) that the ligand EDTMP has a poor bone uptake. Thus a more effective ligand than EDTMP is needed to deliver a high percentage of injected $^{153}Sm$ or $^{166}Ho$ to the bone tumour. [7, 21]

A ligand, HEDP, is being used extensively in $^{99m}Tc$ imaging of bone and some clinical data exist for $^{153}Sm$-HEDP in vivo behaviour [4]. The formation constants of a number of metal ions with the ligand HEDP are required in order to estimate stability constants of this ligand when complexed to trivalent lanthanides such as $^{153}Sm$ and $^{166}Ho$ using the linear free energy relationship.

The formation constants for $^{153}Sm$-HEDP and $^{166}Ho$-HEDP cannot be determined by either GEP or polarography, due to precipitation at potentiometric conditions and these metal ions are polarographically inactive. As a result, the linear free energy relationship (LFER) has been used as predictive tool to estimate the first formation constants for $^{153}Sm$-HEDP and $^{166}Ho$-HEDP [20]. In addition, the formation constants for HEDP with $Cd^{II}$ have been reported by Cukrowski et al [24], wherein the formation constants were attained by Differential Pulse Polarography (DPP) and Glass Electrode Potentiometry (GEP).

The formation constants for trivalent lanthanides $^{153}Sm$ and $^{166}Ho$ with methylene diphosphonic acid (MDP) were estimated using the same approach of linear free energy correlation [22, 23]. This was achieved by studying the metal-MDP systems involving $Cd^{II}$, $Pb^{II}$, $Zn^{II}$, and $Ni^{II}$ by potentiometry and/or polarography and using literature data for the metal ions $Ca^{II}$, $Mg^{II}$ [25] , and $Sn^{II}$ [26, 27] with MDP.

In the quest for more effective pain palliation radiopharmaceuticals for metastatic bone cancer, the stability constants for ligand, APD with several metal ions have been reported [28]. In this study, stability constants for metal ions $Ca^{II}$, $Mg^{II}$, and $Zn^{II}$ (blood plasma metal ions) with APD were measured by potentiometry or polarography. Polarography was

used in systems where metal hydroxide precipitates were formed at $L_T$:$M_T$ ratios applicable for potentiometry. However, the complex formation constants for trivalent metal ions, $^{166}$Ho and $^{153}$Sm with APD could not be determined potentiometrically due to precipitate formation and also because these metal ions are polarographically inactive.

## 1.5 Objectives of this study.

- To determine protonation constants for the bone-seeking ligand, 1-hydroxyl-3-aminopropilydenediphosphonic acid (APD) by Glass Electrode Potentiometry at μ = 0.15 M NaCl and t = 25 °C.
- To determine stability constants for complexation of APD with several metal ions such as $Cd^{II}$, $Pb^{II}$ and $Zn^{II}$, using electrochemical techniques, Glass Electrode Potentiometry and Direct Current Polarography ($DC_{TAST}$) at μ = 0.15 M NaCl and t = 25 °C.
- To use the determined first formation constants (log $K_{ML}$) of the above metal ions as well as literature values for other metal ions to estimate the first formation constants for the trivalent lanthanides $^{153}$Sm and $^{166}$Ho complexed with ligand APD using the linear free energy relationship (LFER) as a predictive tool. The linear free energy relationship can be used in principle for any metal ion to predict the approximate log $K_{ML}$ values provided that the log $K_{M(OH)}$ values for those metal ions are known with high accuracy.
- The concept of virtual potential will be applied in cases were polarography will be used to determine the formation constants.

The structures of the ligand APD (studied in this work) and other related ligands, HEDP and MDP, are shown below:

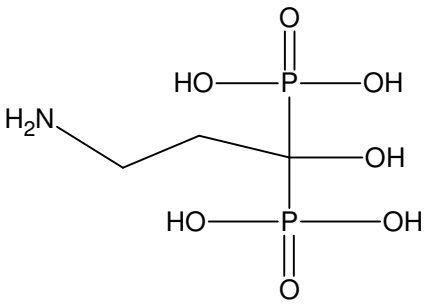

1-hydroxyl-3-aminopropilydenediphosphonic acid (**APD**)

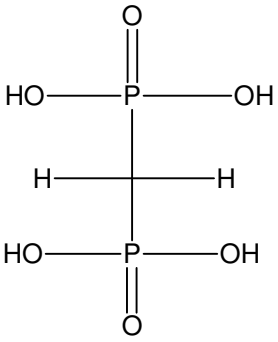

Methylenediphosphonic acid (**MDP**)

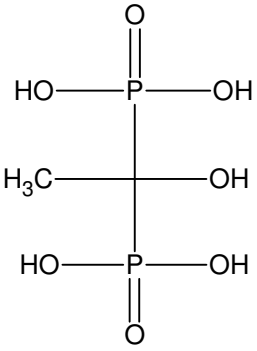

1-hydroxy-ethylene-diphosphonicacid (**HEDP**)

## References


1. Per-Anders Abrahamsson, *European Urology Supplements*, **2004**, *3*, 3.
2. T. Yoneda and T. Hiraga, *Biochemical and Biophysical Research Communications*, **2005**, *328*, 679.
3. T. Hiraga, S. Tanaka, M. Yamamoto, T. Nakajima, and W. Ozawa, *Bone*, January **1996**, *8*, No. 1, 1.
4. J. Simon, D. A. Wilson, J. R. Garlich and D. A. Troutner, *Patent 899734*, Dow Chemical Company, **1989**.
5. USA Food and Drug Administration approval for $^{153}$Sm-EDTMP ($^{TM}$Quadramet), granted during March **1997**.
6. L. G. Bouchet, W. E. Bolch, S. M. Goddu, R. W. Howell, and D. V. Rao, *J. Nucl. Med.*, **2000**, *41*, Iss 4, 682.
7. E. B. Silberstein, *Seminars in oncology*, **1993**, *20*, No. 3, Suppl. 2, 10.
8. H. L. Neville-Webbe, I. Holen, and R. E. Coleman, *Cancer Treatment Reviews*, **2002**, *28*, 305.
9. T. Hiraga, S. Tanaka, M. Yamamoto, T. Nakajima and H. Ozawa, *Bone*, January **1996**, *18*, No. 1, 1.
10. H. Fleisch, *Drugs*, **1991**, *42*, No. 6, 919.
11. P. M. Boonenkamp et al., *Bone. Min.*, **1987**, *2*, 29.
12. B. Thurlimann, R. Morant, W. F. Jungi and A. Rudziwill, *Support Care Cancer*, **1994**, *2*, 61.
13. S. Lipschitz, Bisphosphonates in the management of osteoporosis, National Osteoporosis Society, RSA.
14. Christopher Champallou, *Journal of pain and symptom Management*, **2003**, *25*, 2.
15. www.srsweb.org/radiopharmaceutical
16. M. Calleja, A. Alam, D. Wilson and K. Bradley, *Current Orthopaedics*, **2005**, *19*, 34.
17. E. Larsson, *Z. Phys. Chem. A*, **1934**, *169*, 215.
18. E. Martell and R. D. Hancock, Metal complexes in aqueous solutions, Plenum Press, New York, 1996, pp. 26–27.
19. L. P. Hammett, “Physical Organic Chemistry”, McGraw-Hill, New York, 1940.
20. J. R. Zeevaart, N. V. Jarvis, I. Cukrowski, and G. E. Jackson, *S. Afr. J. Chem.*, **1997**, *50*, No. 4, 189.

21. N. V. Jarvis, J. M. Wagener, and G. E. Jackson, *J. Chem. Soc.*, Dalton Trans, **1995**, 1411.

22. M.D. Mogano, Electrochemical studies of metal-ligand complexation of HEDP and MDP ligands for bone cancer therapy, a dissertation submitted for the degree of Master of Science at the University of the Witwatersrand, June 2004, pp. 2–5, 83–127.

23. I. Cukrowski, D. M. Mogano and J. R. Zeevaart, *J. Inorg. Biochem.*, **2005**, *99*, 2308.

24. I. Cukrowski, J. R. Zeevaart, and N. V. Jarvis, *Analytica Chimica Acta*, **1999**, *379*, 217.

25. NIST Standard Reference Database 46. NIST Critically Selected Stability Constants of Metal Complexes Database. Version 8.0. Data collected and selected by R. M. Smith, A. E. Martell, US Department of Commerce, National Institute of Standards and Technology, 2004.

26. J. R. Zeervaart, Metal Ion Speciation in Blood Plasma as a Tool in Predicting the In vivo Behaviour of Potential Bone-seeking Radiopharmaceuticals, Ph.D. Thesis, Delft University Press, The Netherlands, 2001.

27. R. A. M. J. Claessens and J. G. M. van der Linden, *J. Inorg. Biochem.*, **1984**, *21*, 73.

28. J. R. Zeevaart, N. V. Jarvis, W. K. A. Louw, G. E. Jackson, I. Cukrowski, and C. J. Mouton, *J. Inorg Biochem*, **1999**, *73*, 265.

# CHAPTER 2

# THEORY AND DATA TREATMENT

# 2. Theory and data treatment

## 2.1 Prediction of stability constants by Glass Electrode Potentiometry

Glass electrode potentiometry (GEP) can be used in the determination of stability constants for systems such as the one shown below:

$$pM + qL + rH \leftrightarrow M_pL_qH_r \quad (1)$$

where M represents the metal, L the ligand, and H is either the proton or hydroxide. In solution a large number of complexes shown above can coexist in equilibrium at a definite pH. It is therefore essential to determine which species are present in solution and to determine the formation constants of these species using for example GEP. In GEP, the glass electrode develops potential corresponding to the activities of species in solution, thus the use of large excess of a neutral background electrolyte is required to keep the ionic strength of a solution and activity coefficients of all species present in a solution constant. The stability constants for the reaction (1) shown above can be defined as [1, 2]:

$$\beta_{pqr} = \frac{[M_pL_qH_r]}{[M]^p[L]^q[H]^r} \quad (2)$$

Equation 2 defines in general the equilibrium constants which can be shown according to the following examples:

$$M + L \leftrightarrow ML \qquad K_1 = \beta_1 = \frac{[ML]}{[M][L]} \quad (3)$$

$$ML + L \leftrightarrow ML_2 \qquad K_2 = \frac{[ML_2]}{[ML][L]} \quad (4)$$

$$M + 2L \leftrightarrow ML_2 \qquad \beta_2 = \frac{[ML_2]}{[M][L]^2} = K_1K_2 \quad (5)$$

From Equations 3, 4, and 5, it follows that the overall stability constant $\beta_2 = K_1K_2$ and in general can be expressed as

$$\beta_n = \pi K_n \quad (6)$$

In most cases the experimental potentiometric data are obtained in the form of titrant added and electrode potential. At each titration point the Nernst equation is used to obtain the glass electrode potential corresponding to hydrogen ion concentration, or activity in the solution:

$$E = E^{\circ} - \mathrm{H}_{\mathrm{slope}} \times \mathrm{pH} \qquad (7)$$

where $E^{\circ}$ is the electrode constant, $\mathrm{H}_{\mathrm{slope}}$ is the electrode response slope, and pH is the negative logarithm of the free hydrogen ion activity or concentration if experiments are performed at constant ionic strength.

## 2.2 Analysis of potentiometric data

The potentiometric data was analysed in this study using ESTA (Equilibrium Simulation by Titration Analysis) library of programs as described by May et al [3]. ESTA imposes conditions on mass-balance equations by equating the calculated total concentrations with the real total concentrations in a standard fashion as shown by Equation 8:

$$T_i^r = T_i^c, \quad i = 1, \ldots, NC, \qquad (8)$$

where $T_i^r$ is the real or experimental total concentration, $T_i^c$ is the calculated total concentration of the $i$th component, $NC$ is the number of components appearing in complexes and $i$ is the general index for the components. $T_i^r$ and $T_i^c$ are given by the following equations:

$$T_i^c = [X_i] + \sum_{j=1}^{NJ} r_{ji} \Gamma_j \beta_j \prod_{n=1}^{NC} [X_n]^{r_{jn}} \qquad (9)$$

$$T_i^c = \left( \frac{C_i^V V^{\circ} + \sum_{m=1}^{NB} C_{im}^B v_m}{V^{\circ} + \sum_{m=1}^{NB} v_m} \right) \qquad (10)$$

$$\Gamma_j = \left( \frac{\prod_{n=1}^{NC} \gamma_n{}^{r_{jn}}}{\gamma_j} \right) \tag{11}$$

where $[X_i]$ is the free concentration of the $i$th component, $r_{jn}$ is the stoichiometric coefficient of component $i$ in complex $j$, $NJ$ is the number of complexes, $C_i^V$ is the initial concentration of $i$th component in the vessel, $C_{im}^B$ is the concentration of $i$th component in the $m$th burette, $v_m$ is the total titre volume added from $m$th burette, $V^\circ$ is the initial vessel volume, $NB$ is the number of burettes, $\gamma_n$ and $\gamma_j$ are the activity coefficients of species $n$ and $j$, respectively.

The free hydrogen concentration or the activity of hydrogen ions is known at any given time in glass electrode potentiometry, in a titration it is usually calculated from the observed emf. This emf is linked to the activity of the electrode ion (hydrogen) by ESTA at each $k$th titration step as shown by the following equation:

$$E_k = E_k^\circ + E_k^{IS} + E_k^{LJ}, \qquad k = 1, 2, 3, \ldots n \tag{12}$$

where $E_k^\circ$ is the electrode response intercept, $E_k^{IS}$ is the electrode selectivity as defined by Equation 13, and $E_k^{LJ}$ is the liquid junction potential as defined by Equation 14. ESTA accommodates the effects of other interfering ions in solution using the following Equation:

$$E_k^{IS} = S_k \, log \left[ \{X_k\}^{\frac{1}{\alpha}} + \sum_i \left( K_{ki} \{X_i\}^{\frac{z_k}{z_i}} \right)^{\frac{1}{\alpha}} \right]^\alpha \tag{13}$$

where $S_k$ is the electrode response slope, $K_{ki}$ is the selectivity coefficient of the $i$th component, $\alpha$ is an empirical parameter and $z_i$ is the charge on the $i$th component, the liquid junction potential term can be derived using the form of the Henderson equation as follows:

$$E_k^{LJ} = -\left(\frac{RT}{F}\right) ln\left(1 + \frac{d[XH]}{I}\right) \tag{14}$$

where $I$ is the concentration of the background univalent electrolyte. The above equation is used to correct the changes due to liquid junction potential in the calibration of glass electrode [4].

The Henderson equation is usually used in the prediction of the potentials across the junctions of various electrolytes at constant ionic strength [5] and is given by:

$$E_k^{LJ} = -\frac{RT}{F} \times \left( \frac{\sum_i \gamma_i^s \{S_i^s\} - \lambda_i^b \{S_i^b\}}{\sum_i z_i \left(\lambda_i^s \{S_i^s\} - \lambda_i^b \{S_i^b\}\right)} \times ln \frac{\sum_i \lambda_i^s z_i \{S_i^s\}}{\sum_i \lambda_i^b z_i \{S_i^b\}} \right) - E_k^{LJ0} \tag{15}$$

where $\lambda_i^s$ is the ionic conductance of the $i$th component in solution, $\lambda_i^b$ is the ionic conductance of $i$th component in the bridge solution, $z_i$ is the charge on the species $i$, $\{S_i^s\}$ is the activity of $i$th component in the test solution, $\{S_i^b\}$ is the activity of the $i$th component in the bridge solution and $E_k^{LJ0}$ is the liquid junction between the bridge solution and a solution containing the bridge ions at the reference ionic strength. Equation (15) is applicable at pH smaller than 2 where liquid junction potential becomes significant.

### 2.2.1 The protonation formation function

The total concentrations of the metal, ligand and protons are represented by $M_T$, $L_T$, and $H_T$, respectively, and the free concentration of these components is given by M, L, and H, respectively. The average number of protons bound per ligand (i.e. for protonated ligands) is defined as the protonation formation function, $\overline{Z}_H$ and is given by the following equation in the absence of the metal:

$$\overline{\mathbf{Z}}_{\mathbf{H}} = \frac{[\mathbf{boundH}]}{\mathbf{L_T}} \tag{16}$$

where [boundH] = $H_T$ –H + [$OH^-$] = $H_T$– H + $K_w H^{-1}$ (17)

where $OH^-$ is the hydroxide ion and $K_w$ is the dissociation constant for water and therefore:

$$\bar{Z}_H = \frac{H_T - H + K_w H^{-1}}{L_T} \quad (18)$$

where $H_T$ and $L_T$ are known from the analytically prepared or determined concentrations and $K_w$ is a value attainable from the literature. The $\bar{Z}_H$ can be calculated at any pH values since the glass electrode monitors the H at any experimentally accessible pH value [1]. The graph of $\bar{Z}_H$ *vs*. pH can therefore be plotted; and this graph provides information about the state of the ligand at a particular pH. $\bar{Z}_H$ can be defined as:

$$\bar{Z}_H = \left( \frac{\sum_{J=0}^{J} j H^j \beta_{01j}}{\sum_{J=0}^{J} H^j \beta_{01j}} \right) \quad (19)$$

once the protonation constants have been calculated. Thereafter the calculated and the observed protonation constants are compared and optimised until they have comparable values.

### 2.2.2 The formation function

The formation function for the metal-ligand system is called $\bar{Z}_M$ and is defined as the average number of bound ligand per metal ion as given by:

$\bar{Z}_M = \frac{[\text{L bound to M}]}{M_T}$, which can also be expressed as:

$$\bar{Z}_M = \left( \frac{L_T - [H_T - H + K_W H^{-1}]}{\bar{Z}_H} \right) \Big/ M_T \quad (20)$$

where $\bar{Z}_H$ is defined as in equation (19) above. $\bar{Z}_M$ can also be defined as follows:

$$\overline{Z}_M = L_T + L\left(1 + \sum_{J=0}^{J} jH^j \beta_{01j}\right) \tag{21}$$

$$\text{where } L = \left(\frac{\mathbf{H_T - H + K_w H^{-1}}}{\sum_{\mathbf{J=0}}^{\mathbf{J}} \mathbf{jH^j \beta_{01j}}}\right) \tag{22}$$

Note that $\overline{Z}_H$ must be determined prior determination of $\overline{Z}_M$ from the observed experimental points with the use of Equation (19) above. $\overline{Z}_M$ is plotted against pA, the negative logarithm of the free ligand concentrations.

Titrations with different ligand to metal concentration ratios are performed starting at low pH and ending at high pH using a standardised strong base. The experimentally observed formation curves are then obtained from these titrations and compared with calculated formation curves. The $\overline{Z}_H$ and $\overline{Z}_M$ functions are useful in the analysis of potentiometric data and giving meaningful representation of data and are useful in selection of the plausible potentiometric model. They can also be used for comparison of the observed and calculated data irrespective of the kinds of species forming in solution.

### 2.2.3 Deprotonation function, Qbar.

The deprotonation function is defined as the average number of protons released per metal ion due to the complexation of the metal ion by the ligand of interest and is given by:

$$Qbar = \frac{T_H^{\ *} - T_H}{T_M} \tag{23}$$

where $T_{\mathrm{H}}$ is the total proton concentration, $T_{\mathrm{M}}$ is the total metal concentration and $T_{\mathrm{H}}^{\ *}$ is the calculated total proton concentration that would be observed at a particular pH assuming no complexation occurs. $T_{\mathrm{H}}^{\ *}$ is given by:

$$T_H^{\ *} = [H] - [OH] + \sum_{J=1}^{NJ} r\left[M_p L_q H_r\right] \tag{24}$$

where *NJ* represents the number of complexes. The summation accounts for all the protonated forms of the ligand in solution [5]. Substituting Equation 23 into Equation 24 result in:

$$Qbar = \left( [H] - K_w [H]^{-1} + \sum_{J=1}^{J} r\beta_{pqr} [M]^p [L]^q [H]^r \right) / T_M \tag{25}$$

The deprotonation function assists in the analysis of titration data and complements the formation function. This function is useful in cases where the graphical representation of data by the formation function is not good. It represents very well the mixed systems and regions of titrations were the formation function is ill-conditioned or ill-defined. The deprotonation function can assist in the selection of the appropriate model and can provide the stoichiometry of the predominant species in solution.

### 2.2.4 Formation function, nbar.

The formation function**,** nbar, for binary system is defined as the average number of protons per ligand in the absence of the metal ion. The nbar is given by the equation below:

$$nbar = \left( \frac{T_H{}^* - [H] + [OH]}{L_T{}^r} \right) \tag{26}$$

$$L_T{}^r = L + \sum_{J=1}^{NJ} p\left[ M_p L_q H_r \right] \tag{27}$$

Replacing Equation (27) into Equation (26) results in:

$$nbar = \left( \frac{\sum_{J=1}^{NJ} r\beta_{pqr} \left[ M_p L_q H_r \right]}{L + \sum_{J=1}^{NJ} p\left[ M_p L_q H_r \right]} \right) \tag{28}$$

If $p$ = 0, the formation function will only depend on the free ligand and free proton concentrations in solution. The free proton concentration is obtainable from the glass electrode calibration.

### 2.2.5 ESTA library of programs

Equilibrium Simulation by Titration Analysis (ESTA) is a library of programs used for the simulation of simple equilibrium distribution of chemical species in solution and for analysis of potentiometric data. ESTA can accommodate chemical species of up to 10 components and 99 complexes. ESTA permits titrations involving up to 3 electrodes and 3 burettes. ESTA also takes into account the variations in ionic strength and the associated changes in activity coefficients. It also permits corrections of titration data affected by liquid-junction potentials and imperfect ion-selectivity of electrodes [6]. The ESTA library contains program modules which perform one or two kinds of calculations specified as a different "task". These program modules are discussed below.

***ESTA 1, the simulation module.***

ESTA 1 is the simulation module, which can determine on point-point basis single values for almost any titration parameter by setting up and solving mass balance equations. The calculations performed by ESTA 1 include

**a)** Species distribution calculations

**b)** Potentiometric titration calculations.

The latter include determination of emf values, formation constants values, total analytical concentration values, initial vessel concentrations and initial burette concentrations. This module is useful in the generation of formation function values, for,

a) Formation function (task ZBAR)

b) Deprotonation function (task QBAR) and

c) Protonation function (task NBAR)

ESTA 1 can also calculate appropriate weights, an overall objective function value and the relative contribution of the most important errors based on emf residuals and total concentration residuals. (task OBJE and OBJT, respectively). One can also generate ESTA1 output file which comes in ESTA input format [6].

***ESTA 2, the optimisation module*.**

ESTA 2 module contains two optimisation programs, viz. ESTA2A and ESTA2B which differ only in the way data are weighted [7]. These programs are used to determine the best values for one or more parameters based on least-square minimization procedure applied to the whole system of titrations. These programs allow refinement of the following titration parameters: formation constants, vessel and burette concentrations, electrode slope, and initial vessel volume. It is possible to refine together local parameters of the same type as a single parameter in a combination of titrations.

The objective function may be weighted or unweighted. The sum of squares of residuals may be minimised with respect to either:

i) emf, the task OBJE that optimizes the titration parameters using the weighted or unweighted sum of squares of emf residuals, or
ii) the total concentration, the task OBJT that optimizes titration parameters using weighted or unweighted sum of total electrode ion concentration of residuals.

In ESTA2A, the weights are recalculated during the optimisation cycle from current values of the parameters being optimised. In ESTA2B, the weights are calculated once from the initial estimates of the parameters being optimised [6].

## 2.3 Polarography, a general introduction.

Polarography is a dynamic electrochemical technique that uses current-voltage relationship obtained when the solution is electrolysed between the working electrode (Dropping mercury electrode, DME) and a reference electrode. In modern polarography, a solution is electrolysed between a dropping mercury electrode (a working electrode), a reference

electrode, and an auxiliary electrode (in which a reverse process to the one occurring at the working electrode occurs) by applying the potential between the working and reference electrodes. The dropping mercury electrode consists of a series of small droplets issued from the end of a fine capillary. The potential applied to mercury working electrode is increased at typical rates 2-5 mV/s and the current is recorded as a function of applied potential to give a polarogram. Prior applying potential to the working electrode it is necessary to purge the solution with some inert gas, such as nitrogen or argon, in order to remove dissolved oxygen which interferes with the normal cathodic potential range for DME by undergoing a two-step reduction process. A small current always flows as the potential is increased cathodically, this current is called the residual or background current (BC). This BC arises from the charging of the double layer at each drop and is non-faradaic. When reduction potential of the reducible species in solution is reached, the ions, designated $M^{n+}$, begin to discharge as a result of their reduction by the following process:

$M^{n+} + ne^{-} = M(Hg)$

The product of the electrode process above is written as M(Hg) to account for the fact that when the metal ions are deposited on the mercury drop, they form an amalgam denoted M(Hg) [8-11].

Polarography is advantageous in that it can operate at total metal ion concentration of as low as $10^{-6}$ M and is useful when dealing with situations of low complex stability and easily hydrolysable ions to form hydroxide precipitates**.** Other advantages include the fact that mercury drops are reproducible so that the currents recorded are also reproducible, fresh electrode surface is continuously presented to the electrolyte and is independent on the preceding electrochemical process. The mercury has high $H_2$ over-voltage and as a result it is rare for hydrogen evolution to interfere with deposition of metal ion on the mercury surface. Mercury electrode has small surface area enabling electrolysis of solutions without decrease in the total concentration of ions concerned [12].

Like any other technique, polarography has some disadvantages, which include the reduction of $O_2$ by two-stage process on the entire mercury cathodic potential working range. Therefore the oxygen must be flush out of the solution by purging with an inert gas such $N_2$. When studying metal-ligand equilibria by polarography it is important to accurately and precisely record the free metal ion potential, *E*(M) which serves as the reference in calculating the shift in the potential when complexes are formed. This is a

disadvantage because sometimes the $E$(M) is not available, for example $Bi^{3+}$. Mercury is toxic; its vapour causes cancer [8].

### 2.3.1 Direct Current Polarography (DCP)

DCP involves the measurement of current-potential curves as recorded on the dropping mercury electrode resulting in a DC polarogram. In the presence of substances which undergo reduction or oxidation at the DME, an increase or decrease in current is observed, respectively, over a particular potential range of the current-potential plot. A potential will be reached by which the current will be constant when the applied potential is varied. This current is called limiting current and is diffusion-controlled, hence it is called limiting diffusion current, $I_d$ as shown in Figure 2.1. The limiting diffusion current is directly proportional to the concentration of electroactive species in solution [13].

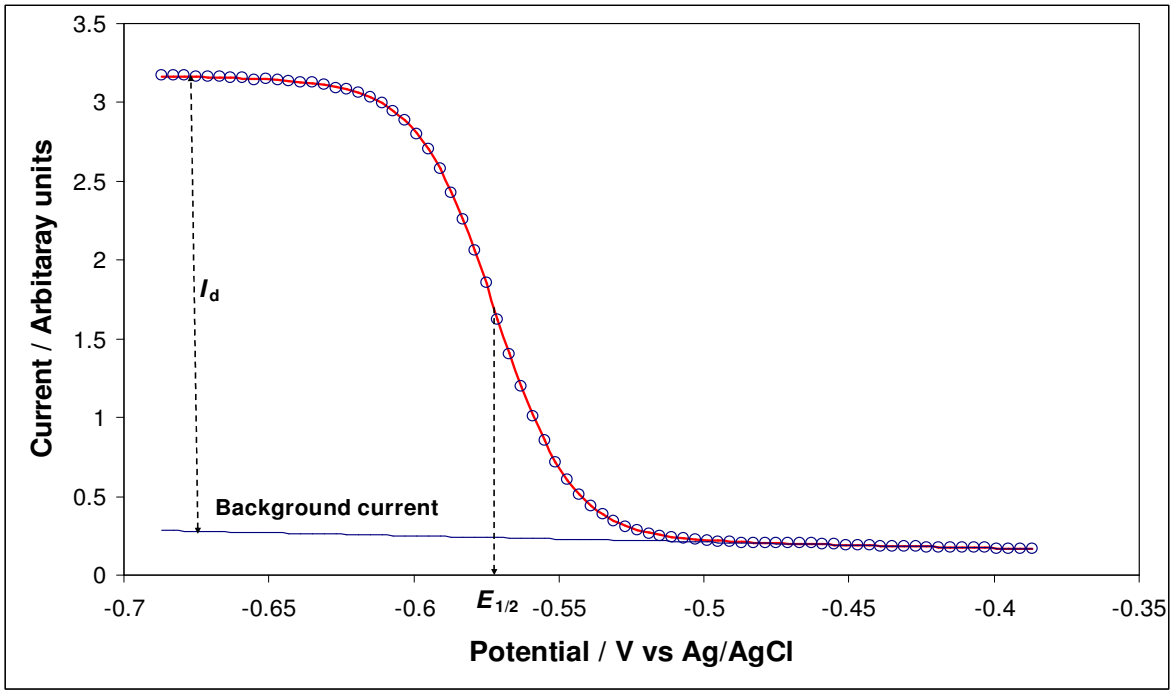


**Figure 2.1**: An example of DC–wave recorded at pH 1.96 for $Cd^{II}$–APD system. $L_T$:$M_T$ ratio 40, initial $[M_T] = 1.14 \times 10^{-4}$ M, experiment performed at ionic strength $\mu$ = 0.15 M (NaCl) and 25.0 °C. The circles represent experimental points and the red line represents the fitted curve.

If an electroactive substance is capable of undergoing a redox process at the DME, an S-shaped or sigmoidal current-potential curve is observed as shown in figure 2.1. This curve is called a polarographic wave. The limiting diffusion current, $I_d$ is proportional to the

concentration of the electroactive species in solution and is essential in analytical measurements. The $I_d$ is related to the concentration of the electroactive species in solution by the Ilkovič equation [14]:

$$I_d = 706nD^{1/2}m^{2/3}t^{1/6}{}_dC \tag{29}$$

where $n$ is the number of electrons, $D$ is the diffusion coefficient, $m$ is the mass flow rate of mercury, $t_d$ is the drop time and $C$ is the concentration of electroactive species in the bulk solution. Another important parameter on the DC polarographic wave is the half-wave potential, $E_{1/2}$ which is the potential at which the limiting diffusion current reaches half its limiting value. The $E_{1/2}$ value is independent of the concentration of electroactive species in solution but dependent on the composition of the solution and therefore is characteristic of species. The shape of the DC polarogram is important for the overall characterisation of an electrode process. If the reduction electrochemical process is reversible and diffusion controlled, the potential $E$ is related to the concentrations by the Nernst equation:

$$E = E^{\circ} + \left(\frac{RT}{nF}\right) ln\left(\frac{C_O(0)}{C_R(0)}\right) \tag{30}$$

where $E^{\circ}$ is the standard redox potential, R is the gas constant, T is the absolute temperature, $C_O(0)$ and $C_R(0)$ are the surface concentrations of species Ox and Red, respectively. The shape of the DC polarographic wave can be characterised by combining the Nernst and Ilkovič equations:

$$E = E_{1/2} + \left(\frac{RT}{nF} ln\left(\frac{(Id - I)}{I}\right)\right) \tag{31}$$

or

$$I = I_d / \left[1 + exp\left(\left(\frac{nF}{RT}\right)(E - E_{1/2})\right)\right] \tag{32}$$

where $E_{1/2} = E^{\circ} + \left(\frac{RT}{nF}\right) ln\left(\frac{D_R}{D_O}\right)$ (33)

Since the diffusion coefficients of oxidised and reduced forms, $D_O$ and $D_R$ are very often nearly equal, then $E_{1/2} \approx E^\circ$.

When the potential of the DME is at the limiting current value, all electroactive species will be reduced immediately when they reach the electrode surface and the magnitude of the limiting current will be diffusion controlled. As a result, the concentration gradient will be created at the electrode-solution interface which will cause the ions to diffuse to the electrode surface. The limiting diffusion current is proportional to the rate at which the ions diffuse to the electrode surface [15].

### 2.3.2 Differential Pulse Polarography (DPP)

This technique is convenient for studying speciation and for determination of stability constants when the electrochemical process is reversible. DPP was introduced in the late 1940's due to slow speed of DCP. The potential wave-form of DPP experiment consists of small pulses with constant amplitude superimposed on the staircase wave-form. The current is sampled before and after the pulse and the difference between these currents is plotted vs. applied potential step. For a reversible electrochemical process, the peak potential recorded from the DPP experiment is close to the $E_{1/2}$ obtained from DCP for the same process. DPP overcame difficulties encountered by Dropping Mercury Electrode by:

1) Recording data at the end of drop life
2) Using a potential pulse to maximise flux
3) Using timed sampling of current to discriminate against charging current, and
4) Subtracting background current

The problem with this technique is that it struggles when the electrochemical process under study is irreversible meaning the electron-transfer kinetics is slow. It this case, the peak width increases causing a difficulty for resolution purposes [17] and also decreases the detection limit slightly.

### 2.3.3 Use of Polarography in Metal-Ligand Equilibrium study

*Polarographic study of metal complexes at fixed pH*

About 65 years ago, Lingane [18] reported an equation that can be used in polarograhic study of metal-ligand system in which a single complex is formed at fixed pH. This equation is based on a shift in half-wave potential to more negative value when complexes are formed and the equation can be written at 25 °C as follows:

$$\Delta E_{1/2} = E_{1/2}(\mathbf{M}) - E_{1/2}(\mathbf{C}) = \frac{0.05916}{n} log\, \beta_{\mathbf{ML_j}} + \frac{0.05916}{n} log[\mathbf{L}]^{\mathbf{j}} \qquad (34)$$

where $E_{1/2}$(M) is the half-wave potential of the free metal ion (i.e. $E_p$(M) in case of DPP), $E_{1/2}$(C) is the half-wave potential of the complexed metal ion. (i.e. $E_p$(C) in case of DPP), [L] is the free ligand concentration and j is the number of ligands in complex $ML_j$.

Ten years later DeFord and Hume [19] reported a mathematical equation for polarographic analysis of shift in half-wave potential of a metal ion, $\Delta E_{1/2}$(M) with the change in concentration of ligand:

$$anti\, log\left(\frac{\mathbf{0.4343 \times nF}}{\mathbf{RT}} \Delta E_{1/2} + log \frac{I_d(\mathbf{M})}{I_d(\mathbf{C})}\right) = \sum_0^n \beta_{\mathbf{ML_j}} [\mathbf{L}_{\mathbf{excess}}]^{\mathbf{j}} \qquad (35)$$

where $\Delta E_{1/2}$ is the difference in half-wave potential of the free metal ion and the half-wave potential of the complexed metal ion, $I_d$(M) and $I_d$(C) are the limiting diffusion currents of the free metal ion and complexed metal ion, respectively. This equation was derived on the similar conditions and assumptions as those used in derivation by Lingane. DeFord and Hume method is advantageous over Lingane in that it allows calculation of stability constants of the metal-ligand system when complexes are formed in consecutive manner:

$$F_0[\mathbf{L}] = \beta_0 + \beta_1[\mathbf{L}] + \beta_2[\mathbf{L}]^2 + \ldots + \beta_n[\mathbf{L}]^n \qquad (36)$$

where $\beta_0$ is the stability constant of the zero complex and by definition has value 1.

$$\mathbf{F_1[L]=\left[\frac{F_0[L]-1}{[L]}\right]=\beta_1+\beta_2[L]+...+\beta_n[L]^{n-1}} \quad (37)$$

$$\mathbf{F_2[L]=\left[\frac{F_1[L]-\beta_1}{[L]}\right]=\beta_2+\beta_3[L]+...+\beta_n[L]^{n-2}} \quad (38)$$

The procedure is continued until all the N complexes are accounted for:

$$\mathbf{F_N[L]=\left[\frac{F_{N-1}[L]-\beta_{N-1}}{[L]}\right]=\beta_n} \quad (39)$$

Schapp and McMasters [20] described a polarographic method of studying mixed complexes and its application in the determination of stability constants at fixed pH. In this case they used metal ions $Cu^{2+}$ and $Cd^{2+}$ with the ethylenediammine-oxalate systems. This method is the extension of DeFord and Hume method applied to metal-ligand systems were two ligands compete for one metal ion in solution. However the weakness of this method is that when several complexes are formed simultaneously at particular fixed pH, the observed shift in $E_{1/2}$ cannot be accounted for all complexes in solution.

*Polarographic study of metal complexes at fixed $L_T$:$M_T$ ratio and varied pH*

All the polarographic methods described above were based on experiments performed at fixed pH. The new approach of polarographic study of metal ions with protic ligands has been recently described by Cukrowski [21–26], in which the Lingane equation is expanded and the effect of pH is taken into account. The expanded Lingane equation is written as follows:

$$\mathbf{\Delta E_{1/2}-\frac{RT}{nF}ln\left(\frac{I(C)}{I(M)}\right)=\frac{RT}{nF}ln\,\beta_{ML_j(OH)_b}+j\frac{RT}{nF}[L]+b\frac{RT}{nF}ln[OH^-]} \quad (40)$$

where $I(\mathrm{C})$ and $I(\mathrm{M})$ are the currents for the complexed and uncomplexed metal ion, respectively, $[\mathrm{L}]$ and $[\mathrm{M}]$ represent the free ligand and metal ion concentrations, respectively. The above equation is applicable to the following overall reaction:

$M + jL + bOH \rightarrow ML_j(OH)_b$ or $M + jL + bH \rightarrow ML_jH_b$

The free ligand concentration $[L]$ is calculated from the known pH value, total ligand concentration $[L_T]$ and the stepwise protonation constants ($Ka_1$, $Ka_2$, $Ka_3$,…) of the ligand under study as follows:

$$[L] = \frac{[L_T]}{(1 + Ka_1[H] + Ka_1Ka_2[H]^2 + ...)} \quad (41)$$

$\Delta E_{1/2}$ in Equation (40) is related to a single β value and if a number of complexes are formed simultaneously in solution, this equation assumes that one complex makes the contribution to the shift, $\Delta E_{1/2}$. This is a huge limitation when simultaneous and consecutive complexes are formed and results in larger stability constant values.

Recently, Cukrowski developed an approach to treat polarographic data. This approach involves the use of an equation based on mass balance equation for labile, non-labile and mixed complexes formed at fixed $L_T$:$M_T$ ratio and varied pH [21-28]. The equation is based on the shift in DPP peak potential and variation in the peak height of the labile metal species due to the changes in the solution composition as follows:

$$\Delta E_p(i) - \frac{RT}{nF} ln \frac{I_p(M_{comp})(i)}{I_p(M_{Free})(i)} = \frac{RT}{nF} ln \frac{[M_T](i)}{[M_{Free}](i)} \quad (42)$$

where $\Delta E_p(i) = E_p(M_{Free}) - E_p(M_{Comp})(i)$ (43)

$\Delta E_p(i)$ in Equation (42) represents the shift in DPP peak potential at each pH(i) value to which the metal-ligand system was adjusted to in the polarographic cell, $[M_T](i)$ and $[L_T](i)$ represent the total metal ion and total ligand concentrations respectively, at each pH(i) value, $I_p(M_{comp})(i)$ is the DPP peak height recorded at an *i*th pH(i) value and represents all labile species in solution, $I_p(M_{Free})(i)$ is the calculated DPP peak height of the free metal ion assuming that no complexes are formed. This approach is applicable to any voltammetric technique.

When the left hand side of Equation (42) is plotted against pH it gives the Experimental Complex Formation Curve (ECFC) which contains parameters obtainable from the experiment and is given by:

$$\Delta E_p(\mathbf{i}) - \frac{\mathbf{RT}}{\mathbf{nF}} ln \frac{I_p(\mathbf{M_{comp}})(\mathbf{i})}{I_p(\mathbf{M_{Free}})(\mathbf{i})} = f(pH) \tag{44}$$

and when the right hand side of Equation (42) is plotted against pH it gives Calculated Complex Formation Curve (CCFC) which contains pH-dependent free metal ion concentration, $[\mathrm{M_{Free}}](\mathrm{i})$:

$$\frac{\mathbf{RT}}{\mathbf{nF}} ln \frac{[\mathbf{M_T}](\mathbf{i})}{[\mathbf{M_{Free}}](\mathbf{i})} = f(pH) \tag{45}$$

The free metal ion concentration $[\mathrm{M_{Free}}](\mathrm{i})$ is calculated from the following mass-balance equations:

$$[\mathbf{M_T}](\mathbf{i}) = [\mathbf{M_{Free}}](\mathbf{i}) + \Sigma\Sigma \mathbf{x}[\mathbf{M_x L_y H_z}](\mathbf{i}) \tag{46}$$

$$[\mathbf{L_T}](\mathbf{i}) = [\mathbf{L_{Free}}](\mathbf{i}) + \Sigma\Sigma \mathbf{y}[\mathbf{M_x L_y H_z}](\mathbf{i}) \tag{47}$$

The $[\mathrm{M_T}](\mathrm{i})$ and $[\mathrm{L_T}](\mathrm{i})$ are known at each pH(i) value. During the simultaneous solution of mass balance Equations (46) and (47) the known hydrolysis constants for the metal ion, $M_x(OH)_y$ and the protonation constants of the ligand studied are fixed. The metal-ligand model is varied and the stability constants are optimized such that the CCFC fits best the ECFC.

## 2.4 Theory of Virtual Potentiometry

Polarography is a dynamic electrochemical technique which involves many processes occurring at the electrode-solution interface and any attempt to rigorously describe these processes must involve many complex processes, among them thermodynamics, kinetics (homogeneous and heterogeneous), transport, etc. It is impossible to get to a point that will

allow theoretical reproduction of observed polarograms. It is for this reason that the polarographic change in signal position, $\Delta E_{1/2}$ or $\Delta E_p$ is used for studying of metal complexes rather the theoretically observed position. The weakness of this approach is evident from different polarographic methodologies (i.e. Lingane, DeFord and Hume, Cukrowski, etc) where all the recorded curves $E_p(M_{Comp})$ or $E_{1/2}(M_{Comp})$ are compared with the single value $E_p(M_{Free})$ or $E_{1/2}(M_{Free})$. It is well known that non-linear curve fitting operations will result in more reliable fitted parameters with an increase in the number of experimental points recorded. The problem of refinement of polarographic data is that the points collected on the solution adjusted to many pH(i) values are compared with a single experimental point, e.g. the shift in the peak or half-wave potential is used and not the observed values ($E_p$ or $E_{1/2}$) at each pH(i). As a result, the calculated optimised stability constants must change with value of $E(M_{Free})$ even though the metal-ligand model, the overall fit of CCFC into ECFC and standard deviations in stability constants will virtually remain the same. This implies that the value of $E(M_{Free})$ must be determined with very high accuracy. However, it is not always possible to obtain the accurate $E(M_{Free})$ value. The study of acidic metal ions such as Bi(III) which undergoes hydrolysis at pH 0 is a perfect example where the $E(M_{Free})$ cannot be determined accurately, and it is not directly available from an experiment. For this metal ion, the recorded polarographic curve represents two Bismuth species, Bi(aq) and Bi(OH) which means that the $E(M_{Free})$ cannot be determined accurately and is not available directly from the experiment [29]. The added advantage of polarography is that one can study metal complexes with very large excess of the ligand. However, this might introduce significant uncertainty in the $E(M_{Free})$ value that might be different in the presence and absence of the ligand.

The term $\frac{I_p(M_{comp})(i)}{I_p(M_{Free})(i)}$ seen in Equation (42) represents the normalized change in the intensity of the polarographic signal. This change in the intensity of the signal $I_p$ or $I_d$ is attributable to the change in the diffusion coefficients of different labile and non-labile metal complexes. According to Cukrowski et al, the theoretically and thermodynamically expected position of the polarographic signal along the potential scale can be written as [29-31]:

$$\left( E_{1/2}(\mathbf{comp}) + \frac{\mathbf{RT}}{\mathbf{nF}} ln\left( \frac{I(\mathbf{comp})}{I(M)} \right) \right)_{\mathbf{x(i)}} = E_{1/2}(\mathbf{virt})_{\mathbf{x(i)}} \quad (48)$$

and can be calculated at any pH(i) from the experimental data. The proposed virtual half-wave potential, $E_{1/2}$(virt) can be interpreted as a thermodynamic potential of a virtual sensor or probe obtained from dynamic, non-equilibrium polarographic data. This virtual sensor must be sensitive to free metal ion concentration when metal complexes are formed. This virtual potentiometric sensor is metal ion non-specific and is applicable to any metal ion which is reversibly reduced. Therefore the virtual potential should have a linear response with Nernstian slope. The $E_{1/2}$(virt) must also result in a linear response shifted in $E°$ by a fixed number of mV in comparison to the linear response of a virtual probe from $E_{1/2}$(virt) values. This proposal of virtual potentiometric probe implies that potentiometric software ESTA can be employed for the refinement stability constants, using data from dynamic electrochemical technique. This concept of virtual potential can also be used in the prediction of slopes for the validation of a proposed model, rather than the observed potentials. This concept will be used in the discussion of results obtained in this work in the following chapters, i.e. plots of $E_{1/2}$(virt) vs. pH, vs. log [L] and vs. log [M] when compared with plots of $E_{1/2}$(observed) vs. pH, vs. log [L].

## References


1. F. R. Hartley, C. Burgess and R. Alcock, "Solution Equilibria", John Wiley and Sons, 1980.
2. F. J. C. Rossotti and H. Rossotti, "The determination of stability constants", McGrow-Hill Book Company, Inc., 1961, pp. 127–170.
3. P. M. May and K. Murray., "Equilibrium Simulation and Titration Analysis", Version 1.0, 1984.
4. B. P. Hay, J. R. Rustad and C. Hostetler, *J. Am. Chem. Soc.*, **1993**, *115*, 158.
5. G. E. Jackson and J. du Toit, *J. Chem. Soc. Dalton. Trans*., **1991**, 1463.
6. P. M. May, K. Murray and D. R. Williams, *Talanta*, **1998**, *35*, No. 11, 825.
7. P. M. May, K. Murray and D. R. Williams, *Talanta*, **1998**, *35*, No. 12, 927.
8. D. R. Crow, Principles and Applications of electrochemistry, pp. 200–208.
9. A. J. Bard and L. J. Faulkner, Electrochemical methods, John Wiley & Sons, New York, 2001, pp. 261–301.
10. D. R. Crow, Polarography of metal complexes, Academic Press, London and New York, 1969, pp. 22–25, 66–73.
11. C. H. Hamman, A. Hamnett and W. Vielstich, Electrochemistry, John Wiley & Sons, New York, 2001, pp. 391–396.
12. A. E. Martell and R. D. Hancock, Metal complexes in aqueous solutions, Plenum Press, New York and London, pp. 40–55, 63, 74, 217, 231–235.
13. A. M. Bond, Modern Polarographic Methods in Analytical Chemistry, New York: M. Dekker, 1980, pp. 9–26.
14. I. S. Longmuir, Advances in polarography, Volume 1, 1960.
15. J. Heyrosky, J. Kuta, Principles of Polarograohy, 1996, pp. 17–46.
16. C. H. Hamman, A. Hamnett and W. Vielstich, Electrochemistry, Wiley-VCH Verlag GmbH, Germany, 1998, pp. 391–396.
17. P. T. Kissinger and W. R. Heineman, Laboratory Techniques in Electroanalytical Chemistry, Marcel Dekker, 1984.
18. J. J. Lingane, *Chem. Rev.*, **1941**, *29*, No. 1, 1.
19. D. D. DeFord and D. N. Hume, *J. Am. Chem. Soc.*, **1951**, *73*, 5321.
20. W. B. Schaap and D. L. McMasters, *J. Am. Chem. Soc.*, **1961**, *83*, 4699.
21. I. Cukrowski, *Anal. Chim. Acta.*, **1996**, *336*, 23.
22. I. Cukrowski, Analyst, **1997**, *122*, 827.

23. I. Cukrowski and M. Adsetts, *J. Electroanal. Chem.,* **1997**, *429*, 129.
24. I. Cukrowski, *Electroanalysis*, **1997**, *9***,** No. 9, 699.
25. I. Cukrowski, *Electroanalysis*, **1997**, *11***,** No. 9, 606.
26. I. Cukrowski and Sharon A. Loader, *Electroanalysis*, **1998**, *10***,** No. 13, 877.
27. I. Cukrowski, *J. Electroanal. Chem.*, **1999**, *460*, 197.
28. I. Cukrowski, E. Cukrowska, R. D. Hancock and G. Anderegg, *Anal. Chim. Acta.*, **1995**, *312*, 307.
29. I. Cukrowski, J. M. Zhang and A. V. Aswegen, *Helv. Chim. Acta.*, **2004**, *87*, 2135.
30. I. Cukrowski and J. M. Zhang, *Electroanalysis*, **2004**, *16*, No. 8, 612.
31. I. Cukrowski and J. M. Zhang, *Chem. Anal.(Warsaw)*, **2005**, *50*, 3.

# CHAPTER 3

# EXPERIMENTAL

# 3. Experimental

## 3.1 Reagents

The ligand 1-hydroxyl-3-aminopropilydene diphosphonic acid, APD was synthesized by Zeevaart [1] using method reported in literature [2] and was used as received. The other reagents were of analytical grade: cadmium nitrate tetrahydrate ($Cd(NO_3)_2.4H_2O$, F.W. 308.47 $g.mol^{-1}$, 98 %), lead nitrate ($Pb(NO_3)_2$, F.W. 331.20 $g.mol^{-1}$, 99 + %), zinc nitrate hexahydrate ($Zn(NO_3)_2.6H_2O$, F.W. 297.48 $g.mol^{-1}$, 98 %) were obtained from SIGMA-ALDRICH. Sodium chloride (NaCl, F.W. 54.44 $g.mol^{-1}$, 99.5 %), sodium hydroxide (NaOH, F.W. 40.00 $g.mol^{-1}$, 98 %), hydrochloric acid (HCl, F.W. 36.46 $g.mol^{-1}$, 32 % pure and density = 1.16 kg/l), nitric acid ($HNO_3$, F.W. 63.01 $g.mol^{-1}$, 55 % pure and density = 1.34 kg/l) were obtained from SAARCHEM. Magnesium chloride hexahydrate ($MgCl_2.6H_2O$, F.W. 203.31 $g.mol^{-1}$, 99 %) was obtained from MERCK. Deionised water used in the preparation of solutions was prepared by passing distilled water through a milli-Q-water purification system (Millipore, Bedford, MA, USA).

## 3.2. Preparation of solutions

The solution of 0.15 M NaCl background electrolyte was prepared by weighing out the appropriate amount of salt and dissolving it in de-ionised water. The titrant solution of NaOH was prepared by weighing out the required amount of NaOH and dissolving with de-ionised water. Two solutions of NaOH were prepared, i.e. 0.15 M solution for calibration of glass electrode and 0.05 M (adjusted to 0.15 M ionic strength by dissolving into 0.10 M NaCl) was used for metal-ligand titrations. The 0.15 M HCl solution was also prepared by diluting the stock solution of the acid with the required amount of de-ionised water. The acid and base solutions were standardised before they were used. The stock solutions of metal ions $Cd^{II}$, $Pb^{II}$, $Zn^{II}$ and $Mg^{II}$ were prepared by weighing out the required mass of appropriate metal salt.

In all the titrations for metal-APD systems, i.e. potentiometric and polarographic, the concentration of the stock metal ions used was about $1 \times 10^{-2}$ M. These solutions were prepared by dissolving the appropriate amount of metal salt in 0.12 M NaCl to adjust the

ionic strength to 0.15 M. The stock solution of the ligand (i.e. $1 \times 10^{-2}$ M) was prepared by weighing out the required amount of the ligand and dissolving it in 0.15 M NaCl.
All the experiments were performed at ionic strength 0.15 M and temperature 25.0±0.1 °C using NaCl as background electrolyte.

## 3.3 Polarography

### 3.3.1 Experimental set-up

All the polarographic experiments were performed in a Metrohm model 6.1418.150 jacketed glass vessel, equipped with a magnetic stirrer and thermostated at 25.0 ± 0.1 °C by water circulating from a temperature bath. The potential of a combination glass electrode and pH = $-\log_{10}$ [H] of solutions were measured to within ± 0.1 mV (± 0.001 pH) with a 713 pH meter (Metrohm). A model 6.0234.100 combination glass electrode (Metrohm) was used. Sampled direct current polarograms were collected with the use of computer-controlled instrumental setup (built in-house and controlled by LabView programs) comprising a CV-27 potentiostat, 713 pH meter (Metrohm), 765 digital burette (Metrohm) and a model 6.1110.100 temperature probe (Metrohm). A multimode electrode (Metrohm model 6.1246.020) was employed as the working electrode and used in the dropping mercury electrode mode with a drop time of 2 s. A model 6.0728.00 silver/silver chloride electrode (3 M KCl, from Metrohm) and a model 6.0343.000 platinum electrode (from Metrohm) were used as the reference and counter electrodes, respectively. A potential step of 4 mV was used and the integration time of 80 ms was used in all the polarographic experiments. High purity nitrogen was used for deaeration of the sample solutions.

### 3.3.2 Experimental procedure

The polarographic cell was cleaned using 0.05 M $HNO_3$ and then rinsed thoroughly with de-ionised water. The combination glass electrode was calibrated prior and after the polarographic experiment using the standardised NaOH and HCl. After cleaning the cell, the required volume of the background electrolyte solution (NaCl) was added to the polarographic cell and the solution was purged with nitrogen to deaerate the solution. The

polarogram for background electrolyte solution was recorded to check the purity of the solution. The required volume of metal ion stock solution was then added to give the total metal ion concentration of interest and the solution was deaerated for 30 minutes. The polarogram was recorded in the presence of the metal ion solution only to determine the $E_{1/2}(M_{Free})$ and this was repeated twice. The required mass of solid ligand or volume of the ligand stock solution was then added to obtain the $L_T$:$M_T$ ratio of interest. The solution was then deaerated after addition of the ligand solution and then the polarogram was recorded in the presence of the ligand. The polarograms were then recorded at pH steps of 0.05 by addition of standardised 0.05 M NaOH solution adjusted to ionic strength of the background electrolyte solution. The solution composition for metal-APD systems studied by polarography in this work is shown in Table 3.1. Experimental data were collected between pH 2.0 to 7.5 depending on the metal-APD system, and a set of 40 to 60 polarograms was obtained for each $L_T$:$M_T$ ratio.

**Table 3.1**: The solution composition for metal-APD systems studied by DC polarography. The stock solution concentrations for the metal ions were 0.0100, 0.0099, and 0.0099 M for $Cd^{II}$, $Pb^{II}$, and $Zn^{II}$, respectively. The concentration of APD stock solution was 0.0100 M.

| **Cation** | **0.15 M NaCl (ml)** | **$V_M$ (ml)** | **$V_L$ (ml)** | **$V_A$/ HCL (ml)** | **$[L_T]$/ (mol.L$^{-1}$)** | **$[M_T]$/ (mol.L$^{-1}$)** | **$[L_T]$:$[M_T]$ ratio** |
|---|---|---|---|---|---|---|---|
| $Cd^{II}$ | 14.500 | 0.500 | 20.000 | 5.000 | $5.00\times10^{-3}$ | $1.25\times10^{-4}$ | 40 |
| $Pb^{II}$ | 9.800 | 0.200 | 10.000 | 0.000 | $5.00\times10^{-3}$ | $9.90\times10^{-5}$ | 50 |
| $Zn^{II}$ | 14.750 | 0.180 | 5.070 | 0.000 | $2.54\times10^{-3}$ | $8.91\times10^{-5}$ | 28 |

The concentration of the HCl solution used was 0.1190 mol.L$^{-1}$

## 3.4 Glass Electrode Potentiometry

### 3.4.1 Experimental set-up

All the potentiometric experiments were performed in a Metrohm model 6.1418.150 jacketed glass vessel, equipped with a magnetic stirrer, thermostated at 25.0 ± 0.1 °C by water circulating from a temperature bath. The potential of a combination glass electrode and pH = $-\log_{10}$ [H] of solutions were measured to within ± 0.1 mV (± 0.001 pH) with a 713 pH meter (Metrohm). A model 6.0234.100 combination glass electrode (Metrohm) was used. A model 6.111.100 temperature probe (Metrohm) was used to monitor the temperature of the solutions.

### 3.4.2 Experimental procedure

A stock solution of NaOH was standardised once a week using potassium hydrogen phthalate KHP. A stock acid solution (HCl) was standardised once a month using standardised NaOH solution. These standardised solutions were used to calibrate the combination glass electrode before and after the experiments were run.

*Standardisation of NaOH with KHP*

A small amount of KHP (about 0.2 g) was weighted out and placed in a cell containing known volume of de-ionised water and dissolved. The KHP solution was then titrated with the NaOH of unknown concentration until the end point was established. The end point of the titration was detected using phenolphthalein indicator which turns from colourless to light pink at the end point. The end point volume of the NaOH was used to calculate the actual NaOH concentration using the Equation 49:

$$[NaOH] = m_{KHP}.1000 / M_{KHP}.V_{NaOH} \quad (49)$$

where $m_{KHP}$ is the mass of KHP dissolved, $M_{KHP}$ is the molecular mass of KHP and $V_{NaOH}$ is the volume of NaOH required to reach endpoint.
This procedure was repeated three times and the average concentration of NaOH was taken as the concentration of the standard base solution.

*Standardisation of HCl with standardised NaOH*

About 10 ml of 0.15 M HCl solution was placed in titration cell. This solution was titrated with standardised solution of 0.15 M NaOH. The volume of NaOH at the end point was used to calculate the concentration of the acid solution as follows:

$$[Acid] = V_{NaOH}.C_{NaOH} / V_{acid} \quad (50)$$

where $V_{NaOH}$ is the volume of NaOH required to reach the end point, $C_{NaOH}$ is the concentration of the standardised NaOH solution and $V_{acid}$ is the volume of the acid solution placed in the cell.

The procedure was repeated three times and the average acid concentration was considered to be the standardised acid concentration.

*Calibration of combination glass electrode*

The glass electrode was calibrated before and after each experiment was run using the standardised acid and base solutions. The glass electrode was calibrated using strong acid-base titration data involving about 10 ml of standardised 0.15 M HCl with standardised 0.15 M NaOH solution in 20 ml of 0.15 M NaCl (as background electrolyte) in a polarographic cell. Data points were collected before and after the end point was reached; these points were then used in fitting a straight line into the titration data to obtain the response slope as well as the $E°$ for the glass electrode.

*Determination of protonation constants for ligand, APD*

For one to study metal complexes of a specific ligand, it is essential to know the form of the ligand throughout the entire pH range of interest. To do this, the protonation constants of the ligand must be determined. The protonation constants of the ligand APD were determined from the following titrations:

**Table 3.2**: Solution composition for determination of protonation constants for the ligand APD by glass electrode potentiometry (GEP).

| **Titration** | **Mass of APD** | **$V_{BG}$ (0.15 M NaCl)** | **Volume 0.1484 M NaOH added** | **$V_T$** | **$L_T$** |
|---|---|---|---|---|---|
| | **(g)** | **(ml)** | **(ml)** | **(ml)** | **(mol.L$^{-1}$)** |
| 1 | 0.0481 | 20.000 | 0.000 | 20.000 | $1.0181\times10^{-2}$ |
| 2* | 0.0472 | 10.000 | 5.455 | 15.455 | $1.2937\times10^{-2}$ |

*0.1382 M HCl used to titrate the ligand solution from pH 11 to pH 2.5. 0.0500 M NaOH was used as titrant in titration 1.

## References

1. J. R. Zeevaart, N. V. Jarvis, W. K. A. Louw, G. E. Jackson, I. Cukrowski and C. J. Mouton, *J. Inorg. Biochem.*, **1999**, *73*, 265.
2. Von. K. H. Worms, H. Blum and H. U. Hempel, *Z. Anorg. Allg. Chem.*, **1979**, *457*, 214.

# CHAPTER 4

# RESULTS AND DISCUSSION

# 4. Results and Discussion

## 4.1 Determination of protonation constants for ligand APD.

The study of metal-ligand equilibria of interest as a function of proton concentration or pH of a solution requires the knowledge of the form of the ligand in the solution as the pH is varied. The form of the ligand tells about the number of protons attached to the ligand at a particular pH and hence the extent to which the protons will compete with the metal ion under study to complex with the ligand in solution when the metal-ligand equilibria are studied. According to the structure of the ligand APD, five protonation constants are expected in accordance to the following reactions:

$$H + L = HL \qquad K_1^H = \frac{[HL]}{[H][L]} \tag{51}$$

$$H + HL = H_2L \qquad K_2^H = \frac{[H_2L]}{[H][HL]} \tag{52}$$

$$H + H_2L = H_3L \qquad K_3^H = \frac{[H_3L]}{[H][H_2L]} \tag{53}$$

$$H + H_3L = H_4L \qquad K_4^H = \frac{[H_4L]}{[H][H_3L]} \tag{54}$$

$$H + H_4L = H_5L \qquad K_5^H = \frac{[H_5L]}{[H][H_4L]} \tag{55}$$

Two titrations were performed and the protonation constants were obtained by fitting the computed curve into the experimental points. The final protonation values which resulted in (i) better fit between experimental and calculated protonation function as well as (ii) the smaller standard deviations for the protonation constants were taken as the final protonation constants. The protonation formation function $\bar{Z}_H$ indicates different forms of the ligand at different pH ranges. The protonation formation function for ligand APD attained in this work is shown in Figure 4.1. It is reasonable to say that the computed curve (with refined protonation constants) reproduced experimental points very well.

The predominant form of the ligand in the pH range between 2.5 and 5.8 is $H_3L$, $H_2L$ is the main form between pH 5.8 and 9.8, and above pH 9.8 the predominant form of the ligand

is HL. The protonation constants are the pH values at which the concentrations of two consecutive forms of the ligand are equal. It is clear that at physiological pH of about 7.4 one would be concerned with $H_2L$ form of the ligand. It means that from the point of view of needs related to bone cancer therapy, the most important protonation constants are $pKa_2$ and $pKa_3$ ($pKa_4$ and $pKa_5$ are of no importance to this study). A similar protonation formation function was obtained when the titration was done using an HCl solution as a titrant, see Figure 4.2.

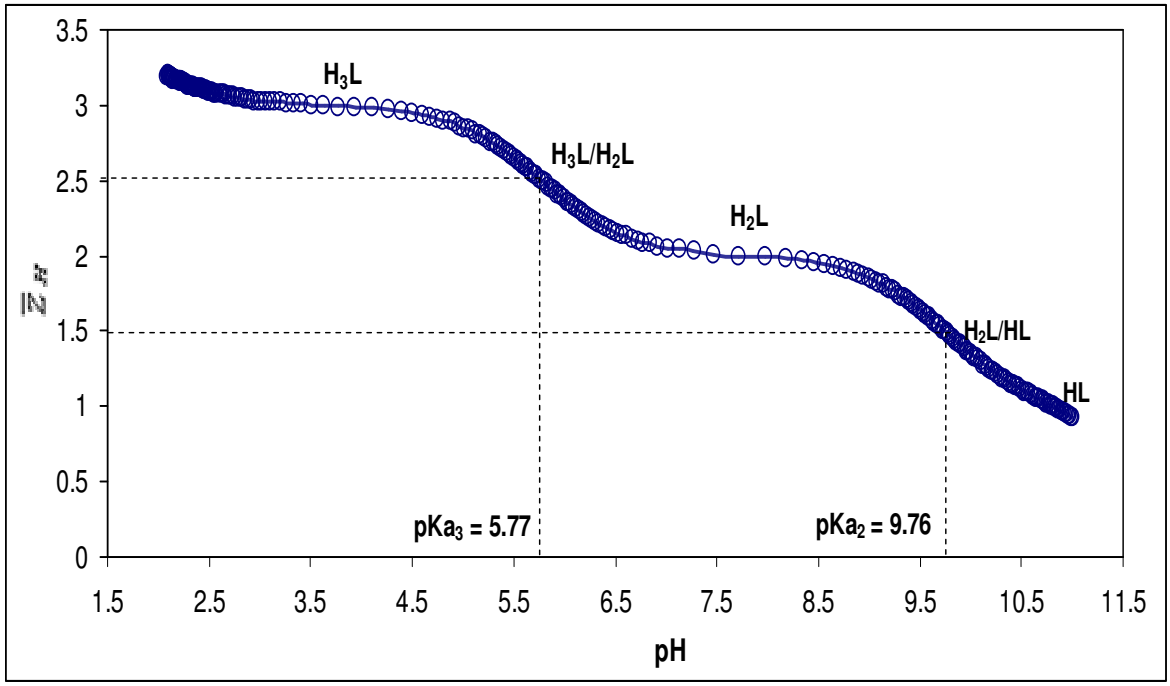


**Figure 4.1:** Experimental (circles) and fitted (solid line) protonation functions from the titration of the ligand APD titrated by 0.05 M NaOH at ionic strength $\mu$ = 0.15 M (NaCl) and 25 °C, $[L_T]$ = $1.0181 \times 10^{-2}$ M. (Computed $\bar{Z}_H$ was plotted using protonation constants shown in Table 4.1)

When looking at Table 4.1, in the first titration (base was used as titrant), the experimental data points up to pH 11 were used in the refinement operations that included all four determined protonation constants. The ESTA program showed correlation between parameters when either base, or acid, or ligand concentration was refined simultaneously with protonation constants. However, the $pKa_3$ gave approximately the same refined value of 5.774 when the above mentioned parameters were refined. In the following refinement operation the $pKa_3$ value was fixed at 5.774 and the base, acid or ligand concentration was refined together with other pKa values. However when the base concentration in the burette, $[OH]_b$, was refined simultaneously with the other pKa values, it gave low standard deviations for all the pKa values, small R-factor and the base concentration value

increased by 1.77 %. This is unexpected provided that the base was well standardised prior the experiment.

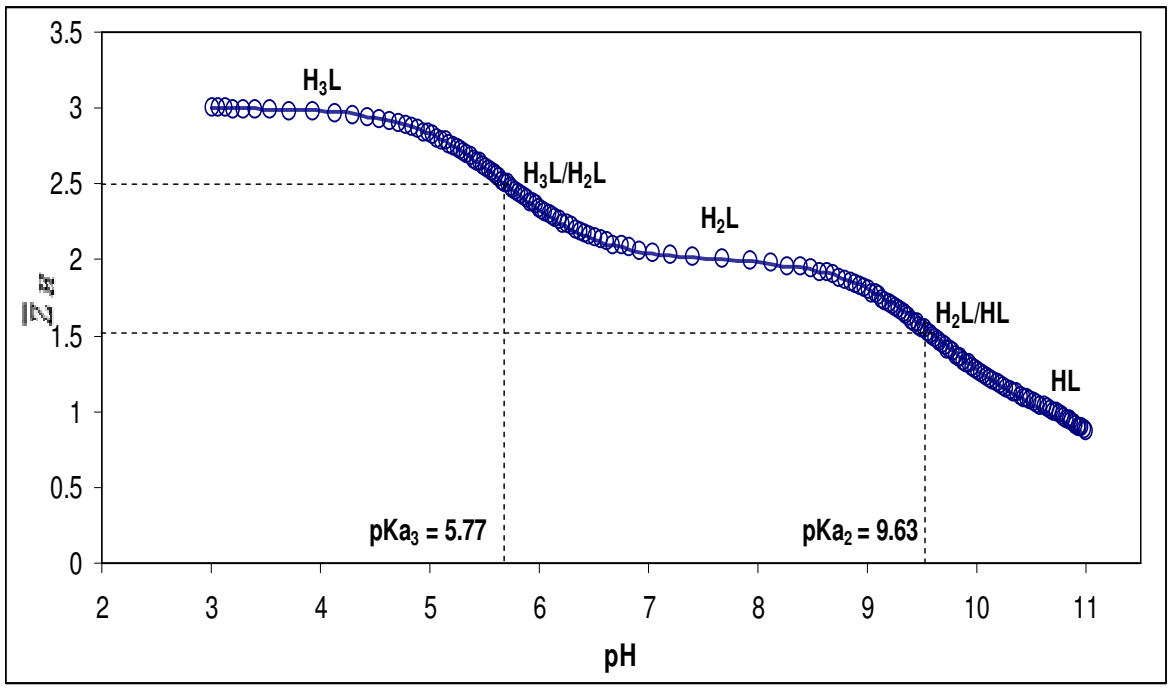


**Figure 4.2:** Experimental (circles) and fitted (solid line) protonation functions from the titration of the ligand APD titrated by 0.15 M HCl at ionic strength μ = 0.15 M (NaCl) and 25 °C, $[L_T] = 1.294 \times 10^{-2}$ M. (Computed $\overline{Z}_H$ was plotted using protonation constants shown in Table 4.1).

The computed protonation function (solid line) for this refinement operation is shown in Figure 4.1. However when the initial acid concentration in the cell $[H]_c$ was refined simultaneously with the pKa values, a slightly larger R-factor 0.0089 was obtained and the refined acid concentration in the cell was about $3\times10^{-4}$ M (note that initially no acid was added into the cell). When the initial ligand concentration in the cell $[L]_c$ was refined simultaneously with the pKa values, similar protonation constants were attained as in the case when the initial base concentration in the burette was refined, but the refined initial ligand concentration value decreased by 1.75 %. This could be attributed to the fact that the ligand was 98 % pure and could absorb some moisture (was not dried in oven) and this contributes to uncertainty in the ligand concentration. Since (i) refined value of $[OH]_b$ increased (this is rather unlikely), and (ii) $pKa_2$ as well as $pKa_3$ values were identical with refinement of $[L]_c$, as well as (iii) the concentration $[L]_c$ decreased slightly and this is expected, therefore we recommend protonation constants obtained with simultaneous refinement of $[L]_c$ as most reliable.

For the second titration (acid was used as titrant), the experimental data below pH 3 were not collected and as a result the protonation constant ($pKa_4$) could not be refined and was excluded in the data refinement. Here again, ESTA program showed correlation of parameters when either base, acid or ligand concentration was refined together with the pKa values.

When the $pKa_3$ was fixed at 5.774 (a value generated from titration 1), the concentration of base, acid, or ligand could be refined. When the acid concentration was refined simultaneously with pKa values (see Table 4.1) a slight decrease of 0.76 % in the acid concentration is seen and this is not expected. When the base or ligand initial concentration in the cell were refined simultaneously with the pKa values (with $pKa_3$ fixed at 5.774), these concentrations increased by 1.32 and 1.36 %, respectively. This might be unreliable considering the fact that the base concentration should rather decrease due to slight exposure to carbon dioxide to form carbonate, or due to exposure of the ligand to moisture. Also since the ligand was not 100 % pure, one expects the initial ligand concentration to decrease when refined. Thus the results from the acid titration are not that reliable when compared with the base titration.

The protonation constants recommended from this work together with the literature values are shown in Table 4.2. It is seen from Table 4.2 that the reported values in [3] are quite different when compared with those in [1] and [2], the latter ones can be seen as very much the same. The data in [1, 2] are from GEP, whereas the results in [3] are from NMR; five protonation constants are reported with additional one at lowest pH values. As it has been pointed out above, the most important pKa values are the 2$^{nd}$ and 3$^{rd}$ ones. When only these two are considered it follows that they are very much the same for all the data sets, including those reported in this work, even though the experimental conditions used in literature data and our work were somewhat different (i.e. temperature and ionic strength). These are the most crucial protonation constants in this study because the ligand exist in theses two forms at blood plasma pH range and therefore they need to be accurately determined. The discrepancy in $pKa_4$ and $pKa_1$ values, which are at very low and high pH values, respectively, can be easily understood when limitations typical to glass electrode potentiometry are accounted for (with the main problem coming from diffusion junction potential). The $pKa_4$ and $pKa_1$ values are not of strict vitality for this kind of studies.

**Table 4.1:** Protonation constants for the ligand APD determined at ionic strength μ = 0.15 M (NaCl) and 25 °C.

| Titration | $pKa_1$ | $pKa_2$ | $pKa_3$ | $pKa_4$ | R-factor | Parameter refined | % change | Comment |
|---|---|---|---|---|---|---|---|---|
| 1 (base) | 11.866 (0.002) | 9.756 (0.002) | 5.775 (0.002) | 1.500 (0.002) | 0.0010 | $[OH]_b$ | +1.76 | Correlation seen, points above pH 11 removed. |
| | 11.998 (0.020) | 9.791 (0.020) | 5.768 (0.020) | 1.356 (0.024) | 0.0083 | $[H]_c$ | $2.86\times10^{-4}$ M | |
| | 11.884 (0.002) | 9.755 (0.002) | 5.776 (0.002) | 1.466 (0.002) | 0.0010 | $[L]_c$ | –1.73 | |
| | 11.884 (0.002) | 9.755 (0.002) | 5.775 (0.002) | 1.466 (0.003) | 0.00104 | $[L]_r$ | – | |
| | | **Average value** | **5.774** | | | | | |
| | 11.614 (0.011) | 9.891 (0.007) | 5.774 (fixed) | 1.600 (0.026) | 0.0252 | _ | ----- | No correlation seen, points above pH 11 removed. |
| | 11.851 (0.001) | 9.755 (0.001) | 5.774 (fixed) | 1.500 (0.001) | 0.0011 | $[OH]_b$ | +1.77 | |
| | 11.826 (0.005) | 9.793 (0.003) | 5.774 (fixed) | 1.349 (0.014) | 0.0089 | $[H]_c$ | $2.95\times10^{-4}$ M | |
| | 11.852 (0.001) | 9.755 (0.001) | 5.774 (fixed) | 1.465 (0.002) | 0.0013 | $[L]_c$ | –1.75 | |
| | **11.852 (0.001)** | **9.755 (0.001)** | **5.774 (fixed)** | **1.465 (0.002)** | **0.0013** | **$[L]_r$** | **–** | |
| 2 (acid) | 11.754 (0.043) | 9.545 (0.041) | 5.583 (0.042) | Excl | 0.0431 | _ | | Correlation seen, points below pH 3 and above pH 11 removed |
| | 11.742 (0.014) | 9.615 (0.014) | 5.715 (0.014) | Excl | 0.0138 | $[OH]_b$ | +1.25 | |
| | 11.815 (0.026) | 9.637 (0.025) | 5.703 (0.027) | Excl | 0.0228 | $[H]_c$ | –0.71 | |
| | 11.868 (0.043) | 9.635 (0.043) | 5.658 (0.045) | Excl | 0.0342 | $[L]_c$ | +1.23 | |
| | 12.211 (0.015) | 9.535 (0.010) | 5.774 (fixed) | Excl | 0.0477 | _ | ----- | No correlation seen, pts below pH 3 and above pH 11 removed |
| | 11.998 (0.007) | 9.612 (0.005) | 5.774 (fixed) | Excl | 0.0187 | $[OH]_c$ | +1.32 | |
| | 11.985 (0.010) | 9.638 (0.006) | 5.774 (fixed) | Excl | 0.0241 | $[H]_b$ | –0.76 | |
| | 12.029 (0.015) | 9.640 (0.009) | 5.774 (fixed) | Excl | 0.0349 | $[L]_c$ | +1.36 | |

$[OH]_b$ is the concentration of the titrant in the burette, $[H]_c$ is the initial proton concentration in the cell and $[L]_c$ is the initial total ligand concentration in the cell. $[OH]_c$ is the concentration of the base in the cell and $[H]_b$ is the concentration of the proton concentration in the burette. $[L]_r$ is the refined concentration of the ligand.

**Table 4.2:** Protonation constants for the ligand APD (charges are omitted for simplicity).

| Equilibrium | pKa | μ and t | Reference |
|---|---|---|---|
| H + L = HL | 10.95(0.02) | 0.15 M NaCl and 37 °C | [1] |
| H + HL = $H_2L$ | 9.80(0.03) | | |
| H + $H_2L$ = $H_3L$ | 6.01(0.03) | | |
| H + $H_3L$ = $H_4L$ | 2.56(0.04) | | |
| H + L = HL | 10.80 | 0.1 M KCl and 25 °C | [2] |
| H + HL = $H_2L$ | 9.90 | | |
| H + $H_2L$ = $H_3L$ | 5.83 | | |
| H + $H_3L$ = $H_4L$ | 2.55 | | |
| H + L = HL | 12.14 | 0.1 M $NaNO_3$ and 25 °C | [3] |
| H + HL = $H_2L$ | 10.18 | | |
| H + $H_2L$ = $H_3L$ | 6.04 | | |
| H + $H_3L$ = $H_4L$ | 1.93 | | |
| H + $H_4L$ = $H_5L$ | 1.24 | | |
| H + L = HL | 11.85(0.01) | 0.15 M NaCl and 25 °C | This work |
| H + HL = $H_2L$ | 9.76(0.01) | | |
| H + $H_2L$ = $H_3L$ | 5.77(0.02) | | |
| H + $H_3L$ = $H_4L$ | 1.47(0.01) | | |

## 4.2 Metal-ligand studies involving ligand APD.

### 4.2.1 $Cd^{II}$–APD system by DCP: Titration at $L_T$:$M_T$ ratio 40, $[M_T] = 1.25 \times 10^{-4}$ M.

#### *4.2.1.1 Fitting of the polarographic data*

The $DC_{TAST}$ wave is the sum of the reduction and background current at any applied potential. The polarograms for the $Cd^{II}$–APD system were fitted using non-linear curve fitting operations where the following equations, which were previously used by Cukrowski et al [4], were applied**:**

$$I_r = \frac{I_d}{\langle 10\text{^}\left(\left(2\delta\left(x - E_{1/2}\right)\right)/0.05916\right) + 1\rangle} \quad (56)$$

$$I_b = a + b \times x \quad (57)$$

$$I_t = I_r + I_b \quad (58)$$

where $I_r$ is the reduction current, $I_d$ is the limiting diffusion current, $\delta$ is the parameter which relates to electrochemical reversibility of the system and is close to 1 for fully reversible system (when $0.5 < \delta < 0.9$ the system is said to be quarsi-reversible and when

$0<\delta<0.5$, the system is said to be irreversible), $x$ is the applied potential, $E_{1/2}$ is the half-wave potential of the recorded polarogram, $I_b$ is the background current, $a$ and $b$ are background current parameters and, $I_t$ is the total recorded current. The selected fitted polarograms for this system are shown in Figure 4.3.

From the fitted polarograms in Figure 4.3, the $Cd^{II}$–APD system can be regarded as fully reversible system because $\delta$ was never lower than 0.9 and did not vary much. It had a value of 0.99 for the free metal ion and after ligand solution addition $\delta$ was 0.98 at pH 2.56, and decreased slightly to 0.95 at pH 7.21. However, the polarographic signal disappeared above pH 7.21, even though no precipitation was observed. This suggests formation of an inert complex; each polarographic wave seen in Figure 4.3 represents all the labile $Cd^{II}$ species present at particular pH.

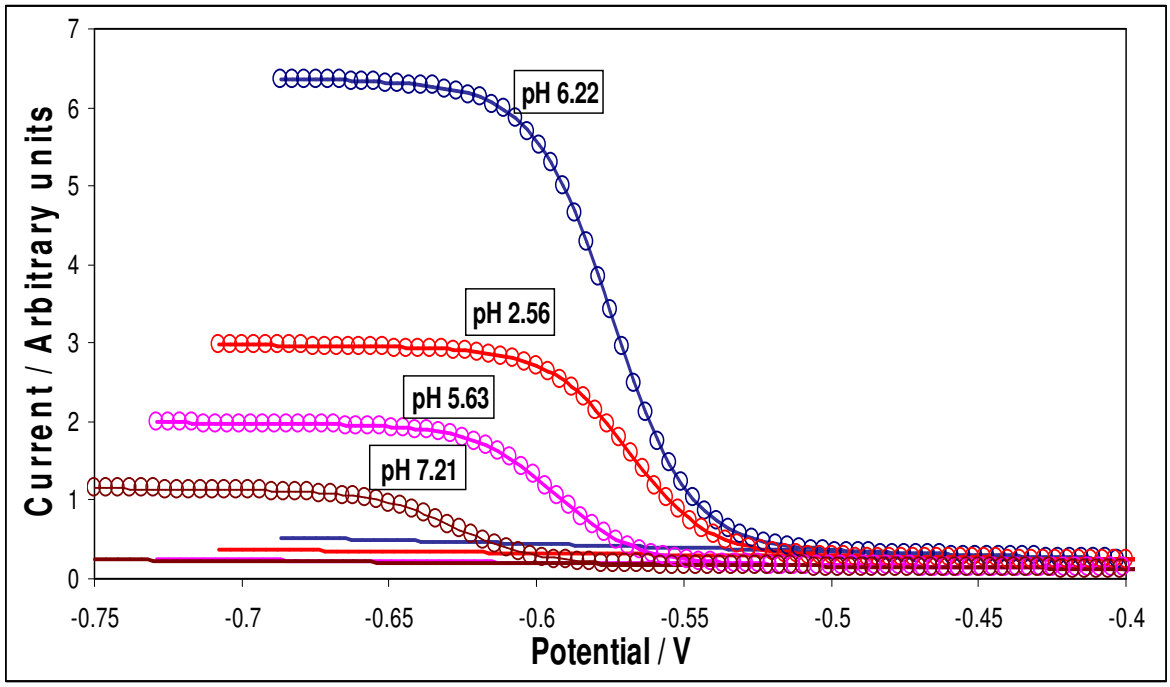


**Figure 4.3**: Selected fitted polarograms for $Cd^{II}$–APD system, the $[L_T]$:$[M_T]$ ratio 40, initial $[M_T]$ = $1.25\times10^{-4}$ M, ionic strength μ = 0.15 M (NaCl) and 25 °C. Circles represent the experimentally recorded points at particular applied potential and the solid lines represent the fitted curves.

### *4.2.1.2 Evaluation of $E_{1/2}$(M)*

Three polarograms were recorded on a sample solution containing only free metal ion in a polarographic cell; an example of DC polarogram recorded at pH 6.22 is seen in Figure 4.3. The average half-wave potential, $E_{1/2}$(M), for the free metal ion was -574.65 mV and

the average limiting diffusion current, $I_d$, for the free metal ion was 5.82 (arbitrary units). It is well known that the limiting diffusion current $I_d$ depends on the concentration of the free metal ion in solution and is independent of pH. However, the $E_{1/2}$(M) of the free metal ion is independent of concentration of the free metal ion and pH of the solution (the pH of the solution after addition of metal ion solution was about 6.2).

After the ligand solution was added to the polarographic cell the pH of the sample solution decreased to about 2.5. The half-wave potential $E_{1/2}$ shifted to more positive value of -568.56 mV after ligand addition. This could be attributed to, for example, adsorption of the metal-ligand complex formed at the mercury electrode, or due to junction potential interference at low pH values. The shift to more positive potential was 6.10 mV. It is important to stress that the shape of DC polarogram has not changed, it showed the same degree of electrochemical reversibility as it was obtained for the free metal ion and no evidence of adsorption at DME was observed– see polarogram at pH 2.56 in Figure 4.3. The limiting diffusion current decreased to 2.62 after ligand solution was added which could be attributed to dilution on ligand solution addition (dilution was more than 100 %). The expected limiting diffusion current after accounting for dilution is given by:

$$I_d = I_d(M) \times (V_{initial}/V_{Total}) = 5.82 \times (15/40) = 2.18$$

where $I_d$(M) is the recorded limiting diffusion current of the free metal ion only, $V_{initial}$ is the volume of the solution containing only the free metal ion, and $V_{Total}$ is the total initial volume of the sample after ligand solution addition. However the recorded limiting diffusion current of 2.62 was larger than the expected 2.18 due to dilution. The small increase in the limiting diffusion current was most likely caused by an increase in the mercury drop area (due to, e.g. a decrease in the surface tension after the addition of the ligand). Because of the shift in potential to the more positive half-wave potential, and change in limiting diffusion current it was assumed that the half-wave potential and the limiting diffusion current for the free metal ion were those obtained after ligand solution was added. These values are needed in refinement of computed stability constants.

### *4.2.1.3 Modelling of $Cd^{II}$–APD system*

a) Variation in limiting diffusion current, $I_d$ vs. pH

From the current vs. pH plot shown in Figure 4.4, the $Cd^{II}$–APD system can be divided into 3 regions. The region I, up to pH of about 4.0 can be treated as fully labile metal-ligand system on the polarographic time scale used because the normalized limiting diffusion current does not change and only one DC–wave was recorded. This means that the association and/or dissociation of metal complexes in solution in this pH range, if at all metal complexes are formed, is fast enough on the used time scale. In region II, between pH 4.0 and 5.0, there is a slight decrease in the normalized limiting diffusion current which can be attributed to the formation of other labile metal complexes with slightly lower diffusion coefficients since there is no significant dilution on addition of base titrant (i.e. the expected limiting diffusion current is constant). In region III, above pH 5.0, the normalized limiting diffusion current decreases abruptly as pH increases. This means that the labile part for the metal-ligand system 'disappears' and non-labile or inert metal complexes are formed in this particular pH range.

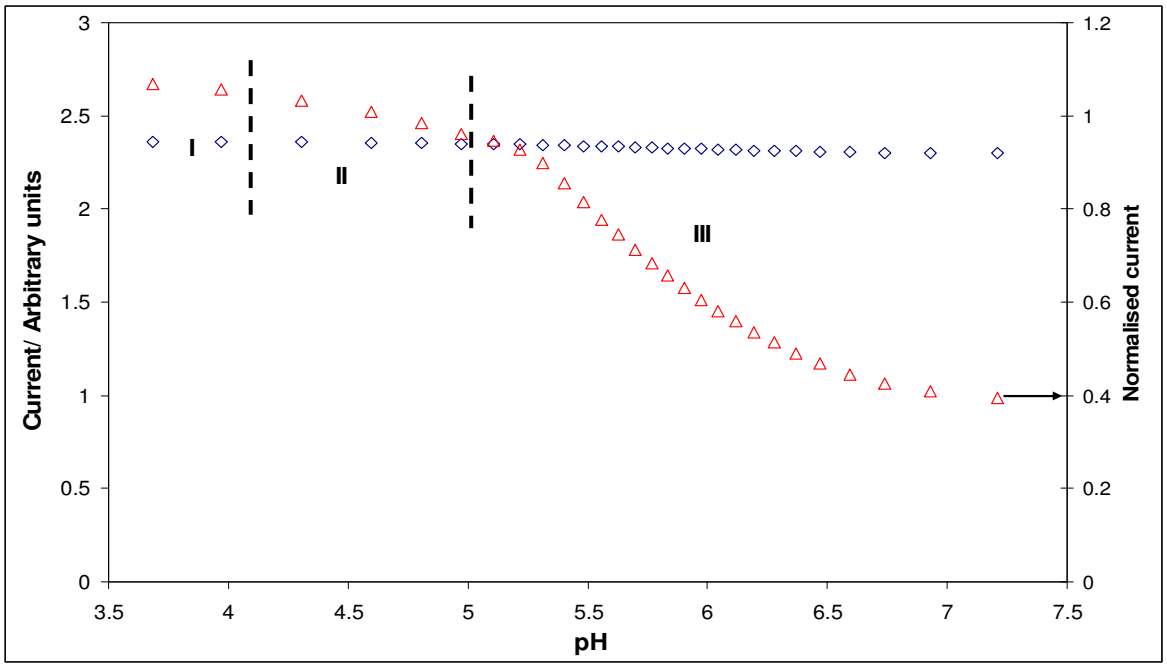


**Figure 4.4**: Variation in limiting diffusion current $I_d$ for $Cd^{II}$–APD system studied by $DC_{TAST}$ at $[L_T]:[M_T]$ ratio 40, initial $[M_T] = 1.25\times10^{-4}$ M, ionic strength $\mu = 0.15$ M (NaCl) and 25 °C. The triangles indicate the normalized limiting diffusion current and the diamonds indicate the expected limiting diffusion current, taking into account dilution on base titrant addition, assuming no complexes are formed.

Unfortunately, the polarographic signal disappeared above pH 7.2 and analysis of the system above this pH could not be performed. The expected current (seen in Figure 4.4 as diamonds) is the current expected in the absence of the complexing agent or ligand, taking into account dilution due to added base titrant. The expected current has not changed much indicating that there was no significant dilution throughout the whole experiment. The normalised limiting diffusion current (seen in Figure 4.4 as triangles) is the ratio between the observed and expected limiting diffusion currents, and represents the normalised change in the intensity of the recorded polarographic signal. The intensity of the recorded polarographic signal can change due to change in diffusion coefficients of different labile metal complexes formed, formation of polarographically inactive metal complexes and decrease in electrochemical reversibility. Since the normalised limiting diffusion current decreases significantly from about 1.0 to about 0.4, there is a need to employ virtual potentials (calculated from Equation 48) in the modelling of the metal-ligand system and refinement of stability constants.

b) Variation in half-wave potential $E_{1/2}$ vs. pH.

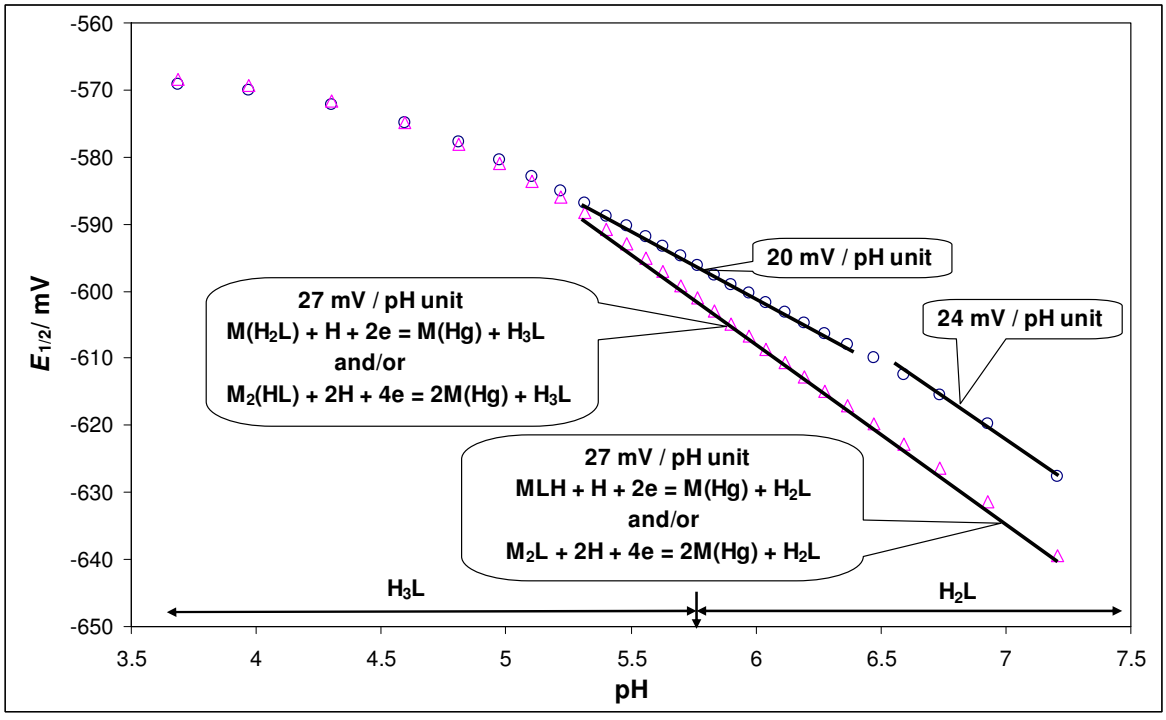


**Figure 4.5**: Half-wave potential $E_{1/2}$ vs. pH for $Cd^{II}$–APD system studied by $DC_{TAST}$ at $[L_T]$:$[M_T]$ ratio 40, $[M_T] = 1.25\times10^{-4}$ M, ionic strength $\mu = 0.15$ M (NaCl) and 25 °C. The circles represent the observed half-wave potentials, $E_{1/2}$(obs), and the triangles represent the virtual half-wave potentials, $E_{1/2}$(virt), calculated from Equation 48. The arrow indicates the protonation constant of APD.

It has been shown previously that the analysis of the shift in peak potential (of a labile peak) vs. pH, such as the one shown in Figure 4.5, can be used for the prediction of labile metal species [5-9]. When labile species are formed, a Nernstian type slope of ($m$(RT/$n$F))/$p$ is expected where $m$ stands for a number of protons, $n$ stands for the number of electrons involved in the electrochemical reduction of the free metal ion, and $p$ is the number of metal ions in the complex. No shift or slope was observed between pH 3.5 and 4.0, since a shift in half-wave potential ($\Delta E_{1/2}$) rather than the observed $E_{1/2}$ is used for prediction of metal complexes formed in solution, there is no information in this pH range which could prove whether metal complexes are formed or not. If complexes are formed in solution below pH 4.0, the most likely metal complex to be formed is M($H_3L$), since the form of the ligand is $H_3L$ and thus the expected shift is zero. The major possible electrochemical reactions between pH 3.5 and 4.0 are therefore (charges omitted for simplicity)

M + 2e = M(Hg), or
M($H_3L$) + 2e = M(Hg) + $H_3L$
in which no proton is involved.

Between pH of about 5.0 and 6.5, a slope of about 20 mV per pH unit was observed (see circles in Figure 4.5). This slope could be attributed to the formation of the metal complexes $M_2$(HL) and/or M($H_2L$) in solution according to the following electrochemical reactions:

M($H_2L$) + H + 2e = M(Hg) + $H_3L$
and/or
$M_2$(HL) + 2H + 4e = M(Hg) + $H_3L$ below pH 5.77.

The expected theoretical slope for these processes is 30 mV per pH unit. Above pH 5.77, the form of the ligand is $H_2L$ and thus the following electrochemical processes are suggested to occur at the mercury electrode surface.

$M_2$(HL) + H + 4e = M(Hg) + $H_2L$
and/or
MHL + H + 2e = M(Hg) + $H_2L$

and/or

$M_2L + 2H + 4e = 2M(Hg) + H_2L$.

The expected theoretical slope for the first process is 15 and 30 mV per pH unit for the latter processes. The observed slope (circles in Figure 4.5) suggests a mixture of these complexes in solution at this pH range.

A maximum slope of 24 mV per pH unit is seen above pH 6.5 (see circles representing the observed $E_{1/2}$), this observed slope is by 6 mV less than the theoretically expected slope. This could be attributed to the inert metal species (MHL) formed in this pH range because the reduction of this metal complex is not fast enough on the polarographic time scale employed. This supposition is confirmed in the current vs. pH graph in Figure 4.4 were a significant drop in normalised limiting diffusion current was observed in the same pH range. Therefore there is a need to use the virtual half-wave potentials in the modelling of metal-ligand system instead of the observed potentials because when inert metal complexes are formed in solution, the observed half-wave potentials (coming only from the labile part of the metal-ligand system) would be more positive than expected.

When the virtual half-wave potentials were analysed as function of pH, as indicated by the triangles in Figure 4.5, a maximum slope of 27 mV per pH unit is observed in the pH range 5.0 to 7.2. Since the form of the ligand below pH 5.77 is $H_3L$, the following electrochemical processes are proposed to be occurring below pH 5.77 at the mercury-solution interface:

$M(H_2L) + H + 2e = M(Hg) + H_3L$

and/or

$M_2(HL) + 2H + 4e = 2M(Hg) + H_3L$

However, above pH 5.77 the form of the ligand is $H_2L$ and the following metal complex is reduced at the electrode surface:

$MHL + H + 2e = M(Hg) + H_2L$

in which one proton is involved in the electrochemical process. The theoretically expected slope for the above electrochemical processes is about 30 mV per pH unit which is close to the slope calculated from the virtual potentials. It is also important to note that an enhanced slope of 27 mV of the virtual half-wave potentials seen at pH below 5.0 is larger than the slope from the observed half-wave potentials seen at pH 6.5 and above, this tells us that the three species proposed from $E_{1/2}$(virt) are formed earlier than predicted by the observed potentials slope. The polarographic signal disappeared above pH 7.2 where MHL is predicted to form, hence one might suggest that MHL is an inert species formed. From this analysis the model for the metal-ligand system at this stage comprises M($H_3L$), $M_2HL$ and/or M($H_2L$) and MHL (analysis of observed $E_{1/2}$ also suggest model M($H_3L$), $M_2HL$ and/or M($H_2L$) and MHL).

The virtual half-wave potentials, $E_{1/2}$(virt) rather than the observed half-wave potentials, $E_{1/2}$(obs) will be used in the modelling of subsequent metal-ligand systems to account for formation of inert metal complexes.

c) Variation in half-wave potential, $E_{1/2}$ vs. log [$H_nL$]

The modified Nernstian type of slope of ($j$(RT/$n$F))/$p$ can be applied in the analysis of slopes of half-wave potential, $E_{1/2}$ vs. log [L] which allows prediction of metal species or complexes formed in solution, where $p$ in this case stands for the number of metal ions involved in the single complex formation reaction, $j$ stands for the number of ligands complexed to the metal ion and $n$ stands for the number of electrons involved in the electrochemical reduction of the free metal ion [5-9].

In principle, this modified Nernstian type of slope can be applied in the analysis of slopes for the plot of half-wave potential, $E_{1/2}$ vs. log [$H_nL$] [10]. Thus complexes of type $M_p(H_nL)$ can be predicted from this kind of analysis. The graph of half-wave potential, $E_{1/2}$ vs. log [$H_2L$] for the $Cd^{II}$–APD system is shown in Figure 4.6, no well defined slopes were observed (the curve is exponential) on this plot and this graph does not provide any evidence as to whether the complex M($H_2L$) is formed in solution as predicted by the plot of half-wave potential, $E_{1/2}$ vs. pH in Figure 4.5. A theoretical slope of about 30 mV per log [$H_2L$] unit is expected when this metal complex is formed in solution. It follows

therefore that presence of the $M(H_2L)$ complex cannot be confirmed from this type of analysis and is evident that this complex is not formed in solution.

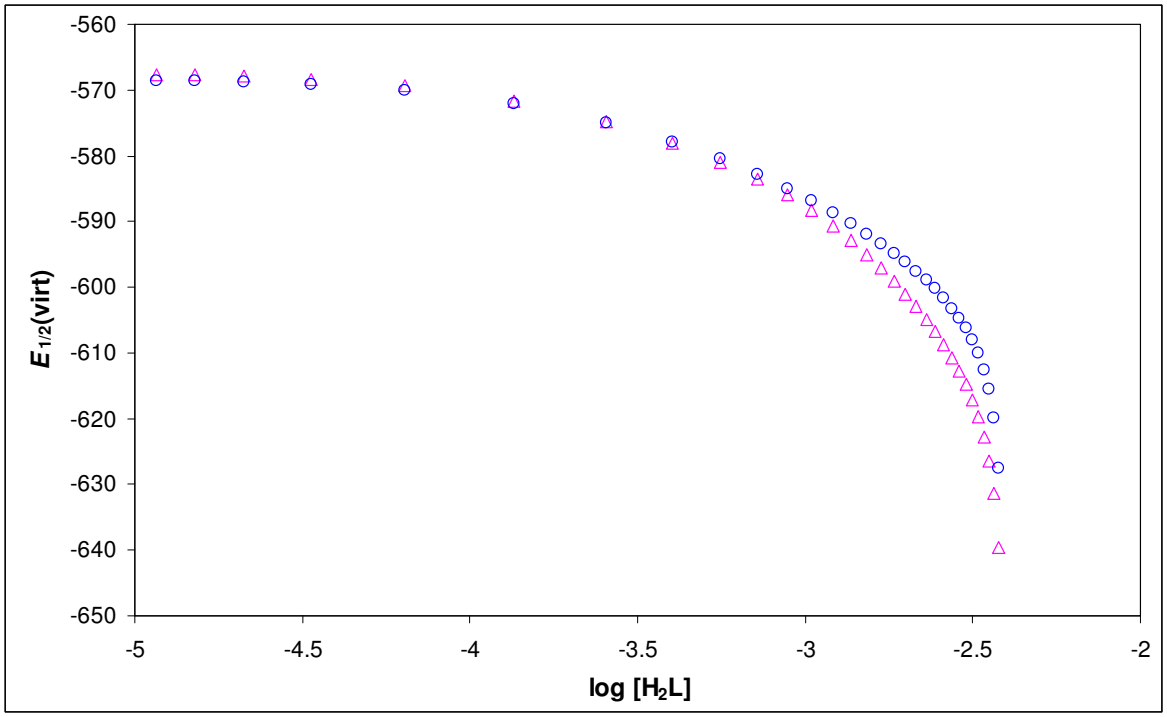


**Figure 4.6**: Half-wave potential $E_{1/2}$ vs. log $[H_2L]$ for $Cd^{II}$–APD system studied by $DC_{TAST}$ at $[L_T]:[M_T]$ ratio 40, $[M_T] = 1.25\times10^{-4}$ M, ionic strength $\mu$ = 0.15 M (NaCl) and 25 °C. The circles represent the observed half-wave potentials and the triangles represent the virtual half-wave potentials calculated from Equation 48.

It is important to mention that the plot of half-wave potential, $E_{1/2}$ vs. log $[H_3L]$ did not have definite slope indicating the presence of $M(H_3L)$ complex.

To confirm the presence of metal complexes containing HL form of the ligand, a plot of half-wave potential, $E_{1/2}$ vs. log [HL] need to be analysed. This graph is shown in Figure 4.7. From this graph a slope of 15 mV per log [HL] unit was seen as far as the virtual half-wave potentials are concerned (triangles in Figure 4.7), this predicts the formation of species $M_2(HL)$ in solution according to the following electrochemical process:

$$2M + HL = M_2(HL)$$

This slope is pinpointing the expected theoretical slope of 15 mV per log [HL] unit for this complex formation reaction. This confirms the presence of the metal complex $M_2(HL)$ in

solution as predicted in the half-wave potential, $E_{1/2}$ vs. pH in the pH range 5.00 to 5.77. It must be pointed out that this species is predicted by the two graphs in the same pH range. A maximum slope of 24 mV per log [HL] unit was observed, this suggest the presence of metal species MHL in solution which is formed according to the complex formation reaction:

M + HL = MHL.

However the expected theoretical slope for this process is 30 mV per log [HL] unit when this complex is fully formed in solution. Thus this slope suggests the complex MHL is not fully formed in solution and there could be traces of preceding species in solution (e.g. $M_2(HL)$) at this particular pH or log [HL] range. This complex, MHL was predicted to be formed in the same pH range in the half-wave potential, $E_{1/2}$ vs. pH plot. Clearly this complex is present in solution and one can conclude that MHL is inert species since the polarographic signal disappeared at the pH or log [HL] range where it is predicted to be formed.

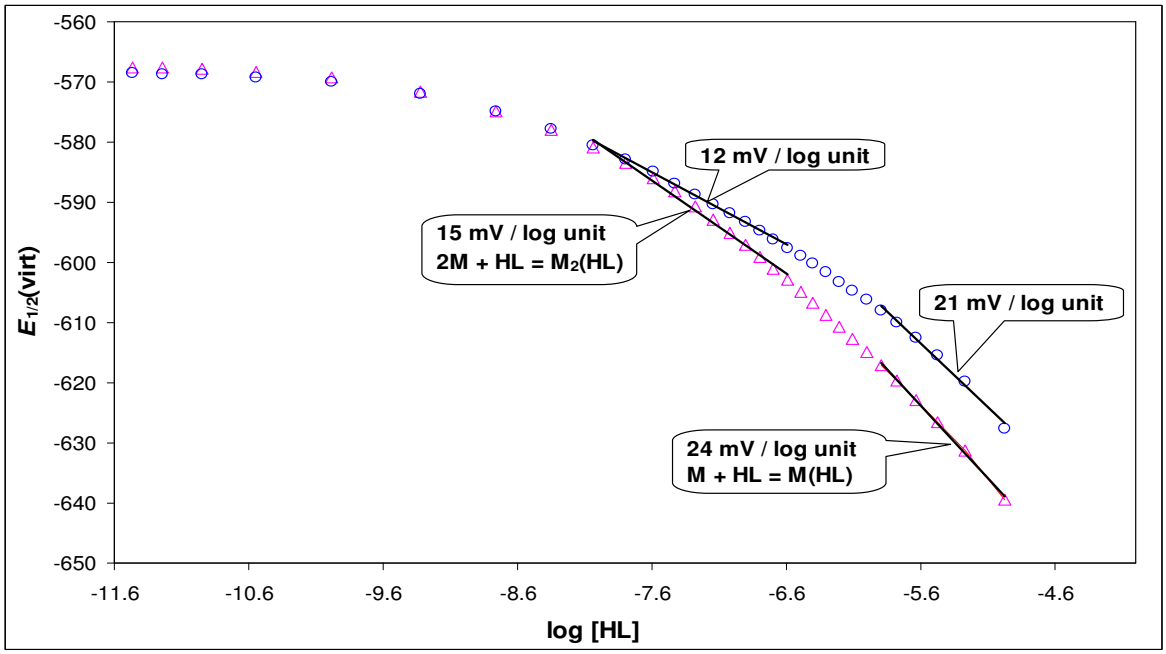


**Figure 4.7**: Half-wave potential $E_{1/2}$ vs. log [HL] for $Cd^{II}$–APD system studied by $DC_{TAST}$ at $[L_T]:[M_T]$ ratio 40, $[M_T] = 1.25\times10^{-4}$ M, ionic strength $\mu$ = 0.15 M (NaCl) and 25 °C. The circles represent the observed half-wave potentials and the triangles represent the virtual half-wave potentials calculated from Equation 48.

It must be said that the observed half-wave potentials (seen as circles in Figure 4.7) gave slopes which are 3 mV less than the virtual potentials. Thus the observed half-wave potentials cannot be used in the modelling of the metal-ligand system because they do not give well defined slopes when inert complexes are formed in solution. This is because only the labile part of the metal-ligand system can be analysed by the $DC_{TAST}$ technique.

The graph of half-wave potential, $E_{1/2}$ vs. log [L] can be used for the prediction of metal complexes of the form $ML_n$, where n is the number of ligands bound to the metal ion ($n \geq 1$). The graph of half-wave potential, $E_{1/2}$ vs. log [L] for the $Cd^{II}$–APD system is shown in Figure 4.8. A well defined slope of 11 mV per log [L] was seen as far as the virtual potentials are concerned (note that 9 mV per log [L] was seen for observed $E_{1/2}$ potentials). This slope suggests formation of metal complex $M_2L$ according to the following complex formation reaction:

$2M + L = M_2L$.

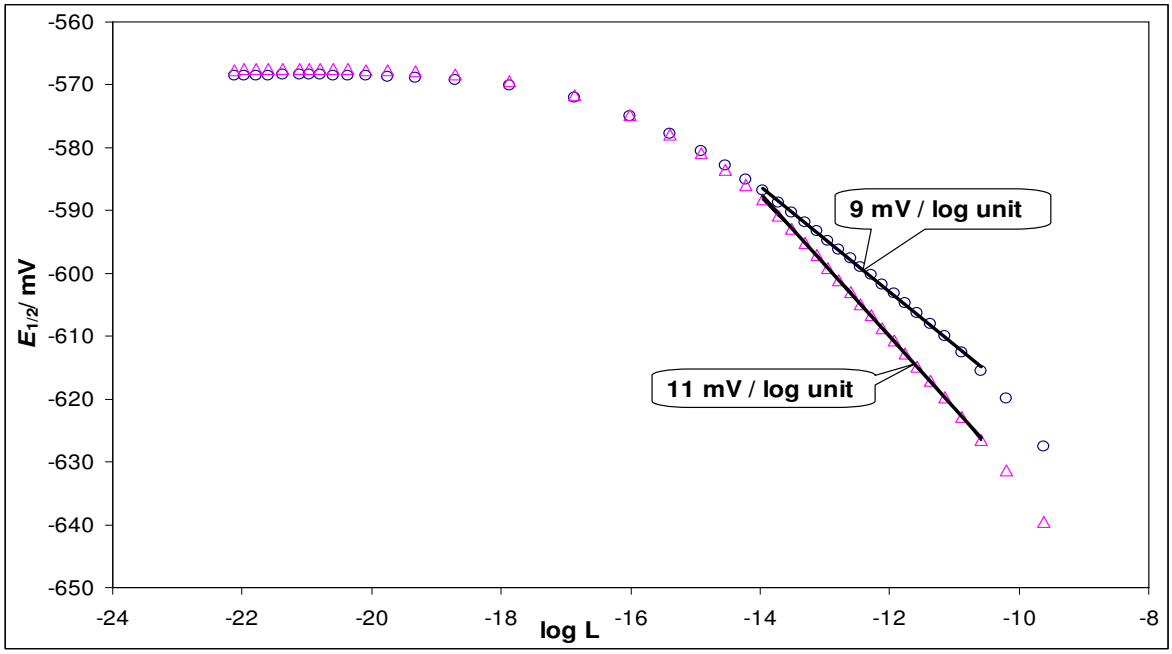


**Figure 4.8**: Half-wave potential $E_{1/2}$ vs. log [L] for $Cd^{II}$–APD system studied by $DC_{TAST}$ at $[L_T]:[M_T]$ ratio 40, $[M_T] = 1.25\times10^{-4}$ M, ionic strength $\mu = 0.15$ M (NaCl) and 25 °C. The circles represent the observed half-wave potentials and the triangles represent the virtual half-wave potentials calculated from Equation 48.

The theoretically expected slope for this process is 15 mV per log [L] unit. It is clear from this plot that there is no evidence of formation of ML species in solution because there is

no slope which predicts the presence or formation of this complex (i.e. a slope of 30 mV per log [L] unit). From the analysis of half-wave potential, $E_{1/2}$ vs. log [$H_2L$] in Figures 4.6, the presence of M($H_2L$) in solution was not evident. In Figure 4.7, the species $M_2HL$ and MHL where confirmed to be formed in solution as suggested by the plot half-wave potential, $E_{1/2}$ vs. pH in the same pH range. While from Figure 4.8, the additional complex $M_2L$ was suggested to be formed in solution. Therefore two models for this metal-ligand system should be considered from the modelling procedures: $M_2$(HL) and M(HL) or $M_2$(HL) and $M_2L$.

#### *4.2.1.4 Optimisation of $Cd^{II}$–APD model and refinement of stability constants.*

The polarographic complex formation curves are used for the optimisation of the final metal-ligand model and refinement of stability constants. The experimental complex formation curve (ECFC), as described by Equation 44, contains parameters available from the polarographic experiment and is characteristic of the metal-ligand system. The calculated complex formation curve (CCFC), as described by Equation 45, contains pH dependent free metal ion concentration which is indirectly available from the experiment and is calculated from mass balance equations written for the metal-ligand system of interest. The metal-ligand model is varied and the stability constants are optimised such that the CCFC fits best the ECFC. For this particular system, the best fit was attained for the model containing complexes $M_2$(HL) and MHL with refined stability constants as shown in Table 4.4 (a) and the corresponding complex formation curve is shown in Figure 4.9.

The best values of the refined stability constants are those values in which the best fit in CCFC into ECFC were attained and small standard deviations for all complexes are attained as well. The proposed best model for this system consists of the species $M_2$(HL) and MHL with the refined stability constants 24.15±0.03 and 19.21±0.02, respectively, as indicated in Table 4.4 (a). This model contains species with low standard deviations and lower overall fit in CCFC into ECFC of ±0.600 mV. However when the model containing species $M_2HL$ and $M_2L$ was tested, it gave a slightly larger overall fit of ±0.664 mV with the refined stability constants 24.18±0.03 and 18.14±0.03, respectively. When the model containing complexes $M_2HL$, MHL and $M_2L$ was fitted, it gave the overall fit of ±0.863

mV of CCFC into the ECFC with refined stability constants as 24.19±0.11, 18.72±0.04 and 18.06±6.42, respectively. It is clear that larger standard deviations for the complexes $M_2HL$ and $M_2L$ were observed.

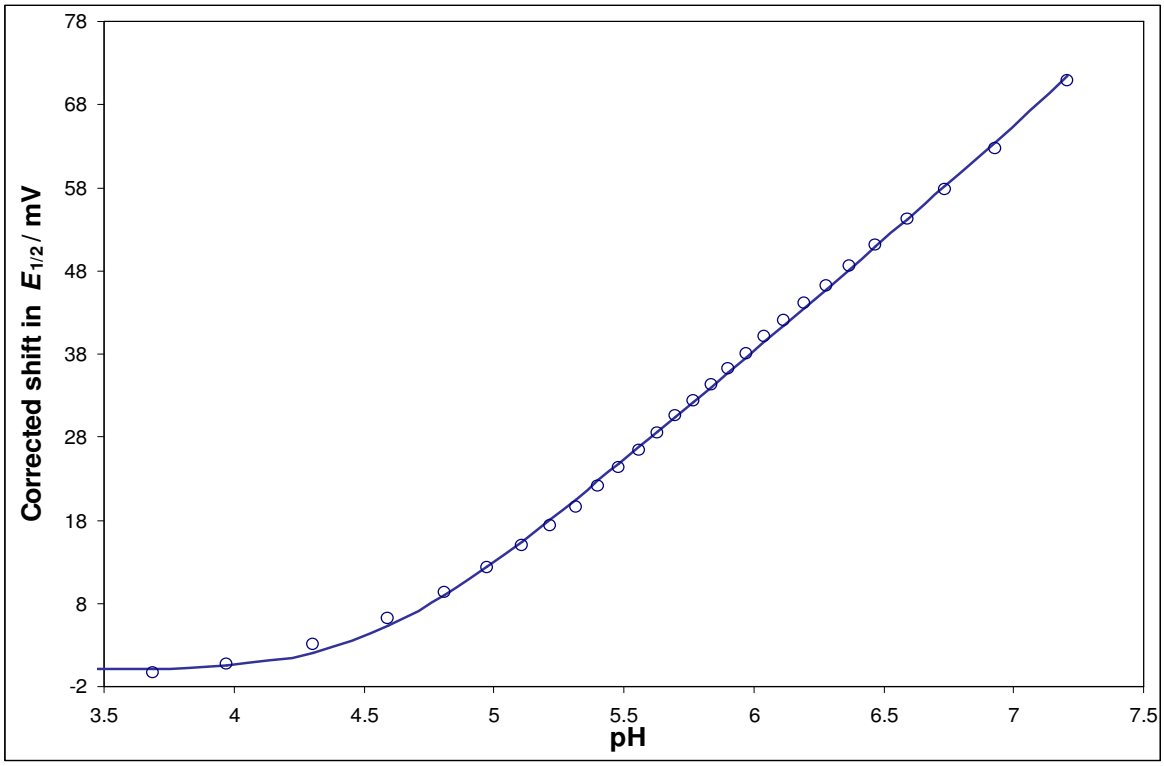


**Figure 4.9**: Experimental and calculated polarographic complex formation curves for $Cd^{II}$–APD system studied by $DC_{TAST}$ at $[L_T]:[M_T]$ = 40, $[M_T] = 1.25\times10^{-4}$ M, ionic strength μ = 0.15 M (NaCl) and 25 °C. The circles represent the experimentally observed points (ECFC) and the solid line represents the theoretically reproduced curve from the refined stability constants (CCFC).

This shows that the complexes MHL and $M_2L$ cannot be incorporated together into the metal-ligand system. The complex $M_2L$ (as suggested by $E_{1/2}$ vs. log [L] plot) could not be fitted at all when included in the model containing $M_2HL$ and MHL species. When $M(H_3L)$ complex is included in the model containing $M_2HL$ and MHL, no change in the overall fit and the stability constants for these complexes is observed. This means that this complex has no contribution in the shift in potential since its reduction does not involve protons or this complex is not formed at all. When $M(H_2L)$ complex is included in the model containing species $M_2HL$ and MHL, no change in overall fit is seen as well. These complexes, $M(H_3L)$ and $M(H_2L)$ gave a log β values < 0 which is meaningless (the theoretically expected values of log β > 0) and indicates that the refinement operations rejected them. It was observed from the plot of half-wave potential, $E_{1/2}$ vs. log$[H_2L]$ that

there was no evidence of formation of metal complex, $M(H_2L)$ in solution and that is the reason why this complex could not be fitted in the metal-ligand model.

However, the final metal-ligand model for this system might be decided using the species distribution diagrams as well as considering the model with the best fit in CCFC into ECFC. The species distribution diagrams for different metal-ligand models are discussed in the following section.

**Table 4.3**: Protonation constants for the ligand APD, dissociation constants of water and overall stability constants of $Cd^{II}$ complexes with $OH^-$ at ionic strength $\mu$ = 0.15 M NaCl and 25.0 °C.

| Equilibrium | log β |
|---|---|
| $H^+ + OH^- = H_2O$ | 13.42 |
| $L + H = HL$ | 11.85 |
| $HL + H = H_2L$ | 9.76 |
| $H_2L + H = H_3L$ | 5.77 |
| $H_3L + H = H_4L$ | 1.47 |
| $Cd^{2+} + OH^- = Cd(OH)^+$ | 4.00 |
| $Cd^{2+} + 2OH^- = Cd(OH)_2$ | 7.70 |
| $Cd^{2+} + 3OH^- = Cd(OH)_3^-$ | 10.30 |
| $Cd^{2+} + 4OH^- = Cd(OH)_4^{2-}$ | 12.00 |
| $2Cd^{2+} + OH^- = Cd_2(OH)^{3+}$ | 5.06 |
| $4Cd^{2+} + 4OH^- = Cd_4(OH)_4^{4+}$ | 24.90 |
| $Cd^{2+} + 2OH^- = Cd(OH)_2(s)$ | -14.30 |

**Table 4.4:** (a) Overall stability constants for $Cd^{II}$ with APD obtained in this work by $DC_{TAST}$ using curve fitting described at ionic strength $\mu$ = 0.15 M NaCl and 25 °C.

| Technique | Ratio | Equilibrium | log β | Overall fit |
|---|---|---|---|---|
| $DC_{TAST}$ | 40 | $2M + HL = M_2(HL)$ | 24.15±0.03 | ±0.600 mV |
| | | $M + HL = MHL$ | 19.21±0.02 | |
| | | $2M + HL = M_2(HL)$ | 24.18±0.03 | ±0.664 mV |
| | | $2M + L = M_2L$ | 18.14±0.03 | |
| | | $2M + HL = M_2(HL)$ | 24.19±0.11 | ±0.863 mV |
| | | $2M + L = M_2L$ | 18.06±6.42 | |
| | | $M + HL = MHL$ | 18.72±0.04 | |
| | | $2M + HL = M_2(HL)$ | 24.15±0.03 | ±0.600 mV |
| | | $M + HL = MHL$ | 19.21±0.02 | |
| | | $M + H_3L = M(H_3L)$ | rejected | |
| | | $2M + HL = M_2(HL)$ | 24.15±0.03 | ±0.600 mV |
| | | $M + HL = MHL$ | 19.21±0.02 | |
| | | $M + H_2L = M(H_2L)$ | rejected | |

(b) Overall stability constants for $Cd^{II}$ with APD obtained in this work by $DC_{TAST}$ using curve fitting described at ionic strength $\mu$ = 0.15 M NaCl and 25 °C (1st protonation constant, i.e. 11.85 excluded). L′ = HL ($pKa_1$ excluded).

| Technique | Ratio | Equilibrium | log β | Overall fit |
|---|---|---|---|---|
| $DC_{TAST}$ | 40 | $2M + L' = M_2L'$ | 12.30±0.03 | ±0.600 mV |
| | | $M + L' = ML'$ | 7.36±0.02 | |

### *4.2.1.5 Species distribution diagrams*

The species distribution diagrams for the proposed plausible final metal-ligand models for this system are shown in Figure 4.10 and 4.11. The species distribution diagram in Figure 4.10 is the one for the model $M_2(HL)$ and MHL and indicates that complexes start to form at pH about 3.5. The species $M_2(HL)$ is the major metal complex until pH about 6.0 and thereafter the complex MHL starts to be the major species in solution above this pH.

It is essential to note that the species $M_2(HL)$ is predominant in the pH range where $H_3L$ is the form of the ligand in solution and MHL is predominant in the pH range where $H_2L$ is the major form of the ligand in solution. This is in agreement with the modelling part of the metal-ligand system as suggested in Figure 4.5. On the other hand, Figure 4.11 shows the species distribution diagram for the model containing species $M_2HL$ and $M_2L$. The species $M_2(HL)$ is the major metal complex until pH about 6.0 and thereafter the complex $M_2L$ start to be the major species in solution above this pH. When comparing the species distribution diagrams for these two models, it is clear that $M_2L$ replaces MHL exactly and they are dominant species in the same pH range. This explains why the two species could not be fitted into the metal-ligand model simultaneously and why they gave larger standard deviations in the stability constants when they were fitted. The species distribution diagram for the model containing complexes $M_2HL$, MHL and $M_2L$ is illustrated in Figure 4.12. From this species distribution diagram one can notice that the complexes MHL and $M_2L$ start to form at the same pH of about 4.5. The metal complex $M_2L$ becomes the major species in solution and constitutes about 60 % of solution at pH about 6.5 while the complex MHL constitute about 20 % of solution composition. When the complexes $M_2L$ and MHL are incorporated into the metal-ligand system, $M_2L$ is favoured over MHL complex as far as % composition in solution but this complex is not favoured when the model $M_2HL$, MHL and $M_2L$ are fitted into the experimental data because it gave larger standard deviation for this $M_2L$ complex. Thus the two plausible metal-ligand models for this system are: $M_2HL$, MHL and $M_2HL$, $M_2L$. The species distribution diagram for the other metal-ligand model containing metal complexes $M(H_2L)$, $M_2(HL)$ and MHL is shown in Figure 4.13. According to Figure 4.13, the species $M(H_2L)$ with refined log β value < 0 is clearly none existing because its percentage is less than 1 and therefore this species could be mathematically generated species.

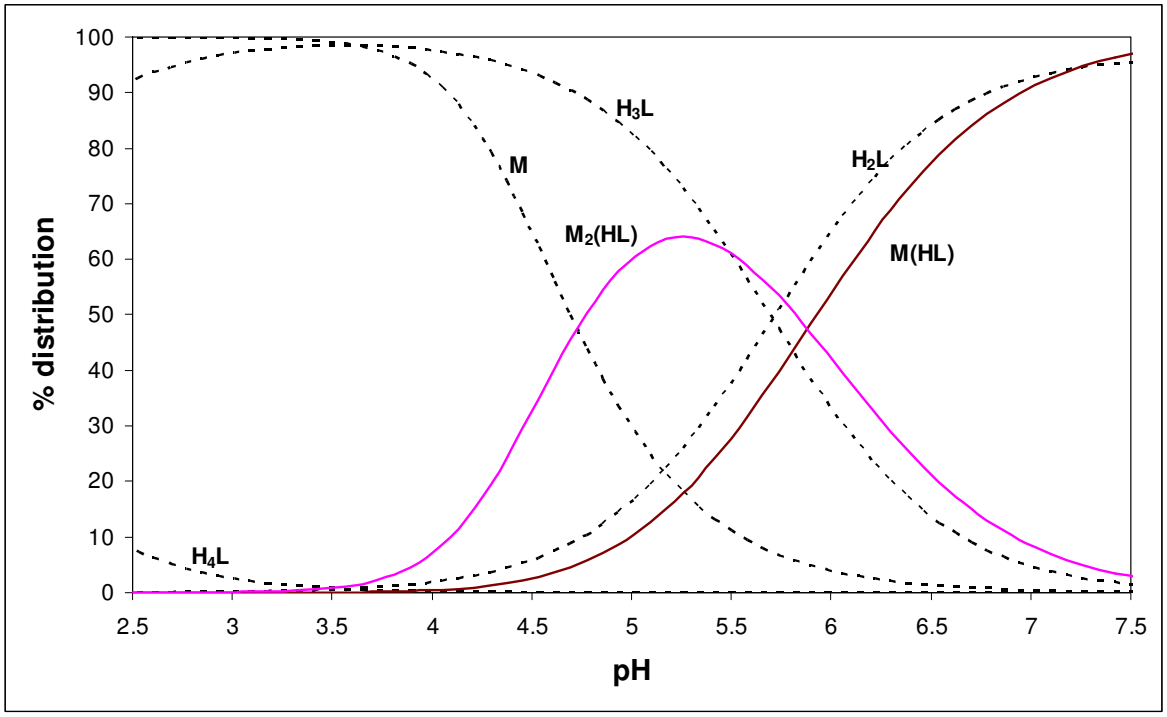


**Figure 4.10**: The species distribution diagram for model $M_2HL$ and MHL for $Cd^{II}$–APD system studied by $DC_{TAST}$ at $[L_T]:[M_T]$ = 40, initial $[M_T]$ = 1.25 × $10^{-4}$ M, ionic strength μ = 0.15 M (NaCl) and 25 °C.

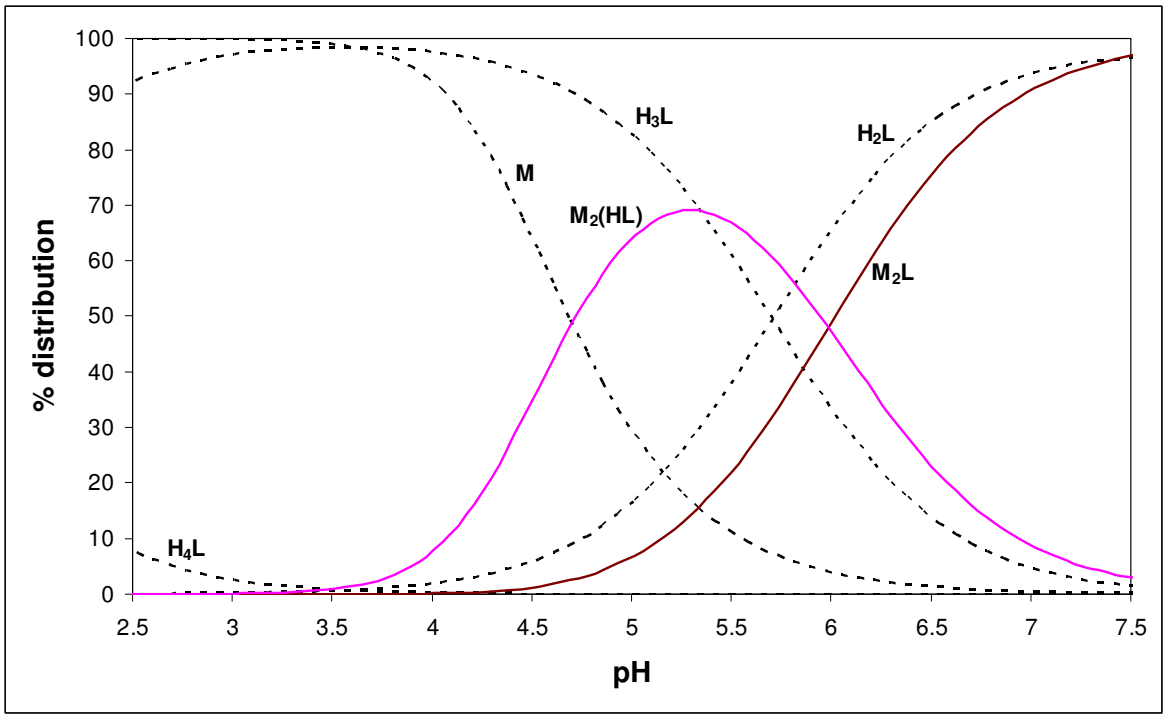


**Figure 4.11**: The species distribution diagram for model $M_2HL$ and $M_2L$ for $Cd^{II}$–APD system studied by $DC_{TAST}$ at $[L_T]:[M_T]$ = 40, initial $[M_T]$ = 1.25 × $10^{-4}$ M, ionic strength μ = 0.15 M (NaCl) and 25 °C.

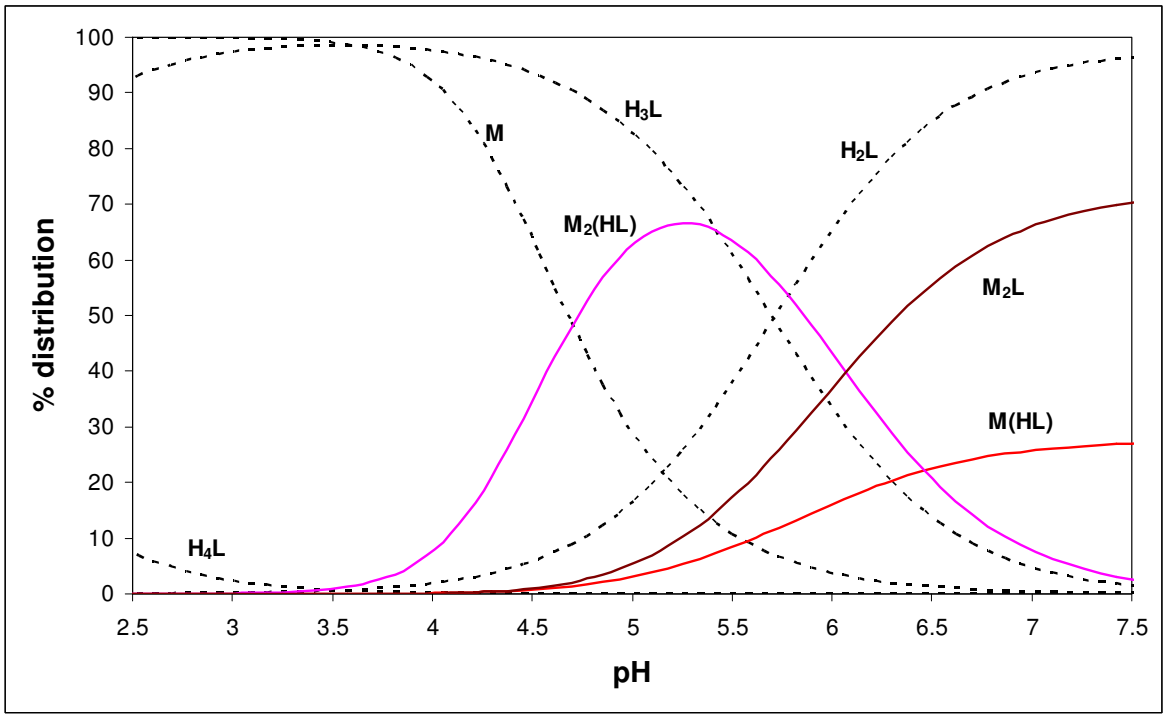


**Figure 4.12**: The species distribution diagram for model $M_2HL$, MHL and $M_2L$ for $Cd^{II}$–APD system studied by $DC_{TAST}$ at $[L_T]:[M_T] = 40$, initial $[M_T] = 1.25 \times 10^{-4}$ M, ionic strength $\mu = 0.15$ M (NaCl) and 25 °C.

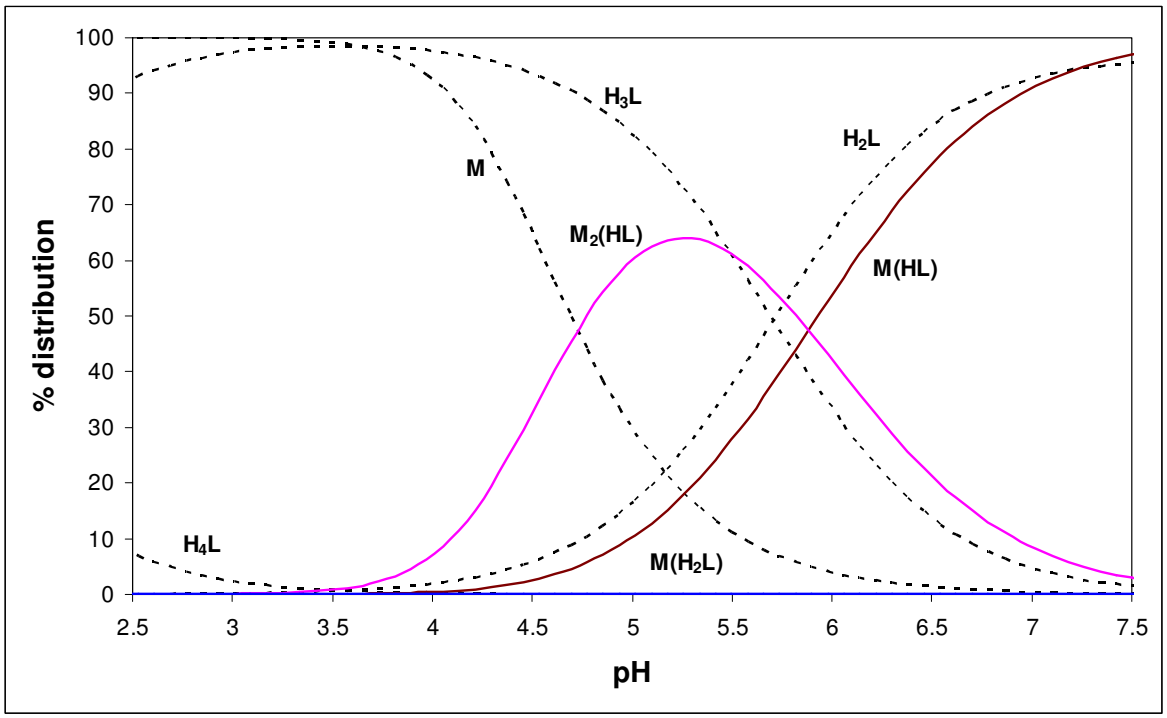


**Figure 4.13**: The species distribution diagram for model $M(H_2L)$, $M_2(HL)$ and MHL for $Cd^{II}$–APD system studied by $DC_{TAST}$ at $[L_T]:[M_T] = 40$, initial $[M_T] = 1.25 \times 10^{-4}$ M, ionic strength $\mu = 0.15$ M (NaCl) and 25 °C.

This species distribution diagram supports the supposition (from the $E_{1/2}$ vs. log [$H_2L$] in Figure 4.6) that M($H_2L$) complex is not formed in solution. The 1st choice for the final metal-ligand model for this particular system is the one containing metal complexes $M_2$(HL) and MHL because this model has the lowest overall fit in CCFC into ECFC with small standard deviations in all the refined stability constants. The model containing species $M_2HL$ and $M_2L$ has a slightly larger overall fit in CCFC into ECFC but this model is also plausible because as the pH increase the metal complex $M_2HL$ deprotonates to form $M_2L$ at high pH.

### *4.2.1.6 Virtual Potentiometry*

It has been demonstrated that the virtual potentiometric sensor should be metal ion non-specific meaning that it should work for any metal ion as long as this metal ion is polarographically active and reduced reversibly. The virtual potentiometric sensor should have a linear response with a theoretical Nernstian type slope. This means that the program such as ESTA can be used to refine data coming from dynamic, non-equilibrium technique such as polarography or any voltammetric technique for that matter.

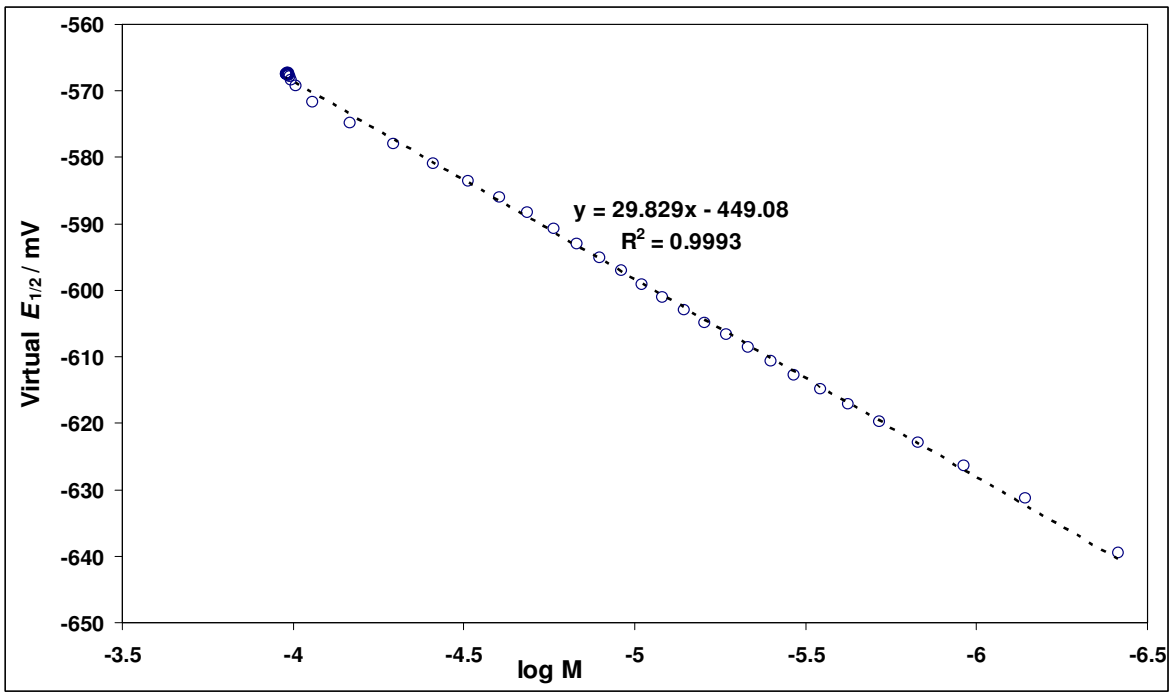


**Figure 4.14**: The plot for virtual half-wave potential $E_{1/2}$(virt) vs. log M for $Cd^{II}$–APD system studied by $DC_{TAST}$ at [$L_T$]:[$M_T$] ratio 40, [$M_T$] = $1.25\times10^{-4}$ M, ionic strength μ = 0.15 M (NaCl) and 25 °C. This plot is for the model containing metal complexes $M_2HL$ and MHL with refined stability constants 24.149±0.028 and 19.210±0.021, respectively.

To do this, the plot of $E_{1/2}(virt)_{x(i)}$ vs. log M for the model containing complexes $M_2HL$ and MHL as indicated in Figure 4.14 was used. From this plot, the slope of 29.83 mV is observed and is close to the theoretical Nernstian slope of 29.58 mV at 25 °C. The response slope was fixed at a theoretical value of 29.58 at 25 °C, with the $E°$ refined and different metal-ligand models were tested/refined by ESTA. Surprisingly, in this case of $Cd^{II}$–APD system ESTA was struggling to refine the polarographic data converted using Equation 48. ESTA could not refine the data irrespective of what parameters were refined together with $E°$ (base, acid, ligand, and metal ion concentrations). Until now it is not yet understood why the virtual potentiometry could not work in this case.

### *4.2.1.7 Comparison of formation constants for Ligands APD and HEDP with $Cd^{II}$ metal ion.*

The general structure of the bisphosponate ligands is R–C(OH)–$(PO_3H_2)_2$ where R = H, $CH_3$, $C_2H_5NH_3^+$ for MDP, HEDP, APD, respectively, except the fact that for the ligand MDP there is no hydroxyl group attached to carbon (no chiral carbon). The structure of the ligands APD and HEDP are similar but the ligand APD has an additional carbon chain with an amine group attached to it. This amine group contains a proton attached to it and as a result the ligand APD has additional protonation constant. The protonation constants for the ligands MDP, HEDP and APD are shown in Table 4.5. The $pKa_1$ values for the ligands MDP and HEDP are 9.97 and 10.11, respectively, these values are similar and can be related to deprotonation at the phosphonate oxygen atoms. These values are similar to the second protonation constant, $pKa_2$ for the ligand APD which is 9.76. The second protonation constants ($pKa_2$) for MDP and HEDP are 7.00 and 6.81, respectively, these values are significantly larger than the third protonation constant ($pKa_3$) for APD which is 5.77. The $pKa_1$ value for the ligand APD is 11.85, this protonation constant can be related to deprotonation of the amine proton of which the ligands MDP and HEDP do not possess.

The polarographic experiment for the $Cd^{II}$–APD system was performed until pH about 7.2; at this particular pH the major form of the ligand is $H_2L$ which means that the ligand has two protons attached to it. The first formation constant (i.e. log $\beta_{ML}$) for the $Cd^{II}$–APD system was not obtained at all in this work, only protonated metal-ligand complexes were obtained as indicated in Table 4.4 (a).

**Table 4.5**: The protonation constants for the ligands MDP, HEDP and APD (charges were omitted for simplicity). Protonation constants for ligands MDP and HEDP were determined at ionic strength μ = 0.15 M (NaCl) and 37 °C.

| Ligand | Equilibrium | p$K_a$ | Reference |
|---|---|---|---|
| MDP | L + H = HL | 9.97(0.01) | [11] |
| | HL + H = $H_2L$ | 7.00(0.01) | |
| | $H_2L$ + H = $H_3L$ | 3.26(0.02) | |
| | $H_3L$ + H = $H_4L$ | 2.19(0.05) | |
| HEDP | L + H = HL | 10.11(0.01) | [12] |
| | HL + H = $H_2L$ | 6.81(0.01) | |
| | $H_2L$ + H = $H_3L$ | 2.97(0.01) | |
| | $H_3L$ + H = $H_4L$ | 2.43(0.02) | |
| | $H_4L$ + 2H = $H_6L$ | 4.66(0.02) | |
| APD | L + H = HL | 11.85(0.01) | This work |
| | HL + H = $H_2L$ | 9.76(0.01) | |
| | $H_2L$ + H = $H_3L$ | 5.77(0.02) | |
| | $H_3L$ + H = $H_4L$ | 1.47(0.01) | |

However for the purposes of comparison of log $\beta_{ML}$ values for the ligand APD and the related ligand HEDP, it was very important to assume that the 1st protonation constant for the ligand APD (i.e. amine protonation constant at 11.85) was not of importance when bond formation during complexation is considered. If this assumption is valid, then the two ligands, HEDP and APD, should in principle form bonds in the same way with the metal ion of interest (i.e. through the diphosphonate oxygen atoms) at physiological pH about 7.2. The reported crystal structures for the ligand APD with metal ions such as $Zn^{II}$ and $Fe^{II}$ [13, 14, 15] shown below indicate that the R–group of the ligand APD is not involved in complex formation or bond formation and the ligand forms the bonds with the oxygen atoms on different phosphonate groups.

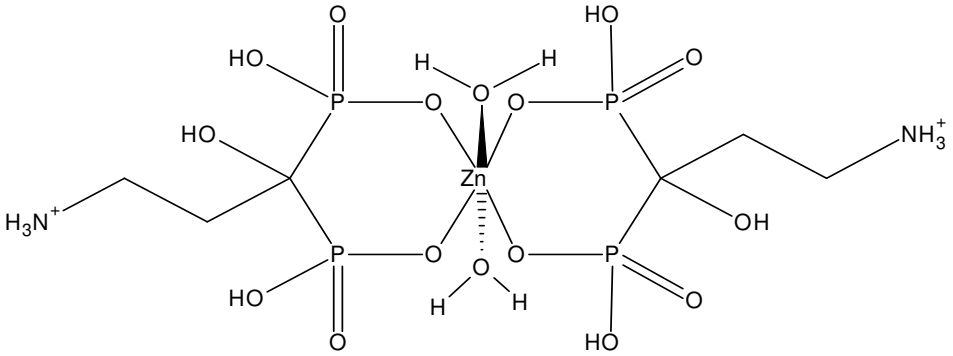


**Figure 4.15**: Crystallographic structure of bis(3–Ammonio–1–hydroxypropylidene–1,1–bisphosphonate–O,O')–diaqua–zinc(II) [13, 15].

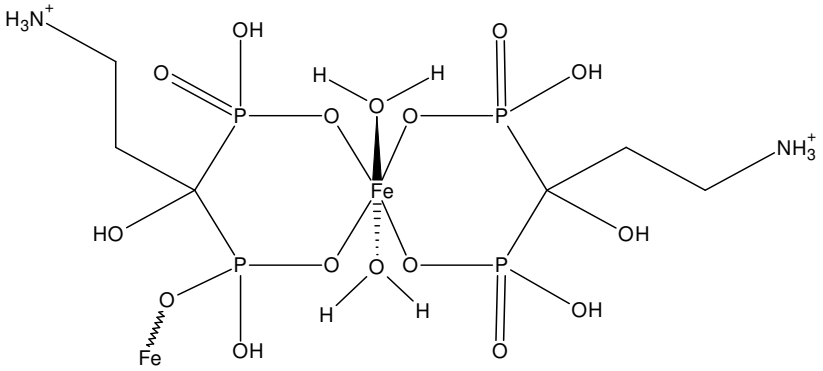


(a)

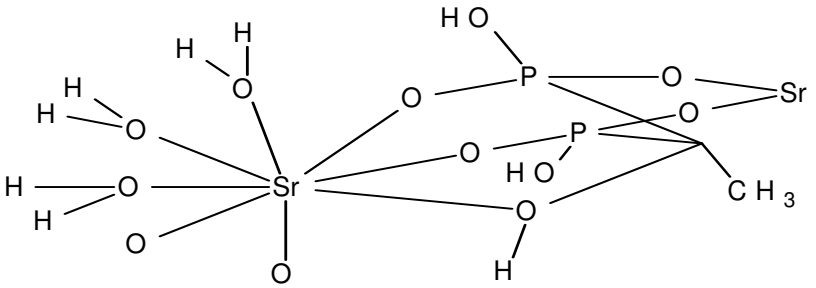


(b)

**Figure 4.16**: Crystallographic structures of a) catena–[bis($\mu_2$–3–Ammonium–1–hydroxypropylidene–1,1–bis(phosphonato)–iron(II) [14, 15] and b) Strontium(II) dihydrogen ethane-1-hydoxy-1,1-diphosphonate trihydrate [15].

Thus the R–group acts as a spectator during complexation and this validates the assumption made in this work. This supports the model $M_2(HL)$ and MHL obtained from the refinement operations in this work. There are no reported crystal structures which show that R-group of the APD ligand being involved in complexation with the metal ion of interest. In addition there are no reported crystal structures for the ligands APD and HEDP which shows these ligands forming bonds with the oxygen atoms on one phosphonate group [15]. Therefore we propose the structures for the $Cd^{II}$ complexes, $M_2(HL)$ and MHL attained in this work as follows:

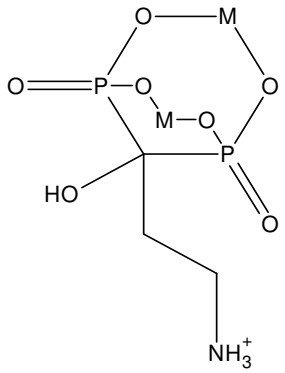


$M_2(HL)$

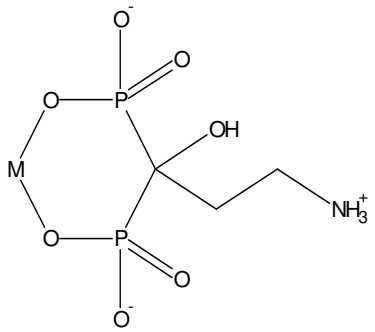


MHL

However these are not the only possible structures for these complexes. Another possibility is that the O-atom of the hydroxyl group can form bonds with the metal ion and similar complexes were reported for a similar ligand HEDP and the Sr complex is shown in Figure 4.16 (b) as an example. Thus one can remove the $pKa_1$ of the APD ligand from the refinement of stability constants and redefine the ligand APD without the first protonation constant as L′ where L′ = HL as indicated in Table 4.4 (b). This means that the stability constants for the $Cd^{II}$–L′ complex as indicated in Table 4.4 (b) were obtained by subtracting $pKa_1$ value from the $Cd^{II}$–HL complex as indicated in Table 4.4 (a). For example, the metal complex MHL has a refined stability constant value of 19.21±0.02 and when the 1st protonation constant is ignored, this metal complex becomes ML′ with refined stability constant value of 7.36±0.02. While the metal complex $M_2$(HL) has a refined stability constant value of 24.15±0.03 and when the 1st protonation constant is ignored, it becomes $M_2$L′ with refined stability constant value of 12.30±0.03 and so on.

The reported stability constants for metal complex $M_2L$ for $Cd^{II}$–HEDP as shown in Table 4.6 are in principle the same as the one obtained for the $Cd_2^{II}$–L′. A value of 12.67±0.03 and 12.99±0.03 for the complex $M_2L$ was obtained by DPP and GEP, respectively, while a value of 12.30±0.03 was attained in this work by $DC_{TAST}$. The polarographic values are within 0.7 log units. On the other hand, the reported stability constants values for metal complex ML for $Cd^{II}$–HEDP are the same as the one determined in this work $Cd^{II}$–L′ by $DC_{TAST}$. The reported values are 7.26±0.02 and 7.10±0.04; they were determined by DPP and GEP, respectively, and the value attained in this work is 7.36±0.02. In this case the polarographic values are within 0.1 log units.

**Table 4.6**: Comparison of stability constant values of $Cd^{II}$ complexes for ligands HEDP and APD determined in this work and elsewhere. (L′ = HL, protonated APD)

| Ligand | Equilibria | log *β* | Reference |
|---|---|---|---|
| HEDP | $2M + L = M_2L$ | 12.67±0.03[a] | [16] |
| | | 12.99±0.03[b] | |
| APD | $2M + L' = M_2L'$ | 12.30±0.03 | This work |
| HEDP | $M + L = ML$ | 7.26±0.02[a] | [16] |
| | | 7.10±0.04[b] | |
| APD | $M + L' = ML'$ | 7.36±0.02 | This work |

[a] results from DPP and [b] results from GEP.

This suggests that the strength of these metal complexes is similar because complexation of the metal ion by the ligand in solution occurs at the phosphonate oxygen atoms for both ligands. In conclusion, it has been reported in literature that the potency of APD is 100 times that of HEDP (i.e. to deliver radionuclei of interest to bone surface). It has been demonstrated in this work that the mode of complex formation for both HEDP and APD is the same. Thus the potency of APD is not related to the strength of the APD complexes, but might be related to interaction of the R-group in APD with the bone environment.

### 4.2.2 $Pb^{II}$–APD system by DCP: Titration at $L_T$:$M_T$ ratio 40, $[M_T] = 9.99 \times 10^{-5}$ M.

#### *4.2.2.1 Fitting of the polarographic data*

Polarograms for the $Pb^{II}$–APD system were initially fitted using the same approach and Equations 56-58 as it was done for $Cd^{II}$–APD system. Selected fitted polarograms for $Pb^{II}$–APD system are shown in Figure 4.17. In polarographic studies, the half-wave potential for the free metal ion, $E_{1/2}$(M), serves as the reference potential in calculating the shift in half-wave potential, $\Delta E_{1/2}$, due to complexation in the presence of ligand at a particular pH (as described by Equation 42). In this case of $Pb^{II}$–APD system, the $E_{1/2}$(Pb) recorded was –379.80 mV, the corresponding $I_d$ was 6.76 in arbitrary units and $\delta$ was 0.98; an example of a recorded DC-wave at pH 4.50 for the free metal ion is shown in Figure 4.17.

After addition of the acidic APD ligand solution, the half-wave potential value of -398.99 mV was recorded, $I_d$ dropped to 3.27, and the degree of electrochemical reversibility $\delta$ remained unchanged (1.0, see Figure 4.17). This means that the half-wave potential shifted by about 20 mV and the limiting diffusion current dropped by more than 50 %. This shift can be attributable to the complexation of the metal ion on addition of the ligand solution and the drop in $I_d$ can be mainly attributable to dilution on addition of the ligand solution (since dilution was 100 %) and slightly due to complexation. Since the dilution on ligand solution addition was significant, it was necessary to account for the drop in limiting diffusion current. The limiting diffusion current, $I_d$ was calculated to be 3.38 after accounting for dilution as follows:

$I_d = I_{d,r} \times (V_{initial}/V_{Total}) = 6.76 \times (10/20) = 3.38$

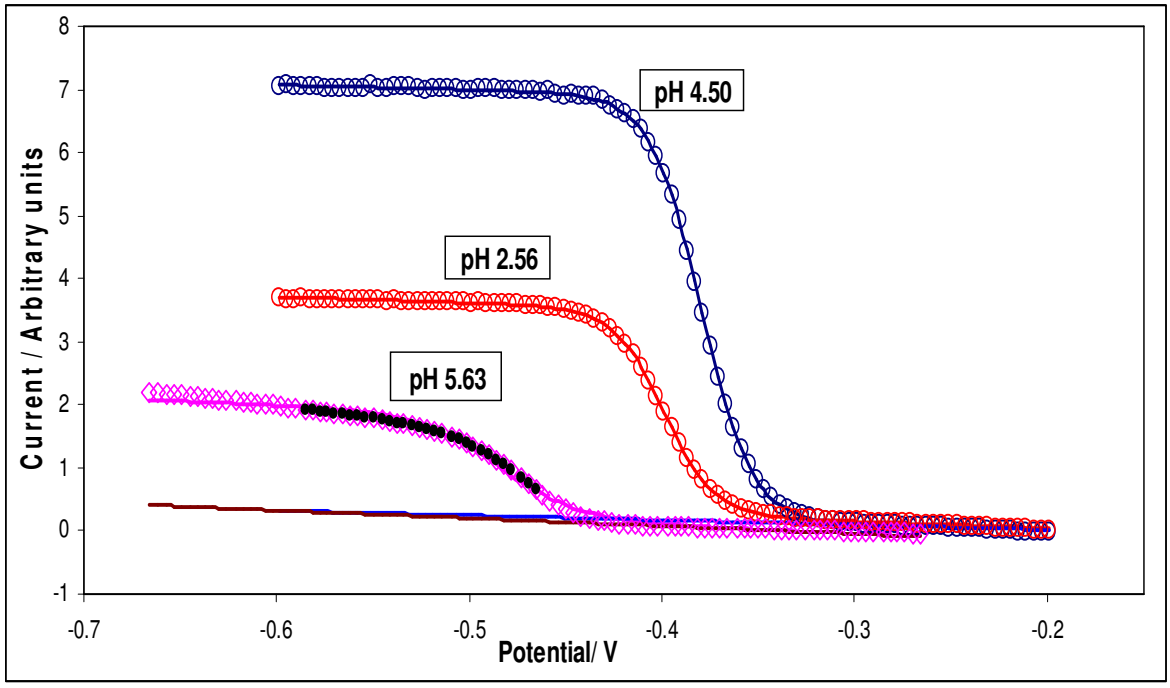


**Figure 4.17:** Selected fitted polarograms for $Pb^{II}$–APD system $L_T$:$M_T$ ratio 50, initial [$M_T$] = 9.99 × $10^{-5}$ M, at ionic strength μ = 0.15 M (NaCl) and 25 °C. The circles represent the experimentally observed points at particular applied potential and the solid lines represent the fitted curves.

where $I_d$ is the limiting diffusion current after accounting for dilution, $I_{d,r}$ is the recorded limiting diffusion current of the free metal ion only, $V_{initial}$ is the volume for the solution containing only the free metal ion and $V_{Total}$ is the total initial volume of the sample after ligand solution addition. The recorded $I_d$ after the addition of the ligand solution is 3.27. This shows that a drop of about 0.11 units in $I_d$ was due to complexation.

Polarograms were fitted initially using Equations 56–58, from this fitting procedure, $\delta$ decreased from 1.0 at pH 2.50 to 0.6 at pH 5.63 which means that the system was fully reversible initially at low pH and departed from electrochemical reversibility as pH increased and became quarsi-reversible at pH 5.63. The fitting of polarograms using Equation 56 in the pH region where departure from electrochemical reversibility is large results in poorly fitted curves and wrong values/estimates for the fitted parameters, i.e. half-wave potential and limiting diffusion current as shown by polarogram recorded at pH 5.63 in Figure 4.17. This will result in erroneous values of refined stability constants. The same scenario occurs when the polarograms are fitted using Equation 56 and correcting the $E_{1/2}$ potentials by deleting points to account for departure from electrochemical reversibility (deleted points shown by filled black points for polarogram recorded at pH

5.63 in Figure 4.17), and fixing delta at 1 assuming the electrochemical process is reversible.

To avoid this complication, Ružić-based curve fitting was employed to account for the departure from electrochemical reversibility [17] and was used were departure was significant, that is from pH 4.30 where $\delta$ was 0.94. Ružić -based curve fitting is based on the following equation:

$$I_r = I_d / ((exp(\frac{nF}{RT} \times (x - E_{1/2}{}^r))) + (exp(\frac{\alpha nF}{RT} \times (x - E_{1/2}{}^{irr}))) + 1) \quad (59)$$

$$I_b = a + b \times x \quad (60)$$

$$I_t = I_r + I_b \quad (61)$$

where $I_r$, $I_b$ and $I_t$ represent the reduction, background and total currents, respectively. $I_d$ is the limiting diffusion current, $E_{1/2}{}^r$ is the reversible half-wave potential, $E_{1/2}{}^{irr}$ is the irreversible half-wave potential corresponding to the irreversible part of the DC wave, $\alpha$ is the cathodic transfer coefficient and $x$ is the applied potential, n, R, F and T have their usual meaning.

Polarograms from pH 4.30 were fitted using Equation 59 with all parameters varied and all points allowed for each curve. An example of a fitted DC polarogram using Equation 59 is shown as circles in Figure 4.18 and the reversible DC wave predicted by the Ružić fitting procedure is shown as solid-bold line in Figure 4.18. The computed reversible half-wave potentials, $E_{1/2}{}^r$ and the limiting diffusion current predicted for the reversible process, $I_d$ were obtained from this fitting procedure and were used for the modelling and refinement of stability constants for this metal-ligand system. Therefore the use of Equation 59 is advantageous when a system departs from electrochemical reversibility and it does not require one to delete some points and no parameters need to be fixed during the fitting process.

The recorded polarograms above pH 5.63 were distorted to such a degree that it was impossible to fit them even with Ružić-based equation and as such they were not used in the interpretation of complexes formed.

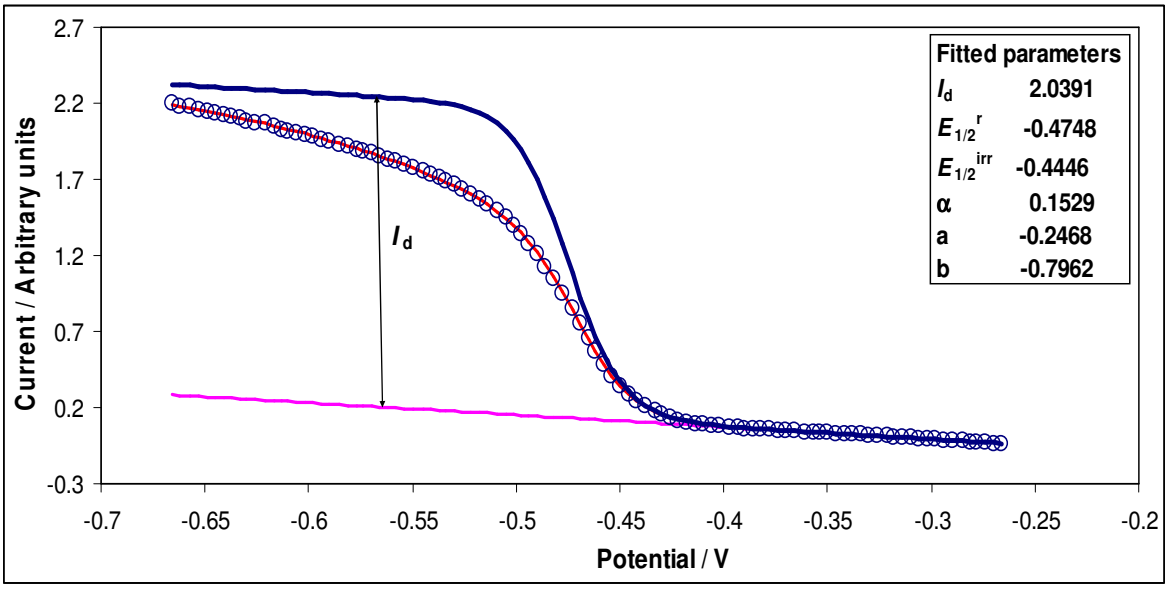


**Figure 4.18:** Selected polarogram for $Pb^{II}$–APD system ratio 50, $[M_T] = 9.99 \times 10^{-5}$ M, recorded at pH 5.63 and fitted using the Ružić-based Equation 58, ionic strength μ = 0.15 M (NaCl) and 25 °C. The circles represent the experimentally observed points at particular applied potential and the line represents the fitted curve. The thick solid line represents the expected sigmoidal observed polarogram if the system was assumed to be fully reversible.

### *4.2.2.2 Modelling of $Pb^{II}$–APD system*

a) Variation in limiting diffusion current, $I_d$ vs. pH

The expected limiting diffusion current decreases slightly in the pH range 2.50 to 5.63, seen in Figure 4.19 as diamonds. This means that the decrease in limiting diffusion current due to dilution on addition of the base titrant solution is not significant. However, the normalised limiting diffusion current (seen as triangles in Figure 4.19) vary from 1.0 at pH about 2.50 to 0.61 at pH 5.63. In region I, the normalised diffusion current is constant, this suggests the formation of labile metal complex(es) in solution on the polarographic time scale used, which means the homogenous equilibria of complexes are fast compared to the time scale of the experiment. In region II, the normalised diffusion current starts to decrease; this indicates the formation of another labile metal complex(es) with slightly lower diffusion coefficient(s) than the preceding metal complex(es). In region III, the normalised limiting diffusion current decreases significantly to a minimum of about 0.61. This indicates the formation of non-labile metal complex(es) in this pH range and the labile part of the metal-ligand system starts to "disappear".

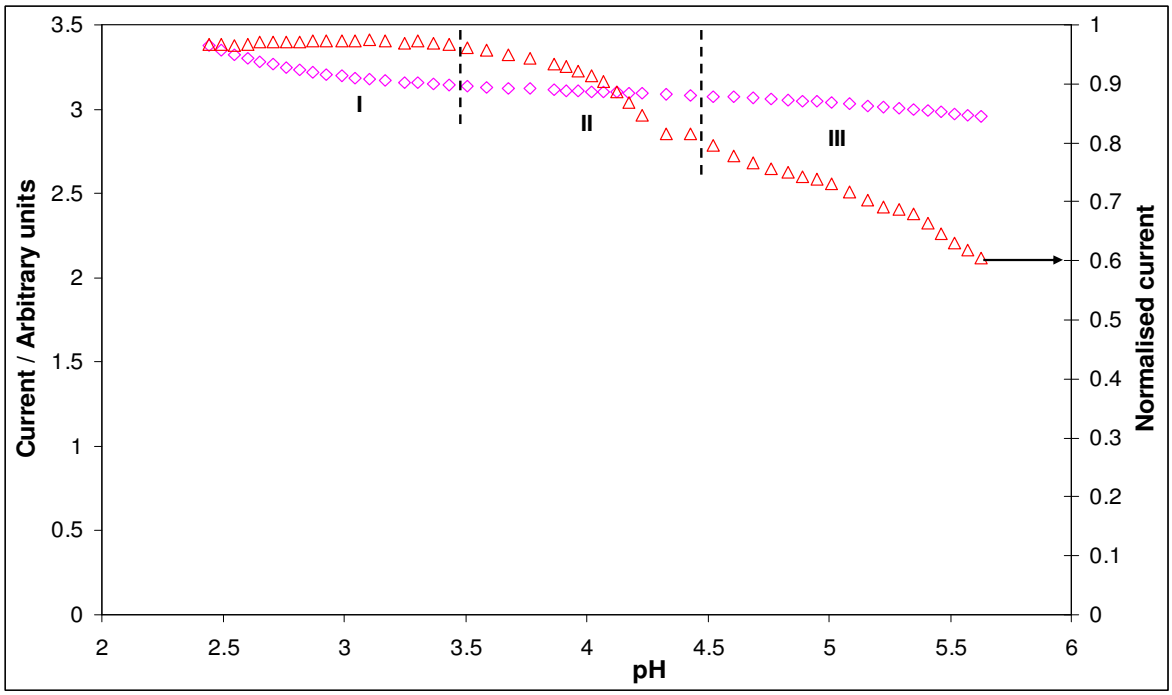


**Figure 4.19:** Variation in limiting diffusion current $I_d$ vs. pH for $Pb^{II}$–APD system studied by $DC_{TAST}$ at $[L_T]$:$[M_T]$ ratio 50, initial $[M_T] = 9.99 \times 10^{-5}$ M, at ionic strength $\mu = 0.15$ M (NaCl) and 25°C. The triangles represent the normalised limiting diffusion current and the diamonds represent the expected limiting diffusion current assuming no ligand is present in solution.

This means that the homogeneous equilibria of metal complex(es) formed in this pH range are sluggish compared to the polarographic time scale employed. The decrease in the normalised limiting diffusion current with increase in pH is attributable to complex formation because in the absence of the ligand, the current does not decrease much. Since there is a decrease in normalised limiting diffusion current, only the virtual half-wave potentials (calculated from Equation 48) will be used in the modelling and refinement of stability constants.

b) Variation in reversible half-wave potential, $E_{1/2}^{r}$(virt) vs. pH

The variation in reversible half-wave potential, $E_{1/2}^{r}$(virt) vs. pH for this particular system is shown in Figure 4.20. There is no shift observed between pH 2.50 and 3.20, this does not provide information as to whether there are complexes formed in solution or not. Since the form of the ligand in the entire pH range in which data was collected is $H_3L$, this suggests reduction of protonated metal complexes (if at all complexes are formed) according to the following electrochemical process:

$M(H_3L) + 2e = M(Hg) + H_3L$

in which no protons are involved in the reduction process and hence no shift is expected when this metal complex is formed in a solution. Although this plot does not provide information regarding the presence of the complex $M(H_3L)$, the drop in the limiting diffusion current of about 0.11 units of current as well as a shift in potential of about 20 mV after addition of the ligand solution support the formation of the complex $M(H_3L)$ in a solution.

A slope of 31 mV per pH unit is observed in the pH range 3.80 and 4.50. This suggests the reduction of the following metal-ligand complexes at the mercury electrode surface:

$M(H_2L) + H + 2e = M(Hg) + H_3L$
and/or
$M_2(HL) + 2H + 4e = M(Hg) + H_3L$.

This slope is in principle the same as the theoretically expected slope for these processes, which is about 30 mV / pH unit. A slope of 41 mV per pH unit can be seen in the pH range of about 4.6 to 5.6 and since the dominant form of the ligand is still $H_3L$, the following electrochemical processes are proposed to be occurring at the mercury-solution interface:

$M(HL) + 2H + 2e = M(Hg) + H_3L$
and/or
$M_2L + 3H + 4e = 2M(Hg) + H_3L$.

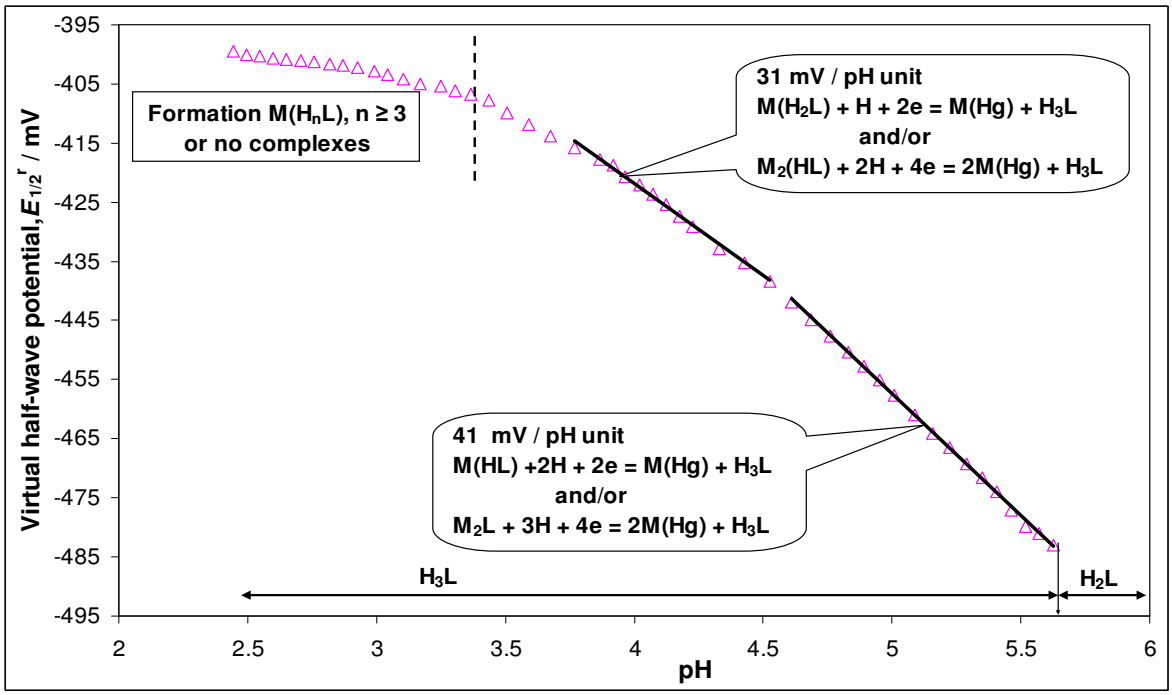


**Figure 4.20:** Variation in reversible half-wave potential $E_{1/2}^r$(virt) vs. pH for $Pb^{II}$–APD system studied by $DC_{TAST}$ at $[L_T]$:$[M_T]$ ratio 50, initial $[M_T] = 9.99 \times 10^{-5}$ M, at $\mu = 0.15$ M (NaCl) and 25 °C.

The expected slopes for these processes are 60 and 45 mV / pH unit, respectively, if these species are fully formed in solution and thus the observed slope of 41 mV / pH unit suggests the presence of a mixture of complexes. If metal complexes with theoretical slopes of 30 and 60 mV / pH unit are present in equal amounts in solution, then a slope of 45 mV / pH unit is expected to be seen.

From this analysis it follows that the following complexes are predicted to be formed in solution: $M(H_3L)$, $M(H_2L)$ and/or $M_2(HL)$, and $M(HL)$ and/or $M_2L$.

c) Variation in reversible half-wave potential, $E_{1/2}^r$(virt) vs. log $[H_nL]$.

To confirm formation of metal complexes suggested by the graph of reversible half-wave potential $E_{1/2}^r$(virt) vs. pH, the plot of reversible half-wave potential $E_{1/2}^r$(virt) vs. log $[H_nL]$ was used [10]. The plot of reversible half-wave potential $E_{1/2}^r$(virt) vs. log $[H_3L]$ is indicated in Figure 4.21. There is not well–defined slope which can confirm the presence of metal complex $M(H_3L)$ in solution.

In Figure 4.22, a graph of reversible half-wave potential, $E_{1/2}^{r}$(virt) vs. log [$H_2L$] is shown. A slope of about 30 mV / log unit is observed, this suggests formation of metal complex M($H_2L$) according to the following complex formation reaction:

$M + H_2L = M(H_2L)$.

This complex is predicted to be formed in the same pH range as in the plot of reversible half-wave potential $E_{1/2}^{r}$(virt) vs. pH. This confirms the presence of this metal complex in solution at this particular pH, or log [$H_2L$] range.

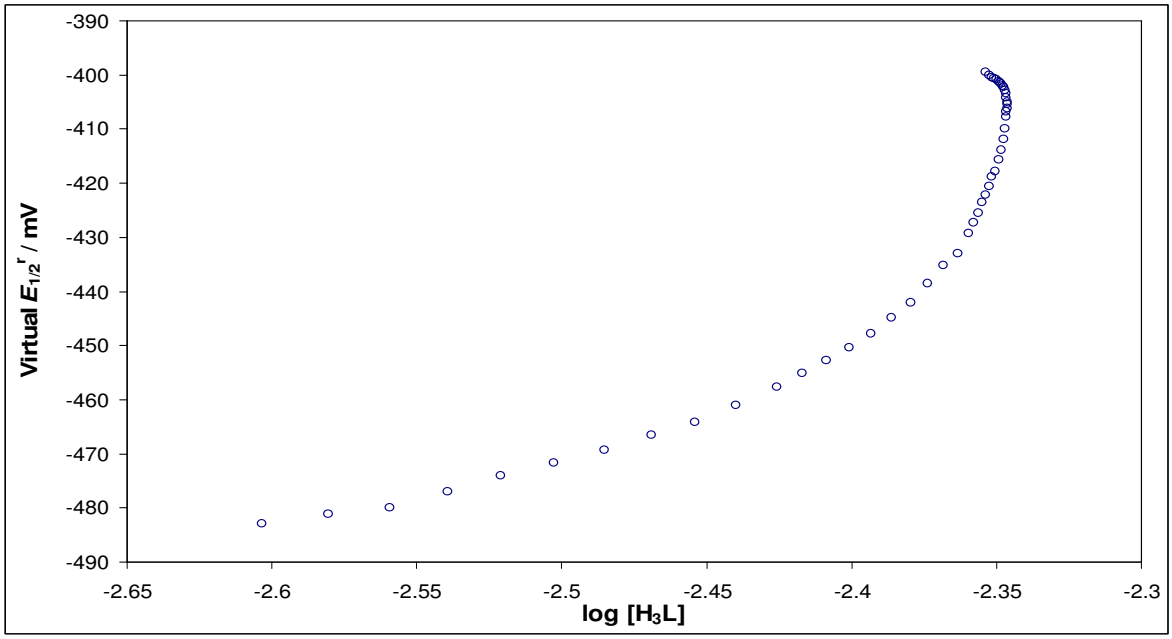


**Figure 4.21:** Variation in reversible half-wave potential $E_{1/2}^{r}$(virt) vs. log [$H_3L$] for $Pb^{II}$–APD system studied by $DC_{TAST}$ at [$L_T$]:[$M_T$] ratio 50, initial [$M_T$] = $9.99 \times 10^{-5}$ M, at ionic strength μ = 0.15 M (NaCl) and 25 °C.

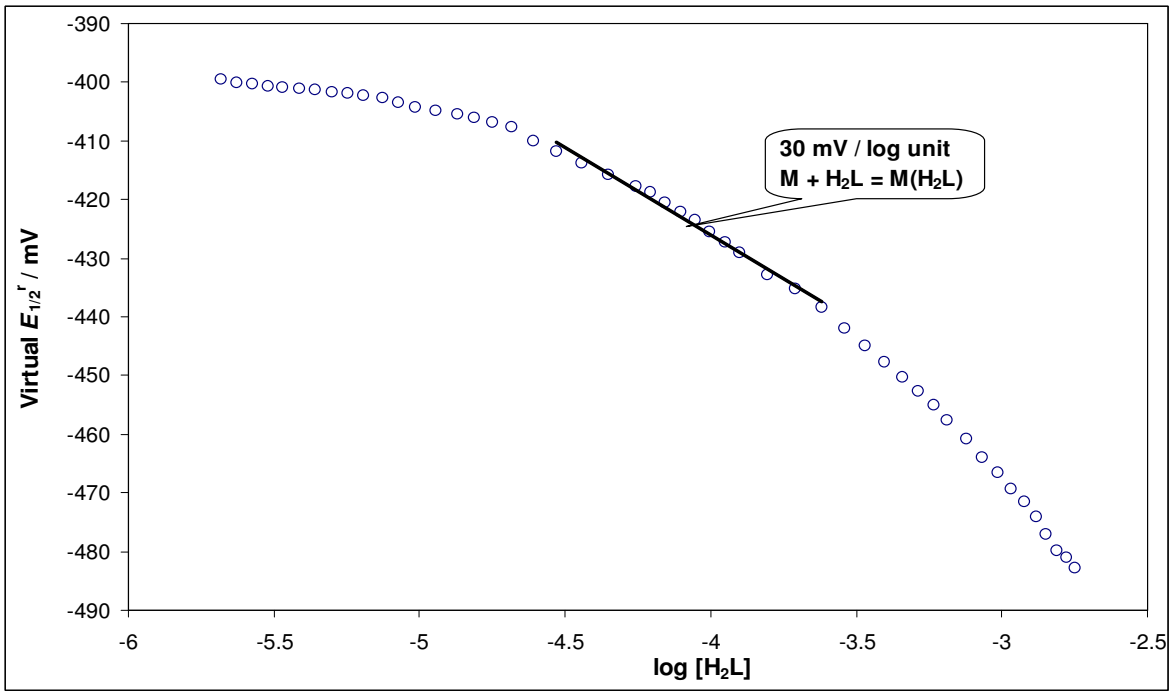


**Figure 4.22:** Variation in reversible half-wave potential $E_{1/2}^{r}$(virt) vs. log [$H_2L$] for $Pb^{II}$–APD system studied by $DC_{TAST}$ at [$L_T$]:[$M_T$] ratio 50, initial [$M_T$] = $9.99 \times 10^{-5}$ M, at ionic strength μ = 0.15 M (NaCl) and 25 °C.

To confirm formation of complexes containing HL form of the ligand, a plot of reversible half-wave potential $E_{1/2}^{r}$(virt) vs. log [HL], as indicated in Figure 4.23 was analysed. A slope of 15 mV / log unit can be seen; this slope indicates the formation of metal complex $M_2$(HL) according to the following complex formation reaction:

$2M + HL = M_2(HL)$.

This slope is pinpoint the theoretically expected slope for this process and indicates that the metal complex $M_2$(HL) is fully formed in solution. It must be stressed that this complex is formed in the same pH range as the predicted by the plot of reversible half-wave potential $E_{1/2}^{r}$ vs. pH in Figure 4.20. This strongly supports the presence of this complex in solution.

A slope of 24 mV / log unit is observed at high [HL] values. This might indicate the formation of the metal complex M(HL) in solution at this log [HL] range at the mercury-electrode interface according to the following complex formation reaction:

$M + HL = M(HL)$.

The expected slope for this process is 30 mV / log unit and thus the observed slope suggest that this complex is not fully formed in solution. Thus the presence of the complex M(HL) is suggested in the same pH range as predicted by the plot of reversible half-wave potential $E_{1/2}^{r}$(virt) vs. pH in the same pH range.

To check the presence of species of type $M_pL_n$ ($n \geq 1$) in solution, a graph of reversible half-wave potential $E_{1/2}^{r}$(virt) vs. log [L] must be analysed. A maximum slope of 15 mV / log unit was observed as indicated in Figure 4.24. This well–developed slope is exactly the expected slope which confirms the presence of the metal complex $M_2L$ species in solution according to the following containing complex formation reaction:

$2M + L = M_2L$.

This slope is observed in the same pH range as predicted to be formed on the graph of reversible half-wave potential, $E_{1/2}^{r}$(virt) vs. pH.

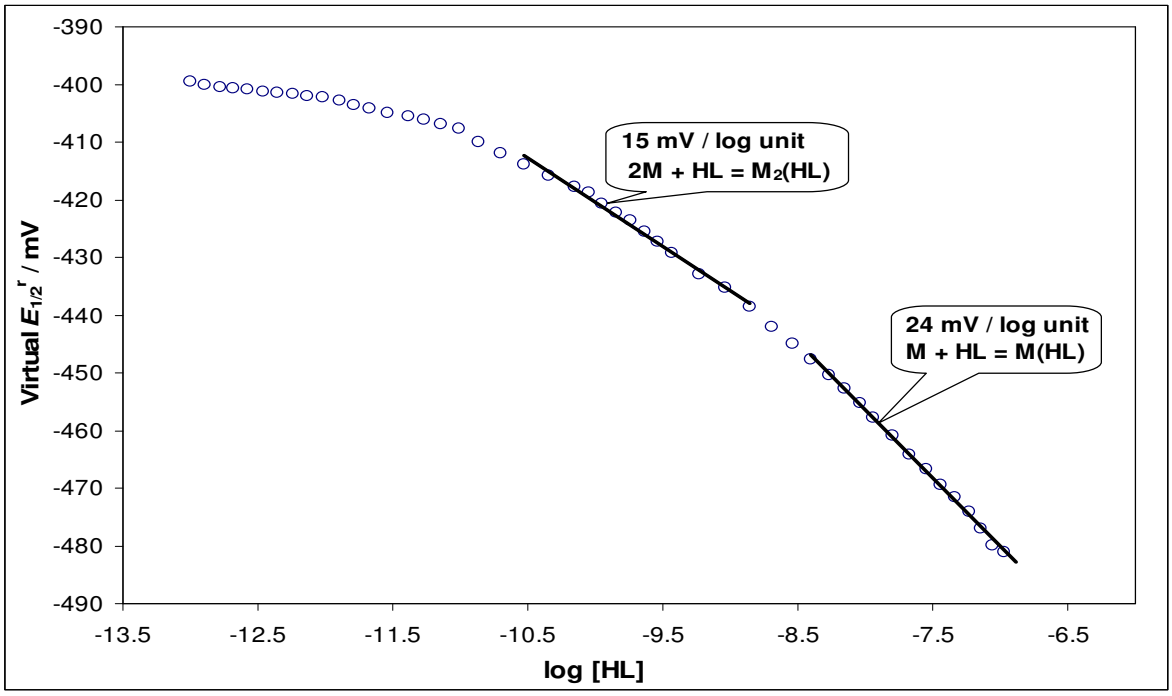


**Figure 4.23:** Variation in reversible half-wave potential $E_{1/2}^{r}$(virt) vs. log [HL] for $Pb^{II}$–APD system studied by $DC_{TAST}$ at $[L_T]$:$[M_T]$ ratio 50, initial $[M_T] = 9.99 \times 10^{-5}$ M, at ionic strength $\mu$ = 0.15 M (NaCl) and 25 °C.

From the analyses of reversible half-wave potential $E_{1/2}^{r}$(virt) vs. log $[H_nL]$ above, there is no evidence of the presence of the complex $M(H_3L)$ in solution as no well defined slope

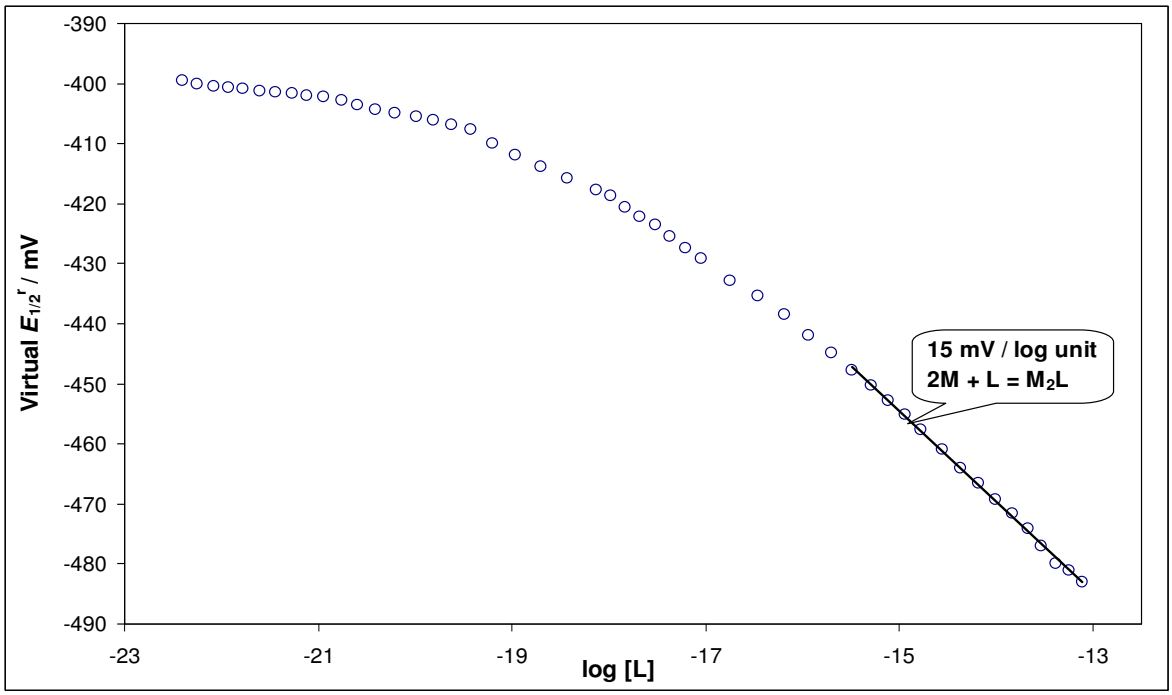


**Figure 4.24:** Variation in reversible half-wave potential $E_{1/2}^{r}$(virt) vs. log [L] for $Pb^{II}$–APD system studied by $DC_{TAST}$ at $[L_T]$:$[M_T]$ ratio 50, initial $[M_T] = 9.99 \times 10^{-5}$ M, at ionic strength $\mu = 0.15$ M (NaCl) and 25 °C.

corresponding to formation of this complex was observed. On the other hand, the presence of complexes $M(H_2L)$, $M_2(HL)$, $M(HL)$ and $M_2L$ was supported.

### *4.2.2.3 Optimisation of the $Pb^{II}$–APD model and refinement of stability constants*

Different metal-ligand models were tested and fitted in order to obtain the refined stability constant values. The complex formation curves were used for the optimisation of the metal-ligand models and refinement of stability constants. The metal-ligand models were optimised until the calculated complex formation curve (CCFC) fits best into the experimental complex formation curve (ECFC). Different metal-ligand models with refined stability constants are shown in Table 4.7 (b).

One can notice that in all the fitted models in Table 4.7 (b), the metal complex $M(H_3L)$ is present and has the most consistent refined stability constant. One can also note that there are many possibilities of models to be considered for this system. The model containing metal complexes $M(H_3L)$, $M_2(HL)$ and $M_2L$ with refined stability constants as log β values

30.35±0.01, 28.05±0.03 and 23.74±0.02, respectively, is one of the plausible models for this system.

**Table 4.7**: (a) Protonation constants for the ligand APD, dissociation constants of water and overall stability constants of $Pb^{II}$ complexes with $OH^-$ at μ = 0.15 M NaCl and t 25.0 °C.

| **Equilibrium** | **log β** |
|---|---|
| $H^+ + OH^- = H_2O$ | 13.42 |
| $L + H = LH$ | 11.85 |
| $LH + H = H_2L$ | 9.76 |
| $H_2L + H = H_3L$ | 5.77 |
| $H_3L + H = H_4L$ | 1.47 |
| $Pb^{2+} + OH^- = Pb(OH)^+$ | 6.00 |
| $Pb^{2+} + 2OH^- = Pb(OH)_2$ | 10.30 |
| $Pb^{2+} + 3OH^- = Pb(OH)_3^-$ | 13.30 |
| $2Pb^{2+} + OH^- = Pb_2(OH)^{3+}$ | 7.60 |
| $3Pb^{2+} + 4OH^- = Pb_3(OH)_4^{2+}$ | 31.70 |
| $4\ Pb^{2+} + 4OH^- = Pb_4(OH)_4^{4+}$ | 35.20 |
| $6Pb^{2+} + 8OH^- = Pb_6(OH)_8^{4+}$ | 67.40 |
| $Pb^{2+} + 2OH^- = Pb(OH)_2(s)$ | –15.00 |

(b) Overall stability constants for $Pb^{II}$ with APD obtained in this work by $DC_{TAST}$ using curve fitting described at ionic strength μ = 0.15 M NaCl and 25 °C.

| **Technique** | **Ratio** | **Equilibrium** | **log β** | **Overall fit/ mV** |
|---|---|---|---|---|
| $DC_{TAST}$ | 50 | $M + H_3L = M(H_3L)$ | 30.35±0.01 | ±0.519 |
| | | $2M + HL = M_2(HL)$ | 28.05±0.03 | |
| | | $2M + L = M_2L$ | 23.74±0.02 | |
| | | $M + H_3L = M(H_3L)$ | 30.32±0.01 | ±0.319 |
| | | $2M + HL = M_2(HL)$ | 28.18±0.02 | |
| | | $M + HL = MHL$ | 22.25±0.01 | |
| | | $M + H_3L = M(H_3L)$ | 30.27±0.02 | ±0.519 |
| | | $M + H_2L = M(H_2L)$ | 26.91±0.03 | |
| | | $2M + L = M_2L$ | 23.68±0.02 | |
| | | $M + H_3L = M(H_3L)$ | 30.22±0.02 | ±0.221 |
| | | $M + H_2L = M(H_2L)$ | 27.02±0.01 | |
| | | $M + HL = MHL$ | 22.19±0.01 | |
| | | $M + H_3L = M(H_3L)$ | 30.31±0.04 | ±0.495 |
| | | $2M + HL = M_2(HL)$ | 27.71±0.45 | |
| | | $M + H_2L = M(H_2L)$ | 26.64±0.38 | |
| | | $2M + L = M_2L$ | 23.71±0.03 | |
| | | $M + H_3L = M(H_3L)$ | 30.25±0.04 | ±0.319 |
| | | $2M + HL = M_2(HL)$ | 27.01±0.48 | |
| | | $M + H_2L = M(H_2L)$ | 27.00±0.19 | |
| | | $M + HL = MHL$ | 22.20±0.03 | |
| | | $M + H_3L = M(H_3L)$ | 30.25±0.05 | ±0.973 |
| | | $2M + HL = M_2(HL)$ | 27.00±0.35 | |
| | | $M + H_2L = M(H_2L)$ | 27.00±0.37 | |
| | | $M + HL = MHL$ | 21.92±0.11 | |
| | | $2M + L = M_2L$ | 23.10±0.40 | |

This model has the overall fit in CCFC into the ECFC of ±0.519 mV. The other plausible model is the one containing species $M(H_3L)$, $M_2(HL)$ and MHL with refined stability values as log β values 30.32±0.01, 28.18±0.02 and 22.25±0.01, respectively, with the

overall fit in CCFC into the ECFC of ±0.319 mV. From the modelling part of the metal-ligand system (see Figure 4.20), either one or both species $M_2L$ and MHL are formed in solution in the same pH range. This is consistent with the fitted models as discussed earlier. The other possibility is to incorporate the metal complex $M(H_2L)$ into the metal-ligand system instead of the complex $M_2HL$ as these two complexes are predicted to be in solution in the same pH range. Thus when the model containing metal complexes $M(H_3L)$, $M(H_2L)$ and $M_2L$ was fitted the following refined stability constants 30.27±0.02, 26.91±0.03 and 23.68±0.03, respectively. The overall fit of CCFC into the ECFC for this system is ±0.519 mV which is the same as for the model containing complexes $M(H_3L)$, $M_2(HL)$ and $M_2L$. This confirms the fact that either one or both of these complexes are formed in the same pH range. When the model containing species $M(H_3L)$, $M_2(HL)$ and MHL was fitted (i.e. $M_2L$ being replaced by MHL) the following refined stability constants as log β values 30.22±0.02, 27.02±0.01 and 22.19±0.01, respectively, were obtained. This particular model has the best overall fit of CCFC into the ECFC of ±0.221 mV.

From the modelling point of view (see Figure 4.20), the complexes $M_2(HL)$ and $M(H_2L)$ were predicted to be formed in solution in the same pH range. It was important to check the effect of incorporating both complexes in the metal-ligand models containing species $M(H_3L)$ and $M_2L$ or/and MHL. For the model $M(H_3L)$, $M_2(HL)$, $M(H_2L)$ and $M_2L$, the following refined stability constants were attained 30.31±0.031, 27.71±0.45, 26.64±0.38 and 23.71±0.03, respectively, with the overall fit of CCFC into ECFC of ±0.495 mV. Larger standard deviations in the refined stability constant values for complexes $M_2(HL)$ and $M(H_2L)$ were attained. This is in agreement with the modelling part of the metal-ligand system that these complexes are formed in the same pH range, hence the larger standard deviations in their refined stability constants is attained when they are both incorporated into the metal-ligand system. The same scenario was observed when the model containing metal complexes $M(H_3L)$, $M_2(HL)$, $M(H_2L)$ and MHL, (i.e. replacing the $M_2L$ complex by MHL). The refined stability constants for these complexes are 30.25±0.04, 27.01±0.48, 27.00±0.19 and 22.20±0.03, respectively, with the overall fit of CCFC into ECFC of ± 0.319 mV.

When all the metal complexes suggested from the modelling part of the metal-ligand system (see Figure 4.20), i.e. $M(H_3L)$, $M_2(HL)$, $M(H_2L)$, $M_2L$ and MHL, were fitted the following refined stability constants were attained 30.25±0.05, 27.00±0.35, 27.00±0.37,

21.92±0.11 and 23.10±0.40, respectively. The largest overall fit of CCFC into the ECFC of ±0.973 mV was obtained. All the refined stability constants in this case have larger standard deviations except for the metal complex $M(H_3L)$. This indicates that all the metal species suggested are present in solution because they could all be fitted into the metal-ligand model.

There are two final models which can be suggested for this metal-ligand system, namely:

1) $M(H_3L)$, $M(H_2L)$ and MHL.
2) $M(H_3L)$, $M_2(HL)$ and MHL.

The complex formation curve for the model 1) above with refined stability constants as indicated in Table 4.7 (b) is shown in Figure 4.25. This model has the lowest overall fit in CCFC into the CCFC. These final models are consistent with the models reported for $Cd^{II}$–HEDP system whereby the amine protonation constant is not present [16]. In addition these models are supported by the reported crystal structures of $Zn^{II}$–APD and $Fe^{II}$–APD as shown in Figures 4.15 and 4.16. The species distribution diagrams for different metal-ligand models are discussed in detail in the next section.

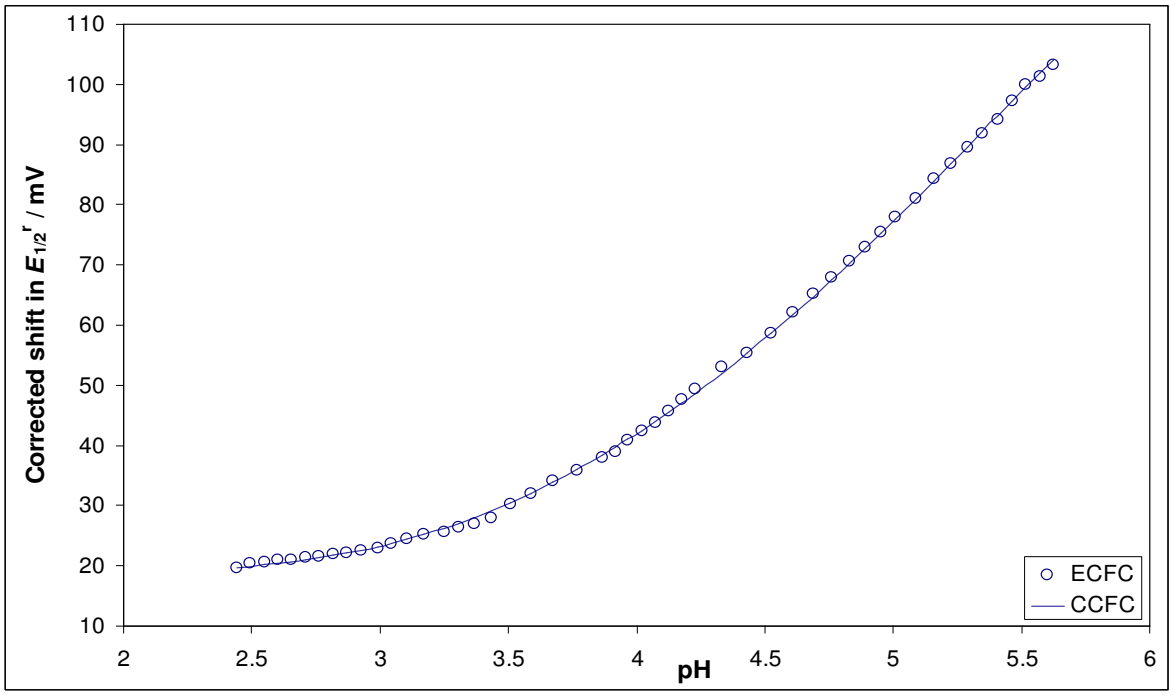


**Figure 4.25**: Experimental and calculated polarographic complex formation curves for $Pb^{II}$–APD system studied by $DC_{TAST}$ at $[L_T]:[M_T]$ = 40, $[M_T]$ = $1.25\times10^{-4}$ M, ionic strength μ = 0.15 M (NaCl) and 25 °C. The circles represent the experimentally observed points (ECFC) and the solid line represents the theoretically reproduced curve (CCFC) from the refined stability constants for the model containing species $M(H_3L)$, $M(H_2L)$ and MHL with refined stability as log β values 30.22±0.02, 27.02±0.01 and 22.19±0.01, respectively.

### *4.2.2.4 Species distribution diagrams*

The species distribution diagram for the model containing metal complexes $M(H_3L)$, $M(H_2L)$, $M_2(HL)$ and $M_2L$ is shown in Figure 4.26. When the experiment is started at pH about 2.5, the complex $M(H_3L)$ is fully formed in solution and forms about 75 % of the solution composition. This is consistent with the suggestion made earlier that this complex (i.e. $M(H_3L)$) is responsible for the drop in current of about 0.11 units and a shift in potential of about 20 mV after addition of the ligand solution into the polarographic cell. The complexes $M(H_2L)$ and $M_2(HL)$ are formed in the same pH range with the complex $M(H_2L)$ being slightly higher than $M_2(HL)$ complex. The metal complex $M(H_2L)$ is the major complex in a narrow pH range 3.6 to 4.0 and constitute about 40 % of solution composition while the $M_2(HL)$ constitute about 30 % of the solution composition. Above pH 4.0, the complex $M_2L$ becomes the major metal complex in solution.

On the other hand, when one looks at the species distribution diagram for the model containing complexes $M(H_3L)$, $M(H_2L)$, $M_2(HL)$ and MHL, as shown in Figure 4.27, the complex $M(H_3L)$ is the major complex at low pH and forms about 70 % of the solution composition. At pH about 3.2 the metal complex $M(H_2L)$ is the major complex in solution and is much higher than the complex $M_2(HL)$ and forms about 70 % of solution composition at pH about 4.0 while $M_2(HL)$ forms about 5 % of solution composition at this particular pH.

The complex MHL is the major complex in solution above pH about 4.7, unlike the complex $M_2L$ in Figure 4.26 which becomes predominant above pH about 4.0. It seems that the when the complex MHL is incorporated into the model instead of the complex $M_2L$, the formation of the complex $M(H_2L)$ is favoured over $M_2(HL)$ complex. From Figure 4.26 and 4.27 it was observed that the complexes $M(H_2L)$ and $M_2(HL)$ are formed in the same pH range as well as the complexes $M_2L$ and MHL. This is consistent with the modelling part of the metal-ligand system.

When one considers the species distribution diagram for the model containing all the species predicted to be formed in solution (i.e. $M(H_3L)$, $M(H_2L)$, $M_2(HL)$, MHL and $M_2L$) as shown in Figure 4.28, one can notice that again $M(H_3L)$ is the major complex at low pH values and forms about 70 % of the solution composition. Between pH about 3.2 and 5.0,

the complex $M(H_2L)$ is the major metal complex in solution and forms about 70 % of solution composition at pH about 4.0 while the complex $M_2(HL)$ forms about 5 % of solution composition at the same pH. Above pH 5.0 the metal complex MHL becomes the predominant species in solution. The complex $M_2L$ forms a maximum of 25 % of solution composition unlike MHL which forms about 70 % maximum.

It seems obvious, as far as the species distribution diagram for all the metal complexes predicted to be formed in solution is concerned, the type of complexes favoured are $M(H_2L)$ and MHL over the complexes $M_2(HL)$ and $M_2L$, but this does not mean that these complexes are not present in solution. When each type of these complexes is considered together with the complex $M(H_3L)$, the species distribution diagrams in Figure 4.29 and 4.30 were obtained. One can notice that the complexes $M(H_2L)$ and $M_2(HL)$ are enhanced in terms of solution composition unlike when they are both included in the metal-ligand model.

This is also the case for the complexes MHL and $M_2L$. This is why these complexes give larger standard deviations for the refined stability constants when fitted together.

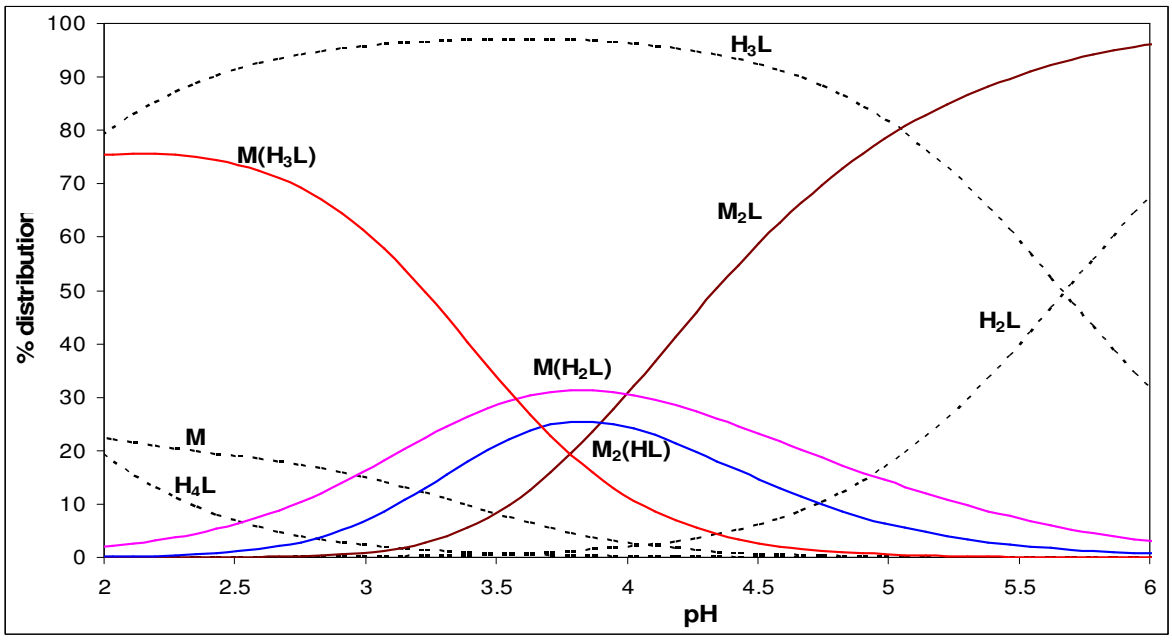


**Figure 4.26**: The species distribution diagram for the model $M(H_3L)$, $M(H_2L)$, $M_2(HL)$ and $M_2L$ for $Pb^{II}$–APD ratio 50 studied by $DC_{TAST}$, $[M_T] = 9.99 \times 10^{-5}$ M, at ionic strength $\mu = 0.15$ M (NaCl) and 25 °C.

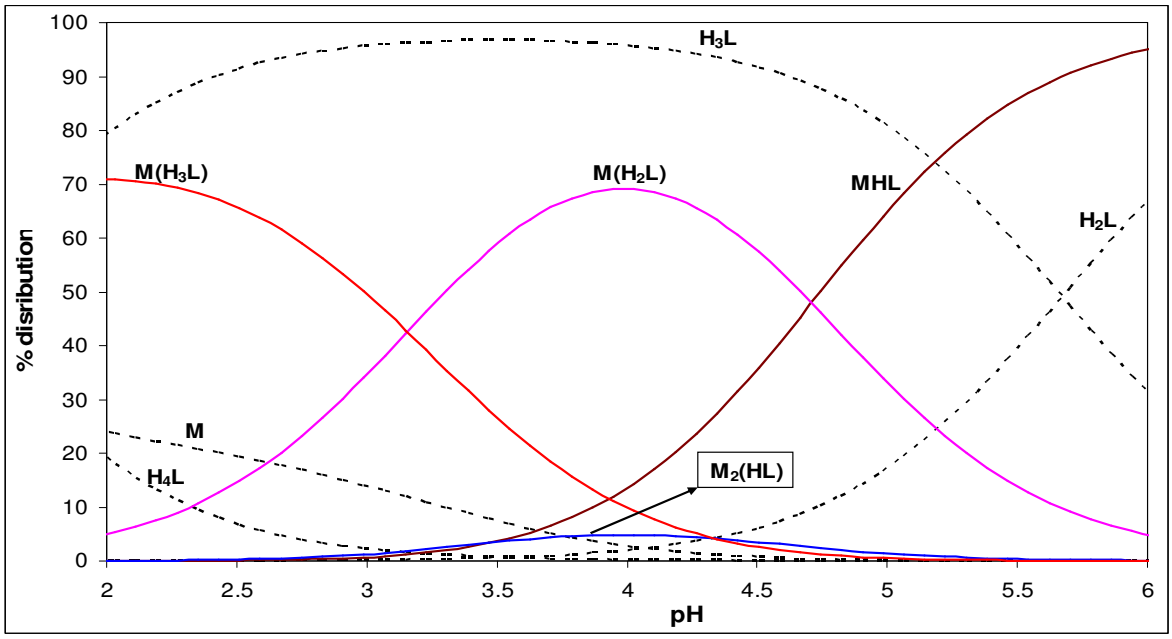


**Figure 4.27**: The species distribution diagram for the model $M(H_3L)$, $M(H_2L)$, $M_2(HL)$ and MHL for $Pb^{II}$–APD ratio 50 studied by $DC_{TAST}$, $[M_T] = 9.99 \times 10^{-5}$ M, at ionic strength $\mu = 0.15$ M (NaCl) and 25 °C.

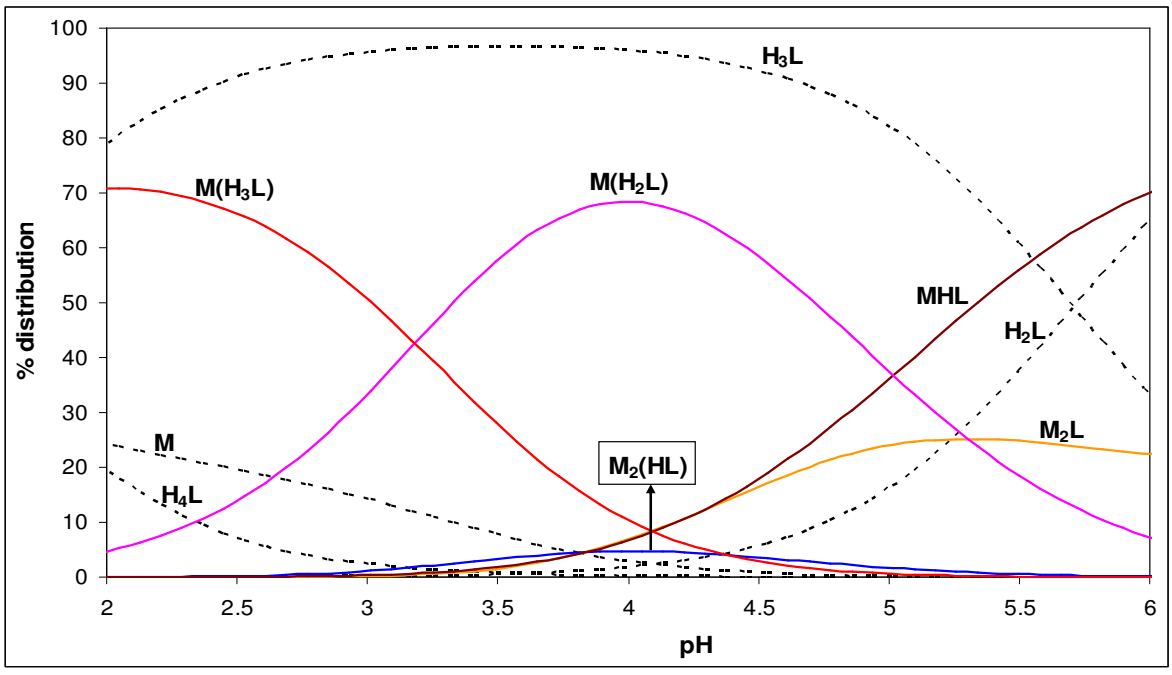


**Figure 4.28**: The species distribution diagram for the model $M(H_3L)$, $M(H_2L)$, $M_2(HL)$, MHL and $M_2L$ for $Pb^{II}$–APD ratio 50 studied by $DC_{TAST}$, $[M_T] = 9.99 \times 10^{-5}$ M, at ionic strength $\mu = 0.15$ M (NaCl) and 25 °C.

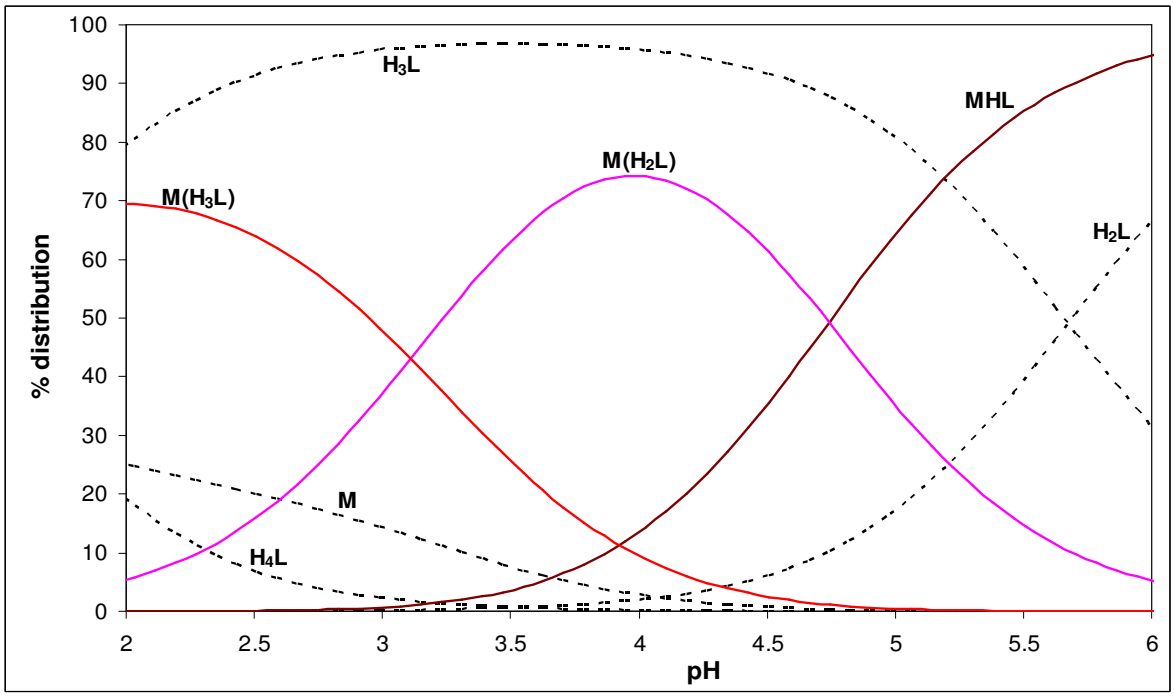


**Figure 4.29**: The species distribution diagram for final model $M(H_3L)$, $M(H_2L)$ and MHL for $Pb^{II}$–APD ratio 50 studied by $DC_{TAST}$, $[M_T] = 9.99 \times 10^{-5}$ M, at ionic strength $\mu = 0.15$ M (NaCl) and 25 °C.

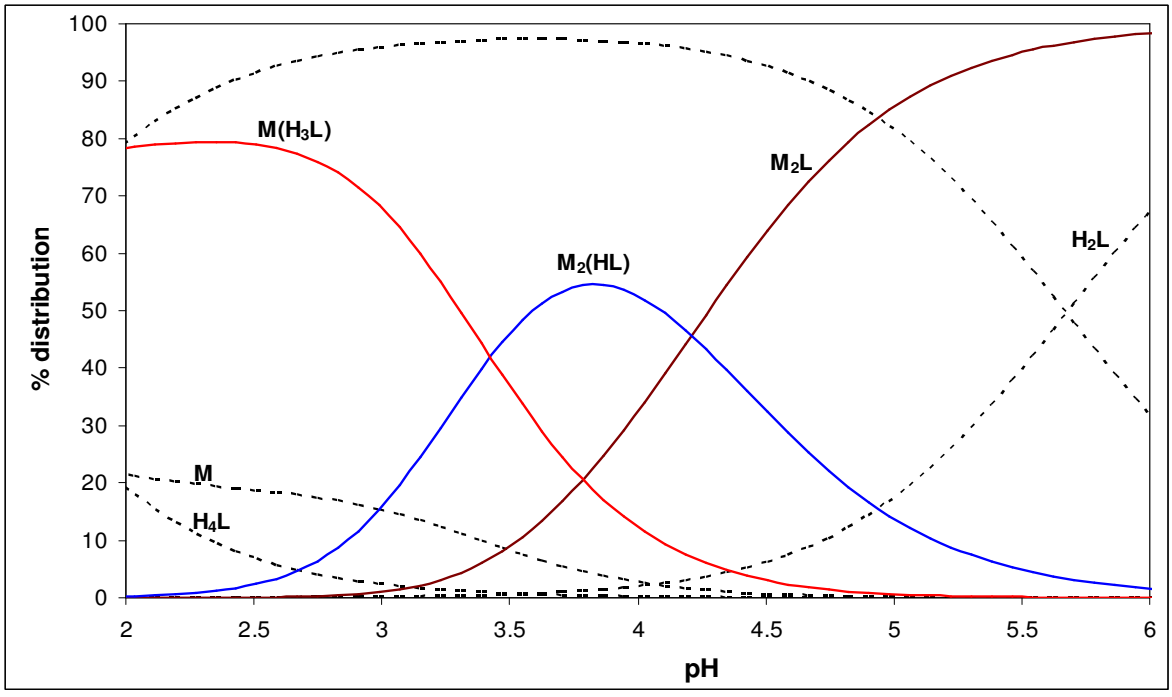


**Figure 4.30**: The species distribution diagram for model $M(H_3L)$, $M_2(HL)$ and $M_2L$ for $Pb^{II}$–APD ratio 50 studied by $DC_{TAST}$, $[M_T] = 9.99 \times 10^{-5}$ M, at ionic strength $\mu = 0.15$ M (NaCl) and 25 °C.

### *4.2.2.5 Comparison of formation constants for ligands APD and MDP with $Pb^{II}$ metal ion.*

In this work the metal complexes attained were all protonated except for the metal complex $M_2L$. The metal complexes such as $M_2(HL)$ and MHL have been attained for the $Pb^{II}$–APD system just like as it is the case for $Cd^{II}$–APD system. The proposed structures for these metal complexes are the same as for the $Cd^{II}$–APD system. The new metal complexes attained from the $Pb^{II}$–APD system are $M(H_3L)$, $M(H_2L)$ and $M_2L$. The proposed structures for these complexes are shown below.

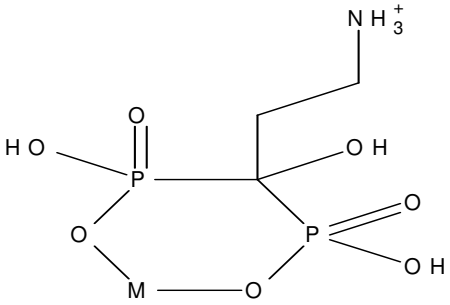

6–membered ring structure

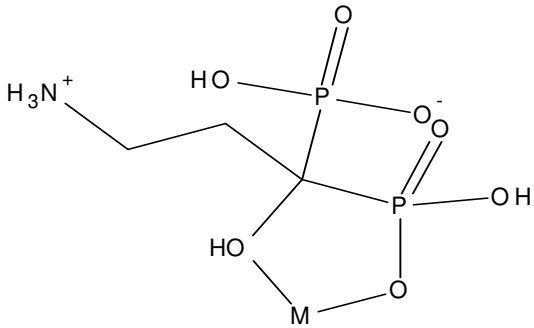

5–membered ring structure

**$M(H_3L)$**

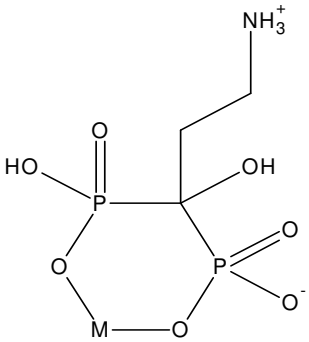

6–membered ring structure

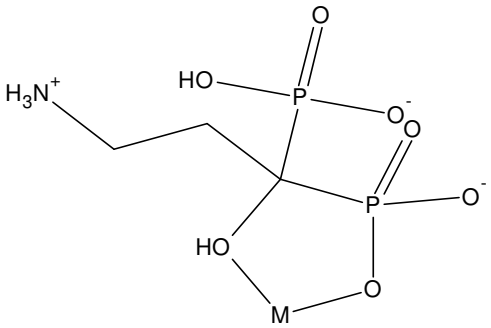

5–membered ring structure

**$M(H_2L)$**

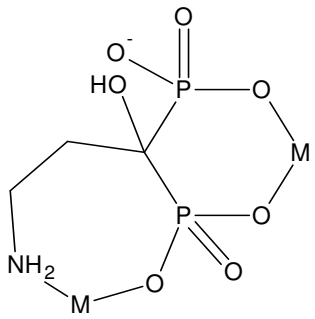

**$M_2L$**

According to the proposed structures of the complexes above, one possibility is that the amino group on the APD ligand is not involved in bond formation as it was assumed to be the case for the metal complexes $M_2(HL)$ and MHL. This was proved to be correct when one looks at the reported crystal structures for the ligand APD as discussed during the analysis of the $Cd^{II}$–APD system [13, 14, 15]. However, there are many possibilities on how the ligand APD can form bonds with the $Pb^{II}$ metal ion, since $Pb^{II}$ is a large metal ion it is possible to form complexes with 5-membered ring rather than complexes with 6-memebered ring. It is difficult to really prove which type of complexes (5 or 6-membered ring complexes) are formed in solution. An attempt was made to grow crystals for these complexes to check the crystal structures but failed. The formation of the metal complex $M_2L$ according to the proposed structure above suggests that the nitrogen atom is involved in complexation reaction. It has been previously reported that at least 14 different types of coordination for the similar ligand HEDP with any metal is possible. The crystal structures from this study shows that the oxygen atom on the hydroxyl group is always involved in coordination with the metal ion of interest [18]. Therefore when one considers the ligand such as APD, it is highly likely that this ligand form more different coordination types than HEDP ligand because it has an additional carbon atom with an amine group attached to it. So the structures suggested above are not the only possible ones.

If one assumes that the 1st protonation constant is not involved in complex formation and then redefine the ligand L′ = HL which is the APD ligand with the 1st protonation constant excluded, the stability constants attained are indicated in Table 4.8.

**Table 4.8**: Overall stability constants for $Pb^{II}$ with APD obtained in this work by $DC_{TAST}$ using curve fitting described at ionic strength μ = 0.15 M NaCl and 25 °C (1st protonation constant, i.e. 11.85 excluded). L′ = HL ($pKa_1$ excluded).

| Technique | Ratio | Equilibrium | log $\beta$ | Overall fit |
|---|---|---|---|---|
| $DC_{TAST}$ | 50 | $M + H_2L' = M(H_2L')$ | 18.37±0.02 | ±0.221 |
| | | $M + HL' = MHL'$ | 15.17±0.01 | |
| | | $M + L' = ML'$ | 10.34±0.01 | |
| | | $M + H_2L' = M(H_2L')$ | 18.47±0.01 | ±0.319 |
| | | $2M + L' = M_2L'$ | 16.33±0.02 | |
| | | $M + L' = ML'$ | 10.40±0.01 | |
| | | $M + H_2L' = M(H_2L')$ | 18.40±0.04 | ±0.210 |
| | | $M + HL' = MHL'$ | 15.07±0.16 | |
| | | $M + L' = ML'$ | 10.35±0.03 | |
| | | $2M + L' = M_2L'$ | 15.63±0.63 | |
| | | **Average value log $\beta_{ML'}$** | **10.36** | |
| | | **Average value log $\beta_{M_2L'}$** | **15.71** | |

One can therefore compare the stability constants attained for $Pb^{II}$–L′ as shown in Table 4.8 with the stability constants of $Pb^{II}$ with a similar type of ligand methylene diphosphonic acid MDP as indicated in Table 4.9. The $Pb^{II}$–HEDP system was not reported in literature and was never studied in our research laboratories but from the point of view that these two ligands have similar protonation constants as indicated in Table 4.5 one expects the metal complexes of these ligands to be similar for a specific metal ion.

**Table 4.9:** Comparison of stability constant values of $Pb^{II}$ complexes for ligands MDP and APD determined in this work and elsewhere. (L′ = HL, protonated APD)

| Ligand | Equilibria | log $\beta$ | Reference |
|---|---|---|---|
| MDP | $2M + L = M_2L$ | 15.58±0.02[a]<br>15.32±0.06[b] | [19] |
| APD | $2M + L' = M_2L'$ | 15.71 | This work |
| MDP | $M + L = ML$ | 9.42±0.01[a]<br>9.51±0.06[b] | [19] |
| APD | $M + L' = ML'$ | 10.36 | This work |

[a] results from $DC_{TAST}$ and [b] results from GEP.

From Table 4.9, one can note that the $\log \beta_{M_2L}$ values for MDP ligand determined by different techniques are comparable to the average $\log \beta_{M_2L'}$ value of 15.71 for APD ligand determined in this work. The values for MDP differ by about 0.25 log units and compared to the value of $\log \beta_{M_2L'}$ they differ by 0.4 log units. When looking at the log $\beta_{ML}$ values for ligand MDP determined by different techniques as well and comparing to them to log $\beta_{ML'}$ for the ligand APD they differ by about 1 log unit maximum with the APD log $\beta_{ML'}$ value being larger. These stability constants values can be regarded as similar taking into account different techniques employed in their determination. Thus if the assumption that the 1st protonation constant for APD is not involved in complexation, then the ligands MDP, HEDP and APD will form bonds with a specific metal ion in the same way. Hence their stability constants will not differ much.

### *4.2.2.6 Virtual potentiometry*

The plot of virtual half-wave potential, $E_{1/2}^{r}(virt)_{x(i)}$ vs. log [M] for the final metal-ligand model containing species $M(H_3L)$, $M(H_2L)$ and MHL for this system is shown in Figure 4.31.

This graph is linear and has a slope close to Nernstian slope for a fully reversible process at 25 °C (i.e. 29.58 mV) and from this graph the $E°$ (i.e. –262.75) from the response equation was refined and the slope was fixed at the Nernstian slope 29.58 at 25 °C by definition. The converted polarographic data was then refined by dedicated potentiometric software, ESTA and the results are shown in Table 4.10.

The virtual potentiometric data was then refined initially with models obtained from DC polarography and no convergence was attained (i.e. ESTA failed to solve mass balance equations for protons for these models). ESTA could not refine these models when the $E°$ was refined alone and concurrently with parameters such as base, acid or ligand concentration. The polarographic model containing species $M(H_3L)$, $M(H_2L)$ and MLH was tested with the stability constant for the complex $M(H_3L)$ fixed at 30.22, a value attained from DCP. Correlation of different parameters was observed when this refinement operation was performed. An example of the results from this refinement operation is shown in Table 4.8 whereby the acid concentration in the cell was refined together with the $E°$.

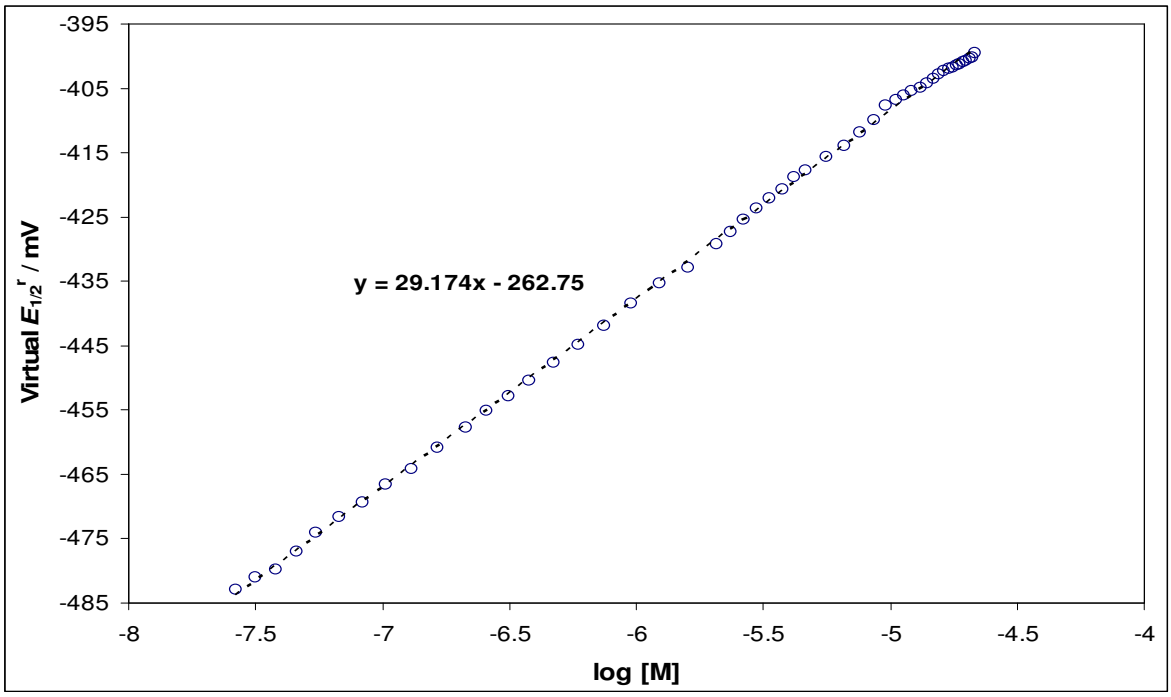


**Figure 4.31**: The plot for virtual half-wave potential $E_{1/2}^{r}$(virt) vs. log [M] for $Pb^{II}$–APD system studied by $DC_{TAST}$ at $[L_T]$:$[M_T]$ ratio 50, $[M_T] = 9.99\times10^{-5}$ M, at ionic strength $\mu$ = 0.15 M (NaCl) and 25 °C. This plot is for model: $M(H_3L)$, $M(H_2L)$ and MHL with refined stability constants as log $\beta$ values 30.22±0.02, 27.02±0.01 and 22.17±0.01, respectively.

In the next refinement operation, the stability constants for the metal complexes $M(H_3L)$ and $M(H_2L)$ or $M_2(HL)$ were fixed at values attained from DCP and only the metal complex MHL or $M_2L$ was varied.

As far as the model $M(H_3L)$, $M(H_2L)$ and MHL is concerned, the best refinement operation can be regarded as the one when the acid concentration in the cell was refined together with the $E°$. Not only was the smallest R-factor attained in this refinement operation but also the smallest refined acid concentration in cell of $5\times10^{-4}$ M attained bearing in mind that the ligand is itself acidic and no acid was added initially in the cell. The stability constants attained from this refinement operation are 30.22(fixed), 27.01(fixed) and 21.68±0.03 for complexes $M(H_3L)$, $M(H_2L)$ and MHL, respectively. One can notice from Table 4.10 that when the base or ligand concentrations were refined together with $E°$ for this particular model, the base concentration increased by 11 % and the ligand concentration decreased by 10.5 %. The increase in base concentration is very large and unexpected because the base concentration was well standardised prior the experiment. On the other hand, the decrease in ligand concentration is very huge even if the ligand was not 100 % pure and it was not exposed to moisture. For the model containing species $M(H_3L)$, $M_2(HL)$ and MHL, the same scenario was observed. The best refinement operation is the one attained when the acid concentration in the cell was refined together with the $E°$. The refined stability constants in this case were 30.22(fixed), 28.18(fixed) and 21.69±0.05 for the complexes $M(H_3L)$, $M_2(HL)$ and MHL, respectively.

Again the base concentration increased by 9.6 % and the ligand concentration decreased by 8.9 %. Although the concentration changes in the base and ligand were drastic, the refined stability constants values for the metal complex MHL were similar and within 0.5 log units in all the refinement operations. The average value for the complex MHL from all the refinement operations is 21.62. One must stress that this value is slightly lower than the polarographic values (i.e. 22.19 and 22.25).

For the other plausible model containing species $M(H_3L)$, $M(H_2L)$ or $M_2(HL)$ and $M_2L$, the best refinement operation was the one when the acid concentration was refined together with the $E°$ as well for the same reason as mentioned earlier. The refined stability constants for the complexes $M(H_3L)$, $M(H_2L)$ and $M_2L$ were 30.22(fixed), 28.18(fixed) and 22.82±0.08, respectively.

For the other model containing species $M(H_3L)$, $M_2(HL)$ and $M_2L$, the refined stability constants when the acid was refined together with $E°$ are 30.22(fixed), 28.18(fixed) and 22.81±0.08, respectively. The average value for the refined stability constant for the metal complex $M_2L$ is 22.74. This value is within 1 log unit of the polarographic values found in this work (i.e. 23.68 and 23.74).

**Table 4.10**: Overall stability constants for $Pb^{II}$–APD system found in this work by Virtual Potentiometry (VP-DC) at ionic strength μ = 0.15 M NaCl and 25 °C. R-factor stands for a statistical Hamilton R-factor generated by the program ESTA.

| Technique | log β | | | $-E^0$(virt) / mV | | Other parameter | % change | R-factor |
|---|---|---|---|---|---|---|---|---|
| | **$M(H_3L)$** | **$M(H_2L)$** | **MLH** | **Initial** | **Refined** | | | |
| VP-DC | 30.22(f) | 26.29 ±0.18 | 21.58 ±0.03 | 262.75 | 265.34 | acid | $8\times10^{-4}$ M* | 0.004 (correlated) |
| | 30.22(f) | 27.01(f) | 21.81 ±0.11 | 262.75 | 270.41 | – | – | 0.015 |
| | 30.22(f) | 27.01(f) | 21.49 ±0.04 | 262.75 | 263.14 | base | 11 | 0.006 |
| | 30.22(f) | 27.01(f) | **21.68 ±0.03** | 262.75 | 262.58 | acid | $5\times10^{-4}$ M* | 0.005 |
| | 30.22(f) | 27.01(f) | 21.53 ±0.04 | 262.75 | 263.84 | ligand | –10.5 | 0.005 |
| | **$M(H_3L)$** | **$M_2(HL)$** | **MLH** | | | | | |
| | 30.22(f) | 28.18(f) | 21.73 ±0.15 | 262.75 | 271.58 | – | – | 0.014 |
| | 30.22(f) | 28.18(f) | 21.48 ±0.08 | 262.75 | 264.84 | base | 9.6 | 0.007 |
| | 30.22(f) | 28.18(f) | **21.69 ±0.05** | 262.75 | 264.24 | acid | $5\times10^{-4}$ M* | 0.005 |
| | 30.22(f) | 28.18(f) | 21.52 ±0.07 | 262.75 | 265.29 | ligand | –8.9 | 0.006 |
| | | **Average** | **21.62** | | | | | |
| | **$M(H_3L)$** | **$M(H_2L)$** | **$M_2L$** | | | | | |
| | 30.22(f) | 27.01(f) | 23.13 ±0.16 | 262.75 | 269.93 | – | – | 0.015 |
| | 30.22(f) | 27.01(f) | 22.55 ±0.07 | 262.75 | 263.24 | base | 11 | 0.006 |
| | 30.22(f) | 27.01(f) | **22.82 ±0.06** | 262.75 | 262.79 | acid | $5\times10^{-4}$ M* | 0.005 |
| | 30.22(f) | 27.01(f) | 22.56 ±0.06 | 262.75 | 263.94 | ligand | –10.3 | 0.006 |
| | **$M(H_3L)$** | **$M_2(HL)$** | **$M_2L$** | | | | | |
| | 30.22(f) | 28.18(f) | 22.95 ±0.20 | 262.75 | 271.45 | – | – | 0.014 |
| | 30.22(f) | 28.18(f) | 22.52 ±0.12 | 262.75 | 264.97 | base | 9.6 | 0.007 |
| | 30.22(f) | 28.18(f) | **22.81 ±0.08** | 262.75 | 264.49 | acid | $5\times10^{-4}$ M* | 0.006 |
| | 30.22(f) | 28.18(f) | 22.55 ±0.11 | 262.75 | 265.42 | ligand | –8.8 | 0.006 |
| | | **Average** | **22.74** | | | | | |

* no acid was added into the solution

It is clear from Table 4.10 that the metal complex MHL is favoured over $M_2L$ when incorporated into the model containing species $M(H_3L)$ and $M(H_2L)$ or $M_2(HL)$ when acid

concentration in the cell is refined together with $E°$. The standard deviation for the refined stability constant for the MHL complex is always better than the one for the $M_2L$ complex. Also the percentage change in potential $E°$ is smaller when the complex MHL incorporated instead of $M_2L$. For the model $M(H_3L)$, $M(H_2L)$ and MHL, the refined stability constant value of 21.68±0.03 was attained for MHL. When $M_2L$ is incorporated instead of MHL, the refined stability constant value of 22.82±0.06 was attained. The same situation is observed when the metal complex $M_2(HL)$ is incorporated instead of $M(H_2L)$. The refined stability constant of 21.69±0.05 was attained for the complex MHL compared to 22.81±0.08 for the metal complex $M_2L$. It is also important to note that the change in potential is very small when the acid concentration is refined together with the $E°$ value irrespective of which species in incorporated into the metal-ligand system. The concept of virtual potential was successfully employed in this metal-ligand system and one can realise that the stability constants attained from the refinement of polarographic data converted to static type of data by using virtual potentials are similar as those attained by DCP. These values differ by utmost 1 log unit with the VP-DC data being low.

### 4.2.3 $Zn^{II}$–APD system by DCP: Titration at $L_T$:$M_T$ ratio 28, $[M_T] = 8.961 \times 10^{-5}$ M.

#### *4.2.3.1 Evaluation of $E_{1/2}(M)$ and fitting of the polarograms.*

Three polarograms for the background solution containing free metal ion were recorded initially at pH 6.4. These polarograms were then fitted initially using Equation 56 to check the degree of electrochemical reversibility given by the parameter, delta ($\delta$). The average value of $\delta$ was 0.82 which indicates that the reduction of the free metal ion on its own is a quasi-reversible process. Thereafter a ligand solution was added to the sample solution and polarograms were recorded in the presence of the ligand in pH steps of 0.05–0.10. After addition of the ligand, the electrochemical reversibility improved to 0.90 at pH 2.6. However the reversibility decreases as pH increases with $\delta$ equal to 0.26 at pH 5.6. Therefore the system is initially reversible and becomes totally irreversible at high pH as shown by the polarograms in Figure 4.32 and poorly fitted polarograms were obtained at high pH when using Equation 56. To account for the departure from the electrochemical reversibility, Ružić–based curve fitting approach was employed using Equations 59–61. The examples of the fitted polarograms using this approach are shown in Figure 4.33.

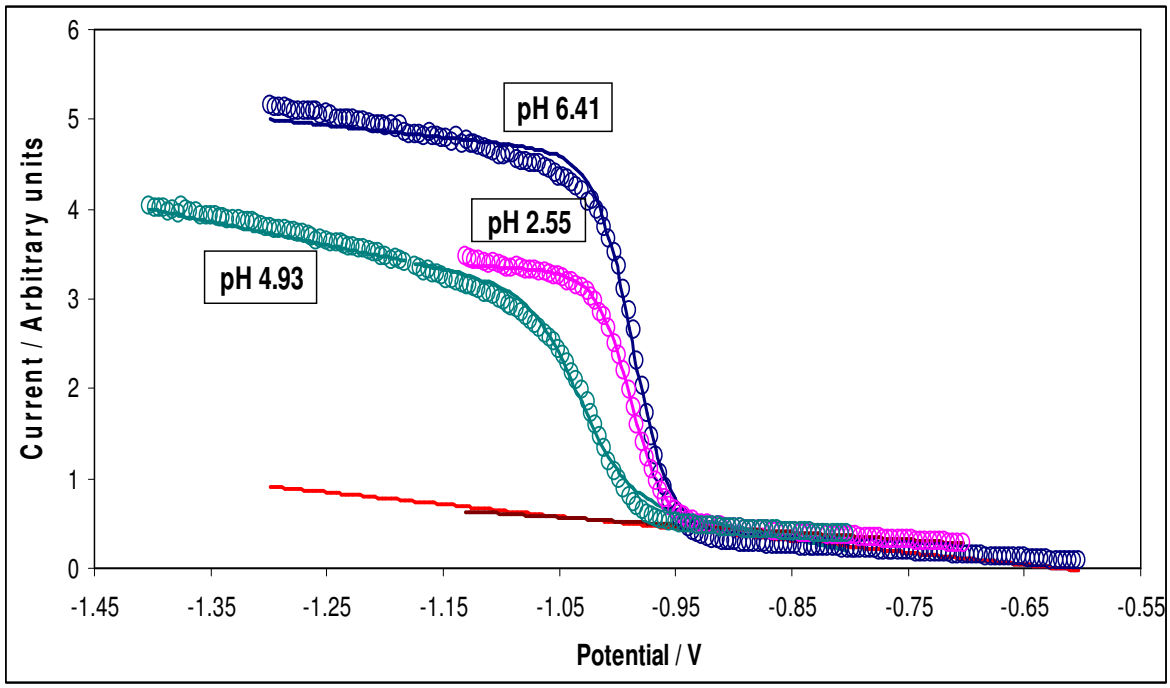


**Figure 4.32:** Selected fitted polarograms for $Zn^{II}$–APD system studied by $DC_{TAST}$ at $[L_T]:[M_T]$ = 28, $[M_T] = 8.961\times10^{-5}$ M, at ionic strength $\mu$ = 0.15 M (NaCl) and 25 °C. Polarograms were fitted using Equation 56. The circles represent the experimentally observed points as potential is applied and the solid lines represent the fitted curves.

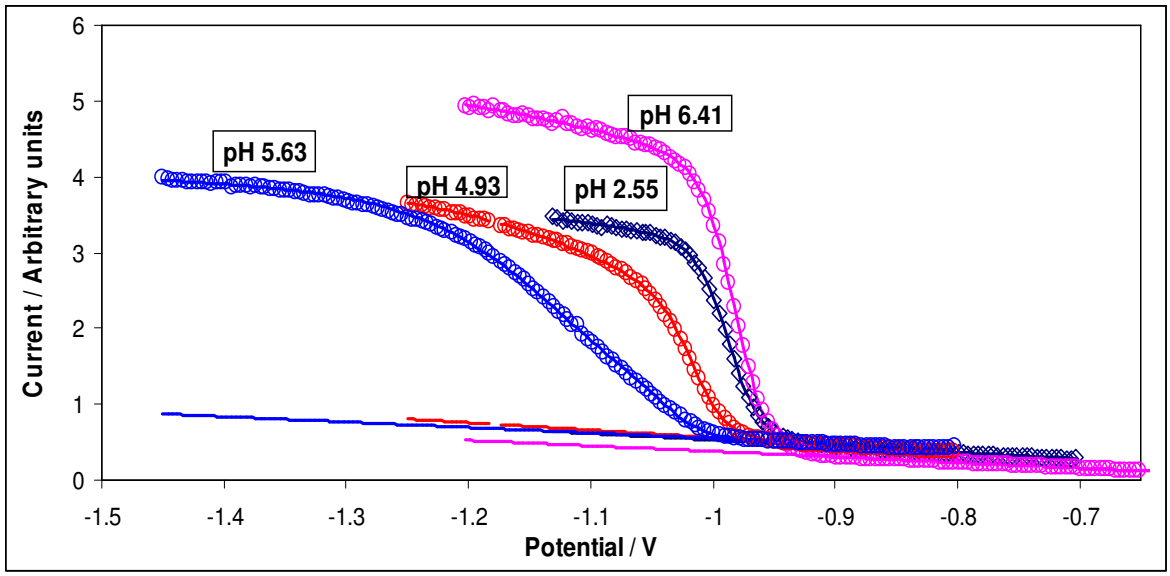


**Figure 4.33:** Selected fitted polarograms for $Zn^{II}$–APD system studied by $DC_{TAST}$ at $[L_T]:[M_T]$ = 28, $[M_T] = 8.961\times10^{-5}$ M, at ionic strength $\mu$ = 0.15 M NaCl and 25 °C. Polarograms were fitted using Equation 58. The circles represent the experimentally observed points as potential is applied and the solid lines represent the fitted curves.

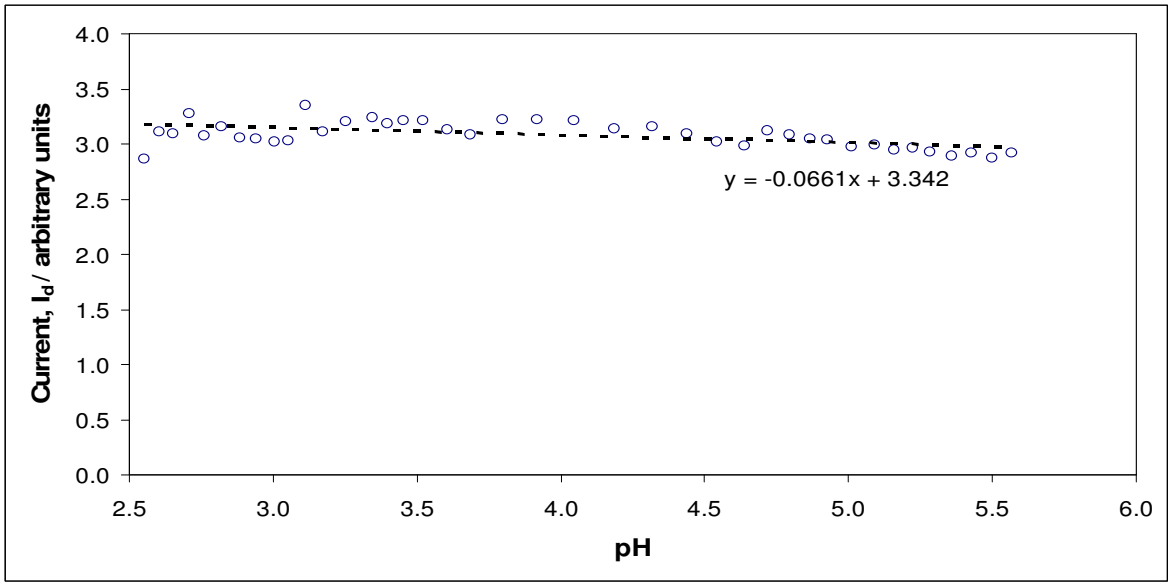


**Figure 4.34:** Variation in current vs. pH for $Zn^{II}$–APD system studied by $DC_{TAST}$ at $[L_T]:[M_T]$ = 28, $[M_T]$ = $8.961\times10^{-5}$ M, at ionic strength μ = 0.15 M NaCl and 25 °C. The circles represent the observed limiting diffusion currents $I_d$ attained for each fitted polarogram and the broken line shows the trend line for the observed limiting diffusion currents.

All parameters were allowed to vary during the fitting operation. It was observed from fitted curves that the limiting diffusion current $I_d$ of the fitted polarograms does not change much with the increase in pH. The limiting diffusion current $I_d$ vs. pH plot for the polarograms recorded is shown in Figure 4.34 as circles; the trend line indicate the overall small decrease in current. Since the recorded $I_d$ was slightly scattered, the limiting diffusion current $I_d$ used further in calculations was calculated at each pH value from the trend line equation.

### *4.2.3.2 Modelling of Zn–APD system*

a) Variation in limiting diffusion current $I_d$ vs. pH

The plot of calculated limiting diffusion current $I_d$ vs. pH for $Zn^{II}$–APD system is shown in Figure 4.35. It can be observed that the normalised limiting diffusion current (seen as triangles) does not vary much as pH increases. It decreases from 1.08 at pH about 3.0 to 1.06 at pH about 5.5. This indicates that inert and/or electrochemically inactive complexes were not formed. Lability of the metal-ligand system relates to the fact that homogeneous equilibria for this metal-ligand system are fast at the mercury-electrode interface. A single polarogram was recorded throughout the experiment, hence one would classify the Zn–

APD system as labile on the time scale of the $DC_{TAST}$ experiment. A few percent increase in the signal intensity is observed after addition of the ligand APD. This can be attributed either to (i) adsorption, or (ii) formation of metal species. Adsorption of a ligand was not investigated here since when the Cd–APD system was investigated (with $L_T$ being slightly larger than being used in this experiment) no evidence of adsorption was observed. Neither increase in signal intensity (Figure 4.4) nor shift in recorded polarogram after ligand addition (Figure 4.9) took place. In case of Pb–APD system, that also shown departure from electrochemical reversibility (as observed for Zn–APD system) no increase in $I_d$ was recorded, but a significant shift in $E_{1/2}$ was seen. From the above, it is most likely that $Zn(H_nL)$ were formed instantly after addition of the ligand, as it was observed for Pb–APD system. Even though the normalised current should not be larger than 1, no correction was made here since the observed initial increase has insignificant influence in computed stability constants. Ideally or in principle, the limiting diffusion current for the free metal (i.e. $I_d$ should be adjusted) if after ligand addition an increase in current is observed.

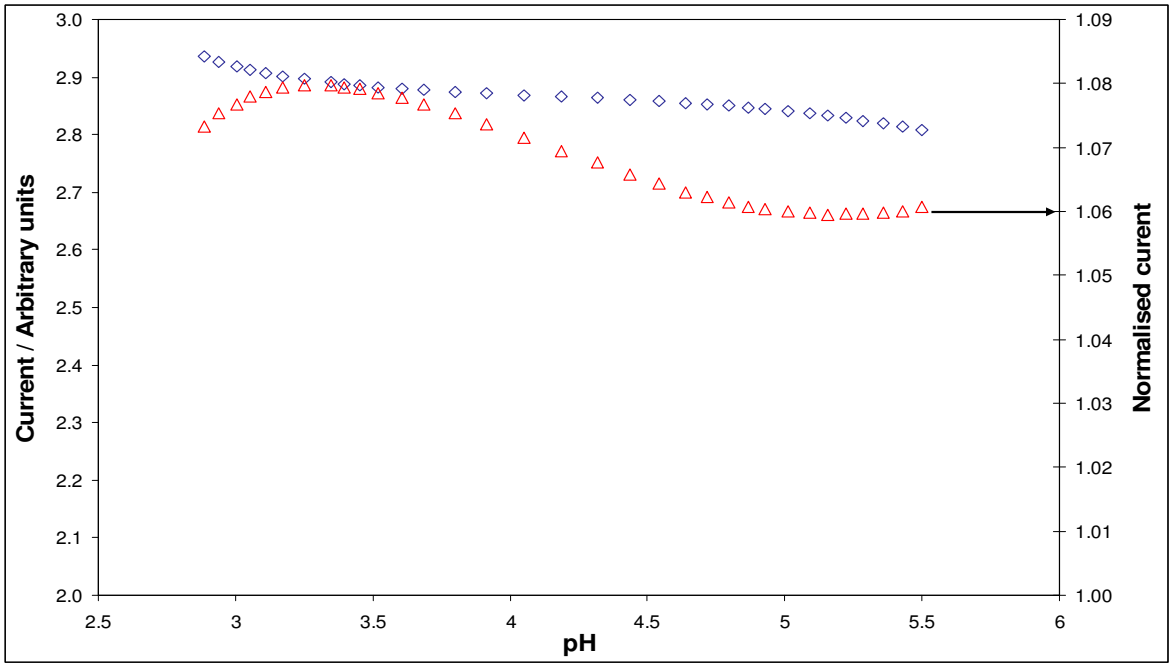


**Figure 4.35**: Limiting diffusion current $I_d$ vs. pH for $Zn^{II}$–APD system studied by $DC_{TAST}$ at $[L_T]:[M_T] = 28$, $[M_T] = 8.961\times10^{-5}$ M, at ionic strength $\mu = 0.15$ M NaCl and 25 °C. The triangles indicates the normalized limiting diffusion current and the diamonds indicates the expected limiting diffusion current that would be observed in the absence of the ligand.

The expected limiting diffusion current $I_d$(exp) seen as diamonds in Figure 4.35 is the limiting diffusion current expected in the absence of the ligand and decreases from 2.94 to 2.81 units. This indicates that the decrease in the intensity of the polarographic signal due

to dilution was insignificant. Since there is only a slight decrease in the normalised intensity of the recorded polarographic signal in the entire pH range either the virtual potential or $E_{1/2}^{r}$ obtained from Ružić–based fitting can be used in the modelling of the metal-ligand system. This slight decrease in $I_d$ can be attributed to the formation of different labile species with different diffusion coefficients as pH increases.

b) Variation in reversible half-wave potential $E_{1/2}^{r}$(virt) vs. pH

The graph of reversible half-wave potential $E_{1/2}^{r}$(virt) vs. pH shown in Figure 4.36 was analysed using the same approach as previously done for $Pb^{II}$–APD system. Between pH 2.8 and 4.0 there is no shift observed which does not provide information as to whether complexes are formed in solution or not. The metal complex $M(H_3L)$ might be considered since the form of the ligand in solution is $H_3L$ at this pH range and no shift is expected when this complex is reduced:

$$M(H_3L) + 2e = M(Hg) + H_3L$$

whereby no proton is involved in the reduction of $M(H_3L)$ complex. A slope of 29 mV/ pH unit is observed between pH 4.5 and 5.2.

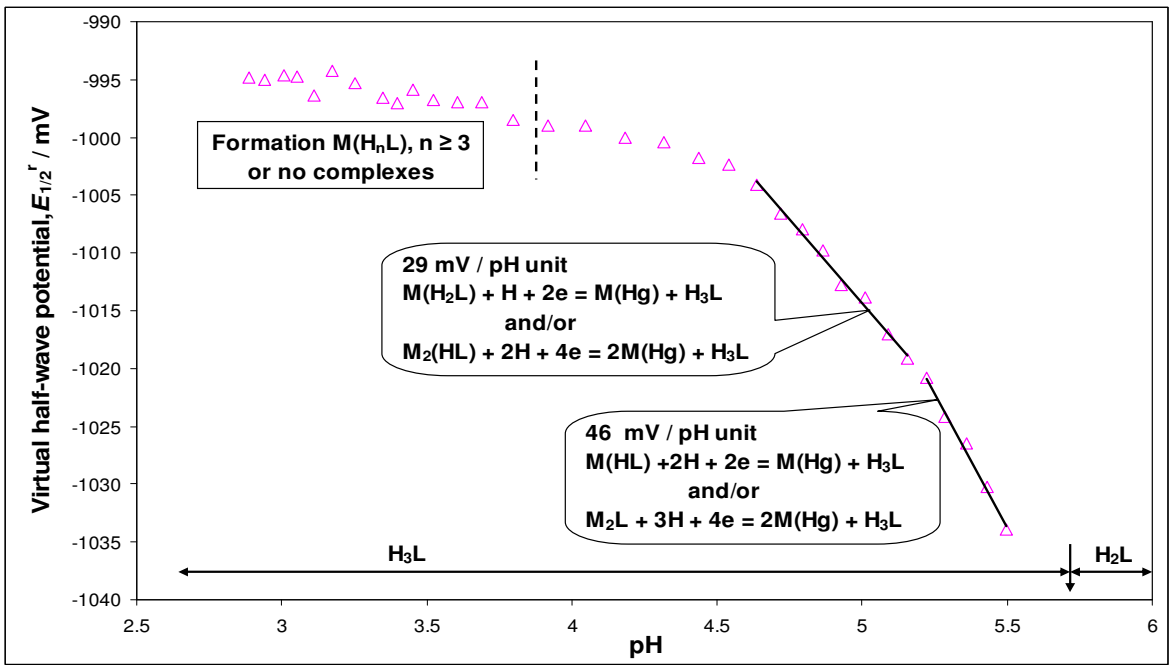


**Figure 4.36**: Reversible half-wave potential $E_{1/2}^{r}$(virt) vs. pH for $Zn^{II}$–APD system studied by $DC_{TAST}$ at $[L_T]$:$[M_T]$ ratio 28, $[M_T] = 8.961\times10^{-5}$ M, at ionic strength $\mu$ = 0.15 M (NaCl) and 25 °C.

Since the form of the ligand in this pH range is $H_3L$, the following electrochemical processes are suggested:

$M(H_2L) + H + 2e = M(Hg) + H_3L$
or/and
$M_2(HL) + 2H + 4e = 2M(Hg) + H_3L$

for which a theoretical slope of 30 mV / pH unit is expected.

A slope of 46 mV / pH unit is observed between pH 5.2 and 5.5; this suggests formation of species with theoretical slopes 30 and 60 mV/ pH unit coexisting in solution. This suggests that at this pH range, the species $M(H_2L)$ or/and $M_2(HL)$ is/are still in solution in addition to the species with theoretical slope of 60 mV/ pH unit:

$MHL + 2H + 2e = M(Hg) + H_3L$.

A slope of about 45 mV / pH unit is also expected for the following electrochemical process:

$M_2L + 3H + 4e = 2M(Hg) + H_3L$.

From this analysis it follows that the metal-ligand system might consist of species $M(H_3L)$, $M(H_2L)$ and/or $M_2(HL)$, MHL and/or $M_2L$.

c) Variation in reversible half-wave potential $E_{1/2}^{r}$(virt) vs. log $[H_3L]$.

The plot of reversible half-wave potential $E_{1/2}^{r}$(virt) vs. log $[H_3L]$ is indicated in Figure 4.37. This does not provide any evidence for the presence of the metal complex $M(H_3L)$. One must note however that similar relationship was obtained for Pb–APD system (Figure 4.21) where the complex $M(H_3L)$ was incorporated into the final model.

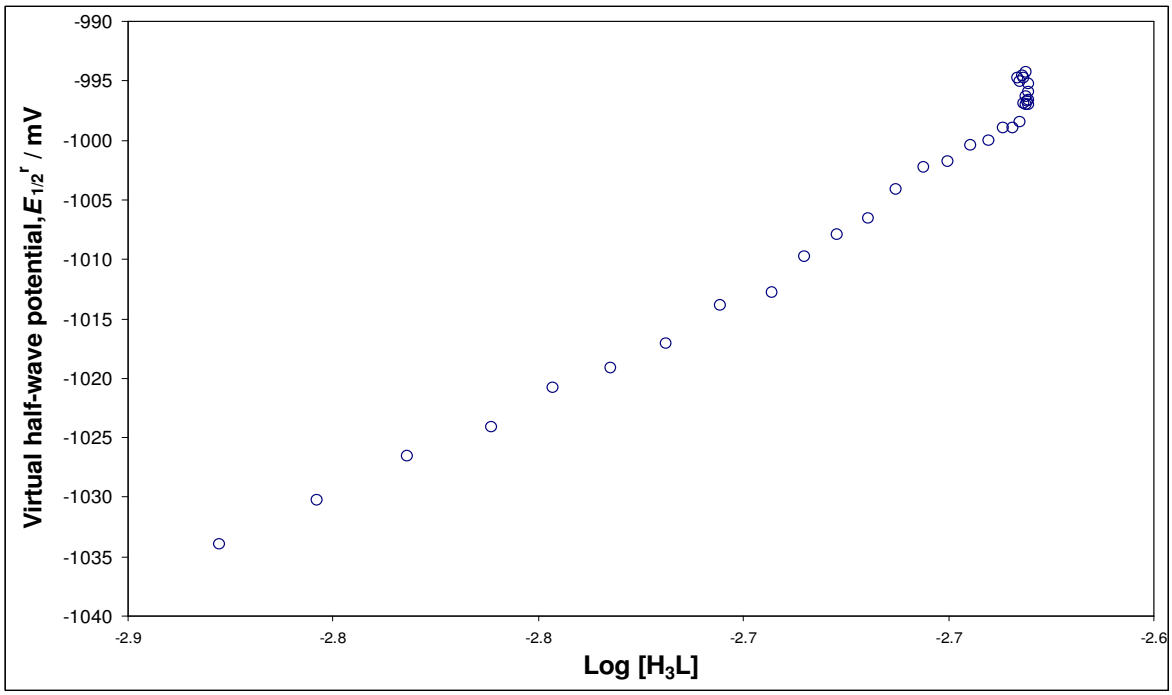


**Figure 4.37**: Reversible half-wave potential $E_{1/2}^r$(virt) vs. log [$H_3L$] for $Zn^{II}$–APD system studied at [$L_T$]:[$M_T$] ratio 28, [$M_T$] = $8.961\times10^{-5}$ M, at ionic strength μ = 0.15 M (NaCl) and 25 °C.

d) Variation in reversible half-wave potential $E_{1/2}^r$(virt) vs. log [$H_2L$].

The presence of the metal complexes of the type $M_x(H_2L)$ might be suggested by analysing the plot of reversible half-wave potential $E_{1/2}^r$(virt) vs. log [$H_2L$] as shown in Figure 4.38. A slope of 30 mV / log unit is observed according to the following complex formation reaction:

$$M + H_2L = M(H_2L)$$

This slope is observed in the same pH range as it is predicted to be formed in the plot of reversible virtual potential $E_{1/2}^r$(virt) vs. pH in Figure 4.36.

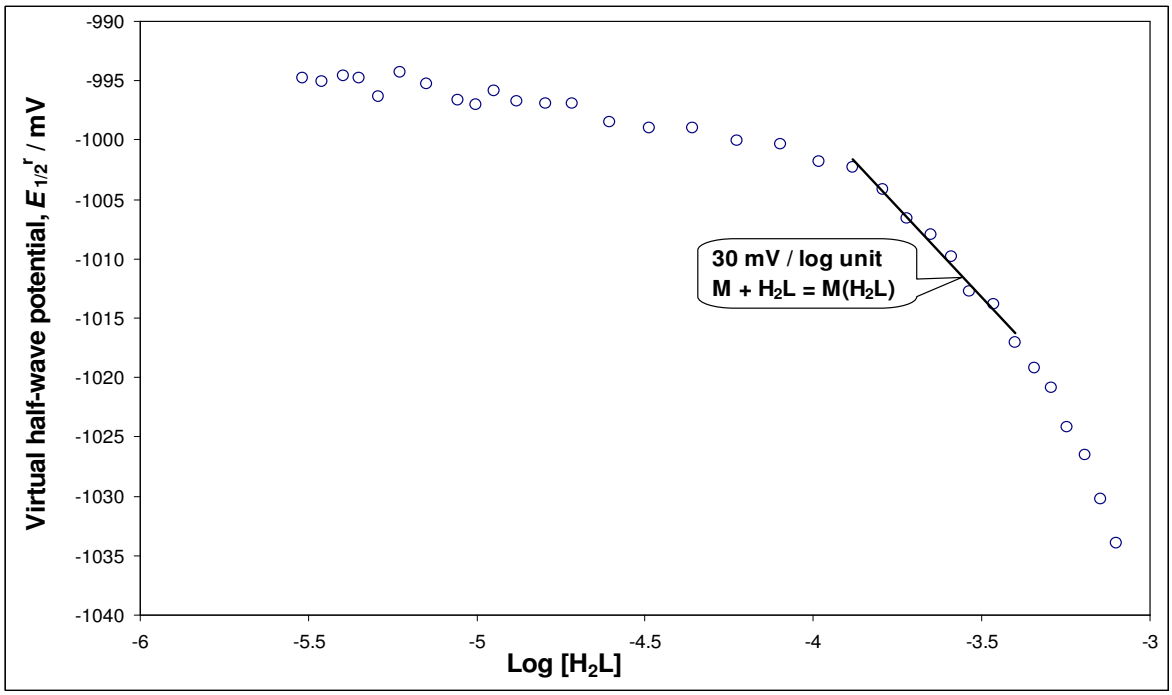


**Figure 4.38**: Reversible half-wave potential $E_{1/2}^r$(virt) vs. log [$H_2L$] for $Zn^{II}$–APD system studied at [$L_T$]:[$M_T$] ratio 28, [$M_T$] = $8.961\times10^{-5}$ M, at ionic strength μ = 0.15 M (NaCl) and 25 °C.

e) Variation in reversible half-wave potential $E_{1/2}^r$(virt) vs. log [HL].

To verify the presence of complexes of the type $M_p$(HL) in solution, the plot of $E_{1/2}^r$ vs. log [HL] was analysed as shown in Figure 4.39. Two slopes are observed. The value of 15 mV / log unit is in support of $M_2$(HL), whereas 27 mV / log unit supports M(HL). Formation of $M_2$(HL) is predicted by the same set of points seen in Figure 4.38 that indicated M($H_2L$). Hence no strong evidence in favour of either $M_2$(HL) or M($H_2L$) was established (see also Figure 4.36).

f) Variation in reversible half-wave potential $E_{1/2}^r$(virt) vs. log [L].

The presence of complexes of the type $M_pL_n$ ($n \geq 1$) in solution can be usually verified by analysis of the plot of reversible half-wave potential $E_{1/2}^r$(virt) vs. log [L] shown in Figure 4.40. A slope of 16 mV / log unit was observed that suggests the formation of the metal complex $M_2L$. Unfortunately the same set of points in Figure 4.39 indicated possibility of M(HL).

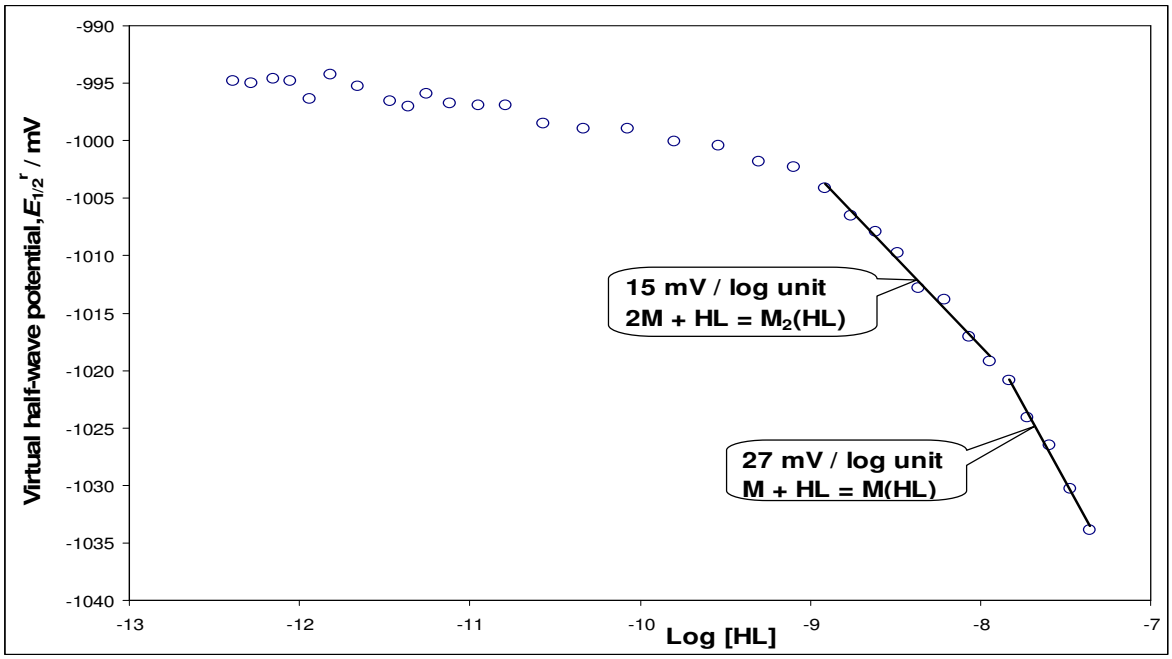


**Figure 4.39**: Reversible half-wave potential $E_{1/2}^{r}$(virt) vs. log [HL] for $Zn^{II}$–APD system studied at $[L_T]$:$[M_T]$ ratio 28, $[M_T] = 8.961\times10^{-5}$ M, at ionic strength μ = 0.15 M (NaCl) and 25 °C.

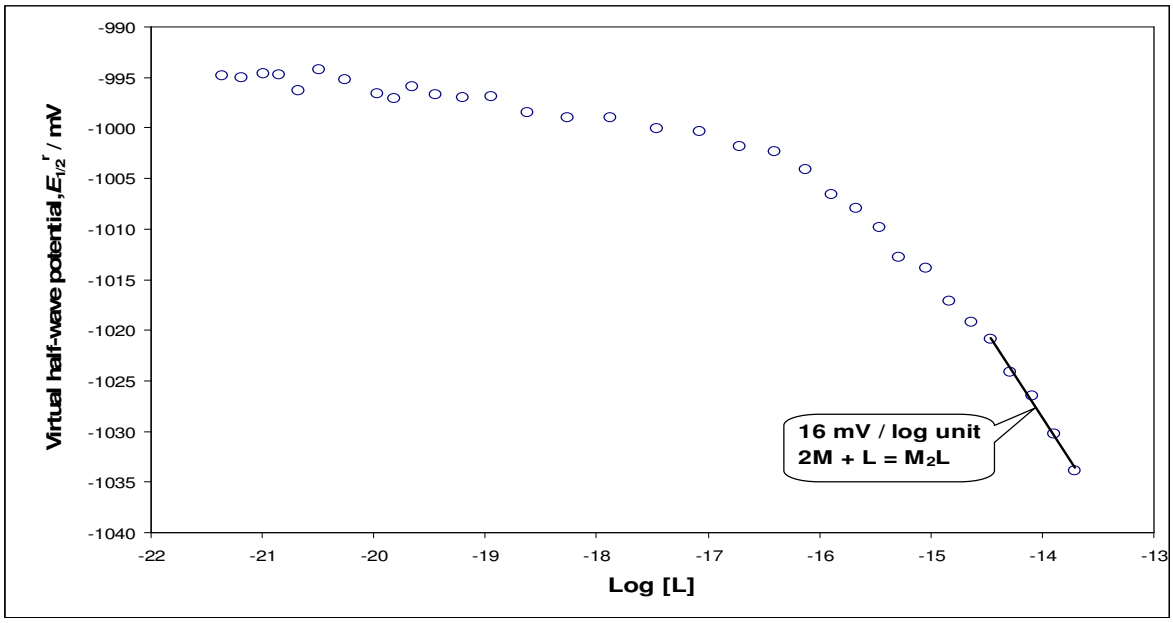


**Figure 4.40**: Reversible half-wave potential $E_{1/2}^{r}$(virt) vs. log [L] for $Zn^{II}$–APD system studied at $[L_T]$:$[M_T]$ ratio 28, $[M_T] = 8.961\times10^{-5}$ M, at ionic strength μ = 0.15 M (NaCl) and 25 °C.

From the above analyses of $E_{1/2}^{r}$ (virt) vs. log $[H_nL]$ it follows that it is impossible to arrive to a single metal-ligand model. Exactly the same was observed for the Pb–APD system. It was necessary to further test at least two most likely models, such as identified for the Pb–APD system.

### *4.2.3.3 Optimization of $Zn^{II}$–APD model and refinement of stability constants.*

Different metal-ligand models were tested and fitted to obtain refined stability constants values. The polarographic complex formation curves (i.e. ECFC and CCFC) were used in the optimization of the metal ligand models and refinement of stability constants. The results from this optimization procedure are indicated in Table 4.11. The best fit in CCFC into the ECFC was attained for the model containing species $M(H_3L)$, $M(H_2L)$ and MHL with refined stability constants as log β values as 30.15±0.02, 25.64±0.05 and 20.72±0.03, respectively. The complex formation curves for this particular model are shown in Figure 4.41.

When looking at Table 4.11 b), it can noticed that the refined log β value for the metal complex $M(H_3L)$ is consistent irrespective of the model being fitted. Also, the three last models seen in Table 4.11 b) could be rejected due to large overall fit obtained. These three models tested simultaneous refinement of competing complexes, such as $M_2(HL)$ and $M(H_2L)$, or M(HL) and $M_2L$.

In all cases, the complex $M_2(HL)$ was rejected indicating that refinement procedures favour $M(H_2L)$ complex. Also, the complex M(HL) was retained by software when it had a choice between M(HL) and $M_2L$. From the use of complex formation curves it would follow that most likely model should be $M(H_3L)$, $M(H_2L)$ and M(HL). When this model is compared with the one obtained for Pb–APD system, the only difference is a presence of $M(H_2L)$ in case of Zn–APD, whereas $M_2(HL)$ was identified for the Pb–APD system. One must stress here, however, that experimental points obtained for Zn–APD system are by far more scattered when compared with the points obtained for lead. This might be a reason that from statistics point of view the refinement operations were a bit more in favour of $M(H_2L)$ than $M_2(HL)$.

One can see in Table 4.11 that standard deviations for individual complexes, in two models containing $M(H_3L)$, $M_2(HL)$, M(HL) and $M(H_3L)$, $M(H_2L)$, M(HL) are very much the same, and hence these two models might be considered as plausible.

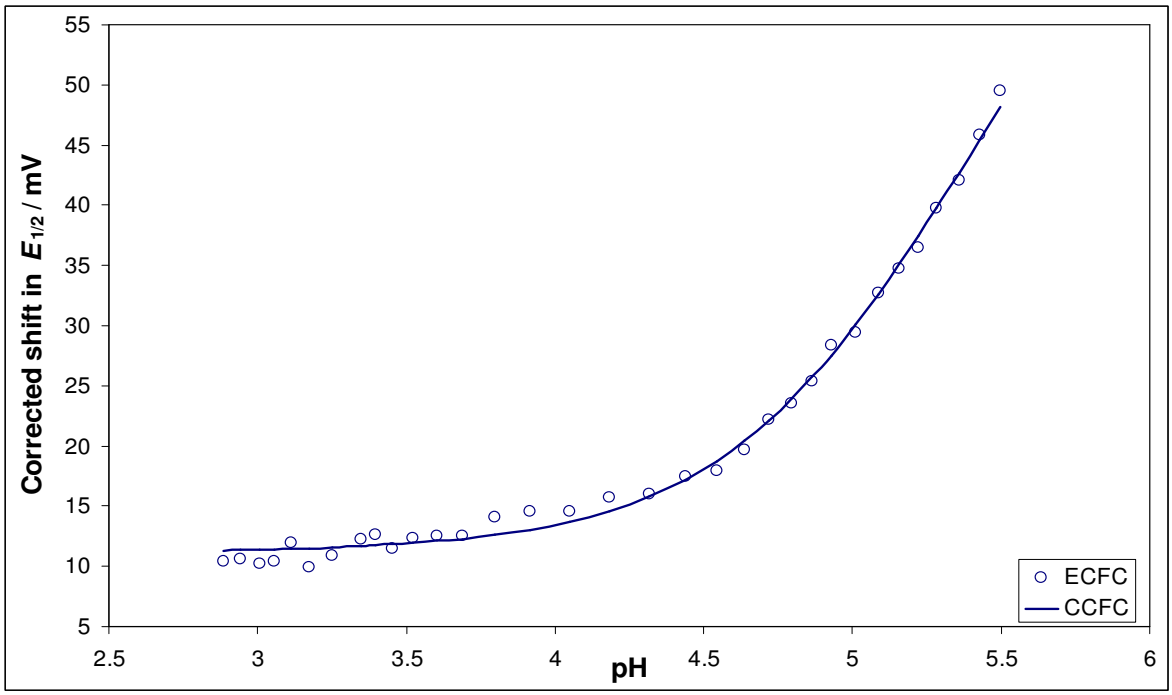


**Figure 4.41:** Experimental (ECFC) and calculated (CCFC) polarographic complex formation curves for $Zn^{II}$–APD system studied by $DC_{TAST}$ at $[L_T]$:$[M_T]$ ratio 28, $[M_T] = 8.961\times10^{-5}$ M, at ionic strength $\mu$ = 0.15 M (NaCl) and 25 °C. The curves are for the model $M(H_3L)$, $M(H_2L)$ and MHL with refined stability constants as log $\beta$ values 30.15±0.02, 25.64±0.05 and 20.72±0.03, respectively.

**Table 4.11**: a) Protonation constants for the ligand APD, dissociation constants of water and overall stability constants of $Zn^{II}$ complexes with $OH^-$ at ionic strength 0.15 M (NaCl) and 25.0 °C.

| **Equilibrium** | **log β** |
|---|---|
| $H^+ + OH^- = H_2O$ | 13.42 |
| $L + H = LH$ | 11.85 |
| $LH + H = H_2L$ | 9.76 |
| $H_2L + H = H_3L$ | 5.77 |
| $H_3L + H = H_4L$ | 1.47 |
| $Zn^{2+} + OH^- = Zn(OH)^+$ | 5.00 |
| $Zn^{2+} + 2OH^- = Zn(OH)_2$ | 10.20 |
| $Zn^{2+} + 3OH^- = Zn(OH)_3^-$ | 13.90 |
| $Zn^{2+} + 4OH^- = Zn(OH)_4^{2-}$ | 15.50 |
| $2Zn^{2+} + OH^- = Zn_2(OH)^{3+}$ | 5.50 |
| $4Zn^{2+} + 4OH^- = Zn_4(OH)_4^{4+}$ | 27.94 |
| $Zn^{2+} + 2\ OH^- = Zn(OH)_2(s)$ | –14.84 |

b) Overall stability constants for $Zn^{II}$ with APD obtained in this work by $DC_{TAST}$ using curve fitting described at ionic strength μ = 0.15 M NaCl and 25 °C.

| Technique | Ratio | Equilibrium | log β | Overall fit/ mV |
|---|---|---|---|---|
| $DC_{TAST}$ | 28 | $M + H_3L = M(H_3L)$ | 30.19±0.01 | ±1.378 |
| | | $2M + HL = M_2(HL)$ | 25.39±0.09 | |
| | | $2M + L = M_2L$ | 20.57±0.05 | |
| | | $M + H_3L = M(H_3L)$ | 30.19±0.01 | ±1.109 |
| | | $2M + HL = M_2(HL)$ | 25.38±0.07 | |
| | | $M + HL = MHL$ | 20.75±0.03 | |
| | | $M + H_3L = M(H_3L)$ | 30.16±0.02 | ±0.901 |
| | | $M + H_2L = M(H_2L)$ | 25.64±0.06 | |
| | | $2M + L = M_2L$ | 20.54±0.05 | |
| | | $M + H_3L = M(H_3L)$ | 30.15±0.02 | ±0.663 |
| | | $M + H_2L = M(H_2L)$ | 25.64±0.05 | |
| | | $M + HL = MHL$ | 20.72±0.03 | |
| | | $M + H_3L = M(H_3L)$ | 30.16±0.03 | ±3.357 |
| | | $2M + HL = M_2(HL)$ | rejected | |
| | | $M + H_2L = M(H_2L)$ | 25.64±0.03 | |
| | | $2M + L = M_2L$ | 20.54±0.35 | |
| | | $M + H_3L = M(H_3L)$ | 30.15±0.04 | ±4.269 |
| | | $2M + HL = M_2(HL)$ | rejected | |
| | | $M + H_2L = M(H_2L)$ | 25.64±0.10 | |
| | | $M + HL = MHL$ | 20.72±0.11 | |
| | | $M + H_3L = M(H_3L)$ | 30.15±0.05 | ±14.332 |
| | | $2M + HL = M_2(HL)$ | rejected | |
| | | $M + H_2L = M(H_2L)$ | 25.64±0.09 | |
| | | $M + HL = MHL$ | 20.75±2.90 | |
| | | $2M + L = M_2L$ | rejected | |

#### *4.2.3.4 Species distribution diagrams*

Species distribution diagrams were generated for several M–L models discussed above. As one would expect from the similar analysis performed on the Pb–APD system, the diagrams were of no help in deciding on most likely model. As examples, the species distribution diagrams are shown for the two plausible models–see Figures 4.42 and 4.43.

On both the diagrams the predominance of $M(H_3L)$ and $M(HL)$ is indicated with $M_2(HL)$ and $M(H_2L)$ being predicted to form in the same pH range and with a similar maximum amount of about 35 % of the total metal concentration.

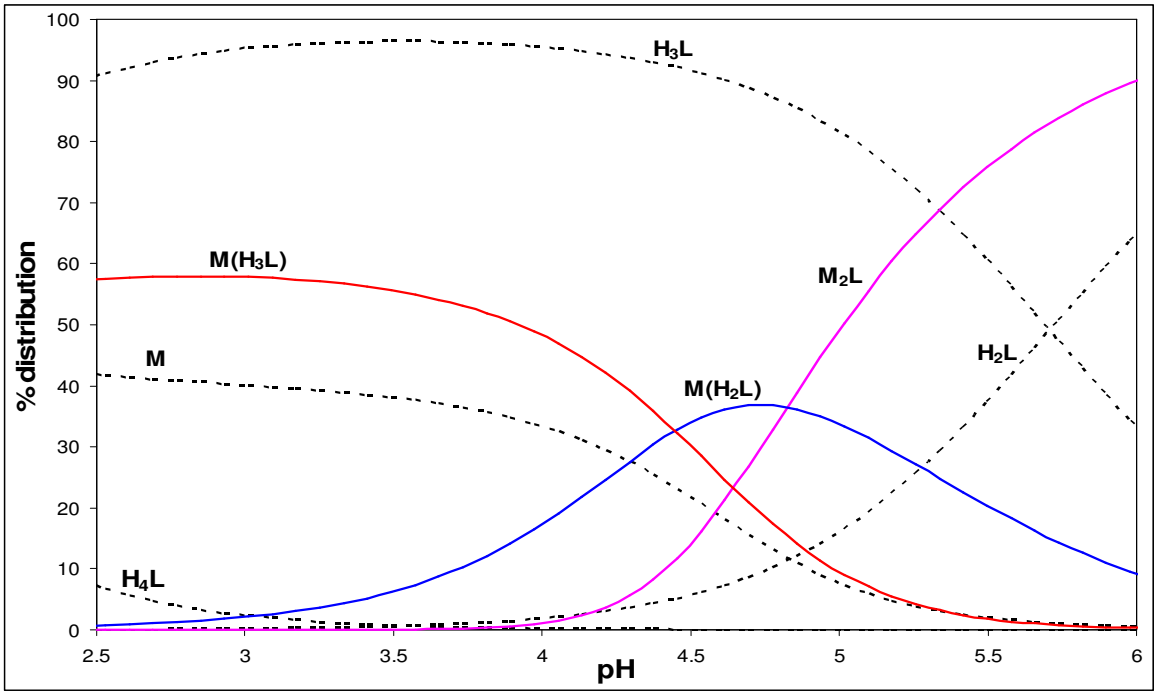


**Figure 4.42:** The species distribution diagram for the $Zn^{II}$–APD system studied by $DC_{TAST}$ at $[L_T]:[M_T]$ = 28, initial $[M_T]$ = $8.961\times10^{-5}$ M, at ionic strength μ = 0.15 M NaCl and 25 °C. The model consists of species $M(H_3L)$, $M(H_2L)$ and $M_2L$ with refined stability constants as log β values 30.16±0.02, 25.64±0.06 and 20.54±0.05, respectively.

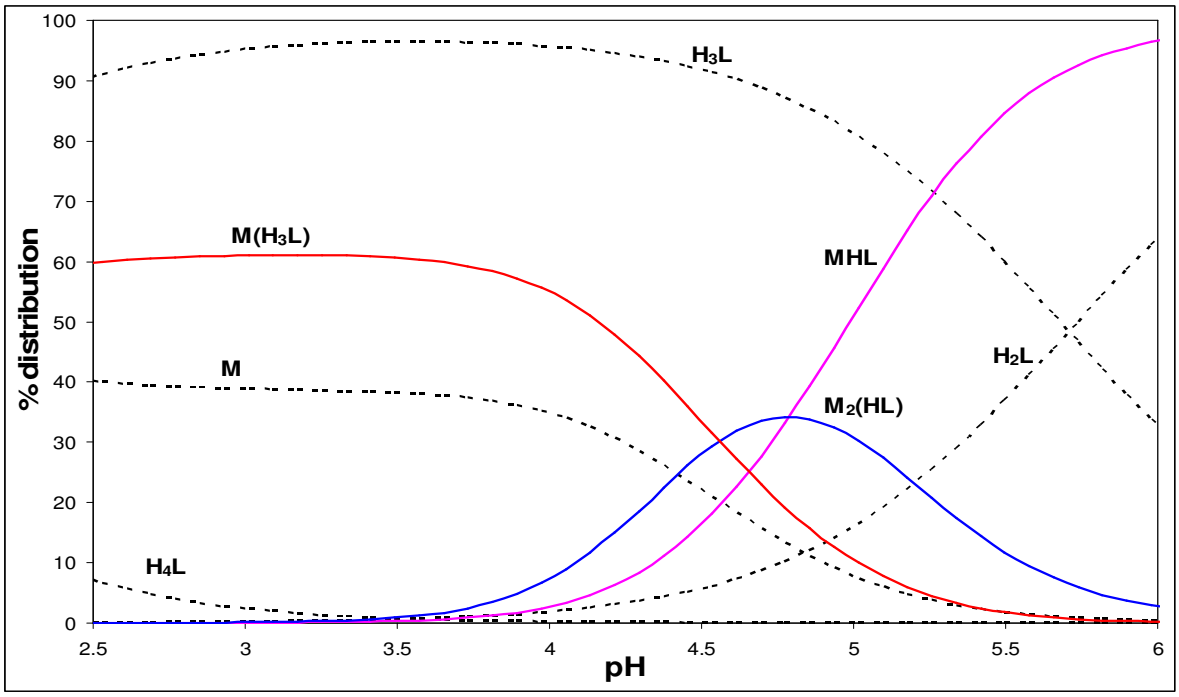


**Figure 4.43:** The species distribution diagram for the $Zn^{II}$–APD system studied by $DC_{TAST}$ at $[L_T]:[M_T]$ = 28, initial $[M_T]$ = $8.961\times10^{-5}$ M, at ionic strength μ = 0.15 M NaCl and 25 °C. The model consists of species $M(H_3L)$, $M_2(HL)$ and MHL with refined stability constants as log β values 30.19±0.01, 25.38±0.07 and 20.75±0.03, respectively.

### *4.2.3.5 Comparison of formation constants for ligands APD and HEDP with $Zn^{II}$ metal ion*

As it was stated already, the reported crystal structures for the APD ligand indicate that the amino group is not involved in complex formation [13–15]. On the other hand, when one considers a similar ligand HEDP, it has been previously reported that at least 14 different types of coordination with a metal is possible [18]. The crystal structures from that study showed that the oxygen atom on the hydroxyl group was always involved in coordination with the central metal ion [18]. In principle, it is possible that the ligand APD can form more different coordination types than HEDP ligand due to the nitrogen donor atom.

However, if the amino group is not involved in complex formation [13–15], then the metal complex such as $M_2L$ is not likely to form in solution since its formation will involve the nitrogen atom. Thus the refined stability constants, as indicated in Table 4.12, were attained from the refinement operation with the 1st protonation constant being excluded.

**Table 4.12**: Overall stability constants for $Zn^{II}$ with APD obtained in this work by $DC_{TAST}$ using curve fitting described at ionic strength μ = 0.15 M NaCl and 25 °C (1st protonation constant, i.e. 11.85 excluded). L′ = HL ($pKa_1$ excluded).

| Technique | Ratio | Equilibrium | log $\beta$ | Overall fit/ mV |
|---|---|---|---|---|
| $DC_{TAST}$ | 28 | $M + H_2L' = M(H_2L')$ | 18.30±0.02 | ±0.663 |
| | | $M + HL' = MHL'$ | 13.79±0.05 | |
| | | $M + L' = ML'$ | 8.87±0.03 | |
| | | $M + H_2L' = M(H_2L')$ | 18.34±0.01 | ±1.109 |
| | | $2M + L' = M_2L'$ | 13.53±0.07 | |
| | | $M + L' = ML'$ | 8.90±0.03 | |
| | | **Average value log $\beta_{ML'}$** | **8.89±0.03** | |

When the amine protonation constant was excluded from the refinement operations then the same overall fit in CCFC into the ECFC was attained when compared with the relevant models seen in Table 4.11. The average log $\beta_{ML'}$ of 8.89 was generated from both the models as indicated in Table 4.12.

One can, in principle, compare the stability constants for $Zn^{II}$–L′ system attained in this work with the stability constant of $Zn^{II}$–HEDP reported from the literature as shown in Table 4.13. Unlike the $Cd^{II}$–APD and $Pb^{II}$–APD systems, the stability constants for the $Zn^{II}$–L′ system do not compare well with those of $Zn^{II}$–HEDP system reported in the literature [11]. The literature value of log $\beta_{M_2L}$ for HEDP is more than 2 log units higher

than the log $\beta_{M_2L'}$ value for the ligand APD. The log $\beta_{ML}$ value for HEDP is 1 log unit higher than the log $\beta_{ML'}$ value for ligand APD.

**Table 4.13:** Comparison of stability constant values of $Zn^{II}$ complexes for ligands APD and HEDP determined in this work and elsewhere. (L′ = HL, protonated APD)

| Ligand | Equilibria | log $\beta$ | Reference |
|---|---|---|---|
| HEDP | $2M + L = M_2L$ | 16.46±0.06 | [19] |
| APD | $2M + L' = M_2L'$ | 13.53±0.07 | This work |
| HEDP | $M + L = ML$ | 10.30±0.05 | [19] |
| APD | $M + L' = ML'$ | 8.89±0.03 | This work |

Analysis of data in [11] indicates that differential pulse polarography was used and the observed peak potential $E_p$ was used for the refinement operations. As a matter of fact it is obvious that the departure from electrochemical reversibility was not considered in that work. The use of DPP had to result in significant decrease in recorded polarograms due to departure from reversibility. Also, the observed potentials had to be more negative than reversible potentials. These two non-rigorous data treatments must have resulted in larger stability constants reported in [11]. From this follows that one would have to re-examine Zn–HEDP system by use of $DC_{TAST}$ and Ružić–based curve fitting procedure employed in this study.

### *4.2.3.6 Virtual potentiometry*

The polarographic data was also refined by potentiometric software ESTA using virtual potentials. The slope for $E_{1/2}^{r}(virt)_{x(i)}$ vs. log M was fixed at 29.58, which is a theoretically expected value when the experiment is performed at 25 °C with $E°$ (i.e. being –865.24) refined simultaneously with stability constants. An initial $E°$ value of –865.24 was obtained from relationship seen in Figure 4.44. Initially, different polarographic models (as indicated in Table 4.11 (b)) were tested with the $E°$ being refined and no convergence was attained by ESTA. This means that the program could not solve mass balance equations for protons for these models. No convergence was attained even when the polarographic models were tested with $E°$ refined together with the base, acid or ligand concentration. One must take into account the fact that large $[L_T]$:$[M_T]$ ratios are involved as far as polarographic experiment is concern and very much low initial $[M_T]$ concentration is used.

This low initial [$M_T$] concentration makes it difficult for the ESTA program to solve mass balance equations for protons for the polarographic models because it was designed to work at typical potentiometric conditions (i.e. initial [$M_T$] = $10^{-3}$ M). In the next refinement operation, the stability constant for the metal complex M($H_3L$) was fixed at 30.15 (a value obtained from DCP). The reason for that is a fact that M($H_3L$) is formed where $H_3L$ is the only form of the ligand present in a solution.

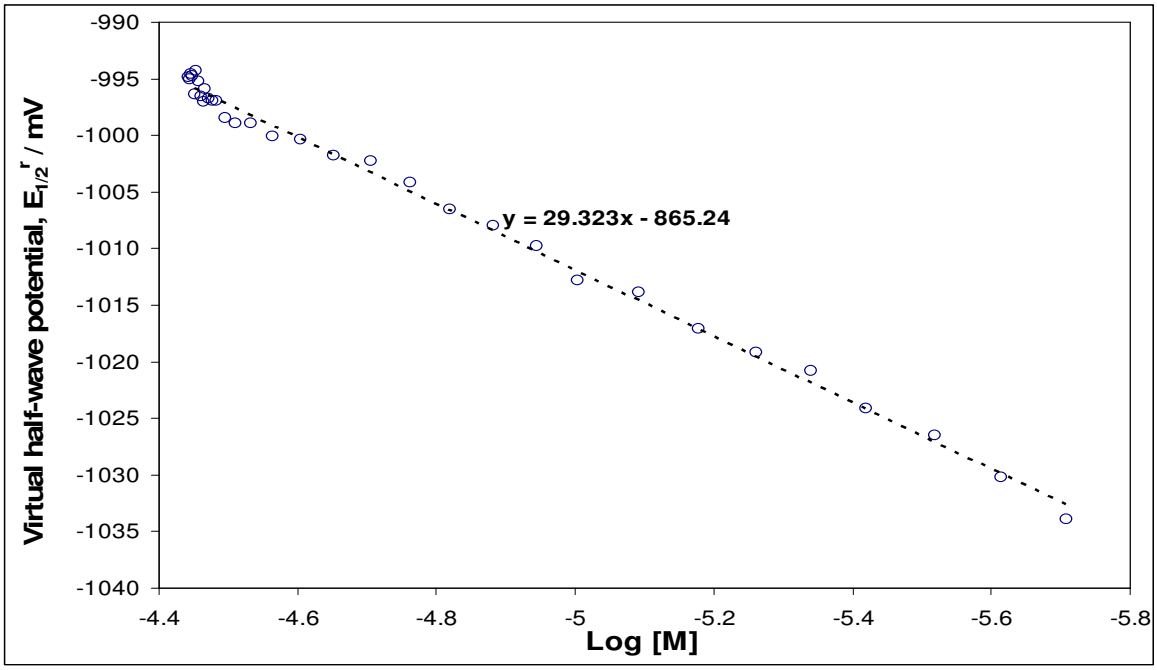


**Figure 4.44**: The plot for virtual half-wave potential, $E_{1/2}^{r}$(virt) vs. log [M] for $Zn^{II}$–APD system studied by $DC_{TAST}$ at [$L_T$]:[$M_T$] ratio 28, [$M_T$] = $8.961\times10^{-5}$ M, at ionic strength μ = 0.15 M (NaCl) and 25 °C. This plot is for model: M($H_3L$), M($H_2L$) and MHL with refined stability constants as log β values 30.15±0.02, 25.64±0.05 and 20.72±0.03, respectively.

Formation of this complex does not change the free proton concentration hence solving mass balance equation for protons is of no use here. A model containing metal complexes M($H_3L$), M($H_2L$) and MHL, together with $E°$, was refined without a problem with the complex M($H_3L$) fixed at log β of 30.15. The refined stability constant for metal complexes, as log β, of 30.15(f), 25.24±0.05 and 20.63±0.01 were obtained, respectively, with the R-factor of 0.0007 (see Table 4.14). The stability constants obtained from VP–DC data compare well with those seen in Table 4.11.

It was predicted during the modelling of the metal-ligand system that either M($H_2L$) or $M_2$(HL) is formed in solution in the same pH range. Thus in the next refinement operation, the data was refined with the metal complex $M_2$(HL) incorporated into model instead of

$M(H_2L)$. The refined stability constant values for the complexes $M(H_3L)$, $M_2(HL)$ and MHL were 30.15(f), 24.80±0.08 and 20.64±0.02, respectively. The R-factor for 0.0008 was attained in this case. The refined stability constant for the metal complex MHL was the same irrespective of whether the complex $M(H_2L)$ or $M_2(HL)$ was incorporated into the model. However, the VP–DC stability constant for $M_2(HL)$ is significantly lower when compared with the value generated from DC data.

**Table 4.14**: Overall stability constants for $Zn^{II}$–APD system found in this work by Virtual Potentiometry (VP-DC) at ionic strength μ = 0.15 M (NaCl) and 25 °C. R-factor stands for a statistical Hamilton R-factor generated by the program ESTA.

| **Technique** | **Log β** | | | **$-E^0$(virt)** | | **Other parameter Refined** | **% change** | **R-factor** |
|---|---|---|---|---|---|---|---|---|
| | **$M(H_3L)$** | **$M(H_2L)$** | **MHL** | **Initial** | **Final** | | | |
| VP–DC | 30.15(f) | 25.24 ±0.05 | 20.63 ±0.01 | 865.24 | 863.18 | – | – | 0.0007 |
| | **$M(H_3L)$** | **$M_2(HL)$** | **MHL** | | | | | |
| | 30.15(f) | 24.80 ±0.08 | 20.64 ±0.02 | 865.24 | 863.61 | – | – | 0.0008 |

It is important to note that the change in potential $E°$ was in the percentage range 0.16–0.30 %. The refined stability constant values from VP-DC data are comparable to the ones obtained by $DC_{TAST}$, with slightly better statistical parameters for a model containing $M(H_2L)$. This shows that the virtual potentials are essential in the refinement of data coming from dynamic voltammetric data using the ESTA program because it does not take into account the potential of a free metal ion at all; the potentiometric software does not compute a shift in potential as is the case for polarographic experiment. Regardless whether $M_2(HL)$ or $M(H_2L)$ was incorporated in the model, the stability constant for M(HL) was predicted to be virtually the same, log $\beta_{M(HL)}$ = 20.63. This compares well with polarographic value of about 20.73, and in generation of LFER an average of 20.68 was used.

## 4.3 Linear Free Energy Relationship for the ligand APD.

In order for one to establish a linear free energy relationship (in this case, log $K_{ML}$ vs. log $K_{M(OH)}$) for a particular ligand, the first formation constants (log $K_{ML}$) for this ligand and several metal ions are required. The LFER for the ligand APD has never been reported, this is because there was not enough data available in the literature. Only stability

constants for the ligand APD with blood plasma metal ions $Mg^{II}$, $Ca^{II}$, and $Sr^{II}$ were reported [1]. It was therefore important in this work to study several metal ions with ligand APD in order to establish the LFER for this ligand. Only the protonated metal-ligand complexes were found in this work. Hence the LFER in the form of log $K_{MHL}$ vs. log $K_{M(OH)}$ could be directly generated in order to predict relevant values for $^{153}Sm^{III}$–APD and $^{166}Ho^{III}$–APD systems.

Three LFER for APD ligand were derived using the tabulated values shown in Tables 4.15, 4.16 and 4.17. When the log $K_{MHL}$ literature data for $Sr^{II}$, $Ca^{II}$ and $Mg^{II}$ [1] and the log $K_{MHL}$ values for $Cd^{II}$, $Zn^{II}$, and $Pb^{II}$ determined in this work were used, the predicted log $K_{MHL}$ values for $Sm^{III}$–HL and $Ho^{III}$–HL were 21.72 and 21.93, respectively (see Table 4.15 and Figure 4.45). These values were calculated from the trendline equation in Figure 4.45 using the first hydrolysis constants values of $Sm^{III}$ and $Ho^{III}$. From the LFER, it can be assumed that the log $K_{MHL}$ value for $Mg^{II}$–HL of 16.81 is an outlier. Also, since log $K_{M(OH)}$ for $Mg^{II}$ is larger than that for $Ca^{II}$, one would expect the same trend for M(HL) complex.

**Table 4.15**: Data for log $K_{MHL}$ for the ligand APD and log $K_{M(OH)}$ for several metal ions.

| Cation | log $K_{M(OH)}$ | log $K_{MHL}$ | Reference |
|---|---|---|---|
| $Sr^{II}$ | 0.82 | 16.30 | [1] |
| $Ca^{II}$ | 1.3 | 17.27 | [1] |
| $Mg^{II}$ | 2.5 | 16.81 | [1] |
| $Cd^{II}$ | 4.0 | 19.21 | TW |
| $Zn^{II}$ | 5.0 | 20.68 | TW* |
| $Pb^{II}$ | 6.0 | 21.96 | TW* |
| $Sm^{III}$ | 6.1 | **21.72** | Predicted |
| $Ho^{III}$ | 6.3 | **21.93** | Predicted |

TW means this work, *–average value from DC and VP–DC data.

The log $K_{MHL}$ value for $Mg^{II}$–HL was then re-established by studying the $Mg^{II}$–APD system by GEP and the log $K_{MHL}$ for $Mg^{II}$ was determined to be about 19 (results not discussed here as precipitation was observed at typical potentiometric conditions and the experiment was performed at very low initial $[M_T] = 10^{-4}$ M). When this log $K_{MHL}$ value for $Mg^{II}$ was used in addition to the literature data for $Sr^{II}$, $Ca^{II}$ [1] and the log $K_{MHL}$ values for $Cd^{II}$, $Zn^{II}$ and $Pb^{II}$ determined in this work, the predicted log $K_{MHL}$ values for $Sm^{III}$–HL and $Ho^{III}$– HL were 21.86 and 22.06, respectively (see Table 4.16 and Figure 4.46).

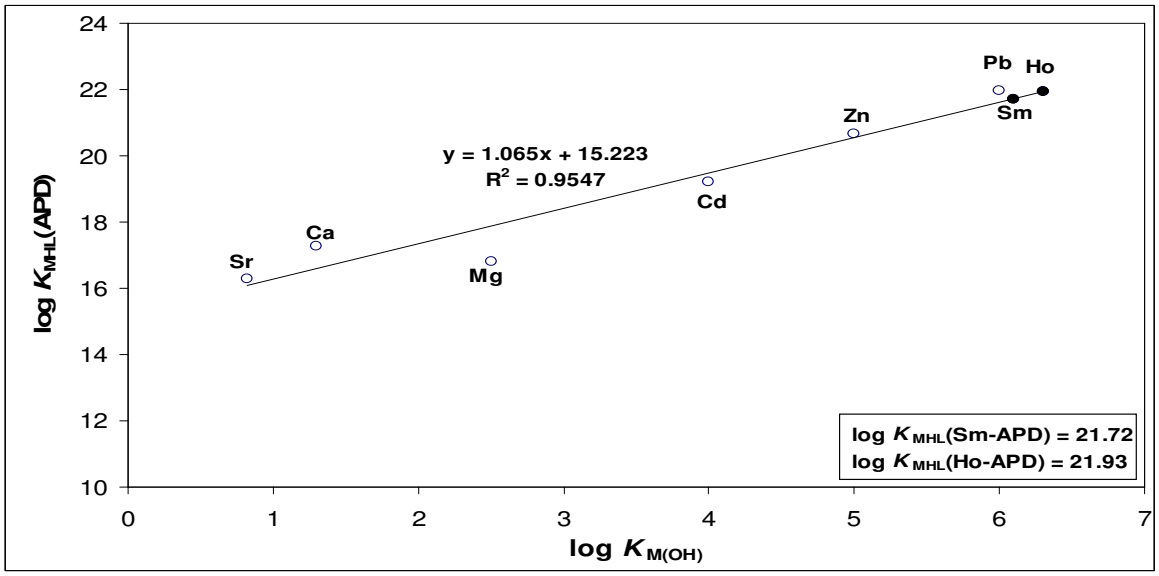


**Figure 4.45:** The linear free energy relationship (LFER) between the log $K_{M(OH)}$ and log $K_{MHL}$ for indicated metal ions (all divalent) and the ligand APD.

**Table 4.16:** Data for log $K_{MHL}$ for the ligand APD and log $K_{M(OH)}$ for several metal ions. Note that the log $K_{MHL}$ for $Mg^{II}$ was obtained in this work.

| Cation | log $K_{M(OH)}$ | log $K_{MHL}$ | Reference |
|---|---|---|---|
| $Sr^{II}$ | 0.82 | 16.30 | [1] |
| $Ca^{II}$ | 1.3 | 17.27 | [1] |
| $Mg^{II}$ | 2.5 | 19.0 | TW |
| $Cd^{II}$ | 4.0 | 19.21 | TW |
| $Zn^{II}$ | 5.0 | 20.68 | TW* |
| $Pb^{II}$ | 6.0 | 21.96 | TW* |
| $Sm^{III}$ | 6.1 | **21.86** | Predicted |
| $Ho^{III}$ | 6.3 | **22.06** | Predicted |

TW means this work, *–average value from DC and VP–DC data.

**Table 4.17:** Data for log $K_{MHL}$ for the ligand APD and log $K_{M(OH)}$ for several metal ions. Note that the log $K_{MHL}$ for $Mg^{II}$ was not included in this case.

| Cation | log $K_{M(OH)}$ | log $K_{MHL}$ | Reference |
|---|---|---|---|
| $Sr^{II}$ | 0.82 | 16.30 | [1] |
| $Ca^{II}$ | 1.3 | 17.27 | [1] |
| $Cd^{II}$ | 4.0 | 19.21 | TW |
| $Zn^{II}$ | 5.0 | 20.68 | TW* |
| $Pb^{II}$ | 6.0 | 21.96 | TW* |
| $Sm^{III}$ | 6.1 | **21.81** | Predicted |
| $Ho^{III}$ | 6.3 | **22.00** | Predicted |

TW means this work, *–average value from DC and VP–DC data.

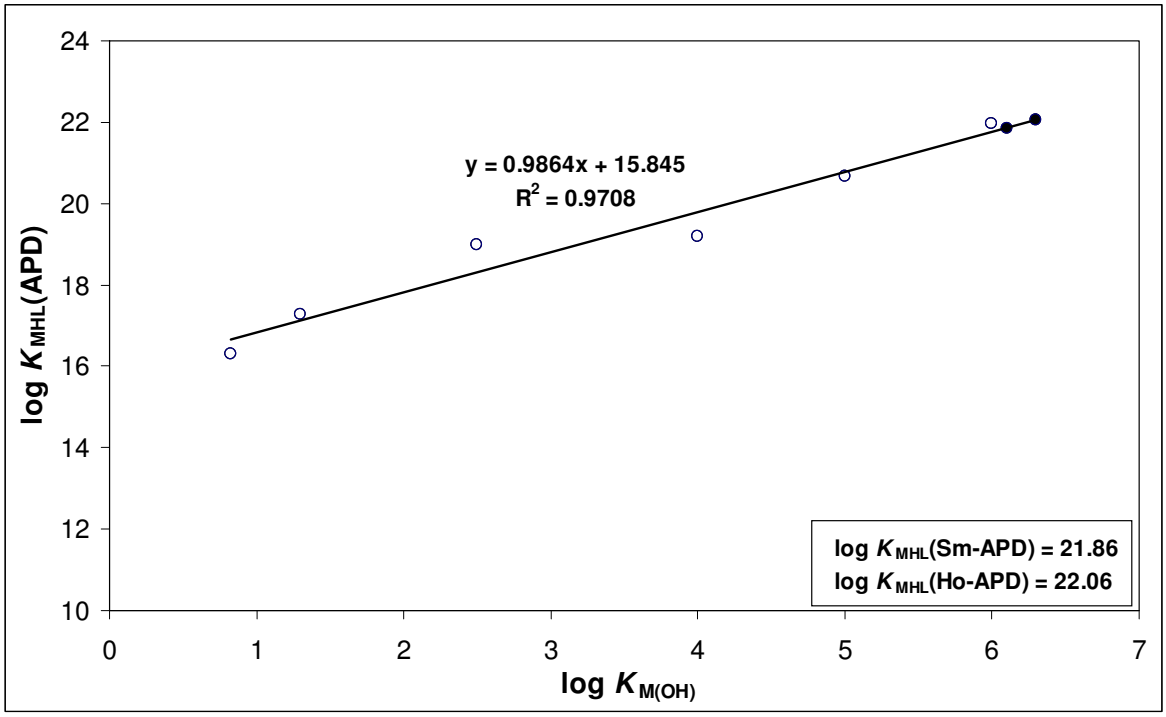


**Figure 4.46**: The linear free energy relationship (LFER) between the log $K_{M(OH)}$ and log $K_{MHL}$ for indicated metal ions (all divalent) and the ligand APD. The log $K_{MHL}$ value for $Mg^{II}$ determined in this work was used.

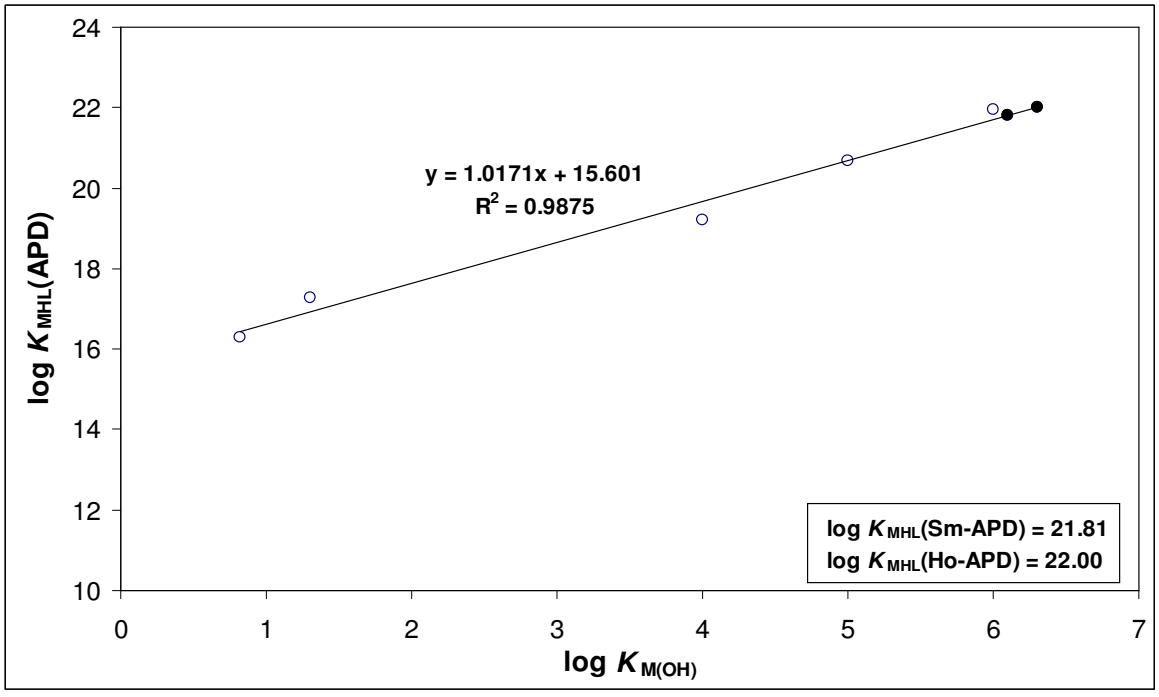


**Figure 4.47:** The linear free energy relationship (LFER) between the log $K_{M(OH)}$ and log $K_{MHL}$ for indicated metal ions (all divalent) and the ligand APD. The log $K_{MHL}$ value for $Mg^{II}$ was not used at all.

From Figure 4.46 it appears that the value of log $K_{MHL}$ = 19 for $Mg^{II}$ is too large. Hence this value was excluded and a new LFER was generated. The predicted log $K_{MHL}$ values for $Sm^{III}$–HL and $Ho^{III}$–HL were 21.81 and 22.00, respectively (as shown in Table 4.17 and figure 4.47).

**Table 4.18:** The estimated first formation constants from the LFER (as log $K_{MHL}$) for $Sm^{III}$ and $Ho^{III}$ with APD at an ionic strength of 0.15 M (NaCl) and 25 °C.

| | **$Sm^{III}$** | **$Ho^{III}$** |
|---|---|---|
| a) With log $K_{MHL}$ for $Mg^{II}$[1] | 21.72 | 21.93 |
| b) With log $K_{MHL}$ for $Mg^{II}$[TW] | 21.86 | 22.06 |
| c) Without log $K_{MHL}$ for $Mg^{II}$ | 21.81 | 22.00 |
| **Average value** | **21.80** | **22.00** |

From Table 4.18 it is clear that the predicted log $K_{MHL}$ values for $Sm^{III}$–HL and $Ho^{III}$–HL are similar irrespective of whether log $K_{MHL}$ value of $Mg^{II}$ was used or not; the spread in predicted stability constants is about 0.10 log unit which is below 1 % of the log $K_{MHL}$ value. From the above it is obvious that in order to predict reliable estimates for $Sm^{III}$ and $Ho^{III}$, one need stability constants for metal ions with as large log $K_{M(OH)}$ as possible.

The reported crystal structures of the ligand APD with the metal ions $Zn^{II}$ and $Fe^{II}$ as seen in Figures 4.15 and 4.16 indicate that the N-atom on the ligand APD is not involved in complexation. Thus one might exclude the first protonation constant from refinement operations. This results in re-defining the ligand from $H_5L$ to $H_4L$, where L′ = HL. This approach might be useful when one wants to compare a binding power of APD with HEDP or MDP. Since the presence of Mg(HL) complex had no significant impact on predicted log $K_{MHL}$ values for $Sm^{III}$ and $Ho^{III}$, this complex was not included in prediction of relevant log $K_{ML'}$ values.

When looking at Table 4.19, the predicted log $K_{ML'}$ values for $Sm^{III}$–L′ and $Ho^{III}$– L′ are 9.96 and 10.16, respectively (see also Figure 4.48). These predicted log $K_{ML'}$ values for $Sm^{III}$– L′ and $Ho^{III}$– L′ are comparable to the reported predicted log $K_{ML}$ values for $Sm^{III}$–HEDP and $Ho^{III}$–HEDP which are 10.10 and 10.40, respectively [11]. The predicted log $K_{ML'}$ value for $Sm^{III}$ is by 0.14 log unit smaller than the predicted value for log $K_{ML}$(HEDP) reported. While the predicted log $K_{ML'}$ value for $Ho^{III}$ is by 0.24 log unit smaller than the predicted value for log $K_{ML}$(HEDP) reported as well. These values could be regarded as virtually the same considering the fact that stability constants from which they were predicted were determined using different polarographic modes.

**Table 4.19**: Data for log $K_{ML'}$ for the ligand APD and log $K_{M(OH)}$ for several metal ions. (where L′ = H–APD)

| Cation | log $K_{M(OH)}$ | log $K_{ML'}$ | Reference |
|---|---|---|---|
| $Sr^{II}$ | 0.82 | 4.45 | [1] |
| $Ca^{II}$ | 1.3 | 5.42 | [1] |
| $Cd^{II}$ | 4.0 | 7.36 | TW |
| $Zn^{II}$ | 5.0 | 8.83 | TW* |
| $Pb^{II}$ | 6.0 | 10.11 | TW* |
| $Sm^{III}$ | 6.1 | **9.96** | Predicted |
| $Ho^{III}$ | 6.3 | **10.16** | Predicted |

TW means this work, *–average value from DC and VP–DC data.

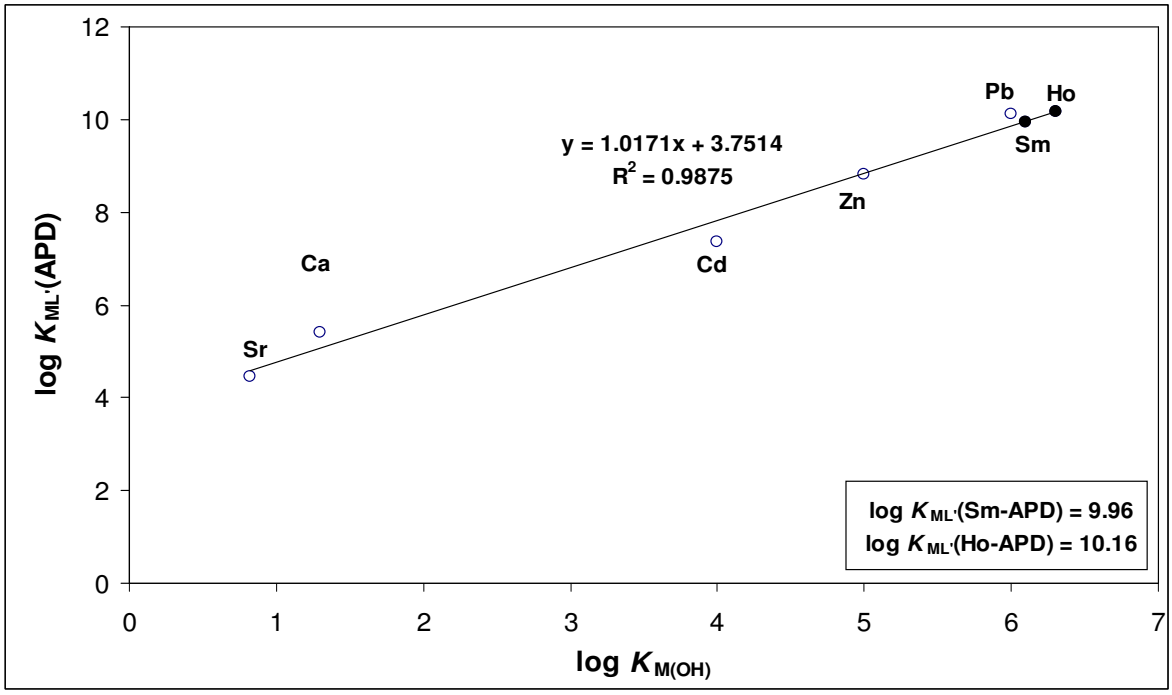


**Figure 4.48:** The linear free energy relationship (LFER) between the log $K_{M(OH)}$ and log $K_{ML'}$ for indicated metal ions (all divalent) and the ligand APD. The log $K_{ML'}$ value for $Mg^{II}$ was not used at all.

In this work the $DC_{TAST}$ mode was utilized while DPP mode was used in [11]. Thus stability constants determined in [11] are less reliable because departure from electrochemical reversibility for the metal-ligand systems was not accounted for. In principle, the predicted log $K_{ML'}$ for $Sm^{III}$ and $Ho^{III}$ should be very much the same as their counterparts for the HEDP ligand.

## References


1. J. R. Zeevaart, N. V. Jarvis, W. K. A. Louw, G. E. Jackson, I. Cukrowski and C. J. Mouton, *J. Inorg. Biochem.*, **1999**, *73*, 265.
2. NIST Standard Reference Database 46. NIST Critically Selected Stability Constants of Metal Complexes Database. Version 8.0. Data collected and selected by R. M. Smith, A. E. Martell, US Department of Commerce, National Institute of Standards and Technology, 2004.
3. Hagele et al.**,** *Heteroatom Chemistry*, **2000**, *11*, No. 7, 562.
4. I. Cukrowski and J. M. Min Zhang, *Electroanalysis*, **2004**, *16*, No. 8, 814.
5. I. Cukrowski, *Anal.Chim. Acta*, **1996**, *336*, 23.
6. I. Cukrowski and M. Adsetts, *J. Electroanal. Chem.,* **1997**, *429*, 129.
7. I. Cukrowski, *Electroanalysis*, **1997**, *9***,** No. 9, 699.
8. I. Cukrowski, *Electroanalysis*, **1997**, *9***,** No. 15, 1167.
9. I. Cukrowski, *Analyst*, **1997**, *122*, 827.
10. I. Cukrowski, unpublished work.
11. J. R. Zeevaart, N. V. Jarvis, I. Cukrowski and G. E. Jackson, *S.A. Journal of Chem.*, **1997**, *50***,** No. 4, 189.
12. J. R. Zeevaart, Metal Ion Speciation in Blood Plasma as a Tool in Predicting the In vivo Behaviour of Potential Bone-seeking Radiopharmaceuticals, Ph.D Thesis, Delft University Press, The Netherlands, 2001.
13. D. Fernandez, G. Polla, D. Vega and J. A. Ellena, *Acta Crystallogr., Sec. C: Cryst. Struct. Commun.*, **2004**, *60*, m73.
14. K. Abu-Shandi and C. Janiak, *Z. Naturforsch., B: Chem. Sci.*, **2005**, *60*, 1250.
15. F. A. Allen, *Acta Cryst.*, **2002**, *B58*, 380.
16. I. Cukrowski, J. R. Zeevaart and N. V. Jarvis, *Anal. Chim. Acta.,* **1999**, *379*, 217.
17. I. Cukrowski, P. Magampa and T. S. Mkwizu, *Helv. Chim. Acta.,* 2006, *89*, 2934.
18. V.N. Serezhkin, L. B. Serezhkina and V. S. Sergienko, *Russ. J. Inorg. Chem.*, **2000**, *45*, 521.
19. M. D. Mogano, Electrochemical studies of metal-ligand complexation of HEDP and MDP ligands for bone cancer therapy, a dissertation submitted to the Faculty of Science of the University of the Witwatersrand, Johannesburg, South Africa. pp 111-126.

# CHAPTER 5

# CONCLUSIONS

## Conclusions and Future work

- The protonation constants for the ligand APD determined in this work are comparable to the reported protonation constant values as shown in Table 4.2 considering the fact that they were determined at different ionic strengths and temperature as well as different background electrolyte solutions. The only discrepancies observed were between the $pKa_1$ and $pKa_4$ from this work and the ones reported in literature. However this is not of importance because the metal-ligand studies were performed in the pH range where these forms were not predominant.

- The LFER for the ligand APD has been established in this work by using data from literature [1] and data attained in this work from the study of the ligand APD with metal ions $Cd^{II}$, $Pb^{II}$ and $Zn^{II}$ by sampled Direct Current Polarography (i.e. $DC_{TAST}$) and from this data the log $K_{ML'}$ values of $Sm^{III}$–APD and $Ho^{III}$–APD were predicted to be 9.96 and 10.16, respectively. These predicted log $K_{ML'}$ values are comparable to the reported predicted log $K_{ML}$ values for $Sm^{III}$–HEDP and $Ho^{III}$–HEDP which are 10.10 and 10.40, respectively [11]. This suggest that the mode of complexation of these ligands to metal ions is the same irrespective of whether the ligand contains the amine–R group attached to the hydroxyl-containing carbon atom and this long chain does not take part in complex formation. This is supported by the reported crystal structures of the ligand APD. Therefore one can come to the conclusion that complexation of bisphosphonate ligands by metal ions occurs at the O-atoms of the phosphonate groups or O-atom of the hydroxyl group and that is why the predicted stability constants for $^{153}Sm^{III}$ and $^{166}Ho^{III}$ are similar.

- An attempt was made to study systems discussed in this work by potentiometry but failed due to precipitation at typical potentiometric conditions.

- The reported literature on the stability constant (i.e. log $K_{MHL}$) of Zn–APD is incorrect (based on the results attained in this work) and this system needs to be re–examined to verify this.

- The Pb–HEDP system was never reported in literature. The knowledge of this system could be beneficial in interpreting and understanding the chemistries of the bisphosphonate ligands MDP, HEDP and APD.

- It is clear from the analysis of stability constants for Pb–APD and literature data on Pb–MDP that the OH group in the ligand APD seems to be involved in complex formation since stability constants for APD are much larger than for MDP.

- An attempt was also made to grow crystals of complexes formed in solution for the $Cd^{II}$, $Pb^{II}$ and $Zn^{II}$–APD systems but failed, thus it is very important for future purposes to verify or understand how the ligand APD forms complexes at different pH values. This will provide answers as to whether the amine group is involved in complexation with the metal ions studied in this work or not. Thus crystals for these metal complexes need to be grown to check the structure of complexes proposed in this work.

- Thus solution chemistry cannot provide answers or explain as to why the potency of bisphosphonate ligands increases with the elongating N-containing chain. i.e. potency increase from HEDP to APD, etc.

## References

1. J. R. Zeevaart, N. V. Jarvis, W. K. A. Louw, G. E. Jackson, I. Cukrowski and C. J. Mouton, *J. Inorg. Biochem.*, **1999**, *73*, 265.
2. I. Cukrowski, D. M. Mogano and J. R. Zeevart, *J. Inorg. Biochem.*, **2005**, *99*, 2308.
3. J. R. Zeevaart, N. V. Jarvis, I. Cukrowski and G. E. Jackson, *S. Afr. J. Chem.*, **1997**, *50*, 189.

# Appendix A

1. **Formation constants for the metal ion complexes with hydroxide ion used in this work** [obtained from: NIST Standard Reference Database 46. NIST Critically Selected Stability Constants of Metal Complexes Database. Version 8.0. Data collected and selected by R. M. Smith, A. E. Martell, US Department of Commerce, National Institute of Standards and Technology, 2004.].

   a) **Formation constants for $Cd^{II}$ complexes with hydroxide ion.**

| Equilibrium | log β | Temperature/ °C | Ionic Strength/ $mol.L^{-1}$ |
|---|---|---|---|
| $Cd^{2+} + OH^- = Cd(OH)^+$ | 4.0 | 25 | 0 |
| $Cd^{2+} + 2\ OH^- = Cd(OH)_2$ | 7.7 | 25 | 0 and 3 |
| $Cd^{2+} + 3\ OH^- = Cd(OH)_3^-$ | 10.3 | 25 | 3 |
| $Cd^{2+} + 4\ OH^- = Cd(OH)_4^{2-}$ | 12.0 | 25 | 3 |
| $2Cd^{2+} + OH^- = Cd(OH)^{3+}$ | 5.06 | 25 | 3 |
| $4Cd^{2+} + 4\ OH^- = Cd_4(OH)^{4+}$ | 24.9 | 25 | 3 |
| $Cd^{2+} + 2\ OH^- = Cd(OH)_2(s)$ | -14.3 | 25 | 3 |

   b) **Formation constants for $Pb^{II}$ complexes with hydroxide ion.**

| Equilibrium | log β | Temperature/ °C | Ionic Strength/ $mol.L^{-1}$ |
|---|---|---|---|
| $Pb^{2+} + OH^- = Pb(OH)^+$ | 6.0 | 25 | 0.5 |
| $Pb^{2+} + 2\ OH^- = Pb(OH)_2$ | 10.3 | 25 | 0 and 3 |
| $Pb^{2+} + 3\ OH^- = Pb(OH)_3^-$ | 13.3 | 25 | 3 |
| $2Pb^{2+} + OH^- = Pb_2(OH)^{3+}$ | 7.6 | 25 | 0 |
| $3Pb^{2+} + 4\ OH^- = Pb_3(OH)_4^{2+}$ | 31.7 | 25 | 0.5 |
| $4Pb^{2+} + 4\ OH^- = Pb_4(OH)_4^{4+}$ | 35.2 | 25 | 0 and 0.5 |
| $6Pb^{2+} + 8\ OH^- = Pb_6(OH)_8^{4+}$ | 67.4 | 25 | 0.5 |
| $Pb^{2+} + 2\ OH^- = Pb(OH)_2(s)$ | -15.0 | 25 | 0 |

   c) **Formation constants for $Zn^{II}$ complexes with hydroxide ion**

| Equilibrium | log β | Temperature/ °C | Ionic Strength/ $mol.L^{-1}$ |
|---|---|---|---|
| $Zn^{2+} + OH^- = Zn(OH)^+$ | 5.0 | 25 | 0 |
| $Zn^{2+} + 2\ OH^- = Zn(OH)_2$ | 11.2 | 25 | 0 |
| $Zn^{2+} + 3\ OH^- = Zn(OH)_3^-$ | 13.6 | 25 | 0 |
| $Zn^{2+} + 4\ OH^- = Zn(OH)_4^{2-}$ | 15.4 | 25 | 3 |
| $2Zn^{2+} + OH^- = Zn_2(OH)^{3+}$ | 5.5 | 25 | 3 |
| $4Zn^{2+} + 4\ OH^- = Zn_4(OH)_4^+$ | 27.94 | 25 | 3 |
| $Zn^{2+} + 2\ OH^- = Zn(OH)_2$ | -14.8 | 25 | 0.1 |

# Appendix B: GEP data

## a) Data for protonation constants for ligand APD (titration 1).

| | | | | | | | | |
|---|---|---|---|---|---|---|---|---|
| TASK | ZBAR | 1 | TITRATION | of | APD:Protonation const. | | | |
| MODL | APD0 | H | 1 | | | | | |
| CPLX | 0 | 0 | -13.79 | H | +1( | -1) | | |
| CPLX | 1 | 0 | 11.85 | APD0( | 1) | H | +1( | 1) |
| CPLX | 1 | 0 | 21.61 | APD0( | 1) | H | +1( | 2) |
| CPLX | 0 | 0 | 27.38 | APD0( | 1) | H | +1( | 3) |
| CPLX | 1 | 0 | 28.88 | APD0( | 1) | H | +1( | 4) |
| CONC | | | | | | | | |
| VESL | IVOL | 20 | 0 | 0 | | | | |
| VESL | H | 1 | 0 | 0 | 0 | | | |
| VESL | APD0 | 0.010181 | 4 | 0 | | | | |
| BUR1 | H | 1 | -0.0509105 | 0 | 0 | | | |
| ELEC | | | | | | | | |
| ZERO | H | 1 | 403.21 | 0 | | | | |
| GRAD | H | 1 | 59.49 | 0 | | | | |
| DATA | | | | | | | | |

| EMF | | PH | | | ZBAR(H) | | POINT | | PA | | | |
|---|---|---|---|---|---|---|---|---|---|---|---|---|
| OBS | ZBAR(M) OBS CALC | CALC RESID | POINT RESID RESID | OBS | CALC | RESID | RESID | OBS | CALC | RESID | OBS | |
| 279.1 | 2.086 | 2.091 | -0.005 | 3.19 | 3.2 | -0.009 | 0.01 | 0 | 0 | 0 | 0 | 0 |
| 278.8 | 2.091 | 2.095 | -0.004 | 3.2 | 3.2 | -0.007 | 0.008 | 0 | 0 | 0 | 0 | 0 |
| 278.5 | 2.096 | 2.099 | -0.003 | 3.2 | 3.2 | -0.005 | 0.006 | 0 | 0 | 0 | 0 | 0 |
| 278.3 | 2.1 | 2.103 | -0.003 | 3.19 | 3.2 | -0.006 | 0.007 | 0 | 0 | 0 | 0 | 0 |
| 278 | 2.105 | 2.107 | -0.002 | 3.19 | 3.2 | -0.004 | 0.005 | 0 | 0 | 0 | 0 | 0 |
| 277.8 | 2.108 | 2.111 | -0.003 | 3.19 | 3.2 | -0.006 | 0.006 | 0 | 0 | 0 | 0 | 0 |
| 277.6 | 2.111 | 2.115 | -0.004 | 3.19 | 3.19 | -0.007 | 0.008 | 0 | 0 | 0 | 0 | 0 |
| 277.3 | 2.116 | 2.119 | -0.003 | 3.19 | 3.19 | -0.005 | 0.006 | 0 | 0 | 0 | 0 | 0 |
| 277.1 | 2.12 | 2.123 | -0.004 | 3.19 | 3.19 | -0.006 | 0.007 | 0 | 0 | 0 | 0 | 0 |
| 276.8 | 2.125 | 2.128 | -0.003 | 3.19 | 3.19 | -0.005 | 0.005 | 0 | 0 | 0 | 0 | 0 |
| 276.6 | 2.128 | 2.132 | -0.004 | 3.18 | 3.19 | -0.006 | 0.007 | 0 | 0 | 0 | 0 | 0 |
| 276.3 | 2.133 | 2.136 | -0.003 | 3.18 | 3.19 | -0.005 | 0.005 | 0 | 0 | 0 | 0 | 0 |
| 276 | 2.138 | 2.14 | -0.002 | 3.18 | 3.19 | -0.003 | 0.004 | 0 | 0 | 0 | 0 | 0 |
| 275.8 | 2.142 | 2.145 | -0.003 | 3.18 | 3.18 | -0.005 | 0.005 | 0 | 0 | 0 | 0 | 0 |
| 275.7 | 2.143 | 2.149 | -0.005 | 3.17 | 3.18 | -0.009 | 0.01 | 0 | 0 | 0 | 0 | 0 |
| 275.3 | 2.15 | 2.153 | -0.003 | 3.18 | 3.18 | -0.005 | 0.006 | 0 | 0 | 0 | 0 | 0 |
| 275 | 2.155 | 2.157 | -0.002 | 3.18 | 3.18 | -0.004 | 0.004 | 0 | 0 | 0 | 0 | 0 |
| 274.7 | 2.16 | 2.162 | -0.002 | 3.18 | 3.18 | -0.003 | 0.003 | 0 | 0 | 0 | 0 | 0 |
| 274.5 | 2.164 | 2.166 | -0.003 | 3.17 | 3.18 | -0.004 | 0.005 | 0 | 0 | 0 | 0 | 0 |
| 274.2 | 2.169 | 2.171 | -0.002 | 3.17 | 3.18 | -0.003 | 0.004 | 0 | 0 | 0 | 0 | 0 |
| 273.9 | 2.174 | 2.175 | -0.002 | 3.17 | 3.17 | -0.002 | 0.003 | 0 | 0 | 0 | 0 | 0 |
| 273.7 | 2.177 | 2.18 | -0.003 | 3.17 | 3.17 | -0.004 | 0.005 | 0 | 0 | 0 | 0 | 0 |
| 273.4 | 2.182 | 2.184 | -0.002 | 3.17 | 3.17 | -0.003 | 0.004 | 0 | 0 | 0 | 0 | 0 |
| 273.1 | 2.187 | 2.189 | -0.002 | 3.17 | 3.17 | -0.003 | 0.003 | 0 | 0 | 0 | 0 | 0 |
| 272.8 | 2.192 | 2.193 | -0.001 | 3.17 | 3.17 | -0.002 | 0.002 | 0 | 0 | 0 | 0 | 0 |
| 272.6 | 2.195 | 2.198 | -0.003 | 3.16 | 3.17 | -0.004 | 0.005 | 0 | 0 | 0 | 0 | 0 |
| 272.3 | 2.201 | 2.203 | -0.002 | 3.16 | 3.17 | -0.003 | 0.004 | 0 | 0 | 0 | 0 | 0 |
| 272 | 2.206 | 2.208 | -0.002 | 3.16 | 3.16 | -0.003 | 0.003 | 0 | 0 | 0 | 0 | 0 |
| 271.7 | 2.211 | 2.212 | -0.002 | 3.16 | 3.16 | -0.002 | 0.003 | 0 | 0 | 0 | 0 | 0 |
| 271.6 | 2.212 | 2.217 | -0.005 | 3.15 | 3.16 | -0.007 | 0.008 | 0 | 0 | 0 | 0 | 0 |
| 271.2 | 2.219 | 2.222 | -0.003 | 3.16 | 3.16 | -0.004 | 0.005 | 0 | 0 | 0 | 0 | 0 |
| 270.8 | 2.226 | 2.227 | -0.001 | 3.16 | 3.16 | -0.001 | 0.002 | 0 | 0 | 0 | 0 | 0 |
| 270.5 | 2.231 | 2.232 | -0.001 | 3.15 | 3.16 | -0.001 | 0.002 | 0 | 0 | 0 | 0 | 0 |
| 270.2 | 2.236 | 2.237 | -0.001 | 3.15 | 3.15 | -0.001 | 0.001 | 0 | 0 | 0 | 0 | 0 |
| 269.9 | 2.241 | 2.242 | -0.001 | 3.15 | 3.15 | -0.001 | 0.001 | 0 | 0 | 0 | 0 | 0 |
| 269.6 | 2.246 | 2.247 | -0.001 | 3.15 | 3.15 | -0.001 | 0.001 | 0 | 0 | 0 | 0 | 0 |
| 269.3 | 2.251 | 2.252 | -0.001 | 3.15 | 3.15 | -0.001 | 0.001 | 0 | 0 | 0 | 0 | 0 |
| 269 | 2.256 | 2.257 | -0.001 | 3.15 | 3.15 | -0.001 | 0.001 | 0 | 0 | 0 | 0 | 0 |
| 268.7 | 2.261 | 2.262 | -0.001 | 3.15 | 3.15 | -0.001 | 0.002 | 0 | 0 | 0 | 0 | 0 |
| 268.4 | 2.266 | 2.267 | -0.001 | 3.14 | 3.15 | -0.002 | 0.002 | 0 | 0 | 0 | 0 | 0 |

| | | | | | | | | | | | | |
|---|---|---|---|---|---|---|---|---|---|---|---|---|
| 268.1 | 2.2710 | 2.2730 | -0.001 | 3.14 | 3.14 | -0.002 | 0.002 | 0 | 0 | 0 | 0 | 0 |
| 267.7 | 2.2780 | 2.2780 | 0 | 3.14 | 3.14 | 0 | 0 | 0 | 0 | 0 | 0 | 0 |
| 267.4 | 2.2830 | 2.2830 | 0 | 3.14 | 3.14 | 0 | 0.001 | 0 | 0 | 0 | 0 | 0 |
| 267.2 | 2.2860 | 2.2890 | -0.002 | 3.14 | 3.14 | -0.003 | 0.004 | 0 | 0 | 0 | 0 | 0 |
| 266.9 | 2.2910 | 2.2940 | -0.003 | 3.13 | 3.14 | -0.003 | 0.004 | 0 | 0 | 0 | 0 | 0 |
| 266.5 | 2.2980 | 2.30 | -0.002 | 3.13 | 3.14 | -0.002 | 0.003 | 0 | 0 | 0 | 0 | 0 |
| 266.1 | 2.3050 | 2.3050 | 0 | 3.13 | 3.14 | -0.001 | 0.001 | 0 | 0 | 0 | 0 | 0 |
| 265.8 | 2.310 | 2.3110 | -0.001 | 3.13 | 3.13 | -0.001 | 0.002 | 0 | 0 | 0 | 0 | 0 |
| 265.4 | 2.3170 | 2.3170 | 0 | 3.13 | 3.13 | 0 | 0 | 0 | 0 | 0 | 0 | 0 |
| 265.1 | 2.3220 | 2.3220 | -0.001 | 3.13 | 3.13 | -0.001 | 0.001 | 0 | 0 | 0 | 0 | 0 |
| 264.7 | 2.3280 | 2.3280 | 0 | 3.13 | 3.13 | 0 | 0 | 0 | 0 | 0 | 0 | 0 |
| 264.3 | 2.3350 | 2.3340 | 0.001 | 3.13 | 3.13 | 0.001 | 0.001 | 0 | 0 | 0 | 0 | 0 |
| 264 | 2.340 | 2.340 | 0 | 3.13 | 3.13 | 0 | 0 | 0 | 0 | 0 | 0 | 0 |
| 263.6 | 2.3470 | 2.3460 | 0.001 | 3.13 | 3.12 | 0.001 | 0.001 | 0 | 0 | 0 | 0 | 0 |
| 263.3 | 2.3520 | 2.3520 | 0 | 3.12 | 3.12 | 0 | 0 | 0 | 0 | 0 | 0 | 0 |
| 262.9 | 2.3590 | 2.3580 | 0 | 3.12 | 3.12 | 0 | 0.001 | 0 | 0 | 0 | 0 | 0 |
| 262.5 | 2.3650 | 2.3640 | 0.001 | 3.12 | 3.12 | 0.001 | 0.001 | 0 | 0 | 0 | 0 | 0 |
| 262.3 | 2.3690 | 2.3710 | -0.002 | 3.12 | 3.12 | -0.002 | 0.003 | 0 | 0 | 0 | 0 | 0 |
| 261.8 | 2.3770 | 2.3770 | 0 | 3.12 | 3.12 | 0 | 0 | 0 | 0 | 0 | 0 | 0 |
| 261.4 | 2.3840 | 2.3830 | 0 | 3.12 | 3.12 | 0 | 0 | 0 | 0 | 0 | 0 | 0 |
| 261 | 2.390 | 2.390 | 0.001 | 3.11 | 3.11 | 0.001 | 0.001 | 0 | 0 | 0 | 0 | 0 |
| 260.6 | 2.3970 | 2.3970 | 0.001 | 3.11 | 3.11 | 0.001 | 0.001 | 0 | 0 | 0 | 0 | 0 |
| 260.2 | 2.4040 | 2.4030 | 0.001 | 3.11 | 3.11 | 0.001 | 0.001 | 0 | 0 | 0 | 0 | 0 |
| 259.8 | 2.4110 | 2.410 | 0.001 | 3.11 | 3.11 | 0.001 | 0.001 | 0 | 0 | 0 | 0 | 0 |
| 259.4 | 2.4170 | 2.4170 | 0.001 | 3.11 | 3.11 | 0.001 | 0.001 | 0 | 0 | 0 | 0 | 0 |
| 258.9 | 2.4260 | 2.4240 | 0.002 | 3.11 | 3.11 | 0.002 | 0.003 | 0 | 0 | 0 | 0 | 0 |
| 258.5 | 2.4330 | 2.4310 | 0.002 | 3.11 | 3.1 | 0.002 | 0.002 | 0 | 0 | 0 | 0 | 0 |
| 258.1 | 2.4390 | 2.4380 | 0.001 | 3.1 | 3.1 | 0.001 | 0.002 | 0 | 0 | 0 | 0 | 0 |
| 257.7 | 2.4460 | 2.4450 | 0.001 | 3.1 | 3.1 | 0.001 | 0.001 | 0 | 0 | 0 | 0 | 0 |
| 257.2 | 2.4540 | 2.4520 | 0.002 | 3.1 | 3.1 | 0.002 | 0.003 | 0 | 0 | 0 | 0 | 0 |
| 256.9 | 2.4590 | 2.460 | 0 | 3.1 | 3.1 | 0 | 0 | 0 | 0 | 0 | 0 | 0 |
| 256.4 | 2.4680 | 2.4670 | 0.001 | 3.1 | 3.1 | 0 | 0.001 | 0 | 0 | 0 | 0 | 0 |
| 255.9 | 2.4760 | 2.4750 | 0.001 | 3.1 | 3.1 | 0.001 | 0.002 | 0 | 0 | 0 | 0 | 0 |
| 255.5 | 2.4830 | 2.4830 | 0 | 3.09 | 3.09 | 0 | 0 | 0 | 0 | 0 | 0 | 0 |
| 255 | 2.4910 | 2.490 | 0.001 | 3.09 | 3.09 | 0.001 | 0.001 | 0 | 0 | 0 | 0 | 0 |
| 254.5 | 2.50 | 2.4980 | 0.001 | 3.09 | 3.09 | 0.001 | 0.002 | 0 | 0 | 0 | 0 | 0 |
| 254 | 2.5080 | 2.5070 | 0.002 | 3.09 | 3.09 | 0.001 | 0.002 | 0 | 0 | 0 | 0 | 0 |
| 253.5 | 2.5170 | 2.5150 | 0.002 | 3.09 | 3.09 | 0.001 | 0.002 | 0 | 0 | 0 | 0 | 0 |
| 253 | 2.5250 | 2.5230 | 0.002 | 3.09 | 3.09 | 0.001 | 0.002 | 0 | 0 | 0 | 0 | 0 |
| 252.5 | 2.5330 | 2.5320 | 0.002 | 3.09 | 3.08 | 0.001 | 0.002 | 0 | 0 | 0 | 0 | 0 |
| 252 | 2.5420 | 2.54 | 0.001 | 3.08 | 3.08 | 0.001 | 0.002 | 0 | 0 | 0 | 0 | 0 |
| 251.4 | 2.5520 | 2.5490 | 0.003 | 3.08 | 3.08 | 0.002 | 0.003 | 0 | 0 | 0 | 0 | 0 |
| 250.9 | 2.560 | 2.5580 | 0.002 | 3.08 | 3.08 | 0.001 | 0.003 | 0 | 0 | 0 | 0 | 0 |
| 250.4 | 2.5690 | 2.5670 | 0.001 | 3.08 | 3.08 | 0.001 | 0.002 | 0 | 0 | 0 | 0 | 0 |
| 249.5 | 2.5840 | 2.5830 | 0.001 | 3.08 | 3.08 | 0.001 | 0.001 | 0 | 0 | 0 | 0 | 0 |
| 248.5 | 2.6010 | 2.5990 | 0.002 | 3.07 | 3.07 | 0.001 | 0.002 | 0 | 0 | 0 | 0 | 0 |
| 247.5 | 2.6170 | 2.6160 | 0.002 | 3.07 | 3.07 | 0.001 | 0.002 | 0 | 0 | 0 | 0 | 0 |
| 246.5 | 2.6340 | 2.6330 | 0.001 | 3.07 | 3.07 | 0.001 | 0.002 | 0 | 0 | 0 | 0 | 0 |
| 245.4 | 2.6530 | 2.6510 | 0.002 | 3.07 | 3.07 | 0.001 | 0.002 | 0 | 0 | 0 | 0 | 0 |
| 244.3 | 2.6710 | 2.6690 | 0.002 | 3.06 | 3.06 | 0.001 | 0.002 | 0 | 0 | 0 | 0 | 0 |
| 243 | 2.6930 | 2.6880 | 0.005 | 3.06 | 3.06 | 0.002 | 0.005 | 0 | 0 | 0 | 0 | 0 |
| 241.8 | 2.7130 | 2.7080 | 0.005 | 3.06 | 3.06 | 0.002 | 0.005 | 0 | 0 | 0 | 0 | 0 |
| 240.5 | 2.7350 | 2.7290 | 0.006 | 3.06 | 3.05 | 0.003 | 0.006 | 0 | 0 | 0 | 0 | 0 |
| 239.2 | 2.7570 | 2.7510 | 0.006 | 3.05 | 3.05 | 0.003 | 0.006 | 0 | 0 | 0 | 0 | 0 |
| 237.8 | 2.780 | 2.7740 | 0.006 | 3.05 | 3.05 | 0.003 | 0.007 | 0 | 0 | 0 | 0 | 0 |
| 236.4 | 2.8040 | 2.7980 | 0.006 | 3.05 | 3.05 | 0.002 | 0.006 | 0 | 0 | 0 | 0 | 0 |
| 234.9 | 2.8290 | 2.8230 | 0.006 | 3.05 | 3.04 | 0.002 | 0.006 | 0 | 0 | 0 | 0 | 0 |
| 233.3 | 2.8560 | 2.85 | 0.006 | 3.04 | 3.04 | 0.002 | 0.006 | 0 | 0 | 0 | 0 | 0 |
| 231.7 | 2.8830 | 2.8780 | 0.005 | 3.04 | 3.04 | 0.002 | 0.005 | 0 | 0 | 0 | 0 | 0 |
| 230 | 2.9120 | 2.9080 | 0.003 | 3.04 | 3.04 | 0.001 | 0.003 | 0 | 0 | 0 | 0 | 0 |
| 228 | 2.9450 | 2.9410 | 0.005 | 3.03 | 3.03 | 0.001 | 0.005 | 0 | 0 | 0 | 0 | 0 |

| | | | | | | | | | | | | |
|---|---|---|---|---|---|---|---|---|---|---|---|---|
| 225.9 | 2.9810 | 2.9750 | 0.005 | 3.03 | 3.03 | 0.001 | 0.005 | 0 | 0 | 0 | 0 | 0 |
| 223.7 | 3.0170 | 3.0130 | 0.005 | 3.03 | 3.03 | 0.001 | 0.005 | 0 | 0 | 0 | 0 | 0 |
| 221.2 | 3.060 | 3.0530 | 0.006 | 3.03 | 3.03 | 0.002 | 0.007 | 0 | 0 | 0 | 0 | 0 |
| 218.6 | 3.1030 | 3.0970 | 0.006 | 3.02 | 3.02 | 0.001 | 0.006 | 0 | 0 | 0 | 0 | 0 |
| 215.7 | 3.1520 | 3.1460 | 0.006 | 3.02 | 3.02 | 0.001 | 0.006 | 0 | 0 | 0 | 0 | 0 |
| 212.6 | 3.2040 | 3.2010 | 0.003 | 3.02 | 3.02 | 0.001 | 0.003 | 0 | 0 | 0 | 0 | 0 |
| 209 | 3.2650 | 3.2630 | 0.002 | 3.01 | 3.01 | 0 | 0.002 | 0 | 0 | 0 | 0 | 0 |
| 204.9 | 3.3340 | 3.3340 | 0 | 3.01 | 3.01 | 0 | 0 | 0 | 0 | 0 | 0 | 0 |
| 200.1 | 3.4140 | 3.4160 | -0.002 | 3.01 | 3.01 | 0 | 0.002 | 0 | 0 | 0 | 0 | 0 |
| 194.4 | 3.510 | 3.5140 | -0.004 | 3 | 3 | 0 | 0.004 | 0 | 0 | 0 | 0 | 0 |
| 187.5 | 3.6260 | 3.6330 | -0.007 | 3 | 3 | 0 | 0.007 | 0 | 0 | 0 | 0 | 0 |
| 179 | 3.7690 | 3.7760 | -0.008 | 2.99 | 3 | 0 | 0.008 | 0 | 0 | 0 | 0 | 0 |
| 169.2 | 3.9340 | 3.9420 | -0.009 | 2.99 | 2.99 | 0 | 0.009 | 0 | 0 | 0 | 0 | 0 |
| 158.9 | 4.1070 | 4.1140 | -0.007 | 2.98 | 2.98 | 0 | 0.007 | 0 | 0 | 0 | 0 | 0 |
| 149.8 | 4.260 | 4.270 | -0.01 | 2.97 | 2.97 | 0 | 0.01 | 0 | 0 | 0 | 0 | 0 |
| 142 | 4.3910 | 4.4020 | -0.011 | 2.96 | 2.96 | 0 | 0.011 | 0 | 0 | 0 | 0 | 0 |
| 135.6 | 4.4980 | 4.5110 | -0.013 | 2.95 | 2.95 | 0 | 0.013 | 0 | 0 | 0 | 0 | 0 |
| 129.9 | 4.5940 | 4.6040 | -0.01 | 2.94 | 2.94 | 0 | 0.01 | 0 | 0 | 0 | 0 | 0 |
| 125.1 | 4.6750 | 4.6840 | -0.009 | 2.92 | 2.92 | 0 | 0.009 | 0 | 0 | 0 | 0 | 0 |
| 120.8 | 4.7470 | 4.7530 | -0.006 | 2.91 | 2.91 | 0 | 0.006 | 0 | 0 | 0 | 0 | 0 |
| 117 | 4.8110 | 4.8150 | -0.004 | 2.9 | 2.9 | 0 | 0.004 | 0 | 0 | 0 | 0 | 0 |
| 113.4 | 4.8720 | 4.8710 | 0 | 2.89 | 2.89 | 0 | 0 | 0 | 0 | 0 | 0 | 0 |
| 110.3 | 4.9240 | 4.9230 | 0.001 | 2.88 | 2.88 | 0 | 0.001 | 0 | 0 | 0 | 0 | 0 |
| 107.5 | 4.9710 | 4.970 | 0.001 | 2.86 | 2.86 | 0 | 0.001 | 0 | 0 | 0 | 0 | 0 |
| 104.9 | 5.0140 | 5.0140 | 0.001 | 2.85 | 2.85 | 0 | 0.001 | 0 | 0 | 0 | 0 | 0 |
| 102.5 | 5.0550 | 5.0550 | 0 | 2.84 | 2.84 | 0 | 0 | 0 | 0 | 0 | 0 | 0 |
| 100.2 | 5.0930 | 5.0930 | 0 | 2.83 | 2.83 | 0 | 0 | 0 | 0 | 0 | 0 | 0 |
| 98 | 5.130 | 5.130 | 0.001 | 2.81 | 2.81 | 0 | 0.001 | 0 | 0 | 0 | 0 | 0 |
| 96 | 5.1640 | 5.1640 | 0 | 2.8 | 2.8 | 0 | 0 | 0 | 0 | 0 | 0 | 0 |
| 94 | 5.1980 | 5.1970 | 0 | 2.79 | 2.79 | 0 | 0 | 0 | 0 | 0 | 0 | 0 |
| 91.9 | 5.2330 | 5.2290 | 0.004 | 2.78 | 2.78 | 0 | 0.004 | 0 | 0 | 0 | 0 | 0 |
| 90 | 5.2650 | 5.260 | 0.005 | 2.76 | 2.76 | 0 | 0.005 | 0 | 0 | 0 | 0 | 0 |
| 88.2 | 5.2950 | 5.2890 | 0.006 | 2.75 | 2.75 | 0 | 0.006 | 0 | 0 | 0 | 0 | 0 |
| 86.5 | 5.3240 | 5.3180 | 0.006 | 2.74 | 2.74 | 0 | 0.006 | 0 | 0 | 0 | 0 | 0 |
| 85 | 5.3490 | 5.3450 | 0.004 | 2.73 | 2.73 | 0 | 0.004 | 0 | 0 | 0 | 0 | 0 |
| 83.4 | 5.3760 | 5.3720 | 0.004 | 2.71 | 2.71 | 0 | 0.004 | 0 | 0 | 0 | 0 | 0 |
| 81.8 | 5.4030 | 5.3980 | 0.004 | 2.7 | 2.7 | 0 | 0.004 | 0 | 0 | 0 | 0 | 0 |
| 80.3 | 5.4280 | 5.4240 | 0.004 | 2.69 | 2.69 | 0 | 0.004 | 0 | 0 | 0 | 0 | 0 |
| 78.8 | 5.4530 | 5.4490 | 0.004 | 2.68 | 2.68 | 0 | 0.004 | 0 | 0 | 0 | 0 | 0 |
| 77.3 | 5.4780 | 5.4730 | 0.005 | 2.66 | 2.66 | 0 | 0.005 | 0 | 0 | 0 | 0 | 0 |
| 75.9 | 5.5020 | 5.4980 | 0.004 | 2.65 | 2.65 | 0 | 0.004 | 0 | 0 | 0 | 0 | 0 |
| 74.4 | 5.5270 | 5.5210 | 0.006 | 2.64 | 2.64 | 0 | 0.006 | 0 | 0 | 0 | 0 | 0 |
| 73 | 5.5510 | 5.5450 | 0.006 | 2.63 | 2.63 | 0 | 0.006 | 0 | 0 | 0 | 0 | 0 |
| 71.6 | 5.5740 | 5.5680 | 0.007 | 2.61 | 2.61 | 0 | 0.007 | 0 | 0 | 0 | 0 | 0 |
| 70.3 | 5.5960 | 5.590 | 0.006 | 2.6 | 2.6 | 0 | 0.006 | 0 | 0 | 0 | 0 | 0 |
| 69 | 5.6180 | 5.6130 | 0.005 | 2.59 | 2.59 | 0 | 0.005 | 0 | 0 | 0 | 0 | 0 |
| 67.7 | 5.640 | 5.6350 | 0.005 | 2.58 | 2.58 | 0 | 0.005 | 0 | 0 | 0 | 0 | 0 |
| 66.4 | 5.6620 | 5.6570 | 0.004 | 2.56 | 2.56 | 0 | 0.004 | 0 | 0 | 0 | 0 | 0 |
| 65.1 | 5.6830 | 5.6790 | 0.004 | 2.55 | 2.55 | 0 | 0.004 | 0 | 0 | 0 | 0 | 0 |
| 63.7 | 5.7070 | 5.7010 | 0.006 | 2.54 | 2.54 | 0 | 0.006 | 0 | 0 | 0 | 0 | 0 |
| 62.5 | 5.7270 | 5.7230 | 0.004 | 2.53 | 2.53 | 0 | 0.004 | 0 | 0 | 0 | 0 | 0 |
| 61.1 | 5.7510 | 5.7450 | 0.006 | 2.51 | 2.51 | 0 | 0.006 | 0 | 0 | 0 | 0 | 0 |
| 59.8 | 5.7730 | 5.7660 | 0.006 | 2.5 | 2.5 | 0 | 0.006 | 0 | 0 | 0 | 0 | 0 |
| 58.5 | 5.7940 | 5.7880 | 0.006 | 2.49 | 2.49 | 0 | 0.006 | 0 | 0 | 0 | 0 | 0 |
| 57.2 | 5.8160 | 5.810 | 0.007 | 2.48 | 2.48 | 0 | 0.007 | 0 | 0 | 0 | 0 | 0 |
| 55.9 | 5.8380 | 5.8310 | 0.007 | 2.46 | 2.46 | 0 | 0.007 | 0 | 0 | 0 | 0 | 0 |
| 54.6 | 5.860 | 5.8530 | 0.007 | 2.45 | 2.45 | 0 | 0.007 | 0 | 0 | 0 | 0 | 0 |
| 53.3 | 5.8820 | 5.8750 | 0.007 | 2.44 | 2.44 | 0 | 0.007 | 0 | 0 | 0 | 0 | 0 |
| 52 | 5.9040 | 5.8970 | 0.006 | 2.43 | 2.43 | 0 | 0.006 | 0 | 0 | 0 | 0 | 0 |
| 50.6 | 5.9270 | 5.920 | 0.008 | 2.41 | 2.41 | 0 | 0.008 | 0 | 0 | 0 | 0 | 0 |
| 49.3 | 5.9490 | 5.9420 | 0.007 | 2.4 | 2.4 | 0 | 0.007 | 0 | 0 | 0 | 0 | 0 |

| | | | | | | | | | | | | |
|---|---|---|---|---|---|---|---|---|---|---|---|---|
| 47.9 | 5.9730 | 5.9650 | 0.008 | 2.39 | 2.39 | 0 | 0.008 | 0 | 0 | 0 | 0 | 0 |
| 46.5 | 5.9960 | 5.9880 | 0.009 | 2.38 | 2.38 | 0 | 0.009 | 0 | 0 | 0 | 0 | 0 |
| 45.1 | 6.020 | 6.0110 | 0.009 | 2.36 | 2.36 | 0 | 0.009 | 0 | 0 | 0 | 0 | 0 |
| 43.8 | 6.0420 | 6.0340 | 0.007 | 2.35 | 2.35 | 0 | 0.007 | 0 | 0 | 0 | 0 | 0 |
| 42.4 | 6.0650 | 6.0580 | 0.007 | 2.34 | 2.34 | 0 | 0.007 | 0 | 0 | 0 | 0 | 0 |
| 40.9 | 6.090 | 6.0830 | 0.008 | 2.33 | 2.33 | 0 | 0.008 | 0 | 0 | 0 | 0 | 0 |
| 39.5 | 6.1140 | 6.1080 | 0.006 | 2.31 | 2.31 | 0 | 0.006 | 0 | 0 | 0 | 0 | 0 |
| 38 | 6.1390 | 6.1330 | 0.006 | 2.3 | 2.3 | 0 | 0.006 | 0 | 0 | 0 | 0 | 0 |
| 36.4 | 6.1660 | 6.1590 | 0.007 | 2.29 | 2.29 | 0 | 0.007 | 0 | 0 | 0 | 0 | 0 |
| 34.8 | 6.1930 | 6.1860 | 0.007 | 2.28 | 2.28 | 0 | 0.007 | 0 | 0 | 0 | 0 | 0 |
| 33.1 | 6.2210 | 6.2130 | 0.008 | 2.26 | 2.26 | 0 | 0.008 | 0 | 0 | 0 | 0 | 0 |
| 31.4 | 6.250 | 6.2410 | 0.009 | 2.25 | 2.25 | 0 | 0.009 | 0 | 0 | 0 | 0 | 0 |
| 29.7 | 6.2790 | 6.2710 | 0.008 | 2.24 | 2.24 | 0 | 0.008 | 0 | 0 | 0 | 0 | 0 |
| 27.9 | 6.3090 | 6.3010 | 0.008 | 2.23 | 2.23 | 0 | 0.008 | 0 | 0 | 0 | 0 | 0 |
| 26.1 | 6.3390 | 6.3320 | 0.007 | 2.21 | 2.21 | 0 | 0.007 | 0 | 0 | 0 | 0 | 0 |
| 24.2 | 6.3710 | 6.3650 | 0.006 | 2.2 | 2.2 | 0 | 0.006 | 0 | 0 | 0 | 0 | 0 |
| 22.2 | 6.4050 | 6.3990 | 0.005 | 2.19 | 2.19 | 0 | 0.005 | 0 | 0 | 0 | 0 | 0 |
| 20 | 6.4420 | 6.4350 | 0.006 | 2.18 | 2.18 | 0 | 0.006 | 0 | 0 | 0 | 0 | 0 |
| 17.6 | 6.4820 | 6.4730 | 0.009 | 2.16 | 2.16 | 0 | 0.009 | 0 | 0 | 0 | 0 | 0 |
| 15.2 | 6.5220 | 6.5140 | 0.008 | 2.15 | 2.15 | 0 | 0.008 | 0 | 0 | 0 | 0 | 0 |
| 12.6 | 6.5660 | 6.5570 | 0.009 | 2.14 | 2.14 | 0 | 0.009 | 0 | 0 | 0 | 0 | 0 |
| 9.7 | 6.6150 | 6.6030 | 0.011 | 2.13 | 2.13 | 0 | 0.011 | 0 | 0 | 0 | 0 | 0 |
| 6.7 | 6.6650 | 6.6540 | 0.011 | 2.11 | 2.11 | 0 | 0.011 | 0 | 0 | 0 | 0 | 0 |
| 3.5 | 6.7190 | 6.7090 | 0.01 | 2.1 | 2.1 | 0 | 0.01 | 0 | 0 | 0 | 0 | 0 |
| 0.1 | 6.7760 | 6.7710 | 0.006 | 2.09 | 2.09 | 0 | 0.006 | 0 | 0 | 0 | 0 | 0 |
| -3.9 | 6.8430 | 6.840 | 0.004 | 2.08 | 2.08 | 0 | 0.004 | 0 | 0 | 0 | 0 | 0 |
| -8.5 | 6.9210 | 6.9190 | 0.001 | 2.06 | 2.06 | 0 | 0.001 | 0 | 0 | 0 | 0 | 0 |
| -14 | 7.0130 | 7.0130 | 0 | 2.05 | 2.05 | 0 | 0 | 0 | 0 | 0 | 0 | 0 |
| -20.9 | 7.1290 | 7.1270 | 0.002 | 2.04 | 2.04 | 0 | 0.002 | 0 | 0 | 0 | 0 | 0 |
| -29.5 | 7.2740 | 7.2710 | 0.002 | 2.03 | 2.03 | 0 | 0.002 | 0 | 0 | 0 | 0 | 0 |
| -41.2 | 7.470 | 7.4630 | 0.007 | 2.01 | 2.01 | 0 | 0.007 | 0 | 0 | 0 | 0 | 0 |
| -56 | 7.7190 | 7.7130 | 0.007 | 2 | 2 | 0 | 0.007 | 0 | 0 | 0 | 0 | 0 |
| -71.3 | 7.9760 | 7.9760 | 0 | 1.99 | 1.99 | 0 | 0 | 0 | 0 | 0 | 0 | 0 |
| -83.6 | 8.1830 | 8.1890 | -0.006 | 1.98 | 1.98 | 0 | 0.006 | 0 | 0 | 0 | 0 | 0 |
| -92.9 | 8.3390 | 8.3490 | -0.009 | 1.97 | 1.97 | 0 | 0.009 | 0 | 0 | 0 | 0 | 0 |
| -100.2 | 8.4620 | 8.4720 | -0.01 | 1.95 | 1.95 | 0 | 0.01 | 0 | 0 | 0 | 0 | 0 |
| -106.1 | 8.5610 | 8.5720 | -0.011 | 1.94 | 1.94 | 0 | 0.011 | 0 | 0 | 0 | 0 | 0 |
| -111.1 | 8.6450 | 8.6560 | -0.01 | 1.93 | 1.93 | 0 | 0.01 | 0 | 0 | 0 | 0 | 0 |
| -115.5 | 8.7190 | 8.7280 | -0.009 | 1.92 | 1.92 | 0 | 0.009 | 0 | 0 | 0 | 0 | 0 |
| -119.4 | 8.7850 | 8.7920 | -0.007 | 1.9 | 1.9 | 0 | 0.007 | 0 | 0 | 0 | 0 | 0 |
| -122.9 | 8.8440 | 8.8490 | -0.005 | 1.89 | 1.89 | 0 | 0.005 | 0 | 0 | 0 | 0 | 0 |
| -126.1 | 8.8970 | 8.90 | -0.003 | 1.88 | 1.88 | 0 | 0.003 | 0 | 0 | 0 | 0 | 0 |
| -128.9 | 8.9450 | 8.9480 | -0.003 | 1.87 | 1.87 | 0 | 0.003 | 0 | 0 | 0 | 0 | 0 |
| -131.6 | 8.990 | 8.9920 | -0.002 | 1.85 | 1.85 | 0 | 0.002 | 0 | 0 | 0 | 0 | 0 |
| -133.9 | 9.0290 | 9.0330 | -0.004 | 1.84 | 1.84 | 0 | 0.004 | 0 | 0 | 0 | 0 | 0 |
| -136.2 | 9.0670 | 9.0710 | -0.004 | 1.83 | 1.83 | 0 | 0.004 | 0 | 0 | 0 | 0 | 0 |
| -138.3 | 9.1030 | 9.1080 | -0.005 | 1.82 | 1.82 | 0 | 0.005 | 0 | 0 | 0 | 0 | 0 |
| -140.3 | 9.1360 | 9.1420 | -0.006 | 1.81 | 1.81 | 0 | 0.006 | 0 | 0 | 0 | 0 | 0 |
| -142.3 | 9.170 | 9.1750 | -0.005 | 1.79 | 1.79 | 0 | 0.005 | 0 | 0 | 0 | 0 | 0 |
| -144.2 | 9.2020 | 9.2070 | -0.005 | 1.78 | 1.78 | 0 | 0.005 | 0 | 0 | 0 | 0 | 0 |
| -146.1 | 9.2340 | 9.2370 | -0.003 | 1.77 | 1.77 | 0 | 0.003 | 0 | 0 | 0 | 0 | 0 |
| -147.9 | 9.2640 | 9.2660 | -0.002 | 1.76 | 1.76 | 0 | 0.002 | 0 | 0 | 0 | 0 | 0 |
| -149.5 | 9.2910 | 9.2940 | -0.003 | 1.74 | 1.74 | 0 | 0.003 | 0 | 0 | 0 | 0 | 0 |
| -151.1 | 9.3180 | 9.3210 | -0.003 | 1.73 | 1.73 | 0 | 0.003 | 0 | 0 | 0 | 0 | 0 |
| -152.7 | 9.3450 | 9.3470 | -0.003 | 1.72 | 1.72 | 0 | 0.003 | 0 | 0 | 0 | 0 | 0 |
| -154.1 | 9.3680 | 9.3730 | -0.005 | 1.71 | 1.71 | 0 | 0.005 | 0 | 0 | 0 | 0 | 0 |
| -155.6 | 9.3930 | 9.3980 | -0.005 | 1.7 | 1.7 | 0 | 0.005 | 0 | 0 | 0 | 0 | 0 |
| -157 | 9.4170 | 9.4220 | -0.005 | 1.68 | 1.68 | 0 | 0.005 | 0 | 0 | 0 | 0 | 0 |
| -158.4 | 9.440 | 9.4460 | -0.006 | 1.67 | 1.67 | 0 | 0.006 | 0 | 0 | 0 | 0 | 0 |
| -159.8 | 9.4640 | 9.4690 | -0.005 | 1.66 | 1.66 | 0 | 0.005 | 0 | 0 | 0 | 0 | 0 |
| -161.2 | 9.4870 | 9.4920 | -0.005 | 1.65 | 1.65 | 0 | 0.005 | 0 | 0 | 0 | 0 | 0 |

| | | | | | | | | | | | | |
|---|---|---|---|---|---|---|---|---|---|---|---|---|
| -162.6 | 9.5110 | 9.5150 | -0.004 | 1.63 | 1.63 | 0 | 0.004 | 0 | 0 | 0 | 0 | 0 |
| -163.9 | 9.5330 | 9.5370 | -0.004 | 1.62 | 1.62 | 0 | 0.004 | 0 | 0 | 0 | 0 | 0 |
| -165.2 | 9.5550 | 9.5590 | -0.004 | 1.61 | 1.61 | 0 | 0.004 | 0 | 0 | 0 | 0 | 0 |
| -166.4 | 9.5750 | 9.580 | -0.005 | 1.6 | 1.6 | 0 | 0.005 | 0 | 0 | 0 | 0 | 0 |
| -167.7 | 9.5970 | 9.6020 | -0.005 | 1.59 | 1.59 | 0 | 0.005 | 0 | 0 | 0 | 0 | 0 |
| -169 | 9.6190 | 9.6230 | -0.004 | 1.57 | 1.57 | 0 | 0.004 | 0 | 0 | 0 | 0 | 0 |
| -170.2 | 9.6390 | 9.6430 | -0.005 | 1.56 | 1.56 | 0 | 0.005 | 0 | 0 | 0 | 0 | 0 |
| -171.4 | 9.6590 | 9.6640 | -0.005 | 1.55 | 1.55 | 0 | 0.005 | 0 | 0 | 0 | 0 | 0 |
| -172.7 | 9.6810 | 9.6840 | -0.004 | 1.54 | 1.54 | 0 | 0.004 | 0 | 0 | 0 | 0 | 0 |
| -173.9 | 9.7010 | 9.7050 | -0.004 | 1.53 | 1.53 | 0 | 0.004 | 0 | 0 | 0 | 0 | 0 |
| -175.1 | 9.7210 | 9.7250 | -0.004 | 1.51 | 1.51 | 0 | 0.004 | 0 | 0 | 0 | 0 | 0 |
| -176.3 | 9.7410 | 9.7450 | -0.004 | 1.5 | 1.5 | 0 | 0.004 | 0 | 0 | 0 | 0 | 0 |
| -177.5 | 9.7610 | 9.7650 | -0.003 | 1.49 | 1.49 | 0 | 0.003 | 0 | 0 | 0 | 0 | 0 |
| -178.6 | 9.780 | 9.7850 | -0.005 | 1.48 | 1.48 | 0 | 0.005 | 0 | 0 | 0 | 0 | 0 |
| -179.8 | 9.80 | 9.8040 | -0.004 | 1.47 | 1.47 | 0 | 0.004 | 0 | 0 | 0 | 0 | 0 |
| -181 | 9.820 | 9.8240 | -0.004 | 1.46 | 1.46 | 0 | 0.004 | 0 | 0 | 0 | 0 | 0 |
| -182.1 | 9.8390 | 9.8440 | -0.005 | 1.44 | 1.44 | 0 | 0.005 | 0 | 0 | 0 | 0 | 0 |
| -183.3 | 9.8590 | 9.8640 | -0.005 | 1.43 | 1.43 | 0 | 0.005 | 0 | 0 | 0 | 0 | 0 |
| -184.5 | 9.8790 | 9.8830 | -0.004 | 1.42 | 1.42 | 0 | 0.004 | 0 | 0 | 0 | 0 | 0 |
| -185.7 | 9.8990 | 9.9030 | -0.004 | 1.41 | 1.41 | 0 | 0.004 | 0 | 0 | 0 | 0 | 0 |
| -186.9 | 9.9190 | 9.9230 | -0.003 | 1.4 | 1.4 | 0 | 0.003 | 0 | 0 | 0 | 0 | 0 |
| -188.1 | 9.940 | 9.9430 | -0.003 | 1.39 | 1.39 | 0 | 0.003 | 0 | 0 | 0 | 0 | 0 |
| -189.2 | 9.9580 | 9.9630 | -0.004 | 1.37 | 1.37 | 0 | 0.004 | 0 | 0 | 0 | 0 | 0 |
| -190.4 | 9.9780 | 9.9820 | -0.004 | 1.36 | 1.36 | 0 | 0.004 | 0 | 0 | 0 | 0 | 0 |
| -191.5 | 9.9970 | 10.0020 | -0.006 | 1.35 | 1.35 | 0 | 0.006 | 0 | 0 | 0 | 0 | 0 |
| -192.7 | 10.0170 | 10.0220 | -0.005 | 1.34 | 1.34 | 0 | 0.005 | 0 | 0 | 0 | 0 | 0 |
| -193.9 | 10.0370 | 10.0430 | -0.005 | 1.33 | 1.33 | 0 | 0.005 | 0 | 0 | 0 | 0 | 0 |
| -195.1 | 10.0570 | 10.0630 | -0.005 | 1.32 | 1.32 | 0 | 0.005 | 0 | 0 | 0 | 0 | 0 |
| -196.3 | 10.0770 | 10.0830 | -0.006 | 1.31 | 1.31 | 0 | 0.006 | 0 | 0 | 0 | 0 | 0 |
| -197.6 | 10.0990 | 10.1040 | -0.004 | 1.3 | 1.3 | 0 | 0.004 | 0 | 0 | 0 | 0 | 0 |
| -198.8 | 10.120 | 10.1240 | -0.005 | 1.28 | 1.29 | 0 | 0.005 | 0 | 0 | 0 | 0 | 0 |
| -200.1 | 10.1410 | 10.1450 | -0.003 | 1.27 | 1.27 | 0 | 0.003 | 0 | 0 | 0 | 0 | 0 |
| -201.3 | 10.1620 | 10.1650 | -0.004 | 1.26 | 1.26 | 0 | 0.004 | 0 | 0 | 0 | 0 | 0 |
| -202.5 | 10.1820 | 10.1860 | -0.005 | 1.25 | 1.25 | 0 | 0.005 | 0 | 0 | 0 | 0 | 0 |
| -203.8 | 10.2040 | 10.2070 | -0.004 | 1.24 | 1.24 | 0 | 0.004 | 0 | 0 | 0 | 0 | 0 |
| -205 | 10.2240 | 10.2280 | -0.005 | 1.23 | 1.23 | 0 | 0.005 | 0 | 0 | 0 | 0 | 0 |
| -206.4 | 10.2470 | 10.250 | -0.002 | 1.22 | 1.22 | 0 | 0.002 | 0 | 0 | 0 | 0 | 0 |
| -207.7 | 10.2690 | 10.2710 | -0.002 | 1.21 | 1.21 | 0 | 0.002 | 0 | 0 | 0 | 0 | 0 |
| -209 | 10.2910 | 10.2920 | -0.001 | 1.2 | 1.2 | 0 | 0.001 | 0 | 0 | 0 | 0 | 0 |
| -210.3 | 10.3130 | 10.3140 | -0.001 | 1.19 | 1.19 | 0 | 0.001 | 0 | 0 | 0 | 0 | 0 |
| -211.6 | 10.3350 | 10.3350 | -0.001 | 1.18 | 1.18 | 0 | 0.001 | 0 | 0 | 0 | 0 | 0 |
| -212.9 | 10.3570 | 10.3570 | 0 | 1.17 | 1.17 | 0 | 0 | 0 | 0 | 0 | 0 | 0 |
| -214.2 | 10.3780 | 10.3790 | 0 | 1.16 | 1.16 | 0 | 0 | 0 | 0 | 0 | 0 | 0 |
| -215.5 | 10.40 | 10.40 | 0 | 1.15 | 1.15 | 0 | 0 | 0 | 0 | 0 | 0 | 0 |
| -216.8 | 10.4220 | 10.4220 | 0 | 1.14 | 1.14 | 0 | 0 | 0 | 0 | 0 | 0 | 0 |
| -218.1 | 10.4440 | 10.4430 | 0.001 | 1.13 | 1.13 | 0 | 0.001 | 0 | 0 | 0 | 0 | 0 |
| -219.4 | 10.4660 | 10.4650 | 0.001 | 1.13 | 1.13 | 0 | 0.001 | 0 | 0 | 0 | 0 | 0 |
| -220.7 | 10.4880 | 10.4860 | 0.001 | 1.12 | 1.12 | 0 | 0.001 | 0 | 0 | 0 | 0 | 0 |
| -222 | 10.5090 | 10.5080 | 0.002 | 1.11 | 1.11 | 0 | 0.002 | 0 | 0 | 0 | 0 | 0 |
| -223.3 | 10.5310 | 10.5290 | 0.003 | 1.1 | 1.1 | 0.001 | 0.003 | 0 | 0 | 0 | 0 | 0 |
| -224.5 | 10.5520 | 10.550 | 0.002 | 1.09 | 1.09 | 0 | 0.002 | 0 | 0 | 0 | 0 | 0 |
| -225.8 | 10.5730 | 10.5710 | 0.003 | 1.09 | 1.08 | 0.001 | 0.003 | 0 | 0 | 0 | 0 | 0 |
| -227 | 10.5940 | 10.5910 | 0.002 | 1.08 | 1.08 | 0.001 | 0.002 | 0 | 0 | 0 | 0 | 0 |
| -228.2 | 10.6140 | 10.6110 | 0.002 | 1.07 | 1.07 | 0.001 | 0.002 | 0 | 0 | 0 | 0 | 0 |
| -229.4 | 10.6340 | 10.6310 | 0.002 | 1.06 | 1.06 | 0.001 | 0.002 | 0 | 0 | 0 | 0 | 0 |
| -230.6 | 10.6540 | 10.6510 | 0.003 | 1.06 | 1.05 | 0.001 | 0.003 | 0 | 0 | 0 | 0 | 0 |
| -231.8 | 10.6740 | 10.6710 | 0.004 | 1.05 | 1.05 | 0.001 | 0.004 | 0 | 0 | 0 | 0 | 0 |
| -232.9 | 10.6930 | 10.690 | 0.003 | 1.04 | 1.04 | 0.001 | 0.003 | 0 | 0 | 0 | 0 | 0 |
| -234.1 | 10.7130 | 10.7090 | 0.004 | 1.04 | 1.03 | 0.001 | 0.004 | 0 | 0 | 0 | 0 | 0 |
| -235.2 | 10.7310 | 10.7270 | 0.004 | 1.03 | 1.03 | 0.001 | 0.005 | 0 | 0 | 0 | 0 | 0 |
| -236.2 | 10.7480 | 10.7450 | 0.003 | 1.02 | 1.02 | 0.001 | 0.003 | 0 | 0 | 0 | 0 | 0 |

| | | | | | | | | | | | | |
|---|---|---|---|---|---|---|---|---|---|---|---|---|
| -237.3 | 10.7670 | 10.7630 | 0.004 | 1.02 | 1.01 | 0.001 | 0.004 | 0 | 0 | 0 | 0 | 0 |
| -238.3 | 10.7830 | 10.780 | 0.003 | 1.01 | 1.01 | 0.001 | 0.003 | 0 | 0 | 0 | 0 | 0 |
| -239.3 | 10.80 | 10.7970 | 0.003 | 1 | 1 | 0.001 | 0.003 | 0 | 0 | 0 | 0 | 0 |
| -240.3 | 10.8170 | 10.8140 | 0.003 | 1 | 1 | 0.001 | 0.003 | 0 | 0 | 0 | 0 | 0 |
| -241.2 | 10.8320 | 10.830 | 0.002 | 0.99 | 0.99 | 0.001 | 0.002 | 0 | 0 | 0 | 0 | 0 |
| -242.1 | 10.8470 | 10.8460 | 0.001 | 0.99 | 0.99 | 0 | 0.001 | 0 | 0 | 0 | 0 | 0 |
| -243.1 | 10.8640 | 10.8620 | 0.002 | 0.98 | 0.98 | 0.001 | 0.003 | 0 | 0 | 0 | 0 | 0 |
| -244.1 | 10.8810 | 10.8770 | 0.004 | 0.98 | 0.97 | 0.002 | 0.004 | 0 | 0 | 0 | 0 | 0 |
| -245 | 10.8960 | 10.8920 | 0.004 | 0.97 | 0.97 | 0.002 | 0.005 | 0 | 0 | 0 | 0 | 0 |
| -245.7 | 10.9080 | 10.9070 | 0.001 | 0.96 | 0.96 | 0.001 | 0.001 | 0 | 0 | 0 | 0 | 0 |
| -246.6 | 10.9230 | 10.9210 | 0.002 | 0.96 | 0.96 | 0.001 | 0.002 | 0 | 0 | 0 | 0 | 0 |
| -247.4 | 10.9360 | 10.9350 | 0.002 | 0.95 | 0.95 | 0.001 | 0.002 | 0 | 0 | 0 | 0 | 0 |
| -248.2 | 10.950 | 10.9480 | 0.001 | 0.95 | 0.95 | 0.001 | 0.002 | 0 | 0 | 0 | 0 | 0 |
| -248.9 | 10.9620 | 10.9620 | 0 | 0.94 | 0.94 | 0 | 0 | 0 | 0 | 0 | 0 | 0 |
| -249.6 | 10.9730 | 10.9750 | -0.001 | 0.94 | 0.94 | -0.001 | 0.002 | 0 | 0 | 0 | 0 | 0 |
| -250.4 | 10.9870 | 10.9880 | -0.001 | 0.93 | 0.93 | 0 | 0.001 | 0 | 0 | 0 | 0 | 0 |
| -251.1 | 10.9990 | 11 0 | -0.001 | 0.93 | 0.93 | -0.001 | 0.002 | 0 | 0 | 0 | 0 | 0 |

AVERAGE OF SUM OF SQUARES

OF RESIDUALS: 2.09E-05 3.20E-06 2.41E-05 0.00E+00 0.00E+00 0.00E+00

NUMBER OF TITRATIONS = 1

TOTAL NUMBER OF POINTS = 301

# b) Data for protonation constants for ligand APD (titration 2).

TASK ZBAR 1 TITRATION of APD:Protonation const.
MODL APD0 H 1
CPLX 0 0 -13.79 H +1( -1)
CPLX 1 0 11.6 APD0( 1) H +1( 1)
CPLX 1 0 21.23 APD0( 1) H +1( 2)
CPLX 0 0 26.92 APD0( 1) H +1( 3)
CONC

VESL IVOL 15.455 0 0

VESL H 1 -0.052395 0 0

VESL APD0 0.0129366 4 0

BUR1 H 1 0.1398627 0 0

ELEC

ZERO H 1 413.67 0

GRAD H 1 61.104 0

DATA

| EMF | PH | ZBAR(H) | POINT | PA | ZBAR(M) | POINT | | | | | |
|---|---|---|---|---|---|---|---|---|---|---|---|
| OBS | OBS CALC | CALC RESID | RESID RESID | OBS | CALC | RESID | RESID | OBS | CALC | RESID | OBS | |
| -258.4 | 10.9990 | 10.9620 | 0.037 | 0.87 | 0.86 | 0.011 | 0.039 | 0 | 0 | 0 | 0 | 0 |
| -257.4 | 10.9820 | 10.9420 | 0.04 | 0.88 | 0.87 | 0.011 | 0.042 | 0 | 0 | 0 | 0 | 0 |
| -256.4 | 10.9660 | 10.9220 | 0.044 | 0.89 | 0.87 | 0.012 | 0.046 | 0 | 0 | 0 | 0 | 0 |
| -255.3 | 10.9480 | 10.9020 | 0.046 | 0.9 | 0.88 | 0.012 | 0.048 | 0 | 0 | 0 | 0 | 0 |
| -254.1 | 10.9280 | 10.8810 | 0.048 | 0.9 | 0.89 | 0.012 | 0.049 | 0 | 0 | 0 | 0 | 0 |
| -252.9 | 10.9090 | 10.8590 | 0.05 | 0.91 | 0.9 | 0.012 | 0.051 | 0 | 0 | 0 | 0 | 0 |
| -251.7 | 10.8890 | 10.8370 | 0.052 | 0.92 | 0.91 | 0.012 | 0.053 | 0 | 0 | 0 | 0 | 0 |
| -250.5 | 10.870 | 10.8150 | 0.055 | 0.93 | 0.92 | 0.012 | 0.056 | 0 | 0 | 0 | 0 | 0 |
| -249.2 | 10.8480 | 10.7920 | 0.057 | 0.94 | 0.93 | 0.012 | 0.058 | 0 | 0 | 0 | 0 | 0 |
| -247.8 | 10.8250 | 10.7680 | 0.057 | 0.95 | 0.94 | 0.011 | 0.058 | 0 | 0 | 0 | 0 | 0 |
| -246.4 | 10.8020 | 10.7440 | 0.058 | 0.96 | 0.95 | 0.011 | 0.059 | 0 | 0 | 0 | 0 | 0 |
| -244.9 | 10.7780 | 10.7190 | 0.059 | 0.97 | 0.96 | 0.01 | 0.059 | 0 | 0 | 0 | 0 | 0 |
| -243.3 | 10.7520 | 10.6940 | 0.058 | 0.98 | 0.97 | 0.01 | 0.058 | 0 | 0 | 0 | 0 | 0 |
| -241.7 | 10.7250 | 10.6680 | 0.057 | 0.99 | 0.98 | 0.009 | 0.058 | 0 | 0 | 0 | 0 | 0 |
| -240.1 | 10.6990 | 10.6420 | 0.057 | 1 | 0.99 | 0.008 | 0.058 | 0 | 0 | 0 | 0 | 0 |
| -238.5 | 10.6730 | 10.6160 | 0.057 | 1.01 | 1 | 0.008 | 0.058 | 0 | 0 | 0 | 0 | 0 |
| -236.7 | 10.6440 | 10.5890 | 0.055 | 1.02 | 1.01 | 0.007 | 0.055 | 0 | 0 | 0 | 0 | 0 |
| -235 | 10.6160 | 10.5610 | 0.054 | 1.03 | 1.02 | 0.007 | 0.055 | 0 | 0 | 0 | 0 | 0 |
| -233.2 | 10.5860 | 10.5340 | 0.053 | 1.04 | 1.03 | 0.006 | 0.053 | 0 | 0 | 0 | 0 | 0 |
| -231.3 | 10.5550 | 10.5060 | 0.049 | 1.05 | 1.04 | 0.005 | 0.05 | 0 | 0 | 0 | 0 | 0 |
| -229.5 | 10.5260 | 10.4780 | 0.048 | 1.06 | 1.05 | 0.005 | 0.048 | 0 | 0 | 0 | 0 | 0 |
| -227.5 | 10.4930 | 10.450 | 0.043 | 1.07 | 1.07 | 0.004 | 0.043 | 0 | 0 | 0 | 0 | 0 |
| -225.6 | 10.4620 | 10.4220 | 0.04 | 1.08 | 1.08 | 0.004 | 0.041 | 0 | 0 | 0 | 0 | 0 |
| -223.7 | 10.4310 | 10.3930 | 0.037 | 1.09 | 1.09 | 0.003 | 0.038 | 0 | 0 | 0 | 0 | 0 |
| -221.8 | 10.40 | 10.3650 | 0.035 | 1.1 | 1.1 | 0.003 | 0.035 | 0 | 0 | 0 | 0 | 0 |
| -219.8 | 10.3670 | 10.3370 | 0.03 | 1.12 | 1.11 | 0.002 | 0.03 | 0 | 0 | 0 | 0 | 0 |
| -217.9 | 10.3360 | 10.3090 | 0.027 | 1.13 | 1.13 | 0.002 | 0.027 | 0 | 0 | 0 | 0 | 0 |
| -216 | 10.3050 | 10.2820 | 0.023 | 1.14 | 1.14 | 0.001 | 0.023 | 0 | 0 | 0 | 0 | 0 |
| -214.1 | 10.2740 | 10.2540 | 0.02 | 1.15 | 1.15 | 0.001 | 0.02 | 0 | 0 | 0 | 0 | 0 |
| -212.3 | 10.2440 | 10.2270 | 0.017 | 1.16 | 1.16 | 0.001 | 0.017 | 0 | 0 | 0 | 0 | 0 |
| -210.4 | 10.2130 | 10.20 | 0.013 | 1.18 | 1.18 | 0.001 | 0.013 | 0 | 0 | 0 | 0 | 0 |
| -208.6 | 10.1840 | 10.1740 | 0.01 | 1.19 | 1.19 | 0 | 0.01 | 0 | 0 | 0 | 0 | 0 |
| -206.8 | 10.1540 | 10.1470 | 0.007 | 1.2 | 1.2 | 0 | 0.007 | 0 | 0 | 0 | 0 | 0 |
| -204.9 | 10.1230 | 10.1210 | 0.002 | 1.21 | 1.21 | 0 | 0.002 | 0 | 0 | 0 | 0 | 0 |
| -203.1 | 10.0940 | 10.0950 | -0.002 | 1.23 | 1.23 | 0 | 0.002 | 0 | 0 | 0 | 0 | 0 |
| -201.4 | 10.0660 | 10.070 | -0.004 | 1.24 | 1.24 | 0 | 0.004 | 0 | 0 | 0 | 0 | 0 |
| -199.7 | 10.0380 | 10.0450 | -0.007 | 1.25 | 1.25 | 0 | 0.007 | 0 | 0 | 0 | 0 | 0 |
| -198 | 10.010 | 10.020 | -0.01 | 1.27 | 1.27 | 0 | 0.01 | 0 | 0 | 0 | 0 | 0 |
| -196.4 | 9.9840 | 9.9960 | -0.012 | 1.28 | 1.28 | 0 | 0.012 | 0 | 0 | 0 | 0 | 0 |
| -194.8 | 9.9580 | 9.9710 | -0.013 | 1.29 | 1.29 | 0 | 0.013 | 0 | 0 | 0 | 0 | 0 |
| -193.2 | 9.9320 | 9.9470 | -0.016 | 1.31 | 1.31 | 0 | 0.016 | 0 | 0 | 0 | 0 | 0 |
| -191.6 | 9.9060 | 9.9240 | -0.018 | 1.32 | 1.32 | 0 | 0.018 | 0 | 0 | 0 | 0 | 0 |
| -190.1 | 9.8810 | 9.90 | -0.019 | 1.33 | 1.33 | 0 | 0.019 | 0 | 0 | 0 | 0 | 0 |

| | | | | | | | | | | | | |
|---|---|---|---|---|---|---|---|---|---|---|---|---|
| -188.6 | 9.8560 | 9.8770 | -0.02 | 1.35 | 1.35 | 0 | 0.02 | 0 | 0 | 0 | 0 | 0 |
| -187.1 | 9.8320 | 9.8530 | -0.021 | 1.36 | 1.36 | 0 | 0.021 | 0 | 0 | 0 | 0 | 0 |
| -185.6 | 9.8070 | 9.830 | -0.023 | 1.37 | 1.37 | 0 | 0.023 | 0 | 0 | 0 | 0 | 0 |
| -184.1 | 9.7830 | 9.8070 | -0.024 | 1.39 | 1.39 | 0 | 0.024 | 0 | 0 | 0 | 0 | 0 |
| -182.7 | 9.760 | 9.7840 | -0.024 | 1.4 | 1.4 | 0 | 0.024 | 0 | 0 | 0 | 0 | 0 |
| -181.2 | 9.7350 | 9.7620 | -0.026 | 1.41 | 1.41 | 0 | 0.026 | 0 | 0 | 0 | 0 | 0 |
| -179.8 | 9.7120 | 9.7390 | -0.026 | 1.43 | 1.43 | 0 | 0.026 | 0 | 0 | 0 | 0 | 0 |
| -178.4 | 9.690 | 9.7160 | -0.027 | 1.44 | 1.44 | 0 | 0.027 | 0 | 0 | 0 | 0 | 0 |
| -176.9 | 9.6650 | 9.6930 | -0.028 | 1.45 | 1.45 | 0 | 0.028 | 0 | 0 | 0 | 0 | 0 |
| -175.5 | 9.6420 | 9.6710 | -0.029 | 1.47 | 1.47 | 0 | 0.029 | 0 | 0 | 0 | 0 | 0 |
| -174.2 | 9.6210 | 9.6480 | -0.027 | 1.48 | 1.48 | 0 | 0.027 | 0 | 0 | 0 | 0 | 0 |
| -172.8 | 9.5980 | 9.6250 | -0.027 | 1.49 | 1.49 | 0 | 0.027 | 0 | 0 | 0 | 0 | 0 |
| -171.4 | 9.5750 | 9.6020 | -0.027 | 1.51 | 1.51 | 0 | 0.027 | 0 | 0 | 0 | 0 | 0 |
| -169.9 | 9.550 | 9.580 | -0.029 | 1.52 | 1.52 | 0 | 0.029 | 0 | 0 | 0 | 0 | 0 |
| -168.4 | 9.5260 | 9.5560 | -0.031 | 1.54 | 1.54 | 0 | 0.031 | 0 | 0 | 0 | 0 | 0 |
| -167 | 9.5030 | 9.5330 | -0.03 | 1.55 | 1.55 | 0 | 0.03 | 0 | 0 | 0 | 0 | 0 |
| -165.5 | 9.4780 | 9.510 | -0.031 | 1.56 | 1.56 | 0 | 0.031 | 0 | 0 | 0 | 0 | 0 |
| -164 | 9.4540 | 9.4860 | -0.032 | 1.58 | 1.58 | 0 | 0.032 | 0 | 0 | 0 | 0 | 0 |
| -162.6 | 9.4310 | 9.4620 | -0.031 | 1.59 | 1.59 | 0 | 0.031 | 0 | 0 | 0 | 0 | 0 |
| -161.1 | 9.4060 | 9.4380 | -0.031 | 1.6 | 1.6 | 0 | 0.031 | 0 | 0 | 0 | 0 | 0 |
| -159.6 | 9.3820 | 9.4130 | -0.031 | 1.62 | 1.62 | 0 | 0.031 | 0 | 0 | 0 | 0 | 0 |
| -158.1 | 9.3570 | 9.3880 | -0.031 | 1.63 | 1.63 | 0 | 0.031 | 0 | 0 | 0 | 0 | 0 |
| -156.6 | 9.3330 | 9.3630 | -0.03 | 1.65 | 1.65 | 0 | 0.03 | 0 | 0 | 0 | 0 | 0 |
| -155 | 9.3070 | 9.3370 | -0.03 | 1.66 | 1.66 | 0 | 0.03 | 0 | 0 | 0 | 0 | 0 |
| -153.4 | 9.280 | 9.310 | -0.03 | 1.67 | 1.67 | 0 | 0.03 | 0 | 0 | 0 | 0 | 0 |
| -151.7 | 9.2530 | 9.2830 | -0.03 | 1.69 | 1.69 | 0 | 0.03 | 0 | 0 | 0 | 0 | 0 |
| -150 | 9.2250 | 9.2550 | -0.03 | 1.7 | 1.7 | 0 | 0.03 | 0 | 0 | 0 | 0 | 0 |
| -148.3 | 9.1970 | 9.2260 | -0.029 | 1.71 | 1.72 | 0 | 0.029 | 0 | 0 | 0 | 0 | 0 |
| -146.5 | 9.1670 | 9.1970 | -0.029 | 1.73 | 1.73 | 0 | 0.029 | 0 | 0 | 0 | 0 | 0 |
| -144.7 | 9.1380 | 9.1660 | -0.028 | 1.74 | 1.74 | 0 | 0.028 | 0 | 0 | 0 | 0 | 0 |
| -142.8 | 9.1070 | 9.1350 | -0.028 | 1.76 | 1.76 | 0 | 0.028 | 0 | 0 | 0 | 0 | 0 |
| -140.9 | 9.0760 | 9.1020 | -0.026 | 1.77 | 1.77 | 0 | 0.026 | 0 | 0 | 0 | 0 | 0 |
| -138.9 | 9.0430 | 9.0670 | -0.024 | 1.78 | 1.78 | 0 | 0.024 | 0 | 0 | 0 | 0 | 0 |
| -136.7 | 9.0070 | 9.0310 | -0.024 | 1.8 | 1.8 | 0 | 0.024 | 0 | 0 | 0 | 0 | 0 |
| -134.5 | 8.9710 | 8.9930 | -0.022 | 1.81 | 1.81 | 0 | 0.022 | 0 | 0 | 0 | 0 | 0 |
| -132.2 | 8.9330 | 8.9530 | -0.02 | 1.83 | 1.83 | 0 | 0.02 | 0 | 0 | 0 | 0 | 0 |
| -129.6 | 8.8910 | 8.910 | -0.019 | 1.84 | 1.84 | 0 | 0.019 | 0 | 0 | 0 | 0 | 0 |
| -126.9 | 8.8470 | 8.8650 | -0.018 | 1.85 | 1.85 | 0 | 0.018 | 0 | 0 | 0 | 0 | 0 |
| -124 | 8.7990 | 8.8150 | -0.016 | 1.87 | 1.87 | 0 | 0.016 | 0 | 0 | 0 | 0 | 0 |
| -120.9 | 8.7490 | 8.7610 | -0.012 | 1.88 | 1.88 | 0 | 0.012 | 0 | 0 | 0 | 0 | 0 |
| -117.5 | 8.6930 | 8.7010 | -0.008 | 1.9 | 1.9 | 0 | 0.008 | 0 | 0 | 0 | 0 | 0 |
| -113.8 | 8.6320 | 8.6340 | -0.002 | 1.91 | 1.91 | 0 | 0.002 | 0 | 0 | 0 | 0 | 0 |
| -109.6 | 8.5640 | 8.5580 | 0.006 | 1.92 | 1.92 | 0 | 0.006 | 0 | 0 | 0 | 0 | 0 |
| -104.8 | 8.4850 | 8.4690 | 0.016 | 1.94 | 1.94 | 0 | 0.016 | 0 | 0 | 0 | 0 | 0 |
| -99 | 8.390 | 8.3620 | 0.028 | 1.95 | 1.95 | 0 | 0.028 | 0 | 0 | 0 | 0 | 0 |
| -91.8 | 8.2720 | 8.2270 | 0.045 | 1.96 | 1.96 | 0 | 0.045 | 0 | 0 | 0 | 0 | 0 |
| -82.9 | 8.1270 | 8.050 | 0.077 | 1.98 | 1.98 | 0 | 0.077 | 0 | 0 | 0 | 0 | 0 |
| -70.9 | 7.930 | 7.810 | 0.12 | 1.99 | 1.99 | 0 | 0.12 | 0 | 0 | 0 | 0 | 0 |
| -55.3 | 7.6750 | 7.5260 | 0.149 | 2.01 | 2.01 | 0 | 0.149 | 0 | 0 | 0 | 0 | 0 |
| -39.1 | 7.410 | 7.2810 | 0.128 | 2.02 | 2.02 | 0 | 0.128 | 0 | 0 | 0 | 0 | 0 |
| -26.3 | 7.20 | 7.10 | 0.1 | 2.03 | 2.03 | 0 | 0.1 | 0 | 0 | 0 | 0 | 0 |
| -16.7 | 7.0430 | 6.9630 | 0.08 | 2.05 | 2.05 | 0 | 0.08 | 0 | 0 | 0 | 0 | 0 |
| -9.5 | 6.9250 | 6.8540 | 0.071 | 2.06 | 2.06 | 0 | 0.071 | 0 | 0 | 0 | 0 | 0 |
| -3.5 | 6.8270 | 6.7640 | 0.063 | 2.08 | 2.08 | 0 | 0.063 | 0 | 0 | 0 | 0 | 0 |
| 1.2 | 6.750 | 6.6870 | 0.064 | 2.09 | 2.09 | 0 | 0.064 | 0 | 0 | 0 | 0 | 0 |
| 5.4 | 6.6820 | 6.6190 | 0.063 | 2.1 | 2.1 | 0 | 0.063 | 0 | 0 | 0 | 0 | 0 |
| 9.2 | 6.6190 | 6.5580 | 0.061 | 2.12 | 2.12 | 0 | 0.061 | 0 | 0 | 0 | 0 | 0 |
| 12.7 | 6.5620 | 6.5040 | 0.058 | 2.13 | 2.13 | 0 | 0.058 | 0 | 0 | 0 | 0 | 0 |
| 15.8 | 6.5110 | 6.4530 | 0.058 | 2.15 | 2.15 | 0 | 0.058 | 0 | 0 | 0 | 0 | 0 |
| 18.9 | 6.4610 | 6.4070 | 0.054 | 2.16 | 2.16 | 0 | 0.054 | 0 | 0 | 0 | 0 | 0 |
| 21.6 | 6.4160 | 6.3640 | 0.053 | 2.17 | 2.17 | 0 | 0.053 | 0 | 0 | 0 | 0 | 0 |

| | | | | | | | | | | | | |
|---|---|---|---|---|---|---|---|---|---|---|---|---|
| 24.2 | 6.3740 | 6.3230 | 0.051 | 2.19 | 2.19 | 0 | 0.051 | 0 | 0 | 0 | 0 | 0 |
| 26.7 | 6.3330 | 6.2850 | 0.048 | 2.2 | 2.2 | 0 | 0.048 | 0 | 0 | 0 | 0 | 0 |
| 29.1 | 6.2940 | 6.2480 | 0.046 | 2.22 | 2.22 | 0 | 0.046 | 0 | 0 | 0 | 0 | 0 |
| 31.4 | 6.2560 | 6.2130 | 0.043 | 2.23 | 2.23 | 0 | 0.043 | 0 | 0 | 0 | 0 | 0 |
| 33.6 | 6.220 | 6.180 | 0.04 | 2.24 | 2.24 | 0 | 0.04 | 0 | 0 | 0 | 0 | 0 |
| 35.7 | 6.1860 | 6.1470 | 0.038 | 2.26 | 2.26 | 0 | 0.038 | 0 | 0 | 0 | 0 | 0 |
| 37.7 | 6.1530 | 6.1160 | 0.037 | 2.27 | 2.27 | 0 | 0.037 | 0 | 0 | 0 | 0 | 0 |
| 39.6 | 6.1220 | 6.0860 | 0.036 | 2.29 | 2.29 | 0 | 0.036 | 0 | 0 | 0 | 0 | 0 |
| 41.5 | 6.0910 | 6.0570 | 0.034 | 2.3 | 2.3 | 0 | 0.034 | 0 | 0 | 0 | 0 | 0 |
| 43.4 | 6.060 | 6.0280 | 0.031 | 2.31 | 2.31 | 0 | 0.031 | 0 | 0 | 0 | 0 | 0 |
| 45.2 | 6.030 | 6.0010 | 0.03 | 2.33 | 2.33 | 0 | 0.03 | 0 | 0 | 0 | 0 | 0 |
| 46.9 | 6.0020 | 5.9730 | 0.029 | 2.34 | 2.34 | 0 | 0.029 | 0 | 0 | 0 | 0 | 0 |
| 48.6 | 5.9750 | 5.9470 | 0.028 | 2.36 | 2.36 | 0 | 0.028 | 0 | 0 | 0 | 0 | 0 |
| 50.3 | 5.9470 | 5.9210 | 0.026 | 2.37 | 2.37 | 0 | 0.026 | 0 | 0 | 0 | 0 | 0 |
| 51.9 | 5.9210 | 5.8950 | 0.026 | 2.38 | 2.38 | 0 | 0.026 | 0 | 0 | 0 | 0 | 0 |
| 53.5 | 5.8940 | 5.8690 | 0.025 | 2.4 | 2.4 | 0 | 0.025 | 0 | 0 | 0 | 0 | 0 |
| 55.1 | 5.8680 | 5.8440 | 0.024 | 2.41 | 2.41 | 0 | 0.024 | 0 | 0 | 0 | 0 | 0 |
| 56.8 | 5.840 | 5.8190 | 0.021 | 2.43 | 2.43 | 0 | 0.021 | 0 | 0 | 0 | 0 | 0 |
| 58.4 | 5.8140 | 5.7940 | 0.02 | 2.44 | 2.44 | 0 | 0.02 | 0 | 0 | 0 | 0 | 0 |
| 59.9 | 5.790 | 5.770 | 0.02 | 2.45 | 2.45 | 0 | 0.02 | 0 | 0 | 0 | 0 | 0 |
| 61.5 | 5.7630 | 5.7450 | 0.018 | 2.47 | 2.47 | 0 | 0.018 | 0 | 0 | 0 | 0 | 0 |
| 63 | 5.7390 | 5.7210 | 0.018 | 2.48 | 2.48 | 0 | 0.018 | 0 | 0 | 0 | 0 | 0 |
| 64.5 | 5.7140 | 5.6970 | 0.018 | 2.5 | 2.5 | 0 | 0.018 | 0 | 0 | 0 | 0 | 0 |
| 66.1 | 5.6880 | 5.6730 | 0.016 | 2.51 | 2.51 | 0 | 0.016 | 0 | 0 | 0 | 0 | 0 |
| 67.6 | 5.6640 | 5.6480 | 0.015 | 2.52 | 2.52 | 0 | 0.015 | 0 | 0 | 0 | 0 | 0 |
| 69.1 | 5.6390 | 5.6240 | 0.015 | 2.54 | 2.54 | 0 | 0.015 | 0 | 0 | 0 | 0 | 0 |
| 70.7 | 5.6130 | 5.5990 | 0.014 | 2.55 | 2.55 | 0 | 0.014 | 0 | 0 | 0 | 0 | 0 |
| 72.2 | 5.5880 | 5.5750 | 0.014 | 2.57 | 2.57 | 0 | 0.014 | 0 | 0 | 0 | 0 | 0 |
| 73.8 | 5.5620 | 5.550 | 0.012 | 2.58 | 2.58 | 0 | 0.012 | 0 | 0 | 0 | 0 | 0 |
| 75.4 | 5.5360 | 5.5250 | 0.011 | 2.59 | 2.59 | 0 | 0.011 | 0 | 0 | 0 | 0 | 0 |
| 77 | 5.510 | 5.50 | 0.01 | 2.61 | 2.61 | 0 | 0.01 | 0 | 0 | 0 | 0 | 0 |
| 78.6 | 5.4840 | 5.4740 | 0.01 | 2.62 | 2.62 | 0 | 0.01 | 0 | 0 | 0 | 0 | 0 |
| 80.3 | 5.4560 | 5.4480 | 0.008 | 2.64 | 2.64 | 0 | 0.008 | 0 | 0 | 0 | 0 | 0 |
| 82 | 5.4280 | 5.4220 | 0.006 | 2.65 | 2.65 | 0 | 0.006 | 0 | 0 | 0 | 0 | 0 |
| 83.7 | 5.40 | 5.3950 | 0.005 | 2.66 | 2.66 | 0 | 0.005 | 0 | 0 | 0 | 0 | 0 |
| 85.4 | 5.3720 | 5.3670 | 0.005 | 2.68 | 2.68 | 0 | 0.005 | 0 | 0 | 0 | 0 | 0 |
| 87.2 | 5.3430 | 5.3390 | 0.004 | 2.69 | 2.69 | 0 | 0.004 | 0 | 0 | 0 | 0 | 0 |
| 89.1 | 5.3120 | 5.310 | 0.001 | 2.71 | 2.71 | 0 | 0.001 | 0 | 0 | 0 | 0 | 0 |
| 90.9 | 5.2820 | 5.2810 | 0.002 | 2.72 | 2.72 | 0 | 0.002 | 0 | 0 | 0 | 0 | 0 |
| 92.9 | 5.250 | 5.250 | -0.001 | 2.73 | 2.73 | 0 | 0.001 | 0 | 0 | 0 | 0 | 0 |
| 95 | 5.2150 | 5.2190 | -0.004 | 2.75 | 2.75 | 0 | 0.004 | 0 | 0 | 0 | 0 | 0 |
| 97 | 5.1820 | 5.1860 | -0.004 | 2.76 | 2.76 | 0 | 0.004 | 0 | 0 | 0 | 0 | 0 |
| 99.2 | 5.1460 | 5.1520 | -0.006 | 2.78 | 2.78 | 0 | 0.006 | 0 | 0 | 0 | 0 | 0 |
| 101.4 | 5.110 | 5.1170 | -0.006 | 2.79 | 2.79 | 0 | 0.006 | 0 | 0 | 0 | 0 | 0 |
| 103.8 | 5.0710 | 5.0790 | -0.008 | 2.8 | 2.8 | 0 | 0.008 | 0 | 0 | 0 | 0 | 0 |
| 106.2 | 5.0320 | 5.040 | -0.008 | 2.82 | 2.82 | 0 | 0.008 | 0 | 0 | 0 | 0 | 0 |
| 108.9 | 4.9880 | 4.9980 | -0.011 | 2.83 | 2.83 | 0 | 0.011 | 0 | 0 | 0 | 0 | 0 |
| 111.7 | 4.9420 | 4.9540 | -0.012 | 2.84 | 2.84 | 0 | 0.012 | 0 | 0 | 0 | 0 | 0 |
| 114.7 | 4.8930 | 4.9060 | -0.013 | 2.86 | 2.86 | 0 | 0.013 | 0 | 0 | 0 | 0 | 0 |
| 118 | 4.8390 | 4.8540 | -0.016 | 2.87 | 2.87 | 0 | 0.016 | 0 | 0 | 0 | 0 | 0 |
| 121.7 | 4.7780 | 4.7980 | -0.02 | 2.89 | 2.89 | 0 | 0.02 | 0 | 0 | 0 | 0 | 0 |
| 125.8 | 4.7110 | 4.7350 | -0.024 | 2.9 | 2.9 | 0 | 0.024 | 0 | 0 | 0 | 0 | 0 |
| 130.6 | 4.6330 | 4.6650 | -0.032 | 2.91 | 2.91 | 0 | 0.032 | 0 | 0 | 0 | 0 | 0 |
| 136.2 | 4.5410 | 4.5840 | -0.043 | 2.93 | 2.93 | 0 | 0.043 | 0 | 0 | 0 | 0 | 0 |
| 142.8 | 4.4330 | 4.490 | -0.057 | 2.94 | 2.94 | 0 | 0.057 | 0 | 0 | 0 | 0 | 0 |
| 151 | 4.2990 | 4.3760 | -0.077 | 2.95 | 2.95 | -0.001 | 0.077 | 0 | 0 | 0 | 0 | 0 |
| 161.3 | 4.130 | 4.2350 | -0.105 | 2.96 | 2.97 | -0.002 | 0.105 | 0 | 0 | 0 | 0 | 0 |
| 173.8 | 3.9260 | 4.0580 | -0.132 | 2.97 | 2.98 | -0.003 | 0.132 | 0 | 0 | 0 | 0 | 0 |
| 186.3 | 3.7210 | 3.8480 | -0.127 | 2.98 | 2.99 | -0.005 | 0.127 | 0 | 0 | 0 | 0 | 0 |
| 197 | 3.5460 | 3.6410 | -0.095 | 2.99 | 2.99 | -0.006 | 0.095 | 0 | 0 | 0 | 0 | 0 |
| 205.4 | 3.4080 | 3.4680 | -0.06 | 2.99 | 2.99 | -0.005 | 0.06 | 0 | 0 | 0 | 0 | 0 |

| | | | | | | | | | | | | |
|---|---|---|---|---|---|---|---|---|---|---|---|---|
| 212.2 | 3.2970 | 3.3330 | -0.036 | 2.99 | 3 | -0.004 | 0.036 | 0 | 0 | 0 | 0 | 0 |
| 217.7 | 3.2070 | 3.2250 | -0.018 | 2.99 | 3 | -0.003 | 0.018 | 0 | 0 | 0 | 0 | 0 |
| 222.3 | 3.1320 | 3.1370 | -0.005 | 3 | 3 | -0.001 | 0.006 | 0 | 0 | 0 | 0 | 0 |
| 226.3 | 3.0660 | 3.0630 | 0.003 | 3 | 3 | 0.001 | 0.003 | 0 | 0 | 0 | 0 | 0 |
| 229.8 | 3.0090 | 30 | 0.009 | 3 | 3 | 0.002 | 0.009 | 0 | 0 | 0 | 0 | 0 |

AVERAGE OF SUM OF SQUARES

OF RESIDUALS: 1.81E-03 1.33E-05 1.82E-03 0.00E+00 0.00E+00 0.00E+00

NUMBER OF TITRATIONS = 1

TOTAL NUMBER OF POINTS = 170

# APPENDIX C: $DC_{TAST}$ data.

## a) Data for $Cd^{II}$–APD system.

41 Experimental points
4 No. of protonation constants
APD Cd [LT]/[MT] = 40.14912
20 5 1980 Date when experiment was performed
CdAPD Files recorded during the experiment
DPP DCT ISE
0 1 0 indicators for mode of experiment
DCT EXPERIMENT
OH-titrant L-titrant M-titrant
1 0 0 indicaters for mode of titration
Titration with protons

| No.: | pH | NaOH/ml | L-sol/ml | M-sol/ml | Ip(obs) | Ip(exp) | Ip(corr) | Log[MF] | Log[LF] | Ep(obs)/m | Init Ep/mV | Shift/mV | ECFC/mV | CCFC/mV | [LT] | [MT] | Virtual E | LOG[HL] | LOG[H2L] | LOG[H3L] | etc. |
|---|---|---|---|---|---|---|---|---|---|---|---|---|---|---|---|---|---|---|---|---|---|
| 1 | 2.556 | 3.85 | 0 | 0 | 2.607 | 2.407865 | 1.082702 | -3.979765 | -22.12492 | -568.6 | -568.64 | -4.00E-02 | -1.060806 | 1.75E-05 | 4.21E-03 | 1.05E-04 | -567.5792 | -12.83092 | -5.626923 | -2.412923 | -3.468923 |
| 2 | 2.608 | 3.95 | 0 | 0 | 2.596 | 2.402812 | 1.080401 | -3.980707 | -21.96589 | -568.56 | -568.64 | -8.00E-02 | -1.073453 | 8.88E-04 | 4.20E-03 | 1.05E-04 | -567.5666 | -12.72389 | -5.57189 | -2.40989 | -3.51789 |
| 3 | 2.666 | 4.05 | 0 | 0 | 2.594 | 2.39778 | 1.081834 | -3.981627 | -21.7889 | -568.49 | -568.64 | -0.150024 | -1.160492 | 1.17E-03 | 4.19E-03 | 1.04E-04 | -567.4796 | -12.6049 | -5.510898 | -2.406898 | -3.572898 |
| 4 | 2.729 | 4.15 | 0 | 0 | 2.589 | 2.392769 | 1.08201 | -3.982548 | -21.5971 | -568.46 | -568.64 | -0.179993 | -1.192549 | 1.56E-03 | 4.18E-03 | 1.04E-04 | -567.4474 | -12.4761 | -5.445097 | -2.404097 | -3.633097 |
| 5 | 2.803 | 4.25 | 0 | 0 | 2.582 | 2.387779 | 1.08134 | -3.983477 | -21.37227 | -568.42 | -568.64 | -0.220032 | -1.224627 | 2.21E-03 | 4.17E-03 | 1.04E-04 | -567.4154 | -12.32527 | -5.368269 | -2.401269 | -3.704269 |
| 6 | 2.888 | 4.35 | 0 | 0 | 2.575 | 2.38281 | 1.080657 | -3.984418 | -21.1146 | -568.41 | -568.64 | -0.230042 | -1.226524 | 3.28E-03 | 4.16E-03 | 1.04E-04 | -567.4135 | -12.1526 | -5.280599 | -2.398599 | -3.786599 |
| 7 | 2.939 | 4.4 | 0 | 0 | 2.568 | 2.380332 | 1.078841 | -3.984899 | -20.96023 | -568.44 | -568.64 | -0.200012 | -1.174887 | 4.16E-03 | 4.16E-03 | 1.04E-04 | -567.4651 | -12.04923 | -5.228226 | -2.397226 | -3.836226 |
| 8 | 2.996 | 4.45 | 0 | 0 | 2.565 | 2.377861 | 1.078701 | -3.985393 | -20.78789 | -568.4 | -568.64 | -0.23999 | -1.213195 | 5.42E-03 | 4.15E-03 | 1.03E-04 | -567.4268 | -11.93389 | -5.169888 | -2.395888 | -3.891888 |
| 9 | 3.061 | 4.5 | 0 | 0 | 2.561 | 2.375394 | 1.078137 | -3.985908 | -20.59159 | -568.45 | -568.64 | -0.190002 | -1.156492 | 7.32E-03 | 4.15E-03 | 1.03E-04 | -567.4835 | -11.80259 | -5.103586 | -2.394586 | -3.955586 |
| 10 | 3.138 | 4.55 | 0 | 0 | 2.558 | 2.372933 | 1.077991 | -3.986535 | -20.35931 | -568.48 | -568.64 | -0.160034 | -1.124785 | 1.25E-02 | 4.15E-03 | 1.03E-04 | -567.5153 | -11.64731 | -5.025314 | -2.393314 | -4.031314 |
| 11 | 3.228 | 4.6 | 0 | 0 | 2.554 | 2.370476 | 1.077421 | -3.987203 | -20.08817 | -568.56 | -568.64 | -8.00E-02 | -1.037968 | 1.90E-02 | 4.14E-03 | 1.03E-04 | -567.6021 | -11.46616 | -4.934164 | -2.392164 | -4.120164 |
| 12 | 3.34 | 4.65 | 0 | 0 | 2.549 | 2.368025 | 1.076425 | -3.988086 | -19.75117 | -568.65 | -568.64 | 1.00E-02 | -0.936061 | 3.18E-02 | 4.14E-03 | 1.03E-04 | -567.704 | -11.24117 | -4.821169 | -2.391169 | -4.231169 |
| 13 | 3.485 | 4.7 | 0 | 0 | 2.54 | 2.365578 | 1.073733 | -3.98955 | -19.31551 | -568.8 | -568.64 | 0.159973 | -0.753937 | 6.19E-02 | 4.13E-03 | 1.03E-04 | -567.8861 | -10.95051 | -4.675508 | -2.390508 | -4.375508 |
| 14 | 3.687 | 4.75 | 0 | 0 | 2.526 | 2.363137 | 1.068918 | -3.993146 | -18.70966 | -569.19 | -568.64 | 0.549988 | -0.306183 | 0.154965 | 4.13E-03 | 1.03E-04 | -568.3339 | -10.54666 | -4.473663 | -2.390663 | -4.577663 |
| 15 | 3.97 | 4.8 | 0 | 0 | 2.497 | 2.360701 | 1.057737 | -4.006688 | -17.86319 | -570.06 | -568.64 | 1.419983 | 0.698899 | 0.542269 | 4.12E-03 | 1.03E-04 | -569.3389 | -9.983191 | -4.193192 | -2.393192 | -4.863192 |
| 16 | 4.304 | 4.85 | 0 | 0 | 2.438 | 2.35827 | 1.033809 | -4.059161 | -16.86925 | -572.09 | -568.64 | 3.450012 | 3.022872 | 2.081168 | 4.12E-03 | 1.03E-04 | -571.6629 | -9.323249 | -3.867249 | -2.401248 | -5.205248 |
| 17 | 4.594 | 4.9 | 0 | 0 | 2.374 | 2.355844 | 1.007707 | -4.16861 | -16.01391 | -574.93 | -568.64 | 6.289978 | 6.19135 | 5.305444 | 4.12E-03 | 1.03E-04 | -574.8314 | -8.757914 | -3.591913 | -2.415913 | -5.509913 |
| 18 | 4.809 | 4.95 | 0 | 0 | 2.315 | 2.353422 | 0.983674 | -4.293866 | -15.38731 | -577.8 | -568.64 | 9.159973 | 9.371434 | 8.997293 | 4.11E-03 | 1.02E-04 | -578.0115 | -8.346313 | -3.395312 | -2.434312 | -5.743312 |
| 19 | 4.973 | 5 | 0 | 0 | 2.262 | 2.351006 | 0.962141 | -4.409613 | -14.9157 | -580.48 | -568.64 | 11.83997 | 12.33576 | 12.40788 | 4.11E-03 | 1.02E-04 | -580.9758 | -8.038694 | -3.251694 | -2.454694 | -5.927694 |
| 20 | 5.106 | 5.05 | 0 | 0 | 2.222 | 2.348595 | 0.946098 | -4.512806 | -14.53862 | -582.83 | -568.64 | 14.19 | 14.90181 | 15.44713 | 4.10E-03 | 1.02E-04 | -583.5418 | -7.794616 | -3.140615 | -2.476615 | -6.082615 |
| 21 | 5.218 | 5.1 | 0 | 0 | 2.177 | 2.346189 | 0.927888 | -4.604406 | -14.22571 | -584.99 | -568.64 | 16.34998 | 17.31145 | 18.14347 | 4.10E-03 | 1.02E-04 | -585.9515 | -7.593707 | -3.051706 | -2.499706 | -6.217706 |
| 22 | 5.314 | 5.15 | 0 | 0 | 2.105 | 2.343787 | 0.898119 | -4.685432 | -13.96146 | -586.88 | -568.64 | 18.23999 | 19.62037 | 20.52706 | 4.09E-03 | 1.02E-04 | -588.2604 | -7.425459 | -2.979459 | -2.523459 | -6.337459 |
| 23 | 5.403 | 5.2 | 0 | 0 | 2.003 | 2.34139 | 0.855475 | -4.762081 | -13.72014 | -588.73 | -568.64 | 20.08997 | 22.09527 | 22.78117 | 4.09E-03 | 1.02E-04 | -590.7353 | -7.273135 | -2.916135 | -2.549135 | -6.452135 |
| 24 | 5.481 | 5.25 | 0 | 0 | 1.904 | 2.338999 | 0.814024 | -4.830158 | -13.51183 | -590.3 | -568.64 | 21.65997 | 24.30332 | 24.78175 | 4.09E-03 | 1.02E-04 | -592.9434 | -7.142827 | -2.863827 | -2.574827 | -6.555827 |
| 25 | 5.558 | 5.3 | 0 | 0 | 1.817 | 2.336612 | 0.777622 | -4.89796 | -13.30927 | -591.87 | -568.64 | 23.22998 | 26.46104 | 26.77421 | 4.08E-03 | 1.02E-04 | -595.1011 | -7.01727 | -2.815269 | -2.60327 | -6.66127 |
| 26 | 5.628 | 5.35 | 0 | 0 | 1.739 | 2.33423 | 0.744999 | -4.959977 | -13.12795 | -593.32 | -568.64 | 24.67999 | 28.4616 | 28.59557 | 4.08E-03 | 1.02E-04 | -597.1016 | -6.905952 | -2.773952 | -2.631951 | -6.759951 |
| 27 | 5.698 | 5.4 | 0 | 0 | 1.662 | 2.331853 | 0.712738 | -5.02225 | -12.94938 | -594.79 | -568.64 | 26.14996 | 30.50028 | 30.4245 | 4.07E-03 | 1.01E-04 | -599.1403 | -6.797377 | -2.735376 | -2.663376 | -6.861376 |
| 28 | 5.766 | 5.45 | 0 | 0 | 1.594 | 2.329481 | 0.684273 | -5.082923 | -12.7786 | -596.15 | -568.64 | 27.51001 | 32.38391 | 32.20612 | 4.07E-03 | 1.01E-04 | -601.0239 | -6.694595 | -2.700595 | -2.696595 | -6.962595 |
| 29 | 5.835 | 5.5 | 0 | 0 | 1.528 | 2.327114 | 0.656607 | -5.144608 | -12.60801 | -597.57 | -568.64 | 28.92999 | 34.33406 | 34.01771 | 4.07E-03 | 1.01E-04 | -602.9741 | -6.593011 | -2.668011 | -2.733011 | -7.068011 |
| 30 | 5.903 | 5.55 | 0 | 0 | 1.466 | 2.324751 | 0.630605 | -5.205497 | -12.44257 | -598.92 | -568.64 | 30.27997 | 36.20311 | 35.80574 | 4.06E-03 | 1.01E-04 | -604.8431 | -6.495566 | -2.638566 | -2.771566 | -7.174566 |
| 31 | 5.972 | 5.6 | 0 | 0 | 1.405 | 2.322393 | 0.604979 | -5.267365 | -12.27733 | -600.24 | -568.64 | 31.59998 | 38.05606 | 37.62275 | 4.06E-03 | 1.01E-04 | -606.696 | -6.399333 | -2.611333 | -2.813333 | -7.285333 |
| 32 | 6.042 | 5.65 | 0 | 0 | 1.349 | 2.32004 | 0.581455 | -5.330214 | -12.11235 | -601.7 | -568.64 | 33.06 | 40.02557 | 39.46878 | 4.05E-03 | 1.01E-04 | -608.6656 | -6.304348 | -2.586348 | -2.858347 | -7.400347 |
| 33 | 6.117 | 5.7 | 0 | 0 | 1.294 | 2.317692 | 0.558314 | -5.397668 | -11.93838 | -603.2 | -568.64 | 34.56 | 42.04729 | 41.45107 | 4.05E-03 | 1.01E-04 | -610.6873 | -6.205376 | -2.562376 | -2.909376 | -7.526376 |
| 34 | 6.193 | 5.75 | 0 | 0 | 1.238 | 2.315349 | 0.534693 | -5.466175 | -11.76489 | -604.67 | -568.64 | 36.02997 | 44.0726 | 43.46449 | 4.04E-03 | 1.01E-04 | -612.7126 | -6.107893 | -2.540893 | -2.963892 | -7.656892 |
| 35 | 6.277 | 5.8 | 0 | 0 | 1.186 | 2.31301 | 0.512752 | -5.542134 | -11.57616 | -606.27 | -568.64 | 37.63 | 46.21091 | 45.69836 | 4.04E-03 | 1.01E-04 | -614.851 | -6.003164 | -2.520164 | -3.027164 | -7.804163 |
| 36 | 6.367 | 5.85 | 0 | 0 | 1.133 | 2.310676 | 0.490333 | -5.62387 | -11.37716 | -608.01 | -568.64 | 39.37 | 48.52523 | 48.10312 | 4.04E-03 | 1.01E-04 | -617.1652 | -5.894163 | -2.501163 | -3.098163 | -7.965163 |
| 37 | 6.47 | 5.9 | 0 | 0 | 1.081 | 2.308347 | 0.468301 | -5.71796 | -11.153 | -609.96 | -568.64 | 41.32001 | 51.06584 | 50.87333 | 4.03E-03 | 1.00E-04 | -619.7059 | -5.773002 | -2.483002 | -3.183002 | -8.153002 |
| 38 | 6.592 | 5.95 | 0 | 0 | 1.028 | 2.306022 | 0.445789 | -5.830305 | -10.89174 | -612.49 | -568.64 | 43.84998 | 54.22867 | 54.18353 | 4.03E-03 | 1.00E-04 | -622.8687 | -5.633739 | -2.465738 | -3.287738 | -8.379738 |
| 39 | 6.737 | 6 | 0 | 0 | 0.981 | 2.303702 | 0.425836 | -5.96524 | -10.58613 | -615.49 | -568.64 | 46.84998 | 57.81692 | 58.16198 | 4.02E-03 | 1.00E-04 | -626.4569 | -5.47313 | -2.45013 | -3.41713 | -8.654129 |
| 40 | 6.927 | 6.05 | 0 | 0 | 0.941 | 2.301387 | 0.408884 | -6.144456 | -10.19184 | -619.83 | -568.64 | 51.19 | 62.67882 | 63.45025 | 0.00402 | 1.00E-04 | -631.3188 | -5.26884 | -2.43584 | -3.59284 | -9.01984 |
| 41 | 7.208 | 6.1 | 0 | 0 | 0.909 | 2.299076 | 0.395376 | -6.41398 | -9.617466 | -627.59 | -568.64 | 58.95001 | 70.87038 | 71.40981 | 4.02E-03 | 1.00E-04 | -639.5104 | -4.975466 | -2.423466 | -3.861466 | -9.569466 |

0.599992 Overall fit of CCFC in ECFC/mV

ini-VT/ml ini-LT/M ini-MT/M ini-Ep/mV ini-Ip
43.7 0.004577 0.000114 -568.6 2.62

4 No. of protonation constants
LogKa:
11.85
9.76
5.77
1.47

2 No. of ML and M(HL) complexes

| Log(Beta) | M | L | H | Refined | RefInd |
|---|---|---|---|---|---|
| 19.20975 | 1 | 1 | 1 | 1 | 1 |
| 2.06E-02 | Stand. deviation in Log(beta) | | | | |
| 4.24E-04 | COVAR for this log | | | | |
| 24.14883 | 2 | 1 | 1 | 1 | 1 |
| 2.77E-02 | Stand. deviation in Log(beta) | | | | |
| 7.67E-04 | COVAR for this log | | | | |

6 No. of MOH and ML(OH) complexes

| Log(Beta) | M | L | OH | Refined | RefInd |
|---|---|---|---|---|---|
| 4 | 1 | 0 | 1 | 0 | 0 |
| 7.7 | 1 | 0 | 2 | 0 | 0 |
| 10.3 | 1 | 0 | 3 | 0 | 0 |
| 12 | 1 | 0 | 4 | 0 | 0 |
| 5.06 | 2 | 0 | 1 | 0 | 0 |
| 24.9 | 4 | 0 | 4 | 0 | 0 |

| Temp. | I-strength | pKw | SLOPE | n-ELECTRONS |
|---|---|---|---|---|
| 25 | 0.5 | 13.74 | 29.57985 | 2 |

AMAX APOS ANEG
4 2 4

Software indicators
1 1 1 1 1 1
0

# b) Data for $Pb^{II}$–APD system.

50 Experimental points
4 No. of protonation constants
APD Pb [LT]/[MT] = 49.9199
17 8 1980 Date when experiment was performed
PbAPDr Files recorded during the experiment
DPP DCT ISE
1 0 0 indicators for mode of experiment
DPP EXPERIMENT
OH-titrant L-titrant M-titrant
1 0 0 indicaters for mode of titration

| Titration No.: | with protons pH | NaOH/ml | L-sol/ml | M-sol/ml | Ip(obs) | Ip(exp) | Ip(corr) | Log[MF] | Log[LF] | Ep(obs)/m | Init Ep/mV | Shift/mV | ECFC/mV | CCFC/mV | [LT] | [MT] | Virtual E | LOG[HL] | LOG[H2L] | LOG[H3L] | etc. |
|---|---|---|---|---|---|---|---|---|---|---|---|---|---|---|---|---|---|---|---|---|---|
| 1 | 2.443 | 0.01 | 0 | 0 | 3.264 | 3.378311 | 0.966163 | -4.697564 | -22.4045 | -398.99 | -379.8 | 19.19 | 19.63221 | 20.61198 | 4.98E-03 | 9.98E-05 | -399.4322 | -12.9975 | -5.680496 | -2.353496 | -3.326496 |
| 2 | 2.495 | 0.18 | 0 | 0 | 3.238 | 3.349851 | 0.96661 | -4.704043 | -22.24745 | -399.7 | -379.8 | 19.90002 | 20.33629 | 20.69496 | 4.94E-03 | 9.90E-05 | -400.1363 | -12.89245 | -5.627451 | -2.352451 | -3.377451 |
| 3 | 2.549 | 0.24 | 0 | 0 | 3.206 | 3.323501 | 0.964646 | -4.710793 | -22.0845 | -399.93 | -379.8 | 20.13 | 20.5924 | 20.79319 | 4.90E-03 | 9.82E-05 | -400.3924 | -12.7835 | -5.572496 | -2.351496 | -3.430496 |
| 4 | 2.6 | 0.48 | 0 | 0 | 3.19 | 3.300781 | 0.966438 | -4.717352 | -21.93077 | -400.28 | -379.8 | 20.48001 | 20.91856 | 20.89908 | 4.87E-03 | 9.75E-05 | -400.7186 | -12.68077 | -5.520774 | -2.350774 | -3.480774 |
| 5 | 2.652 | 0.6 | 0 | 0 | 3.182 | 3.281554 | 0.969663 | -4.724348 | -21.77394 | -400.46 | -379.8 | 20.66 | 21.05576 | 21.03095 | 4.84E-03 | 9.70E-05 | -400.8557 | -12.57594 | -5.467935 | -2.349935 | -3.531935 |
| 6 | 2.708 | 0.72 | 0 | 0 | 3.164 | 3.262548 | 0.969794 | -4.732503 | -21.60522 | -400.78 | -379.8 | 20.98001 | 21.37403 | 21.19758 | 4.81E-03 | 9.64E-05 | -401.174 | -12.46322 | -5.411224 | -2.349224 | -3.587224 |
| 7 | 2.76 | 0.82 | 0 | 0 | 3.151 | 3.246878 | 0.970471 | -4.740859 | -21.44865 | -400.98 | -379.8 | 21.18002 | 21.56508 | 21.38288 | 4.79E-03 | 9.59E-05 | -401.3651 | -12.35865 | -5.358646 | -2.348646 | -3.638646 |
| 8 | 2.818 | 0.92 | 0 | 0 | 3.139 | 3.231358 | 0.971418 | -4.751336 | -21.27409 | -401.32 | -379.8 | 21.52002 | 21.89254 | 21.63124 | 4.77E-03 | 9.55E-05 | -401.6925 | -12.24209 | -5.300091 | -2.348091 | -3.696091 |
| 9 | 2.87 | 1 | 0 | 0 | 3.131 | 3.219048 | 0.972648 | -4.762028 | -21.11766 | -401.61 | -379.8 | 21.81 | 22.16627 | 21.89848 | 4.75E-03 | 9.51E-05 | -401.9662 | -12.13766 | -5.24766 | -2.34766 | -3.747659 |
| 10 | 2.927 | 1.08 | 0 | 0 | 3.12 | 3.206831 | 0.972923 | -4.775439 | -20.94628 | -401.93 | -379.8 | 22.13 | 22.48264 | 22.24633 | 4.73E-03 | 9.48E-05 | -402.2826 | -12.02328 | -5.190281 | -2.347281 | -3.804281 |
| 11 | 2.991 | 1.16 | 0 | 0 | 3.108 | 3.194707 | 0.972859 | -4.792953 | -20.75393 | -402.44 | -379.8 | 22.64001 | 22.99349 | 22.71572 | 4.71E-03 | 9.44E-05 | -402.7935 | -11.89493 | -5.125935 | -2.346935 | -3.867934 |
| 12 | 3.045 | 1.22 | 0 | 0 | 3.097 | 3.185674 | 0.972165 | -4.810014 | -20.5917 | -403.14 | -379.8 | 23.34003 | 23.70268 | 23.18401 | 4.70E-03 | 9.41E-05 | -403.5027 | -11.7867 | -5.071701 | -2.346701 | -3.921701 |
| 13 | 3.104 | 1.28 | 0 | 0 | 3.094 | 3.176692 | 0.973969 | -4.831275 | -20.41453 | -403.93 | -379.8 | 24.13 | 24.46883 | 23.77662 | 4.69E-03 | 9.39E-05 | -404.2688 | -11.66853 | -5.012526 | -2.346526 | -3.980526 |
| 14 | 3.171 | 1.34 | 0 | 0 | 3.078 | 3.16776 | 0.971665 | -4.858927 | -20.21338 | -404.6 | -379.8 | 24.80002 | 25.16928 | 24.55842 | 4.67E-03 | 9.36E-05 | -404.9693 | -11.53438 | -4.945384 | -2.346384 | -4.047383 |
| 15 | 3.248 | 1.4 | 0 | 0 | 3.06 | 3.158879 | 0.968698 | -4.895472 | -19.9823 | -405.03 | -379.8 | 25.23001 | 25.63855 | 25.60333 | 4.66E-03 | 9.33E-05 | -405.4385 | -11.3803 | -4.868301 | -2.346301 | -4.124301 |
| 16 | 3.305 | 1.44 | 0 | 0 | 3.064 | 3.152985 | 0.971778 | -4.925805 | -19.81132 | -405.75 | -379.8 | 25.95001 | 26.31778 | 26.47659 | 4.65E-03 | 9.32E-05 | -406.1178 | -11.26632 | -4.813116 | -2.346316 | -4.181315 |
| 17 | 3.366 | 1.48 | 0 | 0 | 3.05 | 3.147114 | 0.969142 | -4.961275 | -19.62842 | -406.45 | -379.8 | 26.65002 | 27.05268 | 27.50183 | 4.64E-03 | 9.30E-05 | -406.8527 | -11.14442 | -4.750418 | -2.346418 | -4.242417 |
| 18 | 3.435 | 1.52 | 0 | 0 | 3.037 | 3.141264 | 0.966808 | -5.004969 | -19.4216 | -407.24 | -379.8 | 27.44 | 27.87363 | 28.77039 | 4.63E-03 | 9.28E-05 | -407.6736 | -11.0066 | -4.681597 | -2.346597 | -4.311597 |
| 19 | 3.508 | 1.56 | 0 | 0 | 3.014 | 3.135436 | 0.96127 | -5.055054 | -19.20293 | -409.48 | -379.8 | 29.68002 | 30.18746 | 30.22807 | 4.63E-03 | 9.27E-05 | -409.9875 | -10.86093 | -4.608927 | -2.346927 | -4.384927 |
| 20 | 3.589 | 1.6 | 0 | 0 | 2.996 | 3.12963 | 0.957302 | -5.114861 | -18.96043 | -411.32 | -379.8 | 31.52002 | 32.08059 | 31.97334 | 4.62E-03 | 9.25E-05 | -411.8806 | -10.69943 | -4.528425 | -2.347425 | -4.466425 |
| 21 | 3.675 | 1.64 | 0 | 0 | 2.966 | 3.123845 | 0.949471 | -5.182735 | -18.70315 | -413.19 | -379.8 | 33.39001 | 34.0561 | 33.95728 | 4.61E-03 | 9.23E-05 | -413.8561 | -10.52815 | -4.443153 | -2.348153 | -4.553153 |
| 22 | 3.767 | 1.68 | 0 | 0 | 2.939 | 3.118081 | 0.942567 | -5.259764 | -18.42817 | -414.97 | -379.8 | 35.17001 | 35.92986 | 36.21204 | 4.60E-03 | 9.21E-05 | -415.7299 | -10.34517 | -4.352173 | -2.349173 | -4.646173 |
| 23 | 3.865 | 1.72 | 0 | 0 | 2.902 | 3.112339 | 0.932418 | -5.346251 | -18.13556 | -416.91 | -379.8 | 37.11002 | 38.00893 | 38.74662 | 4.59E-03 | 9.20E-05 | -417.8089 | -10.15056 | -4.255558 | -2.350558 | -4.745558 |
| 24 | 3.916 | 1.74 | 0 | 0 | 2.887 | 3.109476 | 0.928452 | -5.392898 | -17.98342 | -417.82 | -379.8 | 38.02002 | 38.97369 | 40.11463 | 4.59E-03 | 9.19E-05 | -418.7737 | -10.04942 | -4.205415 | -2.351415 | -4.797415 |
| 25 | 3.967 | 1.76 | 0 | 0 | 2.863 | 3.106618 | 0.921581 | -5.440598 | -17.83139 | -419.59 | -379.8 | 39.79001 | 40.8391 | 41.51377 | 4.58E-03 | 9.18E-05 | -420.6391 | -9.948388 | -4.155388 | -2.352388 | -4.849388 |
| 26 | 4.019 | 1.78 | 0 | 0 | 2.832 | 3.103765 | 0.91244 | -5.49027 | -17.67649 | -420.96 | -379.8 | 41.16 | 42.33715 | 42.97125 | 4.58E-03 | 9.17E-05 | -422.1371 | -9.845494 | -4.104494 | -2.353494 | -4.902494 |
| 27 | 4.072 | 1.8 | 0 | 0 | 2.803 | 3.100918 | 0.903926 | -5.541942 | -17.51876 | -422.31 | -379.8 | 42.51001 | 43.80759 | 44.48792 | 4.57E-03 | 9.16E-05 | -423.6076 | -9.740757 | -4.052757 | -2.354757 | -4.956757 |
| 28 | 4.124 | 1.82 | 0 | 0 | 2.744 | 3.098075 | 0.885711 | -5.593643 | -17.36415 | -423.89 | -379.8 | 44.09003 | 45.64912 | 46.00546 | 4.57E-03 | 9.15E-05 | -425.4491 | -9.638153 | -4.002153 | -2.356153 | -5.010153 |
| 29 | 4.176 | 1.84 | 0 | 0 | 2.684 | 3.095238 | 0.867138 | -5.646332 | -17.20971 | -425.52 | -379.8 | 45.72 | 47.55133 | 47.55221 | 4.57E-03 | 9.15E-05 | -427.3513 | -9.535706 | -3.951705 | -2.357706 | -5.063705 |
| 30 | 4.229 | 1.86 | 0 | 0 | 2.616 | 3.092406 | 0.845943 | -5.701054 | -17.05246 | -427.03 | -379.8 | 47.23001 | 49.37925 | 49.15911 | 4.56E-03 | 9.14E-05 | -429.1792 | -9.431461 | -3.900461 | -2.359461 | -5.118462 |
| 31 | 4.33 | 1.9 | 0 | 0 | 2.517 | 3.086758 | 0.815419 | -5.808261 | -16.75342 | -430.3 | -379.8 | 50.5 | 53.12135 | 52.30679 | 4.55E-03 | 9.12E-05 | -432.9213 | -9.233419 | -3.803419 | -2.363419 | -5.223419 |
| 32 | 4.43 | 1.94 | 0 | 0 | 2.509 | 3.08113 | 0.814312 | -5.918384 | -16.4582 | -432.62 | -379.8 | 52.82001 | 55.45881 | 55.54076 | 4.55E-03 | 9.10E-05 | -435.2588 | -9.038204 | -3.708204 | -2.368204 | -5.328203 |
| 33 | 4.524 | 1.98 | 0 | 0 | 2.448 | 3.075523 | 0.795962 | -6.025834 | -16.18169 | -435.58 | -379.8 | 55.78 | 58.71159 | 58.69574 | 4.54E-03 | 9.09E-05 | -438.5116 | -8.855686 | -3.619686 | -2.373686 | -5.427687 |
| 34 | 4.609 | 2.02 | 0 | 0 | 2.387 | 3.069937 | 0.777541 | -6.126597 | -15.93265 | -438.74 | -379.8 | 58.94 | 62.1724 | 61.65294 | 4.53E-03 | 9.07E-05 | -441.9724 | -8.691648 | -3.540648 | -2.379648 | -5.518648 |
| 35 | 4.687 | 2.06 | 0 | 0 | 2.344 | 3.06437 | 0.764921 | -6.222348 | -15.7051 | -441.48 | -379.8 | 61.68002 | 65.12263 | 64.46191 | 4.52E-03 | 9.06E-05 | -444.9226 | -8.542095 | -3.469095 | -2.386095 | -5.603094 |
| 36 | 4.761 | 2.1 | 0 | 0 | 2.31 | 3.058824 | 0.755192 | -6.31631 | -15.49018 | -444.09 | -379.8 | 64.29001 | 67.89705 | 67.21804 | 4.51E-03 | 9.04E-05 | -447.697 | -8.401184 | -3.402184 | -2.393184 | -5.684184 |
| 37 | 4.83 | 2.14 | 0 | 0 | 2.292 | 3.053297 | 0.750664 | -6.406813 | -15.29078 | -446.66 | -379.8 | 66.86002 | 70.54432 | 69.87185 | 4.50E-03 | 9.02E-05 | -450.3443 | -8.270779 | -3.340778 | -2.400778 | -5.760778 |
| 38 | 4.892 | 2.18 | 0 | 0 | 2.261 | 3.047791 | 0.741849 | -6.49058 | -15.11255 | -448.94 | -379.8 | 69.14001 | 72.97607 | 72.3265 | 4.50E-03 | 9.01E-05 | -452.7761 | -8.154547 | -3.286547 | -2.408547 | -5.830547 |
| 39 | 4.952 | 2.22 | 0 | 0 | 2.248 | 3.042305 | 0.738914 | -6.573853 | -14.94096 | -451.29 | -379.8 | 71.49002 | 75.377 | 74.76654 | 4.49E-03 | 8.99E-05 | -455.177 | -8.042955 | -3.234955 | -2.416955 | -5.898955 |
| 40 | 5.008 | 2.26 | 0 | 0 | 2.215 | 3.036837 | 0.729377 | -6.653491 | -14.78171 | -453.62 | -379.8 | 73.82001 | 77.87386 | 77.09911 | 4.48E-03 | 8.97E-05 | -457.6739 | -7.939705 | -3.187705 | -2.425705 | -5.963705 |
| 41 | 5.087 | 2.32 | 0 | 0 | 2.171 | 3.028674 | 0.716815 | -6.768779 | -14.55867 | -456.64 | -379.8 | 76.84003 | 81.11706 | 80.47475 | 4.47E-03 | 8.95E-05 | -460.9171 | -7.795667 | -3.122666 | -2.439666 | -6.056666 |
| 42 | 5.157 | 2.38 | 0 | 0 | 2.125 | 3.020554 | 0.703513 | -6.873485 | -14.36285 | -459.58 | -379.8 | 79.78 | 84.29766 | 83.53743 | 4.46E-03 | 8.93E-05 | -464.0977 | -7.669853 | -3.066853 | -2.453853 | -6.140853 |
| 43 | 5.224 | 2.44 | 0 | 0 | 2.079 | 3.012478 | 0.69013 | -6.975525 | -14.17712 | -461.84 | -379.8 | 82.04001 | 86.80441 | 86.52137 | 4.44E-03 | 8.90E-05 | -466.6044 | -7.551123 | -3.015122 | -2.469122 | -6.223123 |
| 44 | 5.288 | 2.5 | 0 | 0 | 2.062 | 3.004445 | 0.686317 | -7.074227 | -14.0014 | -464.5 | -379.8 | 84.70001 | 89.53559 | 89.40668 | 0.004432 | 8.88E-05 | -469.3356 | -7.439403 | -2.967402 | -2.485403 | -6.303403 |
| 45 | 5.349 | 2.56 | 0 | 0 | 2.033 | 2.996454 | 0.678469 | -7.169008 | -13.83559 | -466.59 | -379.8 | 86.79001 | 91.77333 | 92.17606 | 4.42E-03 | 8.85E-05 | -471.5733 | -7.33459 | -2.92359 | -2.50259 | -6.38159 |
| 46 | 5.408 | 2.62 | 0 | 0 | 1.981 | 2.988506 | 0.662873 | -7.260952 | -13.67686 | -468.77 | -379.8 | 88.97 | 94.25207 | 94.86164 | 4.41E-03 | 8.83E-05 | -474.0521 | -7.23486 | -2.88286 | -2.52086 | -6.45886 |
| 47 | 5.463 | 2.68 | 0 | 0 | 1.923 | 2.9806 | 0.645172 | -7.346588 | -13.53048 | -471.43 | -379.8 | 91.63 | 97.25977 | 97.3607 | 4.40E-03 | 8.81E-05 | -477.0598 | -7.143477 | -2.846477 | -2.539476 | -6.532476 |
| 48 | 5.517 | 2.74 | 0 | 0 | 1.87 | 2.972735 | 0.62905 | -7.430326 | -13.38826 | -473.89 | -379.8 | 94.09003 | 100.0449 | 99.8037 | 4.39E-03 | 8.78E-05 | -479.8449 | -7.055261 | -2.812261 | -2.559261 | -6.606261 |
| 49 | 5.571 | 2.8 | 0 | 0 | 1.832 | 2.964912 | 0.617894 | -7.513494 | -13.24758 | -474.86 | -379.8 | 95.06 | 101.2447 | 102.23 | 4.37E-03 | 8.76E-05 | -481.0447 | -6.968579 | -2.779579 | -2.580579 | -6.68158 |
| 50 | 5.625 | 2.86 | 0 | 0 | 1.786 | 2.95713 | 0.603964 | -7.595884 | -13.10848 | -476.47 | -379.8 | 96.67001 | 103.1477 | 104.6333 | 4.36E-03 | 8.74E-05 | -482.9477 | -6.883481 | -2.748481 | -2.603481 | -6.758481 |

0.318714 Overall fit of CCFC in ECFC/mV

| ini-VT/ml | ini-LT/M | ini-MT/M | ini-Ep/mV | ini-Ip |
|---|---|---|---|---|
| 20 | 0.004986 | 9.99E-05 | -379.8 | 3.38 |

4 No. of protonation constants
LogKa:
11.85
9.76
5.77
1.47

3 No. of ML and M(HL) complexes

| Log(Beta) | M | L | H | Refined | RefInd |
|---|---|---|---|---|---|
| 22.252 | 1 | 1 | 1 | 1 | 1 |
| 1.31E-02 | Stand. deviation in Log(beta) | | | | |
| 1.73E-04 | COVAR for this log | | | | |
| 28.183 | 2 | 1 | 1 | 1 | 1 |
| 2.12E-02 | Stand. deviation in Log(beta) | | | | |
| 4.51E-04 | COVAR for this log | | | | |
| 30.323 | 1 | 1 | 3 | 1 | 1 |
| 1.39E-02 | Stand. deviation in Log(beta) | | | | |
| 1.92E-04 | COVAR for this log | | | | |

7 No. of MOH and ML(OH) complexes

| Log(Beta) | M | L | OH | Refined | RefInd |
|---|---|---|---|---|---|
| 6 | 1 | 0 | 1 | 0 | 0 |
| 10.3 | 1 | 0 | 2 | 0 | 0 |
| 13.3 | 1 | 0 | 3 | 0 | 0 |
| 7.6 | 2 | 0 | 1 | 0 | 0 |
| 31.7 | 3 | 0 | 4 | 0 | 0 |
| 35.2 | 4 | 0 | 4 | 0 | 0 |
| 67.4 | 6 | 0 | 8 | 0 | 0 |

| Temp. | I-strength | pKw | SLOPE | n-ELECTRONS |
|---|---|---|---|---|
| 25 | 0.5 | 13.74 | 29.57985 | 2 |

| AMAX | APOS | ANEG |
|---|---|---|
| 6 | 2 | 6 |

| Software | indicators | | | | |
|---|---|---|---|---|---|
| 1 | 1 | 1 | 1 | 1 | 1 |
| 0 | | | | | |

# c) Data for $Zn^{II}$–APD system.

33 Experimental points
4 No. of protonation constants
APD Zn [LT]/[MT] = 28.34505
28 5 1980 Date when experiment was performed
ZAPDr Files recorded during the experiment
DPP DCT ISE
1 0 0 indicators for mode of experiment
DPP EXPERIMENT
OH-titrant L-titrant M-titrant
1 0 0 indicaters for mode of titration
Titration with protons

| No.: | pH | NaOH/ml | L-sol/ml | M-sol/ml | Ip(obs) | Ip(exp) | Ip(corr) | Log[MF] | Log[LF] | Ep(obs)/m | Init Ep/mV | Shift/mV | ECFC/mV | CCFC/mV | [LT] | [MT] | Virtual E | LOG[HL] | LOG[H2L] | LOG[H3L] | etc. |
|---|---|---|---|---|---|---|---|---|---|---|---|---|---|---|---|---|---|---|---|---|---|
| 1 | 2.885 | 0.56 | 0 | 0 | 3.151 | 2.935798 | 1.073303 | -4.441611 | -21.35815 | -995.72 | -984.4 | 11.31995 | 10.41119 | 11.29874 | 2.47E-03 | 8.72E-05 | -994.8112 | -12.39315 | -5.518152 | -2.633152 | -4.048152 |
| 2 | 2.941 | 0.62 | 0 | 0 | 3.148 | 2.927255 | 1.07541 | -4.444048 | -21.18956 | -995.97 | -984.4 | 11.56995 | 10.63599 | 11.3334 | 2.46E-03 | 8.69E-05 | -995.036 | -12.28056 | -5.461563 | -2.632563 | -4.103563 |
| 3 | 3.006 | 0.68 | 0 | 0 | 3.143 | 2.918762 | 1.076826 | -4.446759 | -20.99397 | -995.56 | -984.4 | 11.15997 | 10.20911 | 11.37627 | 2.46E-03 | 8.67E-05 | -994.6091 | -12.14997 | -5.395969 | -2.631969 | -4.167969 |
| 4 | 3.054 | 0.72 | 0 | 0 | 3.14 | 2.913127 | 1.077879 | -4.448733 | -20.84963 | -995.74 | -984.4 | 11.33997 | 10.37654 | 11.40984 | 2.45E-03 | 8.65E-05 | -994.7766 | -12.05363 | -5.347628 | -2.631628 | -4.215628 |
| 5 | 3.111 | 0.76 | 0 | 0 | 3.136 | 2.907514 | 1.078585 | -4.451042 | -20.67824 | -997.33 | -984.4 | 12.92999 | 11.95817 | 11.45335 | 2.45E-03 | 8.63E-05 | -996.3582 | -11.93924 | -5.290243 | -2.631243 | -4.272243 |
| 6 | 3.173 | 0.8 | 0 | 0 | 3.132 | 2.901923 | 1.079284 | -4.453608 | -20.49196 | -995.27 | -984.4 | 10.87 | 9.889842 | 11.50453 | 2.44E-03 | 8.62E-05 | -994.2899 | -11.81496 | -5.227959 | -2.630959 | -4.333959 |
| 7 | 3.252 | 0.84 | 0 | 0 | 3.127 | 2.896353 | 1.079634 | -4.45697 | -20.25464 | -996.25 | -984.4 | 11.84998 | 10.86566 | 11.57928 | 2.44E-03 | 8.60E-05 | -995.2657 | -11.65664 | -5.148642 | -2.630642 | -4.412642 |
| 8 | 3.346 | 0.88 | 0 | 0 | 3.121 | 2.890805 | 1.07963 | -4.461314 | -19.97247 | -997.58 | -984.4 | 13.17999 | 12.19572 | 11.68316 | 2.43E-03 | 8.58E-05 | -996.5958 | -11.46847 | -5.05447 | -2.63047 | -4.50647 |
| 9 | 3.398 | 0.9 | 0 | 0 | 3.117 | 2.888038 | 1.079279 | -4.463953 | -19.81648 | -998.04 | -984.4 | 13.63995 | 12.65986 | 11.74894 | 2.43E-03 | 8.58E-05 | -997.0599 | -11.36448 | -5.00248 | -2.63048 | -4.558479 |
| 10 | 3.452 | 0.92 | 0 | 0 | 3.114 | 2.885277 | 1.079273 | -4.466925 | -19.65458 | -996.88 | -984.4 | 12.47998 | 11.49997 | 11.82453 | 2.43E-03 | 8.57E-05 | -995.9 | -11.25658 | -4.94858 | -2.63058 | -4.612579 |
| 11 | 3.521 | 0.94 | 0 | 0 | 3.109 | 2.882521 | 1.07857 | -4.471104 | -19.44775 | -997.69 | -984.4 | 13.28998 | 12.31833 | 11.93588 | 2.43E-03 | 8.56E-05 | -996.7184 | -11.11875 | -4.879747 | -2.630747 | -4.681747 |
| 12 | 3.605 | 0.96 | 0 | 0 | 3.104 | 2.879771 | 1.077864 | -4.47694 | -19.19608 | -997.94 | -984.4 | 13.53998 | 12.57675 | 12.09623 | 2.42E-03 | 8.55E-05 | -996.9767 | -10.95108 | -4.796084 | -2.631084 | -4.766084 |
| 13 | 3.687 | 0.98 | 0 | 0 | 3.098 | 2.877026 | 1.076807 | -4.483667 | -18.95066 | -997.86 | -984.4 | 13.45996 | 12.50933 | 12.28297 | 2.42E-03 | 8.54E-05 | -996.9094 | -10.78766 | -4.714657 | -2.631657 | -4.848657 |
| 14 | 3.798 | 1 | 0 | 0 | 3.091 | 2.874286 | 1.075398 | -4.494763 | -18.61866 | -999.42 | -984.4 | 15.01996 | 14.08615 | 12.59897 | 2.42E-03 | 8.53E-05 | -998.4861 | -10.56666 | -4.60466 | -2.63266 | -4.96066 |
| 15 | 3.916 | 1.02 | 0 | 0 | 3.083 | 2.871551 | 1.073636 | -4.509889 | -18.26622 | -999.85 | -984.4 | 15.44995 | 14.53721 | 13.03414 | 2.42E-03 | 8.53E-05 | -998.9373 | -10.33222 | -4.488216 | -2.634216 | -5.080215 |
| 16 | 4.048 | 1.04 | 0 | 0 | 3.074 | 2.868821 | 1.07152 | -4.532204 | -17.87263 | -999.83 | -984.4 | 15.42999 | 14.54259 | 13.68199 | 2.41E-03 | 8.52E-05 | -998.9426 | -10.07063 | -4.358625 | -2.636625 | -5.214624 |
| 17 | 4.185 | 1.06 | 0 | 0 | 3.065 | 2.866097 | 1.069399 | -4.563449 | -17.46509 | -1000.94 | -984.4 | 16.53998 | 15.67803 | 14.59402 | 2.41E-03 | 8.51E-05 | -1000.078 | -9.800085 | -4.225085 | -2.640085 | -5.355084 |
| 18 | 4.317 | 1.08 | 0 | 0 | 3.057 | 2.863378 | 1.06762 | -4.603895 | -17.07362 | -1001.24 | -984.4 | 16.83997 | 15.9994 | 15.77821 | 2.41E-03 | 8.50E-05 | -1000.399 | -9.540615 | -4.097615 | -2.644615 | -5.491614 |
| 19 | 4.438 | 1.1 | 0 | 0 | 3.049 | 2.860663 | 1.065837 | -4.65238 | -16.71609 | -1002.64 | -984.4 | 18.23999 | 17.4209 | 17.20019 | 2.41E-03 | 8.49E-05 | -1001.821 | -9.304085 | -3.982085 | -2.650085 | -5.618085 |
| 20 | 4.543 | 1.12 | 0 | 0 | 3.042 | 2.857954 | 1.064398 | -4.705184 | -16.40712 | -1003.11 | -984.4 | 18.70996 | 17.90823 | 18.74996 | 2.41E-03 | 8.49E-05 | -1002.308 | -9.100118 | -3.883118 | -2.656118 | -5.729118 |
| 21 | 4.638 | 1.14 | 0 | 0 | 3.035 | 2.855251 | 1.062954 | -4.762818 | -16.12881 | -1004.9 | -984.4 | 20.5 | 19.71571 | 20.44263 | 2.40E-03 | 8.48E-05 | -1004.116 | -8.916813 | -3.794813 | -2.662813 | -5.830812 |
| 22 | 4.719 | 1.16 | 0 | 0 | 3.03 | 2.852552 | 1.062207 | -4.820025 | -15.89264 | -1007.33 | -984.4 | 22.92999 | 22.15473 | 22.12264 | 2.40E-03 | 8.47E-05 | -1006.555 | -8.761644 | -3.720644 | -2.669644 | -5.918644 |
| 23 | 4.796 | 1.18 | 0 | 0 | 3.025 | 2.849858 | 1.061456 | -4.881597 | -15.66921 | -1008.7 | -984.4 | 24.29999 | 23.53381 | 23.93179 | 2.40E-03 | 8.46E-05 | -1007.934 | -8.615211 | -3.651211 | -2.677211 | -6.003211 |
| 24 | 4.866 | 1.2 | 0 | 0 | 3.02 | 2.84717 | 1.060703 | -4.943713 | -15.46715 | -1010.55 | -984.4 | 26.14996 | 25.39291 | 25.75706 | 2.40E-03 | 8.45E-05 | -1009.793 | -8.483146 | -3.589146 | -2.685146 | -6.081146 |
| 25 | 4.928 | 1.22 | 0 | 0 | 3.016 | 2.844486 | 1.060297 | -5.003529 | -15.28913 | -1013.55 | -984.4 | 29.14996 | 28.39782 | 27.5143 | 2.39E-03 | 8.45E-05 | -1012.798 | -8.367134 | -3.535134 | -2.693134 | -6.151134 |
| 26 | 5.012 | 1.25 | 0 | 0 | 3.011 | 2.840471 | 1.060036 | -5.091401 | -15.04956 | -1014.6 | -984.4 | 30.19995 | 29.45098 | 30.09538 | 2.39E-03 | 8.43E-05 | -1013.851 | -8.211559 | -3.463559 | -2.705559 | -6.24756 |
| 27 | 5.089 | 1.28 | 0 | 0 | 3.006 | 2.836466 | 1.059769 | -5.178303 | -14.83177 | -1017.82 | -984.4 | 33.41998 | 32.67423 | 32.6478 | 2.39E-03 | 8.42E-05 | -1017.074 | -8.070772 | -3.399772 | -2.718772 | -6.337772 |
| 28 | 5.158 | 1.31 | 0 | 0 | 3.001 | 2.832473 | 1.059498 | -5.26072 | -14.6383 | -1019.91 | -984.4 | 35.50995 | 34.76749 | 35.0676 | 2.38E-03 | 8.41E-05 | -1019.168 | -7.946296 | -3.344296 | -2.732296 | -6.420296 |
| 29 | 5.222 | 1.34 | 0 | 0 | 2.997 | 2.828491 | 1.059576 | -5.340455 | -14.4604 | -1021.58 | -984.4 | 37.17999 | 36.43659 | 37.40805 | 2.38E-03 | 8.40E-05 | -1020.837 | -7.832401 | -3.294401 | -2.746401 | -6.498402 |
| 30 | 5.283 | 1.37 | 0 | 0 | 2.993 | 2.82452 | 1.059649 | -5.418905 | -14.29236 | -1024.88 | -984.4 | 40.47998 | 39.73569 | 39.71055 | 2.38E-03 | 8.39E-05 | -1024.136 | -7.725361 | -3.248361 | -2.761361 | -6.574361 |
| 31 | 5.358 | 1.41 | 0 | 0 | 2.988 | 2.819243 | 1.059859 | -5.51795 | -14.08798 | -1027.25 | -984.4 | 42.84998 | 42.10314 | 42.61628 | 2.37E-03 | 8.37E-05 | -1026.503 | -7.595978 | -3.193977 | -2.781977 | -6.669977 |
| 32 | 5.429 | 1.45 | 0 | 0 | 2.983 | 2.813986 | 1.060062 | -5.613628 | -13.89691 | -1031 | -984.4 | 46.59998 | 45.85068 | 45.42244 | 2.37E-03 | 8.36E-05 | -1030.251 | -7.47591 | -3.14491 | -2.80391 | -6.76291 |
| 33 | 5.498 | 1.49 | 0 | 0 | 2.979 | 2.808748 | 1.060615 | -5.707743 | -13.71362 | -1034.69 | -984.4 | 50.28992 | 49.53392 | 48.18241 | 2.36E-03 | 8.34E-05 | -1033.934 | -7.361619 | -3.099619 | -2.827619 | -6.855619 |

0.663099 Overall fit of CCFC in ECFC/mV

ini-VT/ml ini-LT/M ini-MT/M ini-Ep/mV ini-Ip
20 0.00254 8.96E-05 -984.4 3.018

4 No. of protonation constants
LogKa:
11.85
9.76
5.77
1.47

3 No. of ML and M(HL) complexes
Log(Beta) M L H Refined RefInd
20.718 1 1 1 1 1
1.72E-02 Stand. deviation in Log(beta)
2.97E-04 COVAR for this log
25.643 1 1 2 1 1
3.25E-02 Stand. deviation in Log(beta)
1.06E-03 COVAR for this log
30.152 1 1 3 1 1
5.09E-02 Stand. deviation in Log(beta)
2.59E-03 COVAR for this log

6 No. of MOH and ML(OH) complexes
Log(Beta) M L OH Refined RefInd
5 1 0 1 0 0
10.2 1 0 2 0 0
13.9 1 0 3 0 0
15.5 1 0 4 0 0
5.5 2 0 1 0 0
27.94 4 0 4 0 0
Temp. I-strength pKw SLOPE n-ELECTRONS
25 0.5 13.74 29.57985 2

AMAX APOS ANEG
4 1 4

Software indicators
1 1 1 1 1 1
0